Growth Factor Regulation of Preantral Follicle Development in the Mouse Ovary

Victoria Atess

Institute of Reproductive and Developmental Biology

Department of Surgery and Cancer

Imperial College London

Submitted for the degree of Doctor of Philosophy to

Imperial College London

Acknowledgements

First of all, I would like to formally thank my supervisors, Professor Kate Hardy and Professor Stephen Franks, for giving me the opportunity to complete this PhD and for all their advice and generous support to help me along the way.

I would also like to say a big thank you to everyone I have had the pleasure of working with in the IRDB. Especially, I would like to thank Dr Mark Fenwick, Ms Jossie Mora, Dr Mhairi Laird and Dr Avigdor Lerner for their help and guidance in the laboratory and their friendship. A further thank you to Ms Jocelyn Mora for her expert advice and training in confocal microscopy. Special thanks must also go to everyone on the second and fifth floors for making this a lovely place to work and keeping me sane particularly Resha, Rupa, Camilla, and Lil.

Finally, I would like to thank my parents for everything they have done to help support, encourage and reassure me.

Declaration of conjoint work

This is to certify that:

- The data presented in this thesis is my own original work except where indicated
- The data presented in Figure 4.8 and Figure 4.9 was the result of work carried out my Dr Mhairi Laird and Dr Avigdor Lerner, my laboratory colleagues
- All other work that was not my own is appropriately referenced and acknowledged

The copyright of this thesis rests with the author and is made available under a Creative Commons Attribution Non-Commercial No Derivatives licence. Researchers are free to copy, distribute or transmit the thesis on the condition that they attribute it, that they do not use it for commercial purposes and that they do not alter, transform or build upon it. For any reuse or redistribution, researchers must make clear to others the licence terms of this work

Abstract

At, or around, birth female mammals are already endowed with a finite stock of oocytes. The majority are housed within non-growing primordial follicles but, from birth until depletion, a steady trickle initiate growth. The regulation of this process is poorly understood, despite its importance in defining reproductive lifespan. Primordial activation is characterised by oocyte growth, granulosa cell (GC) cuboidalisation and proliferation. N-cadherin is the major cell adhesion molecule (CAM) associated with GC cuboidalisation in mouse. CAMs are known to associate and signal with receptor tyrosine kinases (RTKs). Several RTKs have been implicated in regulating primordial activation and have been localised to GCs. Therefore, we hypothesised that RTKs may regulate primordial activation via interaction with N-cadherin in mouse. Association of candidate RTKs with N-cadherin was assessed by immunofluorescence. The Platelet derived growth factor (PDGF) receptors did not localise to GCs and therefore were not investigated further. In contrast, ErbB2, an RTK member of the Epidermal growth factor (EGF) family, which relies on heterodimerisation to signal co-localised with N-cadherin in cuboidalising GCs. Furthermore, expression of a downstream anti-proliferative protein, transducer of ErbB2 (TOB1), provides evidence that ErbB2 may regulate the onset of GC proliferation during primordial activation. A suitable antibody was not available to identify a dimer partner, but PCR demonstrated *Egfr* and *ErbB3* expression. The sensitivity of isolated preantral follicles to EGF, which stimulated follicle growth, and inhibitors to EGFR, which blocked EGF-stimulated follicle growth, demonstrate that EGFR is expressed and available to dimerise with ErbB2 and also provides strong evidence that EGFR signalling is important in preantral GC proliferation. Crucially, culture of whole d4 ovaries in either EGF of Lapatinib, an inhibitor of EGFR/ErbB2 provide evidence to suggest that these proteins regulate mouse primordial activation.

Contents

Acknowledgements

Declaration of conjoint work

Abstract

Contents

List of Figures

List of Tables

Abbreviations

Chapter 1 Introduction

1.1 The ovary

1.2 Primordial follicle formation

1.3 Follicle development

1.4 Initiation of follicle growth

1.5 Granulosa cell adhesion

1.6 Growth factor regulation of primordial activation

1.7 Growth factor signalling from junctional complexes

1.8 Signalling by RTKs

1.9 PDGF family

1.10 EGF family

1.10.1 ErbB2 is constitutively poised to dimerise

1.10.2 ErbB2 is the preferred heterodimerisation partner of all other ErbBs

1.10.3 ErbB2-containing heterodimers are the most potent ErbB dimers

1.10.4 ErbB2 is often overexpressed in human cancers

1.10.5 The ErbB receptors have critical roles in development

1.10.6 The ErbB ligands are important in reproductive development

1.10.7 ErbB downstream signaling

1.11 Project Strategy – Inhibition of RTKs

1.12 Project strategy: Culture models

1.13 Project strategy: Localisation of RTKs

1.14 Hypothesis

1.15 Aims of Project

Chapter 2 Materials and Methods

2.1 Collection of ovaries

2.2 Isolation of follicles

2.3 Gene expression analysis

2.3.1 RNA extraction of whole tissues

2.3.2 RNA extraction of follicles, oocytes and granulosa cells

2.3.3 Reverse Transcription-PCR (RT-PCR)

2.4 Spatial protein localisation in vivo studies

2.4.1 Fixation of isolated follicles and whole ovaries

2.4.2 Processing of isolated follicles and whole ovaries

2.4.3 Immunofluorescence

2.4.4 Immunohistochemistry

2.4.5 Haematoxylin and Eosin staining

2.4.6 Classification of immunolabelled follicles in ovarian sections

2.4.7 Quantification of Immunofluorescence by follicle stage

2.4.8 Quantification of Immunofluorescence by follicular location

2.5 EGFR protein analysis

2.5.1 Protein extraction for Western blot analysis

2.5.2 Determination of protein concentration

2.5.3 SDS polyacrylamide gel electrophoresis (SDS-PAGE)

2.5.4 Western blotting

2.6 Isolated follicle culture studies

2.6.1 Isolated follicle culture in the presence of insulin

2.6.2 Isolated follicle culture in the absence of insulin

2.6.3 Exogenous ligand

2.6.4 ErbB2 inhibition

2.6.5 Dual ErbB inhibition

2.6.6 EGFR inhibition

2.6.7 Assessment of in vitro follicle growth and morphology

2.7 Whole d4 mouse ovary culture studies

2.7.1 In vitro culture of whole d4 mouse ovary

2.7.2 Fixing and processing of cultured ovaries

2.7.3 Double immunolabelling for VASA and laminin in cultured ovaries

2.7.4 Follicle classification, counting and exclusion during analysis of VASA/laminin labelled cultured ovary sections

2.7.5 Measurement of area of VASA-labelled oocytes in cultured ovary

2.8 Statistical analysis

2.8.1 Assigning statistical significance to isolated preantral follicle culture experiments

Chapter 3 PDGF family expression in the mouse ovary

3.1 Results

3.1.1 PDGF receptor expression

3.1.1.1 PDGF receptor mRNA expression in the mouse ovary

3.1.1.2 PDGF receptor protein expression in the mouse ovary

3.1.2. PDGF ligand expression in the mouse ovary

3.1.2.1 PDGF ligand mRNA expression in the mouse ovary

3.1.2.2 PDGF B ligand protein expression in the mouse ovary

3.1.2.3 PDGF C ligand protein expression in the mouse ovary

3.1.3 Summary of PDGF family results

3.1.4 Summary of comparisons of PDGF family expression in the mouse and rat ovary

3.2 Discussion

3.2.1 The PDGF family are unlikely regulators of N-cadherin

3.2.2 PDGF receptors are candidate markers of theca formation

3.2.3 PDGF family expression in the d4 ovary

3.2.4 Regulation of PDGF-B biosynthesis and secretion

3.2.5 Discordance between PDGFC mRNA and protein expression

3.2.5 Possible regulation of PDGF-C expression by Cingulin

3.3 Conclusions

Chapter 4 EGF family expression in the mouse ovary

4.1 Results

4.1.1 ErbB receptor mRNA expression profile in the mouse ovary

4.1.2 ErbB1 (EGFR) protein expression in the mouse ovary

4.1.3 ErbB2 protein expression in the mouse ovary

4.1.4 Expression of proteins downstream from ErbB2

4.1.5 ErbB ligand mRNA expression profile in the mouse ovary

4.1.6 ErbB receptor PCR screen using bioanalysed samples

4.1.7 Neuregulin 1 protein expression

4.1.8 Summary of EGF family expression results

4.2 Discussion

4.2.1 ErbB2 may have a role in GC cell shape change during primordial activation

4.2.2 ErbB2 may have a role in GC proliferation during primordial activation

4.2.3 ErbB2 is downregulated in late stage follicles

4.2.4 EGFR protein was not detected in mouse ovary

4.2.5 Future studies should examine possible ErbB3 protein expression

4.2.6 Only HB-EGF and TGFα transcripts have been detected in preantral follicles so far

4.3 Conclusions

Chapter 5 Quantification of ErbB2 expression

5.1 Results

5.1.1 Immunolocalisation of ErbB2 in d4, 8, 12, 19 and adult ovaries

5.1.2 Quantitative analysis of ERBB2 immunolabelling

5.1.2.1 How does the level of ERBB2 immunolabelling differ with follicle stage?

5.1.2.2 How does the level of ERBB2 immunolabelling differ with follicle location?

5.1.3 How does ERBB2 immunolabelling in a d16 ovary compare to that of other proteins?

5.2 Discussion

5.2.1 ERBB2 expression may be regulated by something in the blood supply

5.2.2 ERBB2 expression may be regulated by ECM components

5.2.3 ERBB2 expression may be regulated by another growth factor family

5.2.4 ERBB2 expression may be regulated according to GC origin

5.3 Conclusions

Chapter 6 Localisation of EGFR protein by Western blot

6.1 Results

6.1.1 Can we detect EGFR protein in positive mouse tissue controls by Western blot analysis?

6.1.2 Can we detect EGFR in pools of 50 isolated preantral follicles?

6.1.3 How much protein can we extract from pooled preantral follicles?

6.1.4 Is our Western blotting protocol optimal?

6.1.5 How much protein from adult ovaries is needed to detect EGFR?

6.1.6 Can we detect EGFR in protein lysate prepared from 100 follicles?

6.2 Discussion

Chapter 7 ErbB inhibition during in vitro preantral follicle growth

7.1 Results

7.1.1 The effect of ErbB2 inhibition on preantral follicle growth in the presence of insulin

7.1.1.1 Do ErbB2 inhibitors affect preantral follicle growth?

7.1.1.2 Is the isolated follicle culture model suitable to examine ErbB2?

7.1.1.3 Do exogenous ErbB ligands affect preantral follicle growth in vitro?

7.1.1.4 Do ErbB2 inhibitors affect EGF-stimulated preantral follicle growth in vitro?

7.1.2 The effect of ErbB2 inhibition on follicle growth in the absence of insulin

7.1.2.1 Can isolated preantral follicles survive in vitro culture in the absence of insulin?

7.1.2.2 Can EGF stimulate follicle growth in insulin-free conditions?

7.1.2.3 Do ErbB2 inhibitors block EGF-stimulated follicle growth in insulin-free conditions?

7.1.2.4. Does Lapatinib Ditosylate have an effect on EGF-stimulated follicle growth in insulin-free conditions?

7.1.3 Dual inhibition of EGFR and ErbB2 in the presence of insulin

7.1.3.1 Does Lapatinib Ditosylate block EGF-stimulated follicle growth in the presence of insulin?
7.1.3.2 Antibody-mediated ErbB2 inhibition in preantral follicles
7.1.3.3 Is EGF capable of stimulating growth of follicles pre-incubated with Trastuzumab?

7.1.4 EGFR inhibition in preantral follicles

7.1.4.1 Does AG1478 affect basal follicle growth?
7.1.4.2 Does AG1478 affect EGF-stimulated follicle growth?
7.1.4.3 Are the effects of EGF and AG1478 on follicle growth due to changes in GC proliferation?

7.1.5. Summary of results from follicle culture studies

7.2 Discussion

7.2.1 Functional data indicates that EGFR must be expressed in preantral GCs

7.2.2 It is likely that EGFR/ErbB2 heterodimers form in preantral GCs

7.2.3 This data has not demonstrated a role for ErbB2 in in vitro follicle growth

Chapter 8 ErbB stimulation and inhibition during in vitro culture of whole d4 mouse ovaries

8.1 Approach

8.2 Results

8.2.1 Do ovaries exposed to Lapatinib appear healthy during the 8 day culture period?

8.2.2 How does in vitro follicle development differ from in vivo follicle development?

8.2.3 Is ErbB2 expressed in cultured ovaries?

8.2.4 How does Lapatinib treatment affect in vitro primordial activation in these ovaries?

8.2.5 What is the effect of EGF on in vitro primordial activation?

8.3 Discussion

8.3.1 Follicle development in vitro differs to that in vivo

8.3.2 ErbB signalling may be involved in in vitro primordial activation

8.4 Conclusion

Chapter 9 Discussion

References

List of figures

Chapter 1

Figure 1.1 **Summary of follicle development**

Figure 1.2 **The origin of GCs**

Figure 1.3 **Diagram showing the multiple stages of primordial activation in mono-ovular mammals.**

Figure 1.4. **Diagram showing the junctional molecules that have been localised to follicles in the mouse ovary.**

Figure 1.5. **N-cadherin (A) and Nectin-2 (B) immunolocalisation in the mouse ovary.**

Figure 1.6 **Diagram showing all possible dimeric combinations of PDGF ligand and receptors and their specificity for one another.**

Figure 1.7. **Simplified diagram of the domain structure of the EGFR**

Figure 1.8. **The EGF family is comprised of four receptors (ErbB1-4) and eleven ligands**

Figure 1.9. **Diagram illustrating the processes that the LH surge stimulates in a pre-ovulatory follicle via the EGF family.**

Figure 1.10 **Diagram illustrating all possible dimeric combinations of ErbB receptors and the major intracellular signalling pathways common to all of them.**

Figure 1.11 **Different ErbB receptors have a different complement of docking sites on their cytoplasmic tails, once phoshorylated.**

Figure 1.12. **Diagram illustrating the various targets of inhibitors to EGFR and ErbB2.**

Chapter 2

Figure 2.1. **Images of isolated preantral follicles and isolated oocytes.**

Figure 2.2. **Diagram illustrating the morphology used to classify different stages of follicle development.**

Figure 2.3. **Screen shot of FileMaker Pro follicle culture database illustrating the instances in which cultured follicles are excluded from analysis based on their morphology over the 72 hour culture period.**

Figure 2.4. **FileMaker Pro layout with a measurement grid allowing close inspection of follicle development and checking of anamalous sizes.**

Figure 2.5. **Diagram depicting two ovaries cultured in an individual well of a 6 well plate.**

Chapter 3

Figure 3.1. **Diagram showing all the possible dimeric combinations of PDGF ligand and receptors, and their specificity for one another.**

Figure 3.2. **RT-PCR screen showing presence or absence of transcripts for PDGF receptors and N-cadherin in oocytes, GCs, preantral follicles at the primary, secondary or secondary plus stages of development, ovary and oviduct.**

Figure 3.3. **Comparison of PDGF receptor isoforms (α and β) expression in pre-pubertal mouse ovaries.**

Figure 3.4. **PDGF receptor expression and IgG controls in d21 mouse ovary**

Figure 3.5. **PDGF receptor protein expression in mouse ovaries of various ages post-partum.**

Figure 3.6. **An isolated preantral follicle, immunolabelled with antibodies to Ki67, with a single layer of flat (putative) theca cells around the basal lamina.**

Figure 3.7. **RT-PCR screen of oocytes, GCs, follicles and ovaries showing presence or absence of transcripts for the PDGF family and N-cadherin.**

Figure 3.8. **RT-PCR screen of oocytes, GCs, follicles and ovaries and oviduct showing presence or absence of transcripts for the PDGF ligands and N-cadherin.**

Figure 3.9. **PDGF-B expression at successive stages of follicle development, in mouse ovaries of various ages post-partum.**

Figure 3.10. **PDGF-B protein expression in pre-pubertal and adult mouse ovaries.**

Figure 3.11. **PDGF-B expression in positive and negative IgG controls.**

Figure 3.12. **PDGF-C expression in d21 mouse ovaries with respect to cell type and compartment.**

Figure 3.13. **PDGF-C expression in follicles at different stages of development.**

Chapter 4

Figure 4.1. **RT-PCR screen of oocytes, GCs, different stages of preantral follicles, different ages of pre-pubertal ovaries and oviduct control showing presence/absence of transcripts for ErbB family members.**

Figure 4.2. **ErbB2 protein expression in mouse ovaries of various ages post-partum.**

Figure 4.3. **GC-specific ErbB2 protein expression confirmed with two antibodies in d19 ovary.**

Figure 4.4 **Co-localisation of ErbB2 protein with that of N-cadherin and β-catenin.**

Figure 4.5. **Diagram illustrating the phosphorylation status and localisation of the active and inactive forms of TOB1, as regulated by ErbB2.**

Figure 4.6. **Expression of the inactive form of TOB1, pTOB1, in mouse ovaries of various ages post-partum.**

Figure 4.7. **Expression of the active, unphosphorylated form of TOB1 in mouse ovaries of various ages post-partum.**

Figure 4.8. **PCR screen showing presence or absence of transcripts for Btc, Epgn, Hbegf and Tgfα in adult ovary, d16 ovary, pooled preantral follicles, pooled preantral oocytes, antral GCs, positive control specific for each gene and negative water control.**

Figure 4.9. **PCR screen showing presence or absence of transcripts for ErbB1-4 in adult ovary, d16 ovary, pooled preantral follicles, pooled preantral oocytes, antral GCs, lung tissue, and negative water control.**

Figure 4.10. **Neuregulin-1 protein expression (brown) in mouse ovaries of various ages post-partum.**

Figure 4.11. **Model of how ErbB2 may regulate the onset of GC proliferation during primordial activation.**

Chapter 5

Figure 5.1. **ERBB2 protein expression in mouse ovaries of various ages post-partum.**

Figure 5.2. **ERBB2 immunolabelling in central sections from three d16 ovaries.**

Figure 5.3. **Image showing an ovarian section used to measure ERBB2 immunolabelling intensity with respect to distance from OSE.**

Figure 5.4. **Relationship between degree of ERBB2 immunolabelling and follicle stage.**

Figure 5.5. **Diagram illustrating how follicles were staged and separated for analysis.**

Figure 5.6. **Graph showing the effect of follicular location on intensity of ERBB2 immunolabelling.**

Figure 5.7. **The relationship between ERBB2 immunolabelling and that of proteins from the TGF-beta superfamily signalling pathway.**

Chapter 6

Figure 6.1. **Lysates from five adult ovaries were immunoprobed with antibodies to EGFR**

Figure 6.2. **Lysates from pooled preantral follicles and HeLa cells were immunoprobed with antibodies to α-tubulin and β-catenin.**

Figure 6.3. **Lysates from one adult ovary were serially diluted in RIPA buffer to 50, 10, 5, 2 or 1 μg and immunoprobed with antibodies to EGFR and α-tubulin.**

Figure 6.4. **Lysates from adult ovary (10 and 50 μg), pre-pubertal ovary, remnant tissue from a pre-pubertal ovary following follicle isolation ('stroma'), 50 pooled preantral follicles, and 100 pooled preantral follicles were immunoprobed with antibodies to EGFR and α-tubulin.**

Chapter 7

Figure 7.1. **The effect of the small molecule ErbB2 tyrosine kinase inhibitors AG-825 and ErbB2 inhibitor II on in vitro follicle growth over 72 hours.**

Figure 7.2 **Follicles isolated from a d16 ovary, immediately processed for histology and immunolabelled for ErbB2 (green).**

Figure 7.3. **EGF dose response in isolated preantral follicles.**

Figure 7.4. **The effect of ErbB2 inhibition on EGF-stimulated growth.**

Figure 7.5. **Insulin dose response in preantral follicles.**

Figure 7.6. **Follicles cultured in the absence of insulin do not show signs of cell death and atresia.**

Figure 7.7. **EGF dose response in isolated preantral follicles in the absence of Insulin.**

Figure 7.8. **The effect of ErbB2 inhibition on isolated preantral follicle growth in insulin-free conditions in vitro.**

Figure 7.9. **The effect of Lapatinib on EGF-stimulated growth in the absence of insulin.**

Figure 7.10. **The affect of Lapatinib Ditosylate on EGF-stimulated preantral follicle growth in the presence of insulin.**

Figure 7.11. **The effect of Trastuzumab on EGF-stimulated preantral follicle growth in the presence of insulin.**

Figure 7.12. **The effect of EGF on preantral follicles pre-incubated with Trastuzumab.**

Figure 7.13. **The effect of AG1478 on EGF-stimulated preantral follicle growth in the presence of insulin.**

Figure 7.14. **The effect of AG1478, an EGFR inhibitor, on unstimulated preantral follicle growth in the presence of insulin.**

Figure 7.15. **The effect of EGF and AG1478 on TUNEL labelling.**

Chapter 8

Figure 8.1. **Ovaries on the membrane at days 0, 5 and 8 of culture during Lapatinib Ditosylate dose response experiment.**

Figure 8.2. **Representative sections from ovaries cultured with vehicle control, 1 µM Lapatinib or 10 µM Lapatinib stained with Haematoxylin and Eosin.**

Figure 8.3. **Features of follicle development during in vitro culture of whole d4 ovaries that are either similar to follicle development in vivo or peculiar to in vitro model**

Figure 8.4. **ERBB2 immunolocalised in sections from cultured ovaries.**

Figure 8.5. **The distribution of area of oocyte in different stages of follicle development**

Figure 8.6 **Representative sections from control and both treatment groups immunolabelled for VASA and laminin**

Figure 8.7 **The effect of Lapatinib on in vitro primordial activation**

Figure 8.8 **The effect of EGF on in vitro primordial activation**

List of Tables

Table 2.1. **Sequences and properties of primers for PDGF and EGF family genes**

Table 2.2 **Summary of the various targets and optimal conditions of the antibodies characterised in this project.**

Table 2.3 **Recipe for Resolving and Stacking gels for SDS-PAGE**

Table 3.1. **Summary of PDGF family mRNA expression in the mouse ovary**

Table 6.1. **Protein content for juvenile ovary, preantral follicles, and oviduct as determined by BCA total protein assay.**

Abbreviations

1° = Primary follicle

1°+ = Primary Plus Follicle

2° = Secondary Follicle

2°+ = Secondary Plus Follicle

[^{3}H]-Thymidine = Tritiated thymidine

µl = Microlitre

µm= Micrometre

µM = Micromolar

mL = Millilitre

α-MEM = Minimum essential medium alpha

ADCC = Antibody-dependent Cell-mediated cytotoxicity

AJ = Adherens Junction

Akt = Protein kinase B

AMH = Anti- Müllerian Hormone

ANOVA = Analysis of Variance

AREG = Amphiregulin

AT = Annealing temperature

ATP = Adenosine triphosphate

BCA = Bicinchoninic acid

BMP = Bone Morphogenetic Protein

bFGF = basic Fibroblast growth factor

BTC = Betacellulin

BTG = B-cell translocation gene

BSA = Bovine Serum Albumin

CAM = Cell Adhesion Molecule

CI = Confidence interval

cDNA = complimentary deoxyribonucleic acid

cGMP = cyclic guanosine monophosphate

c-Kit = Mast/stem cell growth factor receptor

cKO = Conditional knock-out

COC = Cumulus-oocyte complex

COOH = Carboxy terminal

CREB = cAMP response element-binding protein

Cyp17α = cytochrome P450 17A1

Cyp19 = Cytochrome P450 aromatase

Cx43 = Connexin 43

DAB = 3,3[1] – Diaminobenzidine tetrahydrochloride

DAPI = 4',6-diamidino-2-phenylindole

DMSO = Dimethyl sulphoxide

DNase = Deoxyribonuclease I

E = Embryonic day

ECD = Extracellular domain

ECM = Extracellular Matrix

EGF = Epidermal Growth Factor

EGFR = Epidermal Growth Factor Receptor

EMT = Epithelial-to-Mesenchymal Transition

EPGN = Epigen

EREG = Epiregulin

ERK1/2 = Extracellular signal related kinase 1/2

FBS = Foetal bovine serum

FDA = Food and Drug Administration

FGF = Fibroblast Growth Factor

Foxl2 = Forkhead box L2

FSH = Follicle Stimulating Hormone

GAB = Grb2 associated binding protein 1

GC = Granulosa Cell

GDF9 = Growth Differentiation Factor 9

H&E = Haematoxylin and Eosin

HB-EGF = Heparin-binding epidermal growth factor

hCG = human chorionic gonadotrophin

HCl = Hydrochloric acid

HER1/2/3/4 = Human Epidermal growth factor receptor 1/2/3/4

HPRT1 = Hypoxanthine phosphoribosyltransferase 1

HRP = Horseradish peroxidase

ISH = In situ hybridisation

ITS = Insulin transferrin sodium selenite

JM = Juxtamembrane

JNK = Jun amino-terminal kinases

KL = Kit ligand

L-15 = Leibovitz L-15 medium

LH = Luteinizing Hormone

MAPK = Mitogen activated protein kinase

MAPKK = Mitogen activated protein kinase kinase

MAPKKK = Mitogen activated protein kinase kinase kinase

mc = Monoclonal

mRNA = Messenger ribonucleic acid

$NaCl_2$ = Sodium Chloride

NaF = Sodium Fluoride

Nec2 = Nectin 2

N-cadherin = Neural cadherin

NH_2 = Amino terminal

NHERF2 = Na+/H+ exchanger regulatory factor 2

NRG = Neuregulin

Oo = Oocyte

OSE = Ovarian Surface epithelium

p = primordial follicle

PBS = Phosphate Buffered Saline

Pc = Polyclonal

PDGF = Platelet-Derived Growth Factor

PI3-k = Phosphophatidylinositol-3 kinase

PMSG = Pregnant Mares Serum Gonadotrophins

POF = Primary Ovarian Failure

PTB = Phosphotyrosine binding

PTEN = Phosphatase and tensin homolog

qPCR = quantitative Polymerase Chain Reaction

RGB = Red Green Blue

RIPA = Radioimmunoprecipitation assay

RNase = Ribonuclease

RTK = Receptor Tyrosine Kinase

RT-PCR = Reverse Transcriptase Polymerase Chain Reaction

SDS = Sodium dodecyl Sulfate

SDS-PAGE = Sodium dodecyl Sulfate polyacrylamide gel electrophoresis

SEM = Standard error of the mean

SH2 = Src Homology domain 2

TBST = Tris-Buffered Saline with Tween® 20

TGFα = Transforming Growth Factor alpha

TGFβ = Transforming Growth Factor beta

TJ = Tight Junction

TM = transmembrane

TUNEL = Terminal deoxynucleotidyl transferase dUTP nick end labeling

UV = Ultraviolet

VE-cadherin = Vascular endothelial cadherin

VEGF = Vascular endothelial growth factor

ZO-1 = Zonula occludens 1

TZP = Transzonal Processes

ZP = Zona Pellucida

Chapter 1: Introduction

1.1 The ovary

The ovary is the female reproductive organ that resides in the pelvic cavity of humans and rodents as pairs, one on either side of the uterus. The function of this reproductive, endocrine organ is the production of (i) fertilizable oocytes (eggs) and (ii) hormones required for reproduction.

The ovary consists of ovarian follicles, the basic functional unit of the ovary, nestled in the stroma and surrounded by the ovarian surface epithelium (OSE). Ovarian follicles are comprised of a centrally located oocyte surrounded by somatic granulosa cells (GCs), which are enveloped by a basal lamina and, by the end of their development within the ovary, further enclosed by a somatic theca cell layer.

Follicle development eventually culminates in the production of a single (monoovulatory e.g. human) or several (polyovulatory e.g. rodents) dominant follicle(s) that rupture to release a fertilizable egg into the oviduct. This event is known as ovulation and leads to the formation of a temporary structure called the corpus luteum from the remnants of the ruptured follicle, which produces progesterone necessary to maintain pregnancy.

Initiation of follicle growth can begin in a subset of primordial follicles as soon as they are formed (during gestation in humans and shortly after birth in mice). Follicles continue to enter the growing pool throughout life, until the pool is depleted, but ovulation is only possible once the hypothalamic-pituitary-gonadal axis has been activated during puberty. Many of the physiological changes that occur during this cyclical depletion of an ovary's follicular complement are common to humans and rodents, however, in humans it is referred to as the menstrual cycle and in rodents the

estrous cycle. The major difference between the two is that the endometrium lining of the uterus that is thickened with blood vessels in preparation for egg implantation is shed in the menstrual cycle and reabsorbed during the estrous cycle.

1.2 Primordial follicle formation

Female mammals are born with their entire follicular reserve and so it is therefore both the size of this primordial pool and the rate of primordial activation that determines the mammalian reproductive lifespan (Picton, 2001). There is a dramatic loss in germ cell number even before primordial follicles develop. Germ cells arrive at the gonadal ridge at embryonic day (E) 10.5 in mice and E 28-36 in humans, differentiate into oogonia then mitotically divide with incomplete cytokinesis, four rounds of division in mice and many more cycles in humans, to form oocyte 'nests'. These oogonia then enter meiosis from embryonic day (E) 13.5 in a rostro-caudal gradient before arresting at diplotene of prophase I in the same rostro-caudal gradient by E16.5 in the fetal mouse ovary. Meiotically arrested oocytes can now be incorporated into primordial follicles following 'nest breakdown', a developmentally regulated program which, among other things, is thought to ensure oocytes have a functioning population of mitochondria (Pepling, 2006). During ' nest breakdown' somatic pre-granulosa cells invade the nests, insinuating themselves between the oocytes. Primordial follicle formation is the process whereby a small meiotically arrested oocyte becomes enveloped by flattened somatic cells and a basement membrane known as the basal lamina. During oocyte nest breakdown the GCs interact with the nests and oocytes that survive (approximately one third) are surrounded by these 'invading' GCs.

GCs do not 'invade' uniformly, however. The nests towards the centre of the ovary are surrounded first. Heterogeneity among the GC population was first

observed in ovaries from rat pups that had been prenatally exposed to [^{3}H]-Thymidine , a proliferation marker that is incorporated into newly synthesised strands of DNA during mitotic division (Hirshfield, 1992). This revealed that GCs that became incorporated into cortical follicles had a different proliferative history to those towards the centre of the ovary; they were mitotically active (cortical) and quiescent (medulla) in the embryonic ovary, respectively. It seemed possible that these two contributions of GCs may be originating from different structures or sources. Postulated origins of GCs included the (i) same somatic population in the bipotential gonad that differentiate into Sertoli cells, the male counterpart of GCs, in XY embryos. (ii) the OSE and (iii) the rete ovarii (Mork et al., 2012).

The rete ovarii consists of a network of cords and tubes lined with cuboidalised epithelia, of which a part inhabits the medulla of the ovary for about a week after birth before it begins to degenerate (Byskov and Lintern-Moore, 1973), but to which no postnatal function has been ascribed (Peter R. Smith, 2009). This is in contrast to its homologue in the male, the rete testis, which has an established role in sperm transport (Free et al., 1980). The degeneration of the rete ovarii once follicle formation had completed and the proximity of the rete ovarii with germ cells lead to the hypothesis that the rete ovarii may be involved in follicle formation. This question has not been one of prominence in the reproductive biology field for some time and much of the pioneering studies were done in the 1970's or earlier. The rete system is made up of the intraovarian rete, which has been described so far in this paragraph, the extraovarian rete, which extends into the periovarian tissue and the connecting rete, which connect these two. One study investigated follicle formation in adult female nude strain mice in which foetal mouse ovary, either intact or with the rete system removed, was implanted. Follicle formation was critically perturbed in the

rete-depleted grafts as compared to the intact ovary grafts (Byskov, 1974). This and other data suggested that the intraovarian rete ovarii was critical to follicle formation and therefore the epithelial cells of the rete ovarii may be the source of GCs.

The origin of GCs was recently elucidated, however, with the use of transgenic mice in which expression of GFP-labelled Forkhead box L2 (Foxl2), a forkhead transcription factor, can be switched on under the control of a tamoxifen-inducible CRE recombinase. Foxl2 is expressed in somatic cells of the XX gonad, pre-GCs of the neonatal ovary, and GCs of the postnatal mouse ovary and this study showed that it is a GC marker. Tamoxifen-induced lineage tracing of Foxl2-expressing cells revealed that the vast majority (if not all) of GCs derive from the ovarian surface, similar to the Sertoli cells, but ingress in two temporally distinct waves. The oocytes situated towards the medulla are furnished in the first wave of GC invasion in the fetal ovary whereas cortical oocytes are surrounded in a second wave of GC ingression that is not completed until after birth in mice (Mork et al., 2012). A number of follicles are selected to grow immediately upon their formation and these are always located towards the medulla of the ovary whereas cortical primordial follicles remain dormant for much longer (Hirshfield, 1991a).

1.3 Follicle development

Once activated, growth-factor mediated signalling within and between follicles and, later on, their hormonal environment guide these small (12-15 μm) follicles through a complex series of changes that culminates in either cell death or ovulation of a mature oocyte (Hirshfield, 1991a). Once follicles begin growing, their development can be split into two phases based on their regulation; gonadotrophin-responsive early follicle development and gonadotrophin-dependent late follicle development which are largely characterized by somatic cell proliferation and

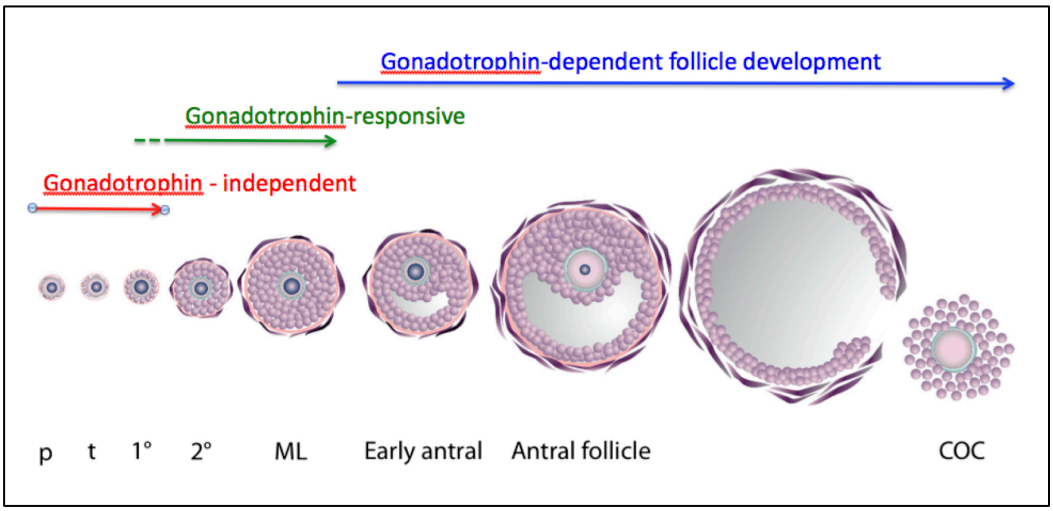


Figure 1.1 *Summary of follicle development. As follicles initiate growth their oocytes increase in size, the granulosa cells change shape, from flattened to cuboidal, and begin to proliferate. As follicles develop GCs continue to proliferate and form multiple layers while a layer of somatic theca cells encloses the follicle. Following this extensive proliferation, a follicular fluid antrum forms between GCs. Development from this point onwards is gonadotrophin-dependent. Upon gonadotrophin stimulation the theca and GCs differentiate and become steroidogenic. This pre-ovulatory follicle may then be selected for ovulation. Key: p; primordial follicle, t; transitional follicle, 1°; primary follicle, 2°; secondary follicle, ML; multilayered follicle, COC; cumulus-oocyte complex.*

differentiation, respectively (Craig et al., 2007). Primordial follicles, on the other hand, are not responsive to gonadotrophins and therefore primordial activation is gonadotrophin-independent. Morphologically, gonadotrophin-dependent follicle development is accompanied by the formation of a follicular fluid-filled antrum between GCs. Hence, the terms preantral and antral follicle development are used (Hirshfield, 1991a). These stages of follicle development are illustrated in Figure 1.1.

Antral follicle development is only possible once the individual has reached puberty as demonstrated by mice in which either the pituitary gland, which produces the gonadotrophins FSH and LH, (Kendall et al., 1991) or FSH receptor (Abel et al., 2000) is disrupted. The ovaries of these mice do not contain antral follicles or corpora lutea. Furthermore, primordial follicles initiate growth during culture of

neonatal mouse ovaries in the absence of gonadotrophins (Eppig and O'Brien, 1996). Up until puberty, the ultimate fate of all growing follicles is atresia (McGee and Hsueh, 2000), which is the co-ordinated apoptosis of the various cell types in the follicle, as orchestrated by hormones (Kaipia and Hsueh, 1997).

Preantral follicle development begins with the transition of a quiescent primordial follicle into a growing primary follicle. During primordial activation the flattened GCs cuboidalise and proliferate while the oocyte grows in size (Lintern-Moore and Moore, 1979) and develops a glycoprotein coat called the zona pellucida, which is important in communication between GCs and oocyte during follicle development (Calongos et al., 2009) and sperm-egg interaction during fertilization (Dean, 1991). There is an intermediate follicle stage between quiescent primordial and growing primary follicles called the transitional follicle in which some but not all of the GCs have cuboidalised (Da Silva-Buttkus et al., 2008; Da Silva-Buttkus et al., 2009). Following the primordial-to-primary transition the cuboidal cells of a primary follicle proliferate extensively until maximal packing density is achieved and these cells become columnar and polarized. The columnar shape of the GCs is a consequence of their close packing, and has the effect of rotating the mitotic axis from parallel to the oocyte surface to perpendicular, resulting in the formation of a second inner layer of GCs (Da Silva-Buttkus et al., 2008). By, or around this point, an additional compartment of somatic cells; the theca layer, is recruited around the follicle outside the basal lamina (Young and McNeilly, 2010). This theca layer is not readily identifiable until it becomes steroidogenic in antral follicles but theca recruitment has been proposed to occur as early as the primordial-to-primary transition (Hirshfield, 1991b). These four follicular stages; primordial (flattened GCs), transitional (some flattened and some cuboidal GCs), primary (one complete

layer of cuboidal GCs) and secondary stage (multiple layers of GCs) follicles, make up the preantral phase of follicle development.

Gonadotrophin-dependent antrum formation separates the GCs into two functionally distinct populations: the mural GCs towards the basal lamina and the cumulus GCs surrounding the oocyte. Alongside this the theca layer also differentiates into an outer collagen- and smooth muscle cell- rich theca externa and a vascularised theca interna that brings circulating gonadotrophins to follicles. Given the relative proximities of the GCs either side of the antrum to the oocyte and vascularised theca, it is not surprising that the cumulus cells function primarily to support oocyte maturation while the mural GCs are more steroidogenic and the first to receive systemic ovulation signals. Having reached full size by the time of antrum formation the oocyte appears morphologically idle in comparison to these dynamic somatic cell layers. However, it is now clear that the oocyte regulates and directs development of the somatic cell layers that serve it (Kidder and Vanderhyden, 2010; Vanderhyden et al., 1990; Vanderhyden et al., 1993; Vanderhyden et al., 1992). The oocyte secretes factors that can act in a paracrine, far reaching manner although obviously whereas the cumulus cells are bathed in these factors, they become much more dilute as they approach the basal lamina. Growth differentiation factor 9 (Gdf9) and Bone morphogenetic protein 15 (BMP15), of the Transforming growth factor beta (TGFβ) superfamily, are two important factors secreted by the oocyte to regulate antral GC development (Dragovic et al., 2005; Otsuka et al., 2000; Su et al., 2008). Furthermore, small metabolites, ions and amino acids can be directly transported between the oocyte and cumulus GCs via gap junctions. There are gap junctions between GCs and also on the end of cellular projections emitting from GCs, across the zona pellucida and touching the oocyte membrane (Kidder and Mhawi, 2002).

Oocyte-derived factors are not solely responsible for their microenvironment however, as the two somatic cell layers now become steroidogenic under the control of gonadotrophins (Hillier, 1994; Hillier, 2001; Hillier et al., 1994). Luteinizing Hormone (LH) stimulates theca production of androgen while Follicle Stimulating Hormone (FSH) stimulates aromatization of androgens in GCs to produce estradiol. Estradiol production causes a mid-cycle LH surge and, in the primate ovulation cycle, a concomitant fall in mid-follicular phase FSH levels causes all but a 'dominant' follicle that has produced and secreted estradiol most efficiently under the control of FSH, to die. This dominant follicle grows further despite the negative feedback loop between estradiol and FSH as (i) it has an adequate amount of FSH in it's follicular fluid and FSH receptors in it's GCs, being the dominant follicle, (ii) the follicle becomes more dependent on LH. The mid-cycle LH surge causes meiosis to resume in these oocytes before expulsion from the dominant follicle into the Fallopian tube. The remaining granulosa and theca cells of the follicle differentiate and become vascularized, with breakdown of the basal lamina, to form a corpus luteum. Only a tiny fraction of oocytes will ever ovulate; the vast majority are destined to die by atresia (Hirshfield, 1991a).

The rate at which follicles initiate growth is critical to determining reproductive lifespan and fertility; too few follicles initiating growth could lead to anovulatory cycles whereas too many may lead to premature exhaustion of the primordial pool, clinically termed primary ovarian failure (POF) (Gosden and Faddy, 1998). Premature, in humans, is defined as before 40. There are several causes of POF but often the cause is unknown (Nippita and Baber, 2007). Elucidation of the mechanisms involved in primordial activation is therefore of great importance as it may shed light on the mechanisms perturbed in some cases of POF and point to

possible targets for treatment. Additionally, it may be possible to identify a 'switch' to activate growth of primordial follicles outside of the mammalian ovary and allow in vitro maturation (IVM) from (usually) the most abundant follicle stage represented in the ovary. This will provide further fertility treatment options for those struggling to conceive, such as some sufferers of polycystic ovarian syndrome (PCOS), or those who may have their fertility affected by chemo or radiotherapy, or even endangered animals and livestock. PCOS is the most common cause of anovulatory infertility in women and again the cause is unknown. Additionally, the precise symptoms and features of PCOS can vary from individual to individual. Excess androgen production is a major feature however, along with the cystic phenotype. Furthermore, it appears that the earlies stages of follicle development, including primordial activation, may be impaired in PCOS (Webber et al., 2003). Therefore, elucidation of this process could point to possible targets to develop therapy for PCOS patients.

In summary, the primordial pool, established at or around the time of birth, constitutes the entire reserve of oocytes that can either remain quiescent, or be selected to grow and ultimately die or ovulate. Of these stages, the initial signal as to whether to grow or not is the least understood.

1.4 Initiation of follicle growth

In a primordial follicle, an oocyte of approximately 12-15 μm in mice is surrounded by a single layer of 2-4 squamous GCs and further by a basal lamina and these are first seen in mice 2-4 days after birth (McLaughlin and McIver, 2009). Follicles in the cortico-medullary border initiate growth immediately after they are formed in one large wave (McGee and Hsueh, 2000; Peters, 1969). Recruitment of cortical follicles into the growing pool is a more measured process up until approximately a decade before menopause in humans when the process is accelerated

(Faddy, 2000; McGee and Hsueh, 2000). Several theories have been developed to explain the central location of the growing pool that expands towards the periphery throughout the reproductive lifespan of mammalian ovaries (Byskov et al., 1997; Da Silva-Buttkus et al., 2009). Henderson and Edwards (Henderson and Edwards, 1968) proposed the 'production line hypothesis' in which the patterns of meiosis entry, arrest and resumption are believed to be the same i.e. surviving rostral oocytes that enter meosis first become central follicles that initiate growth and perhaps ovulate earlier. Jean-Claude Mariana proposed that there were two different origins of GCs in the ovary, each with a different propensity to begin dividing, and the relative contribution from each body in a follicle determined when a follicle initiated growth (Hirshfield, 1992). However, elucidation of GC origin has refuted these hypotheses.

A study from Blanche Capel's group revealed that most (if not all) GCs ingress from the ovarian surface in the mouse but in two temporally distinct waves; one during foetal development that envelopes central oocytes and a second, postnatal wave dedicated to cortical oocytes (Mork et al., 2012) as illustrated in Figure 1.2, and that these two waves of GCs have differential protein expression that can be used to chronologically track these cells. Generation of a tamoxifen-inducible knock-in mouse model in which Foxl2-expressing pre-GCs of the embryonic gonad and GCs of the postnatal ovary can be lineage traced revealed that it is actually the inheritance of either this first or second wave of GC ingression that is associated with either the initial synchronous burst of activation in the centre of the ovary or the lifelong, steady recruitment of cortical oocytes, respectively (Mork et al., 2012). Therefore, the mechanisms governing follicle activation are unlikely to be identical for every growing follicle. Indeed, these two populations of follicles certainly do not behave the same, even once they recruited to the growing pool; the central pool initiate

growth immediately upon their formation, develop quickly with the first antral follicles observed at d23 in mice, and are exhausted by 3 months, whereas cortical primordial follicles have a more measured lifespan (at least 47 days until antral follicles develop) and are still available for recruitment until at least 14 months (Zheng et al., 2014b). It is important to note that it is unlikely that GCs derive from the mature OSE as initially suggested by Mork et al (2011), as this would require basal lamina breakdown during an epithelial-to-mesenchymal (EMT) and subsequent mesenchymal-to-epithelial transition (MET) event once these cells are incorporated into follicles, which is not observed. A study characterising and tracing the various cell types of a developing bovine ovary revealed that the mature OSE and GCs both originate from the same precursor cells, termed gonadal ridge epithelial-like (GREL) cells which proliferate at the gonadal ridge and then either ingress and differentiate into GCs or remain at the surface and differentiate into the OSE (Hummitzsch et al., 2013). To summarise, GCs have a similar lineage to the OSE and there is heterogeneity among the GC population with regards to intiation of follicle growth.

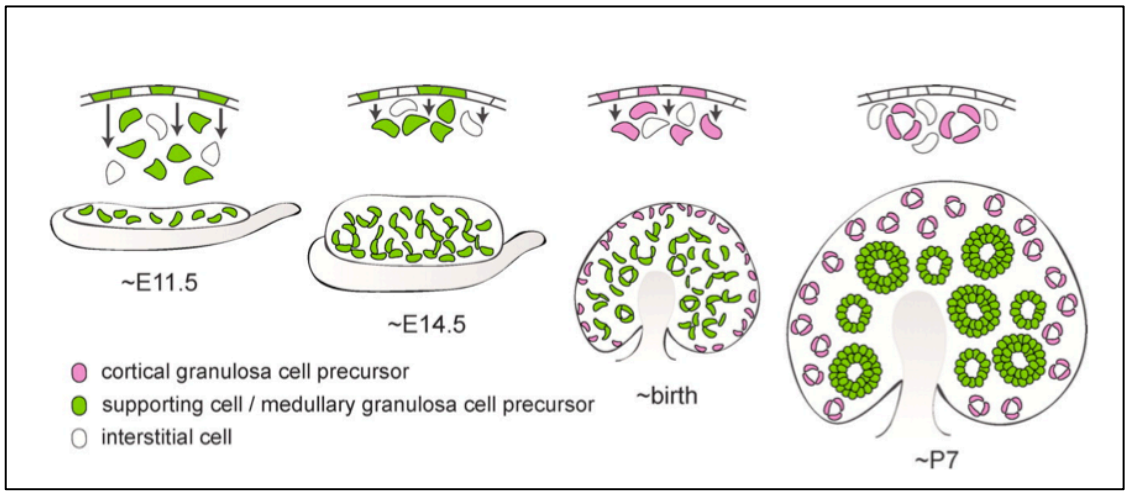


Figure 1.2. *The origin of GCs. The majority (if not all) GCs derive from the ovarian surface but in two temporally distinct waves; a first during foetal mouse development that envelopes central oocytes and a second, postnatal wave that surrounds cortical oocytes. The central oocytes enveloped in the first wave initiate growth in one synchronous burst at birth whereas those oocytes furnished later can remain dormant for much longer. Image obtained from Mork et al (2011).*

Clearly there is a relationship between GC 'origin' and follicle initiation, however, the spontaneous initiation of primordial follicles in cortical strips of primate and baboon ovary in vitro suggested that growth initiation is not (at least wholly) intrinsic to the cortical follicle but rather subject to factors in their environment (Fortune et al., 1998). The simultaneous activation of the majority of follicles in cortical pieces of primate and bovine ovary in vitro also suggests that an inhibitory factor acts in vivo to hold primordial follicles in a quiescent state rather than a diffusion gradient of a stimulatory factor activating growth initiation in nearby follicles (Wandji et al., 1996). This is also in accordance with the observation that primordial follicles are seen in clusters at the periphery of the ovary near the OSE. Recent spatial analysis of juvenile ovaries in our lab identified primordial follicles as the likely source of an inhibitor. This study demonstrated that if a follicle had one or more primordial follicles within 10μm of it, it was likely to be a non-growing

primordial follicle itself (Da Silva-Buttkus et al., 2009). The identity of this inhibitor remains elusive.

While global patterns of follicle activation in mammalian ovaries have been widely studied and manipulated we have still not fully elucidated the actual cellular events that occur during primordial activation, especially in rodents, despite their popularity as a model organism. Primordial activation is characterized by (i) oocyte growth (ii) granulosa cell cuboidalisation and (iii) granulosa cell proliferation but it is not yet clear in what order these events happen and how they relate to, and interact with, one another (Adhikari and Liu, 2009; Lintern-Moore and Moore, 1979). The oocyte grows considerably in size (300 fold by volume in mice) and, while oocytes never reach this size without GC cuboidalisation in vivo, both oocytes which have and have not initiated growth can have at least one cuboidal GC (Da Silva-Buttkus et al., 2008; Lintern-Moore and Moore, 1979). It is therefore unclear whether an oocyte-derived signal causes GCs to cuboidalise or a GC-derived signal causes the oocyte to grow or whether these happen concurrently. The relationship between GC cuboidalisation and proliferation is slightly more coherent as several studies have shown that flattened GCs rarely divide whereas cuboidalised GCs divide at a much higher rate (Da Silva-Buttkus et al., 2008; Hirshfield, 1989). While a model of GC cuboidalisation as a prerequisite of GC proliferation is too simple a model, especially for mouse follicle development, these results do suggest that GC cuboidalisation is a key event during primordial activation. This is greatly supported by the observation that in other mono-ovular mammals, such as humans, oocyte growth occurs only after GC cuboidalisation and proliferation have begun (Figure 1.3) (Gougeon and Chainy, 1987). Molecular markers could help disentangle these events from one another. These would be particularly useful in classifying initiation of changes to the GCs

because simply measuring their diameter or height is inadequate. Regardless of where the initial signal for primordial activation is coming from, GC cuboidalisation is a key event during primordial activation, one that has been overlooked in the literature.

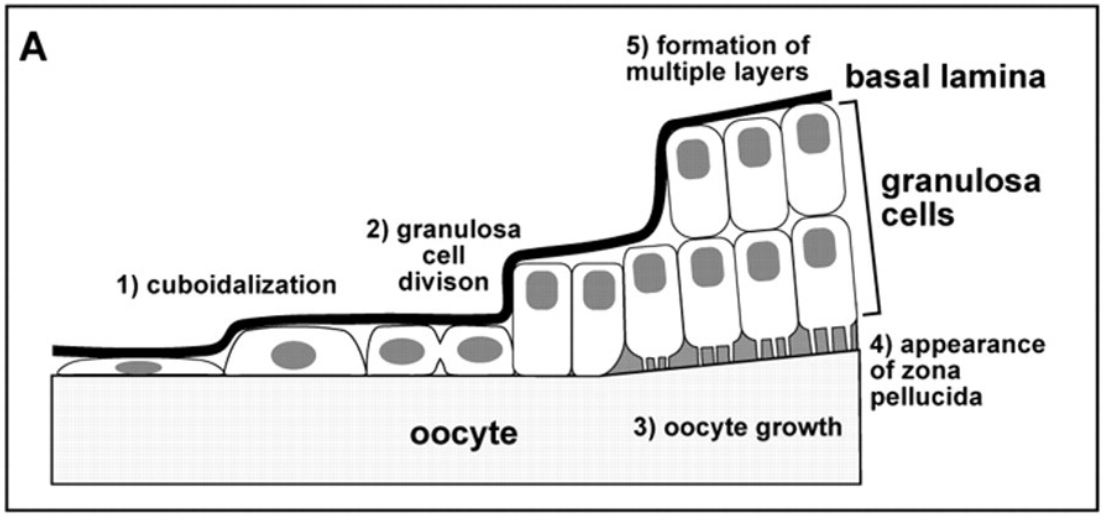


Figure 1.3. *Diagram showing the multiple stages of primordial activation in mono-ovular mammals. Oocyte growth does not occur until GC cuboidalisation and proliferation has begun in these species. It is not yet clear whether follicle development in the mouse occurs exactly in this manner. Diagram obtained from Kate Hardy (Da Silva-Buttkus et al., 2008).*

1.5 Granulosa cell adhesion

Initiation of follicle growth is characterized by a dramatic change in GC cell shape from flattened to cuboidal. Cell shape change is governed by the cytoskeleton and cell adhesion molecules (CAMs) that are organized into junctions at sites of cell-cell and cell-matrix contact. Recent work in our lab (Mora et al., 2012) has demonstrated that the only class of junction present in GCs, other than gap junctions, is adherens junctions (Figure 1.4). This is surprising as GCs have previously been considered epithelial but this recent study has shown GCs do not have juctional complexes typical of true epithelia. GCs are derived from the same cells as the epithelial OSE but ultrastructural studies demonstrate that the inner layers of GCs do

not display apico-basolateral polarity and are instead loosely associated with each other, similar to mesenchymal cells (Mora et al., 2012). Furthermore, GCs do not express tight junctions or desmosomes that are characteristic of epithelia. Therefore, Mora et al. (2012) hypothesize that GCs undergo a partial Epithelial to Mesenchymal transition (EMT) event during preantral follicle development that is completed upon ovulation.

Adherens junctions (AJs) have two, almost conflicting mechanical roles at the cell surface, as they function to both maintain existing tissue architecture and direct assembly and remodelling of new cell-cell contacts. This is achieved by interaction of either the cadherin-catenin or nectin-afadin complexes, or both, with the actin cytoskeleton. The catenin (α- and β-catenin) and afadin proteins are linkers between the actin cytoskeleton and the membrane bound cadherin and nectin proteins (Harris and Tepass, 2010; Takai and Nakanishi, 2003). AJ assembly begins with the actin cytoskeleton arranging into lamellipodial protrusions so that cadherin and nectin molecules on membranes of neighbouring cells can homotypically interact at sites of cell-cell contact. The actin lameillipodial protrusions expand so that the cells become 'zipped up' with clusters of cadherin/catenin or nectin/afadin or both. The actin cytoskeleton rearranges to strengthen contact and form a mature AJ (Harris and Tepass, 2010). Nectin-afadin based AJs are functionally different from cadherin-catenin based AJs as they are weaker and Ca^{2+}-independent (Takai et al., 2008).

These adhesive 'plaques' also have a signalling function. This is mediated by two types of proteins: (i) 'dual function' proteins such as β-catenin which is integral to both AJ assembly at the membrane and Wnt signalling in the nucleus (Willert and Nusse, 1998) and (ii) signalling proteins, such as growth factor receptors, which are enriched at cell junctions and collaborate with cadherins to produce an intracellular signal (Comoglio et al., 2003). This suggests that the increased GC proliferation

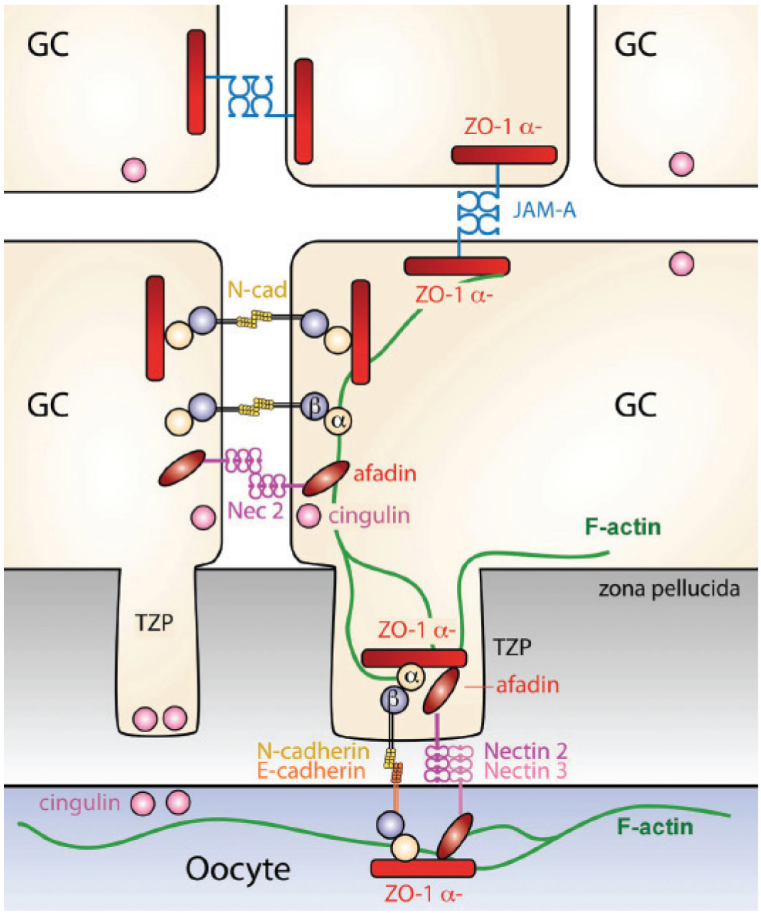


***Figure 1.4**. Diagram showing the junctional molecules that have been localised to follicles in the mouse ovary. The majority of these are Adherens Junctions (AJ) proteins, but tight junctional (TJ) proteins, such as cingulin, JAM-A and ZO-1 are also present. Crucially, this image shows that N-cadherin and Nectin-2 based AJs form between cuboidalised GCs. AJs also appear to tether the GCs to the oocyte via heterophilic cadherin interactions. The TJ proteins ZO-1, JAM-A and cingulin also localise to GCs but recent studies in our lab using biotin tracer assays show they do not form a functional tight junction. Key: GC; granulosa cell, TZP: transzonal processes, ZO-1α; zonula occludens-1 alpha, Nec 2; Nectin 2, Nec 3; Nectin 3, N-cad; N-cadherin, α; alpha-catenin, β; beta-catenin. Diagram obtained from Mora et al, 2012.*

following cuboidalisation may be due to reciprocal regulation between these proteins as AJs form. Therefore, the characterization of these AJ components and signalling molecules present in early follicle stages is critical to understanding primordial activation. There are many cadherin molecules and 3 nectin molecules. Surprisingly, mouse GCs do not express epithelial (E-) cadherin, as oocytes do, but in fact they express neural (N-) cadherin (Mora et al., 2012). This is surprising both because it lends credence to the idea that GCs are not truly epithelial but also suggests the existence of heterophilic interactions between GC specific N-cadherin and oocyte-expressed E-cadherin. GCs also express Nectin-2 and afadin. Crucially, immunolocalisation of these proteins suggests they are key to GC cuboidalisation (Mora et al., 2012).

Electron Microscope (EM) imaging shows that GC cuboidalisation begins with the adjacent membranes of two neighbouring flattened GCs 'zipping up' to form

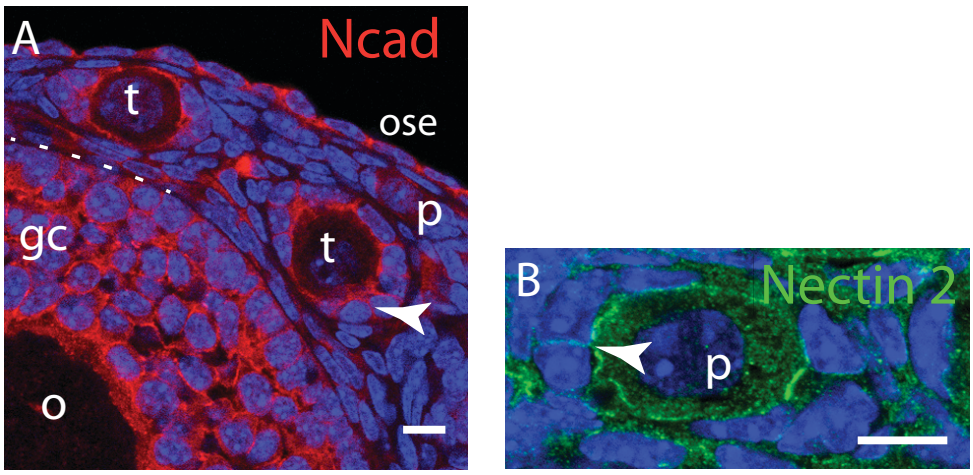


Figure 1.5. *N-cadherin (A) and Nectin-2 (B) immunolocalisation in the mouse ovary. Crucially, distinct N-cadherin and Nectin-2 first appear between cuboidalising GCs of a transitional follicle. Therefore, it is likely that AJs assemble between GCs during initiation of follicle growth. This study will expand on this data by assessing candidate growth factors that are likely regulating these cell adhesion molecules during initiation of follicle growth. Key: ose; ovarian surface epithelium, p; primordial follicle, t; transitional follicle, gc; granulosa cell, o; oocyte, Ncad; N-cadherin. Scale bars represent 10μm. Images courtesy of Jocelyn M. Mora.*

wedge-shaped cells and AJ proteins have been localised to these elongating membranes. Importantly, high intensity N-CADHERIN and NECTIN-2 immunoreactivity first appears between cuboidalising GCs (Figure 1.5). N-cadherin and Nectin-2 are GC-specific CAMs seen faintly between flattened GCs and the oocyte of primordial follicles with much more distinct expression between cuboidalised GCs. Therefore, it has been suggested that the assembly of N-cadherin and Nectin-2 based AJs is involved in GC cuboidalisation (Mora et al., 2012). As both these proteins appear to be upregulated upon initiation of GC cuboidalisation, these could be used to elucidate the order and relationship of events during primordial activation. N-cadherin (Wang and Roy, 2010) and Nectin-2 (Kawagishi et al., 2005) expression has been described in GCs of rodent ovaries previously and the adhesive function of N-cadherin has been shown to prevent apoptosis in GCs in the same pathway as basic Fibroblast Growth Factor (bFGF) (Peluso et al., 1996; Trolice et al., 1997). However, the role of these CAMs has not been investigated in the context of GC shape change. GC shape change has mainly been investigated in the context of later stage follicle characteristics such as steroidogenesis and gonadotrophic regulation (Carnegie et al., 1988; Kreeger et al., 2003; Lawrence et al., 1979). In fact, the only factor I'm aware of to be implicated in GC cuboidalisation is the forkhead transcription factor, Foxl2 (Schmidt et al., 2004). In summary, recent work in our lab has identified two CAMs that are likely to be involved in GC cuboidalisation as they appear to be upregulated at this point. This allows us to search for factors that are likely to be responsible for, or associated with, this upregulation.

1.6 Growth factor regulation of primordial activation

Despite little being known about these early stages, we know that initiation of growth (and therefore GC cuboidalisation) is governed by intraovarian factors as

gonadotrophins are not essential until after antrum formation in vivo and in vitro (McGee and Hsueh, 2000; Wu and Matzuk, 2002). A combination of conditional knockout (cKO) models and culture studies have shown various growth factors to be necessary and sufficient to support early preantral growth (Pangas, 2007). The majority of these belong to the TGFβ superfamily. For example, knocking out oocyte-specific Gdf9 in mice blocks GC proliferation so follicles do not progress past the primary unilamina (one-layered) stage (Dong et al., 1996). In addition, primordial activation is inhibited in ovaries treated with Anti-Müllerian hormone (AMH) (Durlinger et al., 2002) and accelerated in mice lacking AMH (Durlinger et al., 1999), another member of the TGFβ superfamily, which is expressed in columnar GCs (Weenen et al., 2004). These are both expressed once primordial activation has completed. Although there has not been a ligand or receptor belonging to the TGFβ family directly implicated in orchestrating the processes associated with primordial activation, it is likely that there is one as Smad2/3, intracellular signalling molecules downstream of TGFβ family activation, is highly expressed in primordial and recently activated follicles but becomes downregulated as follicles grow further. Interestingly, there was a significant increase in the frequency of nuclear Smad2/3 observed in primordial and newly-activate follicles than follicles of a further stage of development. Furthermore, double immunolabelling with antibodies to Ki67 and Smad 2/3 revealed that Ki67 was predominantly only expressed in nuclei that lacked Smad2/3 labelling (Kate Hardy and Mark Fenwick, unpublished observations). Smad 2/3 is translocated to the nucleus upon phosphorylation by an activated TGFβ family receptor (Moustakas and Heldin, 2009) and this data suggest that Smad 2/3 export into the cytoplasm is required before GCs can proliferate i.e. this suggest that a member of the TGFβ superfamily is preventing the onset of GC division during

primordial activation. Investigations into the regulation and dynamics of this superfamily may identify the putative inhibitor maintaining a dormant pool of primordial follicles.

Primordial activation is not exclusively regulated by the TGFβ superfamily, however. The single most important signalling pathway involved in primordial activation identified to date is the phosphatidylinositol 3-kinase (PI3-K) pathway. Generation of an oocyte-specific knockout of phosphatase and tensin homolog (PTEN)was critical in demonstrating this. PI3-kinases are lipid kinases that phosphorylate the 3'-OH group of the inositol ring of inositol phospholipids in order to regulate cell proliferation, survival, migration and metabolism. PTEN is a phosphatase that removes these phosphate groups and therefore inhibits PI3-K signalling. Oocyte-specific deletion of PTEN driven by the Gdf9 (Reddy et al., 2008) or Vasa (John et al., 2008) promoter caused global activation of the primordial pool and therefore premature depletion of the ovary, which is clinically known as Primary Ovarian Failure (POF) by 16 weeks in mice. This was due to release of PI3-K inhibition, which led to hyperphosphorylation of downstream kinase Akt and the forkhead transcription factor Foxo3a causing Foxo3a nuclear export and initiation of follicle growth. The pathways upstream have not been entirely elucidated but the evidence so far suggests that Kit ligand (KL) is one of the major activators of PI3-K in oocytes. GC-specific KL binds to its receptor, c-kit, on the oocyte surface and can activate PI3-K in oocytes in vitro. Furthermore, KL can stimulate the primordial to primary transition in whole d4 rat ovaries in vitro whereas a c-Kit neutralizing antibody, ACK2 completely blocks the spontaneous initiation of follicle growth in d4 rat ovaries cultured for 8 days (Parrott and Skinner, 1999). In addition, mutations in the genes encoding KL and c-Kit are associated with sterility due to abnormal oocyte and

follicle development (Kuroda et al., 1988). However, KL activation of c-Kit is not the only upstream activator of PI3-K (as demonstrated by normal PI3-K stimulated oocyte growth in mice harbouring a point mutation in the c-kit receptor) or indeed the only receptor tyrosine kinase (RTK) involved in regulating the primordial to primary transition (Adhikari and Liu, 2009).

Several RTK proteins have also been implicated in primordial activation by culturing whole ovaries in either their ligand or inhibitor such as KL (Nilsson and Skinner, 2004), basic Fibroblast Growth Factor (bFGF) (Nilsson et al., 2001) and Platelet-Derived Growth Factor (PDGF) (Nilsson et al., 2001). RTKs are particularly interesting with respect to cell shape change as it is well established that RTKs and CAMs interact. AJs are richly populated with RTKs and the inter-digitation of these molecules generates a signalling centre.

1.7 Growth factor signalling from junctional complexes

Junctional complexes at sites of cell-cell contact do not function solely to regulate cell adhesion, but rather they also function as signalling centres. Importantly, cadherins and RTKs are established to interact and mutually regulate one another. AJs are richly populated with RTKs and the inter-digitation of these molecules can form a local signalling centre and collaborate to induce a cellular response (Comoglio et al., 2003). For example, Vascular endothelial cadherin (VE-cadherin), when in proximity to Vascular endothelial growth factor (VEGF) receptor, can form a complex that promotes downstream activation of Akt (Carmeliet et al., 1999). Cadherins can also induce ligand-independent activation or trafficking of RTKs. For example, AJ assembly is known to lead to Epidermal Growth Factor receptor (EGFR) activation (Pece and Gutkind, 2000). Conversely, EGFR can also phosphorylate β-catenin and therefore hinder its binding to cadherin and assembly into AJs (Hoschuetzky et al.,

1994). It is possible, therefore, that signals stimulating the GCs to proliferate and oocyte to grow may be produced at points of RTK/cadherin co-localisation during GC cuboidalisation. N-cadherin is the major CAM expressed during primordial activation. Therefore, a literature search was performed at the beginning of this project to identify candidate RTKs that were likely to regulate N-cadherin during the GC shape change associated with primordial activation.

1.8 Signalling by RTKs

RTKs all adhere to a general model of signal transduction. A ligand binds an RTK, induces dimerisation and activates its intracellular tyrosine kinase domain. Following kinase domain activation, the cytoplasmic tails of the RTKs become autophosphorylated thus providing high affinity docking sites for intracellular signalling proteins with phosphotyrosine binding domains. A cascade of signalling molecules are activated which ultimately causes changes to gene transcription in the nucleus (Anklesaria et al., 1990; Lemmon and Schlessinger, 2010)

Unsurprisingly, different growth factor families do not share an identical mode of ligand binding, dimerisation or kinase activation. Ligands are usually secreted but there are examples of juxtacrine signalling, in which a membranous ligand binds it's membrane-bound receptor on an adjacent cell (Anklesaria et al., 1990). There are examples of certain growth factors binding as monomers, for example Epidermal growth factor (EGF) (Ogiso et al., 2002), and other growth factors binding as dimers (Fretto et al., 1993). Similarly, the mechanism by which these ligands induce dimerisation can be vastly different between growth factor families. Dimerisation can be mediated either entirely by ligand contacts ((e.g. nerve growth factor receptor dimerisation); (Wehrman et al., 2007)) or entirely by receptor contacts ((e.g. epidermal growth factor receptor dimerisation); (Ogiso et al., 2002;

Schlessinger, 2002)) or a combination of both ((e.g. c-kit dimerisation); (Yuzawa et al., 2007)). In terms of kinase activation, all kinase domains are composed of an N- and a C- lobe and the activated configuration of these is very similar among different RTK families. However, the set of intramolecular interactions that autoinhibit the kinase domain is specific to each RTK. The mechanism of release of autoinhibition is also different between different RTKs. For example, the activation of the majority of kinase domains involves phosphorylation of the 'activation loop'. In contrast, EGFR activation does not involve phosphorylation at all. But rather, dimerisation allows the C-lobe of one monomer to bind the N-lobe of its partner and these interactions disrupt the autoinhibiting interactions therefore causing allosteric activation (Lemmon and Schlessinger, 2010; Lemmon et al., 2014).

The next section will examine RTK families (PDGF and EGF) that the literature identified as likely candidates for having a role in regulating N-cadherin during the GC shape change associated with primordial activation

1.9 PDGF family

Primordial activation has been shown to be subject to regulation by these RTKs, one example of which is the PDGF family (Nilsson et al., 2006). The PDGF family is a comparatively small but widely studied RTK family (Fredriksson et al., 2004). There are two PDGF receptor monomers, PDGFRα and PDGFRβ, which can homo- or heterodimerise and four PDGF ligand subunits (PDGF-A, PDGF-B, PDGF-C, and PDGF-D) which can all homodimerize but only PDGF-A and PDGF-B are known to form a functional heterodimer (Yang et al., 2008). Only specific PDGF ligand isoforms can bind PDGFRβ homodimers and receptor heterodimers whereas all isoforms can bind PDGFRα homodimers (Figure 1.6). The vast repertoire of intracellular signalling messengers are shown in figure 1.6. Whilst PDGF earned its

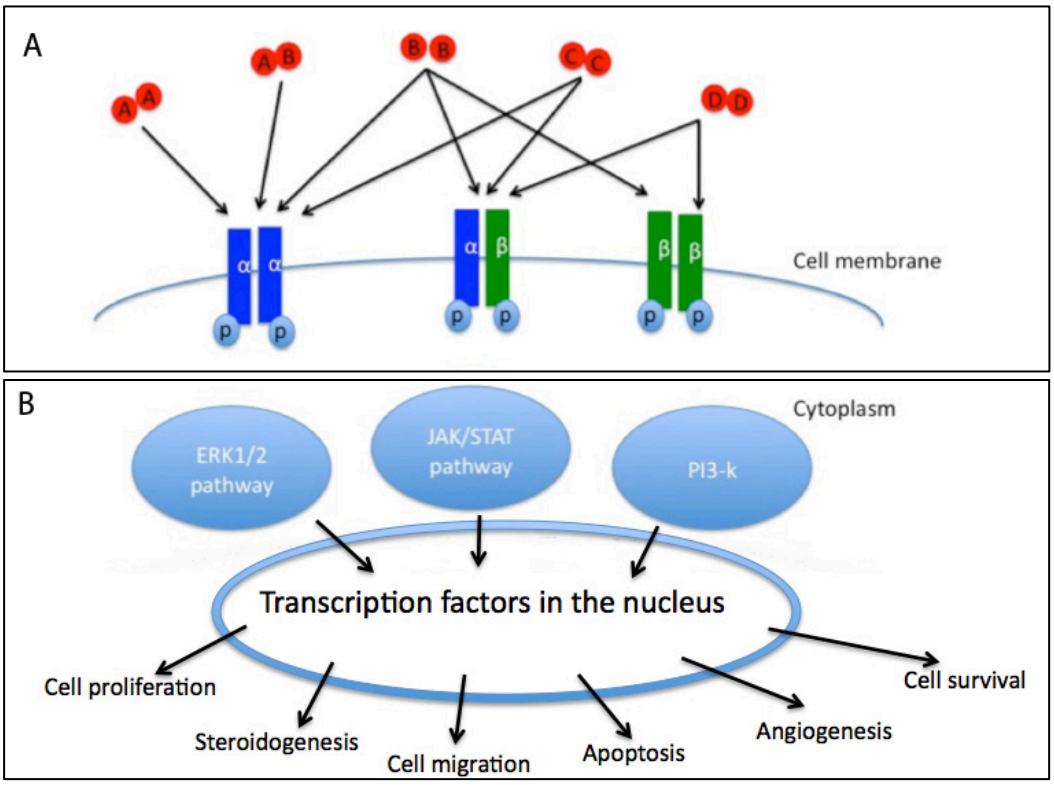


Figure 1.6 *(A) Diagram showing all possible dimeric combinations of PDGF ligand and receptors and their specificity for one another. (B) Diagram showing the major intracellular cascades and biological responses which can be stimulated following PDGF receptor kinase activation. Key: A; PDGF-A, B; PDGF-B, C; PDGF-C, D; PDGF-D, α; PDGF receptor alpha, β; PDGF receptor beta, p: phosphorylation.*

name from its discovery in platelets (Balk, 1971; Ross et al., 1974) and early work focused on its mitogenic activity during wound healing, it is now known to have roles in proliferation, cell migration, angiogenesis, cell survival and steroidogenesis in many different cell types (Betsholtz, 2003).

The role of this growth factor family in the ovary is not fully understood but culture studies have indicated a role for PDGF in promoting the primordial to primary transition in cultured d4 rat ovaries (Nilsson et al., 2006) and Sleer and Taylor (Sleer and Taylor, 2007) found PDGF family expression in rat GCs and primordial follicles. The role of the PDGF family has not been examined in GCs, whereas PDGF was found to stimulate proliferation of rat thecal cells in vitro (Duleba et al., 1999) and also inhibit LH-induced steroid secretion in rat thecal cells (Taylor, 2000). In terms of

a possible link with intercellular adhesion, PDGFRα has been demonstrated to regulate N-cadherin expression during chick gastrulation (Yang et al., 2008) and has also been found to colocalise with N-cadherin via NHERF2 in a fibrosarcoma cell line (Theisen et al., 2007) in both cases causing a functional change in cell adhesion. Therefore literature identified PDGF as candidate for role in GC shape change during primordial activation.

1.10 EGF family

The EGF family is another family of RTK whose receptors are collectively known as the ErbBs. The ErbB family of RTKs are a much more complex network owing to the vastly different properties of each ErbB receptor which can be employed in multiple combinations at the cell membrane (Figure 1.10). The single invertebrate ErbB receptor has evolved to four mammalian RTK members (ErbB1-4), all of which can heterodimerise. However, only EGFR (ErbB1) and ErbB4 can homodimerise as ErbB2 has no known soluble ligand and ErbB3 has a defective kinase domain. Despite being 'defective' in their extracellular and kinase domains, respectively, ErbB2 and ErbB3 combine to form the most potent ErbB dimer and ErbB2 is, in fact, the preferred heterodimerisation partner of all ErbB receptors (Graus-Porta et al., 1997). Although the autonomous receptors evidently differ from the non-autonomous members of this family in aspects of their domain structure and function, they all share a common domain composition. This composition consists of an extracellular domain that binds ligand (except in the case of ErbB2), a transmembrane domain, a juxtamembrane cytoplasmic domain and a kinase domain that becomes active upon ligand-induced receptor dimerization (except in the case of ErbB3) causing phosphorylation of tyrosine residues on the cytoplasmic tail. The domain structure of EGFR is summarised in Figure 1.7. Phosphotyrosines provide docking sites for

signalling molecules with Src Homology 2 (SH2) domains and Phosphotyrosine-binding (PTB) domains. A cascade of signaling molecules are activated which ultimately causes changes to gene transcription in the nucleus leading to important cellular decisions regarding proliferation, differentiation, migration and cell death. Clearly, inappropriate activation or expression of any of these components, which often occurs in cancer, can have profound effects at the cellular, tissue and organ levels (Yarden and Sliwkowski, 2001).

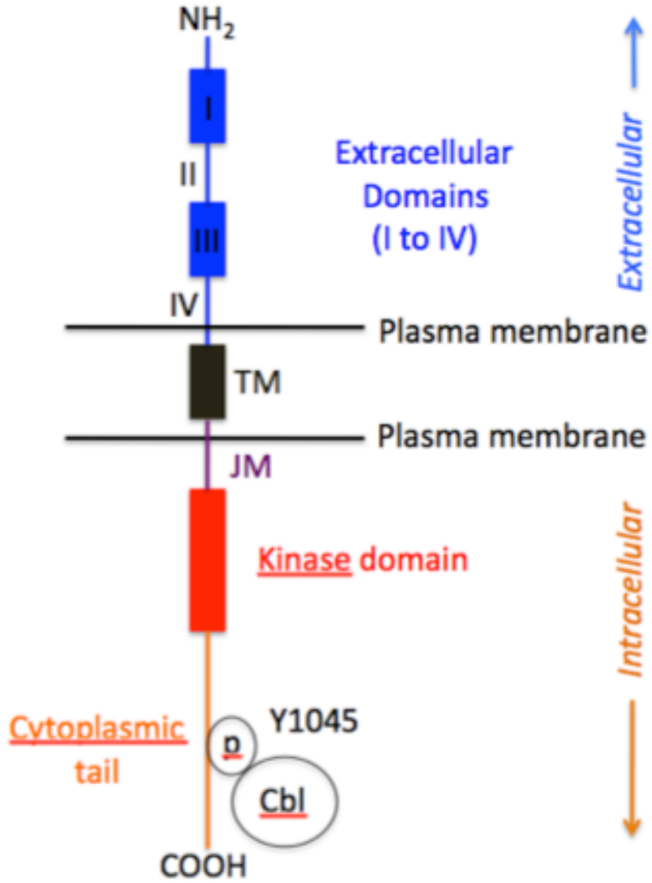


Figure 1.7. *Simplified diagram of the domain structure of the EGFR. There are four extracellular domains at the amino terminus that are involved in ligand binding and heterodimerisation. There is an intracellular kinase domain that, although not depicted here, is composed of N- and C-terminal lobes. The kinase domain is responsible for phosphorylation of tyrosine residues on the cytoplasmic tail which provides sites for proteins that contain SH2 or PTB domains, such as c-Cbl. c-Cbl is an E3 ubiquitin ligase that is involved in targeting EGFR for endocytosis and degradation. It can bind directly to EGFR via phosphorylated tyrosine residue 1045 (Y1045).*

1.10.1 ErbB2 is constitutively poised to dimerise

The EGF family of ligands are similarly complex. Simple details, such as how many ligands there are, have been the subject of considerable research. One major barrier is the difficulty in proving that a soluble ligand does not bind to and activate ErbB2. However, the evidence accumulated so far is convincing. Firstly, extensive activity-based assays that purify mitogenic factors from conditioned medium of specific cell types, and bioinformatic searches for sequence homology, have only identified ligands for EGFR, ErbB3 and ErbB4 (Kochupurakkal et al., 2005). Secondly, the most compelling evidence arises from comparison of the 3D structures of the extracellular domains (ECD's) of both unstimulated and ligand-bound EGFR with that of ErbB2. The ECD of EGFR has four domains, I to IV, that mediate ligand-binding and dimerization. EGF binds to specific sites on domains I and III whereas the dimerization arm is on domain II. In unstimulated cells, the vast majority of cell surface EGFR is in an auto-inhibited state in which domain II is bound to domain IV. This has two consequences. Firstly, the dimerization arm is hidden, preventing receptor dimerisation. Secondly, domains I and III are too far apart for an EGF molecule to bind to both and therefore with high affinity. Ligand binding to EGFR is associated with gross conformational changes in these domains such that domain II is no longer tethered to domain IV. This allows domains I and III to move so close to each other that an EGF molecule can bind to both domains, while additionally exposing the dimerization arm. This EGF:EGFR complex is therefore ready to dimerise with another ligand bound receptor (Ogiso et al., 2002). Elucidation of the crystal structure of the ECD of ErbB2 revealed that it closely resembled that of EGF-bound EGFR. The dimerization arm of ErbB2 is always exposed, therefore it is constitutively poised to dimerise and the preferred

dimerization partner of all other ErbB receptors. Crucially, domains I and III are also always in close proximity but so close that ligand binding is prevented (Garrett et al., 2003). To summarise, ErbB2 is unable to bind ligand despite being in the extended conformation and therefore it is generally agreed that the list of ErbB ligands as it stands is the complete list.

1.10.2 ErbB2 is the preferred heterodimerisation partner of all other ErbBs

There are eleven ErbB ligands that differ in expression, specificity and affinity for ErbB RTK's, intracellular trafficking and therefore biological response. These include the prototypical Epidermal growth factor (EGF), Transforming growth factor

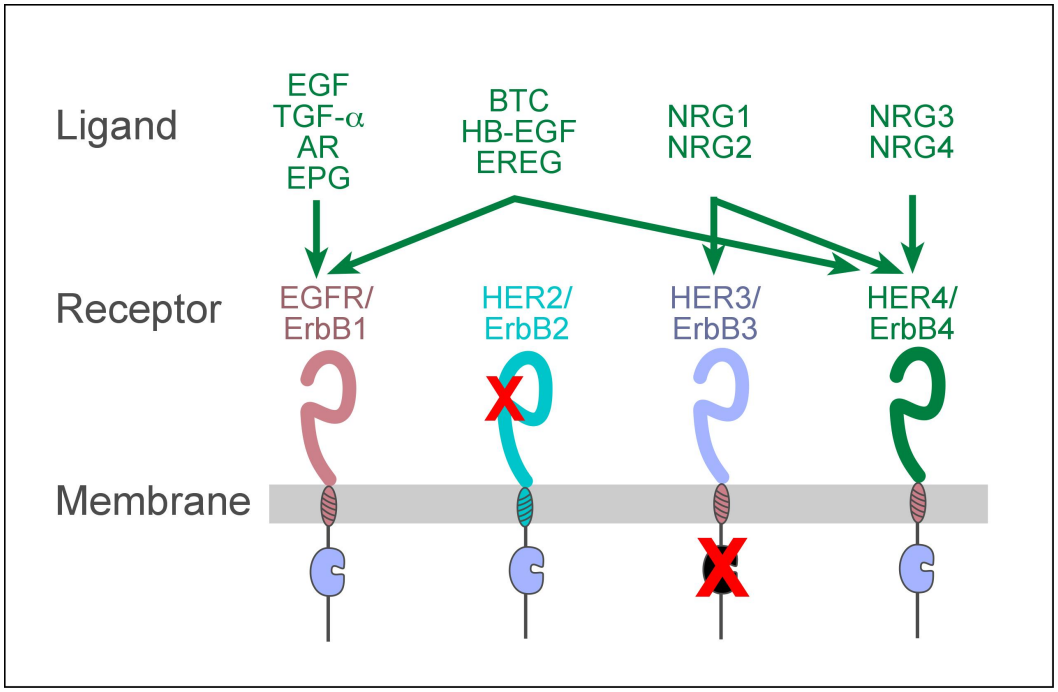


Figure 1.8. *The EGF family is comprised of four receptors (ErbB1-4) and eleven ligands. None of these ligands bind ErbB2 and therefore it requires heterodimerisation to signal, as does kinase-defective ErbB3. The eleven ligands can be divided into those that do bind EGFR and those that don't (the neuregulins). The former group can be further divided into those that bind EGFR only and those that also bind ErbB4 as shown in diagram. The neuregulins can also be split further into those that bind ErbB4 only and those that also bind ErbB3. Key: EGF; epidermal growth factor, TGF-α; transforming growth factor alpha, AR; amphiregulin, EPG; epigen, BTC; betacellulin, HB-EGF; heparin-binding EGF, EREG; epiregulin, NRG1-4; neuregulin1-4.*

alpha (TGFα), Amphiregulin (AREG), Epigen (EPGN), Betacellulin (BTC), Heparin-binding Epidermal growth factor (HB-EGF), Epiregulin (EREG) that all bind EGFR, in addition to the four Neuregulin ligands (NRG1-4) that don't. These groups can be further divided, as summarised in Figure 1.8. BTC, HB-EGF and EREG also bind ErbB4. Of the neuregulins, NRG-1 and NRG-2 bind both ErbB3 and ErbB4 whereas NRG-3 and NRG-4 only bind ErbB4. There is therefore asymmetry in the number of ligands 'assigned' to each receptor (Harris et al., 2003; Schneider and Wolf, 2009).

To add a further level of complexity, the affinity and specificity of ligands for their respective cell surface receptors can differ according to the receptors heterodimerisation partner (Jones et al., 1999). Therefore, examining ligand:receptor interactions in isolation (i.e. in cells engineered to express certain combinations and exposed to specific exogenous ligands) has given what appears to be conflicting results. The use of mammary carcinoma cells that express all ErbB receptors helped increase our understanding. In particular, one study examined EGF, BTC and NRG-1 induced tyrosine phosphorylation of ErbB receptors in the presence and absence of antibodies that caused intracellular retention of either EGFR of ErbB2. The literature prior to this study had demonstrated that EGF bound EGFR only, BTC was capable of binding EGFR and ErbB4 whereas NRG-1 was capable of binding ErbB3 and ErbB4. Downregulation of EGFR at the cell membrane had the expected consequences, namely blocking EGF-induced tyrosine phosphorylation of the other ErbB receptors and having no significant effect on that induced by BTC and NRG-1, which can bind other receptors. Absence of ErbB2 in the cell membrane had more extensive effects, however. Firstly, it impaired BTC and NRG-1 induced tyrosine phosphorylation of ErbB4 as well as EGF and BTC induced phosphorylation of ErbB3 and also EGF-induced tyrosine phosphorylation of EGFR indicating that ErbB2-containing

heterodimers are preferentially formed in response to all these ligands. The contention that ErbB2 was the preferred dimer partner was further supported by the observation that NRG-1 could only stimulate tyrosine phosphorylation of EGFR when ErbB2 was absent from the membrane. This indicates that ErbB2 is such a vastly preferable dimerization partner than EGFR in this instance that its presence causes a total bias towards ErbB2-containing heterodimers. To summarise, these data demonstrate that ErbB2 is the preferred heterodimerisation partner of all other ErbB receptors and, as such, will heterodimerise if co-expressed (Graus-Porta et al., 1997).

1.10.3 ErbB2-containing heterodimers are the most potent ErbB dimers

ErbB2, the preferred dimerisation partner of all other ErbBs, confers a number of properties onto ErbB dimers. Firstly, ligand displacement analysis demonstrated that expression of ErbB2 at the cell membrane increased the affinity of EGF and NRG-1 for their receptors, more so for NRG-1. In addition, ErbB2 slowed the dissociation rates of these ligands, again, more so for NRG-1. This was demonstrated by monitoring the amount of radioactivity released into the medium by cells that had been exposed to saturating amounts of radiolabelled EGF and NRG-1 at 4°C as ligand can only be bound but not internalised at this temperature. This increase in ligand:receptor half life ultimately leads to prolonged signalling (Lenferink et al., 1998). Stabilisation of ligand:receptor interactions is only half the story of why ErbB2-containing heterodimers are more potent. On the inside of the cell membrane, once ligand:receptor complexes have endocytosed, ErbB2 actually de-stabilises ligand-receptor interactions which causes receptors to be routed for rapid recycling back to the cell surface where they are available to signal again (Lenferink et al., 1998). This particular property is only really relevant when ErbB2 dimerises with EGFR or a specific isoform of ErbB4 as the other ErbBs appear to be endocytosis-

impaired regardless (Sundvall et al., 2008). More specifically, in the case of EGFR, it is relevant when EGF but not TGFα is bound. This is because TGFα already dissociates quite readily from EGFR as the endosomes become more acidic, whereas EGF:EGFR interactions are resistant to the drop of pH and their pathway heads towards degradation via late endosomes and finally lysosomes (Ebner and Derynck, 1991). Heterodimerisation of EGFR with ErbB2, however, makes the interactions between EGF and EGFR sensitive to pH. Again, this ultimately leads to further signalling (Lenferink et al., 1998). To summarise, with no ligand of it's own, ErbB2 appears to have evolved to modulate the interactions between it's dimerisation partner and their bound ligand.

1.10.4 ErbB2 is often overexpressed in human cancers

As expression of ErbB2 is associated with a stronger mitogenic response and evasion of downregulation mechanisms it is perhaps not surprising that inappropriate activation or expression is frequently observed in cancer. In fact, ErbB2 was discovered as the normal homolog of the rat oncogene, neu, which differed to ErbB2 by a single point mutation (Schechter et al., 1984). In human cancers however, it is often overexpressed rather than mutated (Slamon et al., 1987). Trastuzumab (also commercially known as Herceptin), a humanized monoclonal antibody that binds the extracellular domain of ErbB2 and blocks signalling, has been one of the most successful anti-cancer drugs developed (Vu and Claret, 2012). Similarly, EGFR is frequently mutated or overexpressed in human carcinomas and again this is associated with poor prognosis (Moscatello et al., 1995; Yarden and Sliwkowski, 2001). Anti-cancer drugs that target both EGFR and ErbB2, such as the small molecule tyrosine kinase inhibitor Lapatinib, have been more successful than those that target EGFR only such as Gefitinib (Tebbutt et al., 2013). Dysregulation of ErbB3, on the other

hand, has been less frequently reported. ErbB3 overexpression/activation was thought to be 'dispensable' for tumour development, or certainly secondary to EGFR/ErbB2-driven tumourigenesis and was therefore never validated as a molecular target (Yarden and Sliwkowski, 2001). One study even offered an explanation as to why this might be. This study examined the affinity of all Src homology 2 (SH2) and phosphotyrosine binding (PTB) domains encoded by the human genome to phosphotyrosine sites on the ErbB receptors. They found that ErbB2 phosphotyrosine sites, in general, bound more SH2 and PTB domains than EGFR and ErbB3. Also, intriguingly, this study found that when you lowered the affinity threshold and therefore included low affinity interactions that are only relevant when the receptor is overexpressed, the phosphotyrosine sites of EGFR and ErbB2 but not ErbB3 became much more promiscuous. The authors therefore hypothesized that overexpression of EGFR and ErbB2 was oncogenic because it lead to activation of additional pathways as opposed to overexpression of ErbB3 that would presumably only lead to enhanced signalling through the same pathways (Jones et al., 2006). However, the role of ErbB3 in cancer development is more appreciated now. In particular, it seems enhanced ErbB3-stimulation of PI3-K pathway is an important mechanism of resistance to cancer therapies that target EGFR and ErbB2 (Lee et al., 2014).

1.10.5 The ErbB receptors have critical roles in development

All ErbB null mice are embryonically lethal, indicating they are critically important in normal embryonic development. Collectively, they are important in several epithelial, mesenchymal and neuronal lineages. EGFR null mice have a general defect in epithelial development that results in multiple organ failure (Miettinen et al., 1995). ErbB2-4 null mice are all embryonically lethal due to different defects in heart development (Erickson et al., 1997; Gassmann et al., 1995;

Lee et al., 1995; Riethmacher et al., 1997). Rescue of organ failure in ErbB null mice revealed important roles in mammary gland development (Luetteke et al., 1999; Troyer and Lee, 2001). Mice in which ErbB ligands are genetically ablated have much less severe defects, indicating redundancy among the 11 ErbB ligands (Wong, 2003).

1.10.6 The ErbB ligands are important in reproductive development

All ErbB ligands are synthesized as membranous proteins composed of one functional EGF module, a transmembrane domain and a cytoplasmic tail. The EGF module is the domain responsible for ErbB binding and always contains the same six cysteine residues with conserved distances between them that form three disulphide bonds (Schneider and Wolf, 2009). Historically, it was thought that the extracellular EGF module was cleaved to release the biologically active ligand into the extracellular space. The process is now known to be much more complex. HB-EGF is the best example of this. The membranous 'pre-cursor' of HB-EGF, known as pro-HB-EGF, can signal in a juxtacrine manner or rather, HB-EGF is biologically active prior to proteolytic cleavage of the EGF module. Transmembrane HB-EGF functions as the diptheria toxin receptor (Mitamura et al., 1995) and is also very important in blastocyst implantation in the mouse (Martin et al., 1998; Paria et al., 2001; Raab et al., 1996).

The ErbB ligands are particularly important in the ovary as expression of EGFR, AREG, BTC and EREG in the GCs is of critical importance in the pre-ovulatory follicle to communicate the LH surge to the cumulus-oocyte complex (COC) which is devoid of LHR (Conti et al., 2006; Park et al., 2004). Furthermore, ErbB ligands are promising possible candidates for regulating GC adhesion and proliferation. Firstly, EGF functions to maintain N-cadherin-mediated AJs in Sertoli

cells (Zhang et al., 2013), the male counterpart of GCs and secondly, membrane-bound TGF is able to bind EGFR on a neighbouring cell causing these cells to adhere and subsequently proliferate (Anklesaria et al., 1990).

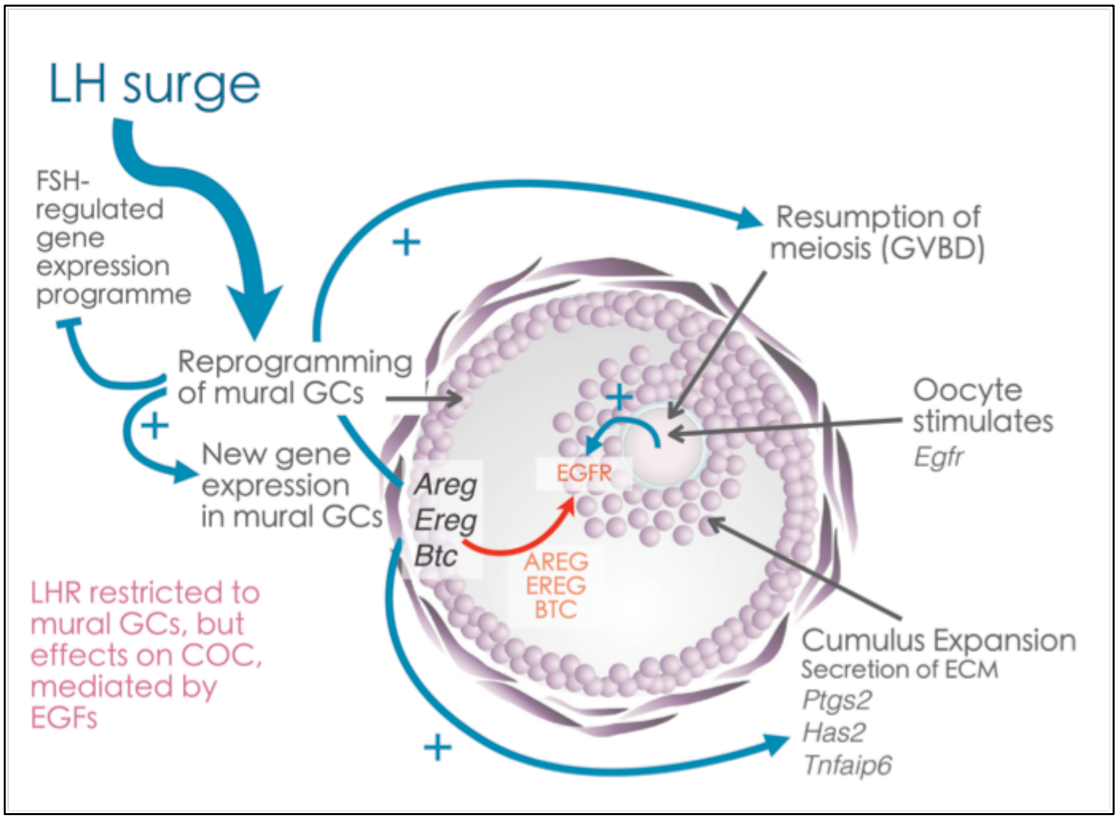


Figure 1.9. *Diagram illustrating the processes that the LH surge stimulates in a pre-ovulatory follicle via the EGF family. Diagram courtesy of K Hardy.*

The LH surge induces many changes necessary for ovulation including oocyte maturation and cumulus expansion (Hillier et al., 1994; Hirshfield, 1991a). However, the COC do not express LH receptor (Peng et al., 1991). This discrepancy was resolved when EREG was one of a number of genes identified by differential display as being upregulated upon hCG injection (Espey and Richards, 2002). Differential display is a PCR that employs a set of primers that will amplify a large amount of random mRNA populations and allows any differentially expressed genes visualized on a gel to be extracted and identified. The Conti group was largely responsible for

elucidation of the EGF network in pre-ovulatory follicles. Park et al (2004) used in situ hybridization (ISH) and northern blotting to show EREG, AREG and BTC are all transcriptionally upregulated in the mural GCs 1-3 hrs post hCG injection. All three of these ligands themselves were able to elicit oocyte maturation and cumulus expansion approximately an hour faster than LH was, indicating that they act downstream of the LH surge. Increased levels of tyrosine phosphorylated EGFR following hCG injection and the inhibitory effect of AG1478 (EGFR tyrphostin, a small molecule inhibitor that specifically inhibits EGFR) on LH-induced oocyte maturation and cumulus expansion show that these ligands mediate the effects of the LH surge on the COCs via binding to their receptor, the EGFR. To summarise, Park et al. (2004) present a model wherein LH signalling in mural GCs stimulates transcription of AREG, BTC and EREG, which diffuse across the antrum and bind to the EGFR on the cumulus cells, thereby mediating the effects of the LH surge (Park et al., 2004), as summarised in Figure 1.9. Therefore, much of the research into the role of the EGF family has focused on antral follicles, specifically pre-ovulatory follicles. For instance, EGFR has been conditionally knocked out in the mouse ovary but under the control of the Cytochrome P450 aromatase (Cyp19) promoter that would confine genetic ablation of EGFR to steroidogenic i.e. mature GCs (Hsieh et al., 2011).

The EGF family also has a role in male reproductive biology. Exactly what this role involves is less clear as gain/loss of expression studies yield conflicting data. Both sialoadenectomy (removal of the salivary gland, and therefore circulating EGF) and overexpression of EGF in transgenic mice (human EGF under control of beta actin promoter) caused a decrease in sperm counts (Liu et al., 1994; Wong et al., 2000). Both studies do at least agree that EGF is important for testicular function. A few similarities between the role of EGF factors in the testes and ovary have emerged.

For instance, EGF regulation of connexins, the gap junctional proteins, appears to be important in both male and female reproductive biology. In the female, cyclic guanosine monophosphate (cGMP) moves from GCs to the oocyte via gap junctions and meiotic arrest is maintained. LH transactivation of EGFR induces gap junction closure via phosphorylation of connexin (Cx43), which prevents entry of cGMP into the oocyte, resulting in resumption of meiosis (Hsieh et al., 2011). In the male, Cx43 is critical for Sertoli cell differentiation and a decrease in EGFR is thought to underlie the decreased expression of Cx43 in azoospermic patients (Dube et al., 2012). While this thesis is more concerned with EGF family regulation of adhesive junctions rather than gap junctions, it is promising that EGF functions in Sertoli cells, the male counterpart of GCs. More relevantly, RT-PCR and immunohistochemistry revealed that N-cadherin is downregulated in Sertoli cells of testes from sialoadenectomised mice and that this underlies the reason why EGF quickens recovery following testicular injury (Zhang et al., 2013).

Excitingly, there is evidence that EGFR signaling may be capable of mediating cell-cell adhesion without involvement of adhesive junctions. Anklesaria et al (1990) found that a haematopoietic cell line expressing EGFR adheres to stromal cells expressing pro-TGFalpha, unless in the presence of soluble EGFR ligand, and these adherent EGFR-expressing cells were proliferating, as shown by BrdU uptake. Therefore, this is an interesting example of where juxtacrine signaling by the EGF family appears solely responsible for regulating cell adhesion and subsequent proliferation. This is particularly interesting when we are looking at regulating of cell shape change and proliferation during primordial activation.

1.10.7 ErbB downstream signalling

Initiation of follicle growth is characterised by GC shape change, GC proliferation and oocyte growth. The reciprocal regulation between AJ assembly and EGFR signalling in other cell types (Hoschuetzky et al., 1994; Pece and Gutkind, 2000) and the effect of removal of the salivary gland (and therefore the majority of circulating EGF) on N-cadherin expression in Sertoli cells (Zhang et al., 2013) demonstrate that the ErbB family are a good candidate for having a role in GC shape change during primordial activation. It is well known that the ErbB activation is often associated with mitogenic activity, and it is therefore entirely possible that the ErbB family may regulate proliferation during primordial activation. Indeed, the Mitogen-activated Protein Kinase (MAPK) pathway is activated downstream of all ErbB dimers (Figure 1.10). This cascade involves three sequential phosphorylation events such that MAPKKK (MAPK kinase kinase) phosphorylates MAPKK (MAPK kinase), which phosphorylates MAPK. There are four distinct MAPKK/MAPKK/MAPK cascades in mammals. The two major cascades involve either the extracellular signal-related kinases (ERK) 1/2 MAPK or the Jun amino-terminal kinases (JNK) MAPK, and the phosphorylation of these is often used as an assay for ErbB activation. This cascade eventually leads to phosphorylation of transcription factors such as cAMP response element-binding protein (CREB) and c-Fos and ultimately leads to changes in transcription of genes involved in cell cycle progression. MAPKs can also regulate post-transcriptional processes in the cytoplasm (Chang and Karin, 2001).

The PI3-K pathway is another major pathway frequently activated downstream of ErbB activation (Figure 1.10). This is another kinase cascade that ultimately regulates proliferation, survival, apoptosis and migration. Of the ErbB

family, only ErbB3 and certain ErbB4 isoforms can directly activate PI3-K (Elenius et al., 1999). However, EGFR and ErbB2 are able to indirectly couple to the PI3-K pathway via adaptor molecules such as Grb2 and GAB (Grb2 associated binding protein 1) (Soltoff and Cantley, 1996). The cytoplasmic tail of ErbB3 is the most equipped to activate PI3-K as it has the most phosphotyrosine sites to which PI3-K can directly dock (Figure 1.11). Indeed, as already discussed, it seems that ErbB3-activation of PI3-K is an important mechanism underlying resistance to anti-cancer drugs targeting (Hynes and Dey, 2009). Again, phosphorylation of PI3-K or its downstream kinase Akt is often used as an assay of ErbB activation.

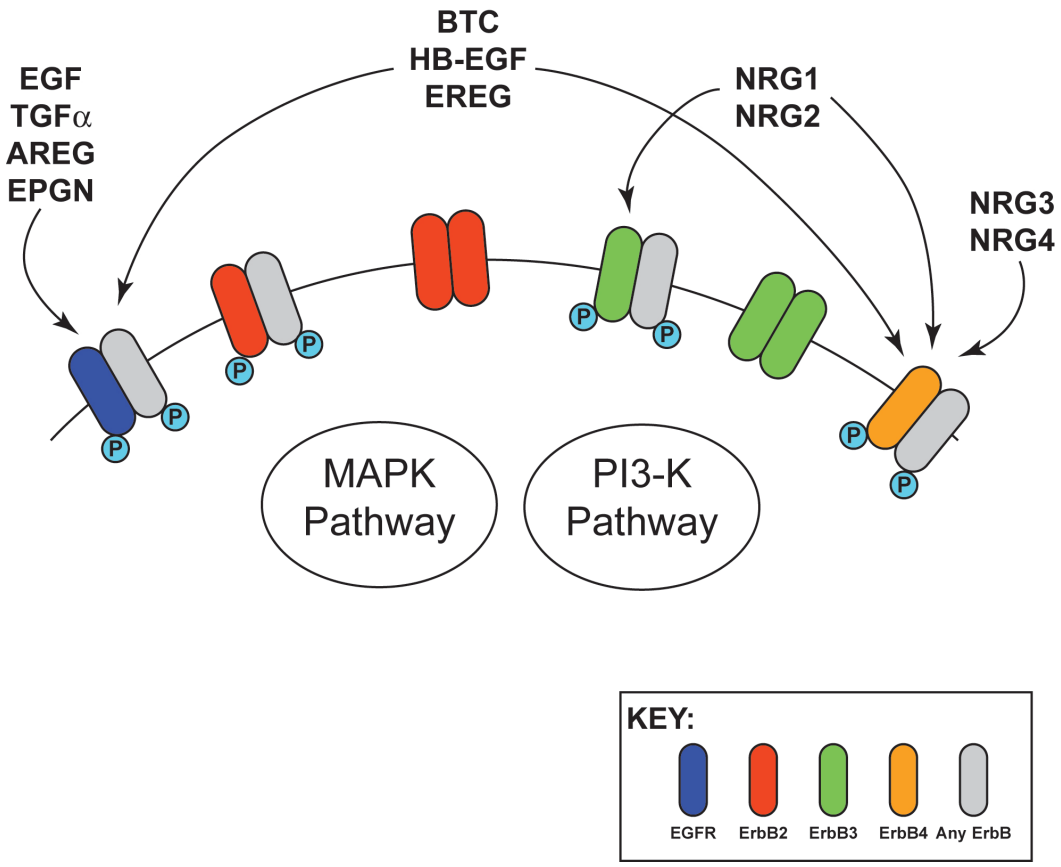


Figure 1.10. *Diagram illustrating all possible heterodimeric combinations of ErbB receptors and the major intracellular signalling pathways common to all of them. No known soluble ligand binds ErbB2 and it requires heterodimerisation to signal, as does ErbB3 (as indicated by the lack of phosphorylation of ErbB2 homodimers and ErbB3 homodimers in image). The MAPK pathway is common to all ErbB dimers and the PI3-K pathway is common to the vast majority.*

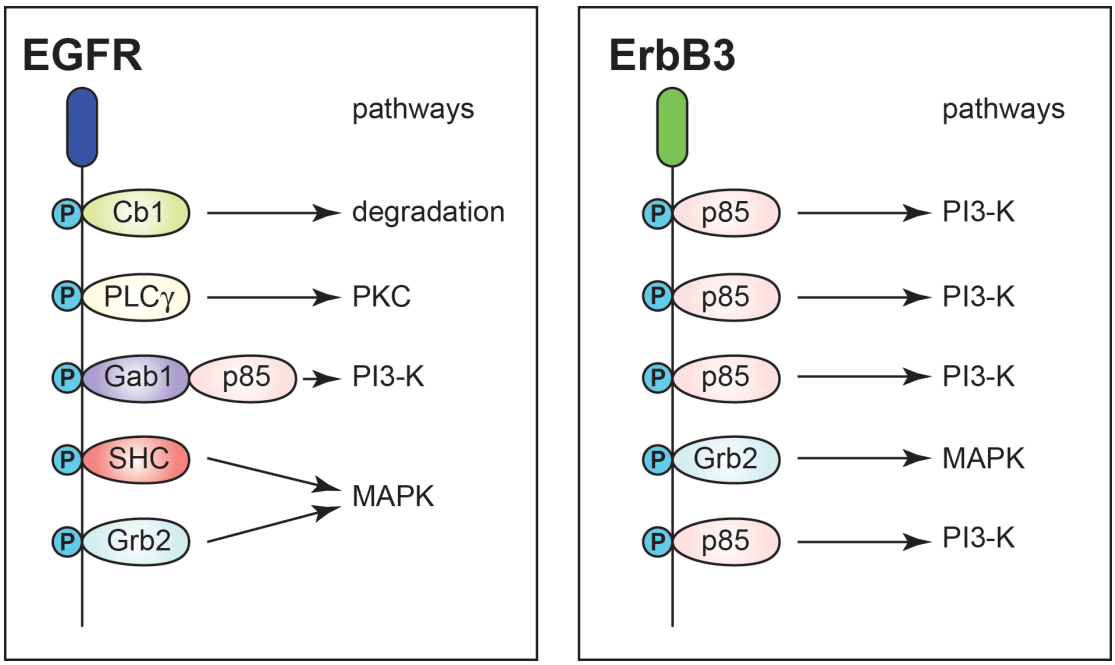


Figure 1.11. *Different ErbB receptors have a different complement of docking sites on their cytoplasmic tails, once phoshorylated. For example, EGFR is the only ErbB receptor to which c-Cbl docks and therefore EGFR is the only ErbB receptor that is efficiently targeted to lysosomes following ligand stimulation. ErbB3, on the other hand, is unique in that it can stimulate the PI3-k pathway directly via several different phosphotyrosine binding sites.*

One downstream pathway that is particularly intriguing with respect to onset of proliferation during primordial activation is ErbB2-mediated inactivation of TOB1 (transducer of ErbB2). TOB1 is a member of the B-cell translocation gene (BTG) family of anti-proliferative proteins that is inactivated downstream of ErbB2 signalling; its N-terminal has homology to BTG1 and ErbB2 inactivation of TOB1 involves the C-terminal of TOB1 (Matsuda et al., 1996). Regulation of its activation is such that when ErbB2 is absent or not activated, TOB1 is active, not phosphorylated and localises to the nucleus where it inhibits proliferation. In contrast, when ErbB2 is activated TOB1 becomes phosphorylated, is exported from the nucleus into the cytoplasm and the brake on proliferation is lifted (Kawamura-Tsuzuku et al., 2004; Matsuda et al., 1996). It inhibits proliferation in the nucleus by interacting with transcription factors via the conserved BTG domain. This is

intriguing, with respect to this project, as the majority of follicles are maintained in the ovary as primordial follicles, with flattened non-proliferating GCs, and a key event in initiation is the onset of proliferation. Therefore, it is possible ErbB2 inactivation of TOB1 may regulate this. Additionally, TOB1 is also an antagonist of Smad signalling proteins that are downstream of TGF-β family signalling (Yoshida et al., 2000), a growth factor family of critical importance in the ovary (Pangas, 2007). Importantly, it has been hypothesized that an antagonist of the TGF-β superfamily is the putative inhibitor maintaining the primordial pool in a dormant state (Da Silva-Buttkus et al., 2009).

To summarise, the ErbB family of receptors are good candidates to investigate their possible role in GC shape change and proliferation during initiation of follicle growth.

1.11 Project Strategy – Inhibition of RTKs

The role of the PDGF and EGF families in primordial activation can be investigated using inhibitors specific to these receptors and exogenous ligands that stimulate them in various culture models. As members of the ErbB families are commonly inappropriately activated in several types of human cancers, a vast amount of research has been and still is devoted to developing drugs that target these (Tebbutt et al., 2013). The successful agents so far can be divided into antibodies, which usually target the extracellular domain, or small molecule inhibitors that block signalling by inhibiting the intracellular tyrosine kinase domain (Figure 1.12). Trastuzumab (commercially known as Herceptin) is a humanized monoclonal antibody that binds to the juxtamembrane domain (extracellular domain IV) of HER2 (human ErbB2) and was the first HER2-targetted cancer therapy to be approved by the Food and Drug Administration (FDA). Its precise mechanism of action is unclear,

though it is thought to slow tumour progression in three major ways. Firstly, binding of trastuzumab is thought to enhance ErbB2 degradation by recruiting c-Cbl, an E3 ubiquitin ligase that normally only ubiquitinates EGFR. Secondly, it is also thought to block mitogenic MAPK and the PI3-K pathway that promotes cell survival by interfering with ErbB2 dimerisation. Trastuzumab is also thought to cause death of ErbB2-overexpressing tumour cells via Antibody-Dependent Cell-mediated Cytotoxicity (ADCC) in which the body's immune cells recognise the human IgG portion of Trastzumab. Trastuzumab was found to significantly improve survival of various subsets of HER2-positive breast cancer patients, particularly when in combination with other therapies although it is used as a single agent in certain cases. Trastuzumab is one of the great success stories in targeted anti-cancer drugs but it still does have some drawbacks. One of these drawbacks is intrinsic to its very nature/form/structure/size; as a large antibody it cannot cross the blood-brain barrier efficiently and therefore cannot efficiently block tumour metastasis to the central nervous system (Vu and Claret, 2012). Development of small molecule tyrosine kinase inhibitors addressed this issue. The kinase domain is highly conserved among receptor and non-receptor tyrosine kinases but many inhibitors have been developed that are highly specific to one receptor. For example, Gefitinib is a tyrosine kinase inhibitor that specifically inactivates EGFR and has been successful in a clinical setting (Gridelli et al., 2011; Muhsin et al., 2003). The kinase domain is composed of an N- and C-terminal lobe with a cleft in between that ATP occupies when the kinase is active. Kinase activity is associated with a conformational change. The first inhibitors to be developed bound competitively and reversibly to ATP-binding site of kinases in the active conformation. These are known as type I tyrosine kinases inhibitors. A second class of inhibitors, type II, targets an additional hydrophobic

pocket that is created by conformational change to the inactive form. Importantly, this pocket is less conserved than the ATP-binding cleft, which allows development of more specific inhibitors. Furthermore, as dissociation of the inhibitor requires a conformational change the inhibitor off-rates are much slower (Liu and Gray, 2006). The first of these type II inhibitors were not designed and developed to specifically target the hydrophobic region, but rather were found afterwards to have different kinetics (off-rates for example) to those developed beforehand. The crystal structure of these inhibitors with their complex was determined as used to retrospectively classify these inhibitors and also to facilitate rational design of these type II inhibitors. Lapatinib, a dual tyrosine kinase inhibitor of EGFR and ErbB2, was found to be a type II tyrosine kinase inhibitor following elucidation of the crystal structure of EGFR with the drug (Wood et al., 2004). Lapatinib is the only small molecule tyrosine kinase inhibitor that has been approved by the FDA. However, there are several tyrosine kinase inhibitors that also competitively and reversibly bind the ATP binding site of ErbB2, and are commercially available for laboratory research, such as AG-825 and ErbB2 inhibitor II. Similarly, there are those for EGFR including AG1478. Furthermore, another antibody targeted to the ECD of ErbB2 has since been developed; Pertuzumab targets a different domain to Trastuzumab and blocks homo- and heterodimerisation of ErbB2. In contrast to AG1478, AG-825 and ErbB2 inhibitor II, Pertuzumab is not readily commercially available for laboratory research.

Although PDGF has not been as prolific as EGF in terms of validation as a molecular target in human cancers, there are several small molecule inhibitors of PDGF receptors available, including AG-1296, should PDGF receptor be a likely candidate for regulating primordial activation.

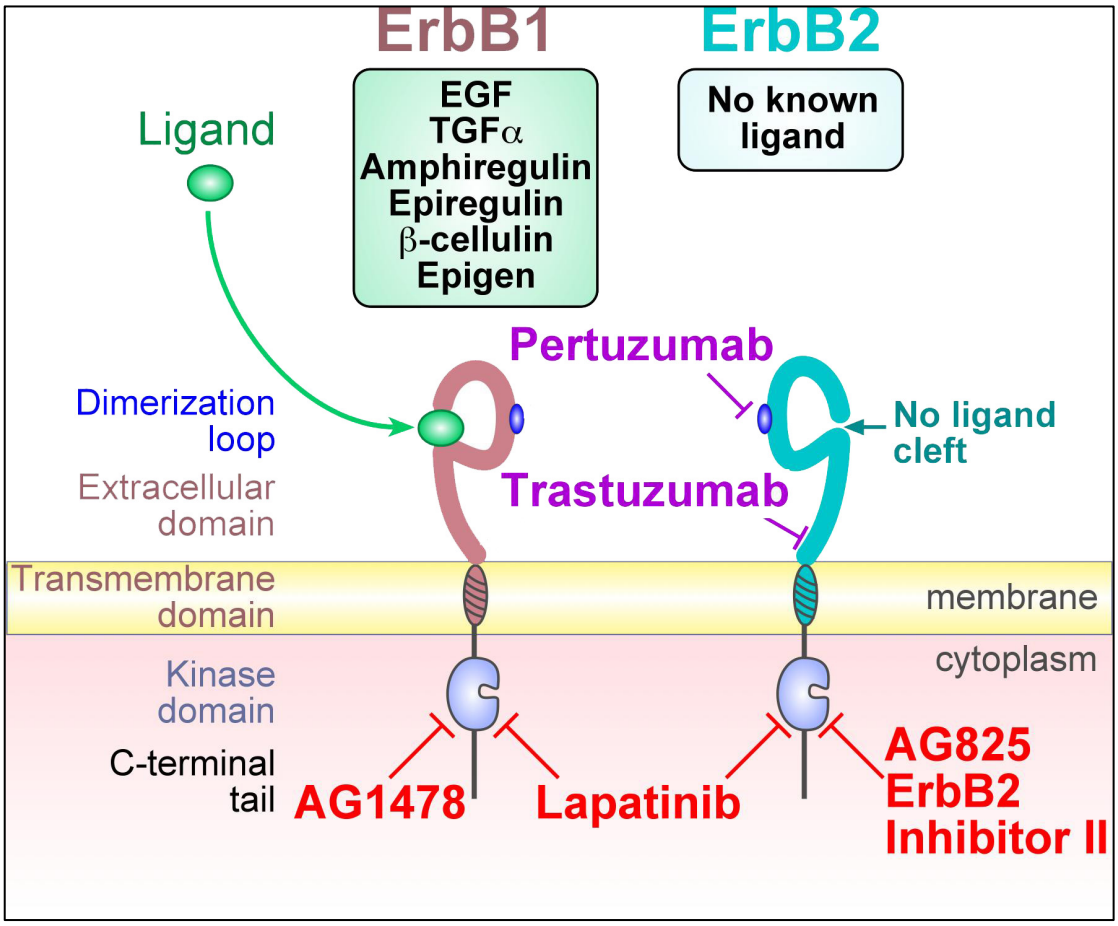


Figure 1.12. *Diagram illustrating the various targets of inhibitors to EGFR and ErbB2. EGFR and ErbB2 are commonly dysregulated in human carcinomas, therefore, several drugs have been developed to inhibit their signalling. These can be divided into small molecule inhibitors, such as AG1478, which target the intracellular kinase domain, and antibodies, such as Trastuzumab, which target the extracellular domains. AG-825 and ErbB2 inhibitor II are specific to the kinase domain of ErbB2. AG1478 is specific to the kinase domain of EGFR. Lapatinib is a dual inhibitor that is specific to the kinase domain of EGFR and ErbB2. Trastuzumab is a humanised monoclonal antibody targeted to the extracellular domain of ErbB2. Pertuzumab is an antibody that blocks ErbB2 dimerisation.*

1.12 Project strategy: Culture models

There are several culture models available to examine the effect of these inhibitors, as well as exogenous ligand, on follicle development. This project is concerned with the changes to GCs during primordial activation. There is an established protocol for primary GC culture in our laboratory. However, it is only possible to culture GCs from antral follicles, which are highly divergent from the squamous GCs of a primordial follicle. There is a preantral GC cell line (KK1)

available (Kananen et al., 1995) but previous studies in our laboratory suggest that these are similarly divergent from preantral GCs in vivo due to a high number of passages (data not shown). Importantly, our laboratory has optimised and established protocols for the culture of isolated preantral follicles and also of whole d4 ovaries.

Several different culture models have been developed by different groups. We use a model in which follicles are mechanically isolated and individually cultured in 96 well plates in 100 µL of medium. The medium is supplemented with antibiotics, BSA and ITS (Insulin 5 µg/mL, transferrin 5µg/mL, selenium 5 ng/mL) but remains serum-free. Follicles incubated in this medium will increase their relative follicular volume by approximately 20%. The huge benefits of this culture model include that (i) follicle growth can be easily measured and tracked, (ii) data are very robust due to the high n numbers (it's possible to isolate up to ~80 healthy follicles from a d16 mouse ovary, although more generally around 30-40 are isolated), and (iii) follicles can be easily processed for molecular or histological techniques to examine the molecular mechanisms underlying follicle development in vitro. The main drawback of this culture in terms of my project is that follicles between the primordial and primary stage are too small, fragile, few in number and too firmly embedded in the tougher/stiffer cortex to mechanically isolate for an experiment. Therefore the effects of inhibitors on primordial activation cannot be directly answered in this model. However, follicle growth, oocyte growth and GC proliferation, three variables that change dramatically upon activation of follicle growth, can be measured in this model. Other drawbacks include the loss of inter-follicular communication and the 'weakening' of intra-follicular communication as endogenous factors secreted by the follicle are diluted into the medium. However, follicles cultured in this model can be stimulated with hormones and growth factors and be induced to form an antrum and

ovulate so developmental checkpoints that occur in vivo can be recapitulated in this in vitro model (Murray and Spears, 2000). Furthermore, it is now becoming increasingly appreciated how important the physical environment is to follicle development and so new follicle culture models using hydrogel encapsulation are continually being developed. This is still an ongoing process in our lab so we have not been able to examine the role of the ErbBs in a 3D isolated follicle culture model. However, we have been able to examine the function of these inhibitors in 3D follicle development within a whole d4 ovary culture model.

The whole d4 mouse ovary culture model that we use was first established by Eppig and O'Brien (1996). This model entails the culture of a whole d4 ovaries (bursa removed) coated in a thin film of medium on top on membrane inserts on 6 well plates with 1.5 mL of medium beneath the inserts for 8 days. At this point, healthy multi-layered follicles are observed towards the centre of the ovary. Importantly, primordial follicles are still present near the OSE, indicating that follicles have not undergone global activation and that the primordial pool is maintained. Furthermore, Eppig and O'Brien (1996) were able to isolate multi-layered follicles from these ovaries and culture them individually to produce mature, fertilizable oocytes. The main benefit of this model in comparison to the isolated follicle model is that the process of primordial activation can be studied. Furthermore, intra- and inter-follicular follicle signalling is maintained and a similar physical environment is maintained. Drawbacks include low n numbers, variation between ovaries, mice and litters and also a fairly labour intensive and time-consuming tissue processing and image analysis methodology for acquisition of data. These d4 ovaries also are not capable of growing in serum-free media, therefore the confounding effects of serum are unavoidable. However, several growth factors have been shown to affect

primordial effects in this, or a similar ovary culture model, indicating serum does not completely mask effects.

1.13 Project strategy: Localisation of RTKs

As discussed in section 1.7, RTKs and cadherins can intermingle in microdomains of the membrane to mutually regulate one another and form a signalling centre (Comoglio et al., 2003). N-cadherin is the major CAM in GCs and distinct N-CADHERIN immunolabelling is first observed between cuboidalising GCs in transitional follicles (Mora et al., 2012). Primordial activation is characterised by oocyte growth, GC shape change from flat to cuboidal and GC proliferation. Regulation of this process is poorly understood though it is likely governed by growth factor signalling as gonadotrophins are not essential until after antrum formation (McGee and Hsueh, 2000). Several RTK families have been implicated in rat primordial activation such as PDGF (Nilsson et al., 2006), c-Kit (Parrott and Skinner, 1999) and fibroblast growth factor receptor (FGFR) (Nilsson et al., 2001) and ErbB2 (Li-Ping et al., 2010). FGFR is particularly interesting as N-cadherin association with FGFR in rat GCs has been shown to regulate FGFR signalling (Trolice et al., 1997). This project was focused on identifying possible RTK association with, and mutual regulation of, CAMs during GC cuboidalisation and proliferation. Therefore, a crucial first step in the project was to localise a candidate RTK to GCs and, more specifically, co-localise this RTK with N-cadherin in follicles initiating growth. Therefore, this project began with a large literature search to establish which RTKs were good candidates worthy of investigation based on the following criteria: (i) whether they had been implicated in primordial activation, (ii) whether they had been localised to GCs and (iii) whether they had been known to associate with N-cadherin in ovarian or other cell types. Based on this criteria and the literature search alone,

the FGF family was the strongest candidate as this had been shown to associate with N-cadherin in rodent GCs (Trolice et al., 1997). The FGF family was investigated simultaneously with other families during this project and expression analyses of other proteins was more fruitful and relevant to this project, therefore the thesis is shaped according to this. Good candidates were investigated by PCR (in whole ovaries, isolated follicles, GCs aspirated from antral follicles and isolated oocytes) and immunofluorescence (in sections from pre- and post-pubertal mouse ovary) first, before culture experiments, to establish which were likely to have a role in GC cuboidalisation and proliferation during primordial activation.

1.14 Hypothesis

We hypothesise that the change of granulosa cell shape from flattened to columnar is a key event during the initiation of follicle growth and that this event is regulated by local growth factor signalling.

1.15 Aims of Project

The overall aim of the project is to investigate whether local growth factor signalling by Receptor Tyrosine Kinases regulates the dramatic cell shape change and GC proliferation associated with initiation of follicle growth. The individual aims and objectives were too:

(i) Identify candidate RTKs that co-localise with adhesion molecules that have been localised in preantral follicles, and hence which are likely to regulate GC shape change during activation of follicle growth.

(ii) Investigate which candidate RTKs are expressed in follicles of different stages of development, in both adolescent and adult mice.

(iii) Identify and spatiotemporally localise growth factor ligands that are likely to be activating these receptors.

(iv) Examine the role of these receptors in preantral follicle growth by investigating the effect of RTK inhibitors and exogenous ligand on in vitro follicle growth in the isolated preantral follicle culture model

(v) Examine the role of these receptors in primordial activation by investigating the effect of RTK inhibitors and exogenous ligand on rate of primordial activation in a whole d4 mouse ovary cultured for 8 days

Chapter 2: Materials and Methods

2.1. Collection of ovaries

Female mice (strain C57BL/6) were killed by cervical dislocation at various dpp (days post partum). All mice were housed in accordance with the Animals (Scientific procedures) Act of 1986 and associated Codes of Practise. Ovaries were removed and collected in Leibovitz L-15 medium (L-15, Gibco, Invitrogen, UK) supplemented with 1% bovine serum albumin (BSA, Cat no A7030, Sigma-Aldrich, UK) for transport to the laboratory. The uterus, oviduct, fat and ovarian bursa and other membranes were aseptically dissected from the ovary using insulin syringes (Terumo, UK), in L-15 medium supplemented with 1% BSA. Ovaries were either cultured (see section 2.8.1), fixed in formalin for immunohistochemistry (see section 2.4.1, or snap frozen in liquid nitrogen and stored at -80°C for molecular studies (see section 2.3.1).

2.2 Isolation of follicles

Individual follicles were manually isolated from the ovary using either insulin needles or disposable acupuncture needles (AcuMedic, UK), in L-15 medium supplemented with 1% BSA. Follicles with an intact basement membrane (as shown by a smooth outline to the follicle), centrally located oocyte, and as few theca/stroma cells attached as possible were selected for future study (Figure 1.1A). Follicles were either cultured further (see section 2.7), fixed in formalin or, snap frozen in 8µl culture medium and stored at -80°C for molecular analyses. Oocytes that 'popped out' during mechanical isolation of follicles were also pooled (Figure 1.1B), snap frozen in 8 µl culture medium and stored at -80°C for molecular analyses.

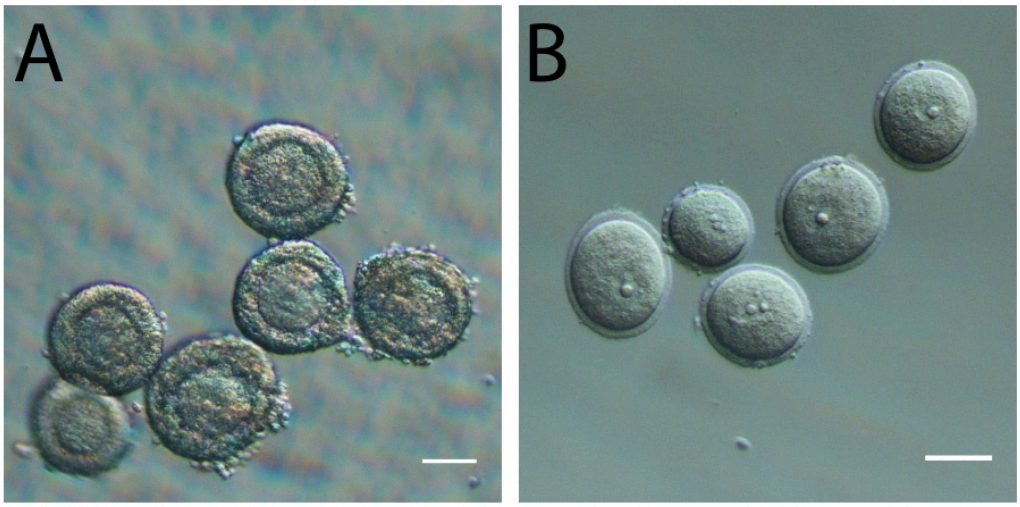


Figure 2.1. *Images of isolated preantral follicles (A) and isolated oocytes (B). Scale bars represent 50 μm.*

2.3 Gene expression analysis

2.3.1 RNA extraction of whole tissues

Total RNA was extracted from whole ovaries/oviduct using the TRIzol method in accordance with the manufacturers instructions (Invitrogen, UK). In brief, tissue samples were thawed in 800μl TRIzol (Invitrogen, UK). Large tissue samples (whole post-natal ovaries, pieces of control tissue such as liver) were physically cut up and ground with sterile scissors and pestle. Tissue fragments were then allowed to dissociate in TRIzol for at least 5 minutes at room temperature. Chloroform (400 μl) was used to separate RNA into an aqueous phase and RNA was subsequently precipitated from the aqueous phase using isopropyl alcohol. The RNA pellet produced was washed in 75% ethanol, dried and dissolved in Tris-EDTA (TE) buffer for 10 minutes at 55 °C. Yield and purity of RNA was measured by spectrophotometry (Nanodrop ND-1000; Nanodrop Technologies Inc., Wilmington, DE). RNA was also electrophoresed on an agarose gel to determine RNA integrity. 500 ng of RNA from each sample was then treated with Deoxyribonuclease I

(Invitrogen) to remove any contaminating DNA. RNA was either stored at -80 °C or used immediately for RT-PCR.

2.3.2 RNA extraction of follicles, oocytes and granulosa cells

Total RNA was extracted from follicles, oocytes and GCs using RNeasy microcolumns (QIAGEN, Crawley, West Sussex, UK) in accordance with the manufacturers instructions. In brief, samples are lysed and the RNA bound to the silica gel-based membrane. RNA is then washed through a series of steps involving ready to use buffers and subsequent centrifugation. DNase-treatment is performed on column before RNA is eluted with 14 μL RNase-free water and either stored at -80 °C or used immediately for RT-PCR. The amount of RNA extracted from isolated follicles, oocytes and GCs is immeasurable using the Nanodrop ND-1000 (Nanodrop Technologies Inc., Wilmington, DE). Therefore, for the PCR screens shown in Figure 3.2, 3.7, 3.8 and 4.1, appropriate PCR application of *Amh* and *Gdf9* from cDNA was used as an indicator of adequate yield and purity of RNA. However, for the PCR screens shown in Figure 4.8 and 4.9, RNA yield and purity was assessed using a Bioanalyser (Agilent 2100 Bioanalyser, RNA pico analysis service, Clinical Sciences Centre, Imperial College London).

2.3.3 Reverse Transcription-PCR (RT-PCR)

cDNA was synthesized from extracted RNA using random hexamer primers and Superscript III reverse transcriptase in accordance with the manufacturers instructions (Invitrogen). cDNA synthesized from follicle, oocyte and GC samples was diluted 2x for the PCR screens shown in Figure 3.2, 3.7, 3.8, and 4.1. Where possible, 250 ng of RNA extracted from whole tissues was reverse transcribed and cDNA synthesized from this RNA was diluted 4x for the PCR screens shown in

Figure 3.2, 3.7, 3.8, and 4.1. However, for the PCR screens shown in Figure 4.8 and 4.9, 25ng of bioanalysed RNA was loaded into the PCR reaction. Primers were designed for PDGF receptors and ligands and ErbB receptors and ligands using the Primer 3 web version 4.0.0 (http://primer3.ut.ee/). PCR using these primers was simulated using the programme Amplify 3X (http://engels.genetics.wisc.edu/amplify/) to check for possible primer dimers and multiple products. Expected product size and primer sequences used in this study are summarised in table 2.1

A presence/absence PCR screen for PDGF receptors and ligands and ErbB receptors and ligands was performed using the above mentioned cDNA samples and KAPA 2G Fast Readymix (Labtech International, East Sussex, UK). cDNA samples were then subject to 34 (Figure 3.2 and 3.8) or 32 (Figure 3.7, 4.1, 4.7 and 4.8) cycles of amplification in a TC-3000 thermal cycler (Techne). The cycle number used for each individual PCR screen was determined by initially using *Gdf9* and *Amh* as controls i.e. a cycle number which ultimately produced a distinct *Amh* product in GC and follicle samples but not oocyte and a distinct *Gdf9* product in oocyte and follicle samples but not GC samples was used in each case. Briefly, following an initial 2 minute denaturation step at 95 °C, each cycle consisted of a 15 second denaturation step at 95°C, a 15 second annealing step at a temperature specific to each primer and a 1 second extension step at 72 °C, before a final extension for 2 minutes at 72 °C. *Hprt1* was also included as a housekeeper control that should be detected in all samples and genes specific to either the oocyte (*Gdf9),* GCs *(AMH),* or theca *(Cyp17α),* were also included as positive controls to establish that samples were not 'contaminated' with unwanted cells.

PCR products were separated according to size, with respect to a molecular weight marker (500 bp DNA ladder, NEB), on a 2% agarose (Sigma) gel by gel

electrophoresis. Ethidium bromide (Sigma) was added to the agarose gel in solution to a final concentration of 0.2 μg/mL. Ethidium bromide-bound DNA was visualised under Ultra Violet (UV) light in a Alpha Imager mini (Alpha Innotech).

Table 2.1. *Sequences and properties of primers for PDGF and EGF family genes*

Key: AT; Annealing temperature

Gene Symbol	**Primer Sequence (5′→3′)**	**GenBank Accession**	**AT (°C)**	**Product Size (bp)**
Pdgfrα	Fwd tgtgtataaggcaggagaaacg Rev gtttgatggatgggagtttgat	NM_001083316.1 and NM_011058.2	59	143
Pdgfrβ	Fwd catggatatgagcaaggatgaa Rev tggtgagtcgttgattaaggtg	NM_001146268.1 and NM_008809.2	59	169
Pdgf-α	Fwd ctcgaagtcagatccacagcat Rev cttctcgggcacatggttaat	NM_008808.3	56.4	131
Pdgf-b	Fwd tcttccttcctctctgctgcta Rev gtcatgttcaagtccagctca	NM_011057.3	56.4	175
Pdgf-c	Fwd gcctgttgtctccataattgc Rev ctgcgtttcctctacacacaca	NM_019971.2	61.6	178
Pdgf-d	Fwd tttagtctccattctcctgtgc Rev tggtacaagtctgtgaggtgatt	NM_027924.2	56.4	138
Egfr	Fwd actggactgacctccatgct Rev ctgatctccttgagggaacg	NM_007912.4 and NM_207655.2	59	133
ErbB2	Fwd gcaatttggagcttacctacct Rev acgtgtttcactcggttgtg	NM_001003817.1	59	109
ErbB3	Fwd gactcaagatgtgtgagccttg Rev cccatcgatattgctagagtcc	NM_010153.1	59	104
ErbB4	Fwd acttgcctctggagaatttacg Rev ttctggtctacatagactccacca	NM_010154.1	59	169
Betacellulin	Fwd aagtgaaaacccacttctctcg Rev taaaacaggtccactcgctcac	NM_007568.5	60	193
Epigen	Fwd agcaagccatttgcagatc Rev gcatctgcaaatggcttgct	NM_053087.2	60	137
Hb-egf	Fwd caggacttggaagggacagat Rev cgtggatgcagtagtccttgta	NM_010415.2	60	172
Tgf-α	Fwd ctagcgctgggtatcctgttag Rev cttctcttcctgcaccaaaaac	NM_031199.3	60	171

2.4 Spatial protein localisation in vivo studies

2.4.1 Fixation of isolated follicles and whole ovaries

Isolated follicles were fixed in 10% neutral buffered formalin (BDH Prolabo Chemicals) for 30 minutes, washed in PBS and then embedded in a drop of 2 % agarose (low gelling temperature agarose, Sigma) on a microscope slide on top of a stage heated to 50 °C. Once the follicles were embedded, the slides were removed from the heated stage. The drop of agarose containing the follicles was allowed to set for approximately 10 minutes. Once completely set, the agarose drop was covered in Nuclear Fast Red solution (Sigma) and left for a further 45 minutes to allow time for the follicles to be stained. This stain ensures the follicles are visible and therefore not lost during sectioning. Once follicles are visibly stained, excess Nuclear Fast Red solution is washed off and the agarose droplet is placed in 70% ethanol, ready for processing. Whole ovaries (as described in section 2.1) were fixed in formalin overnight at room temperature. Ovaries were then washed and stored in 70% ethanol ready for processing.

2.4.2 Processing of isolated follicles and whole ovaries

Ovaries or agarose embedded follicles were processed through the following series of increasing concentrations of ethanol: 70 % ethanol (1 hour), 90 % ethanol (1 hr), 100 % ethanol (3 x 1.5 hrs). The ovaries and agarose-embedded follicles were then placed in Histoclear (National Diagnostics) overnight under a 24 x 50 mm glass cover slip (VWR) to keep the agarose droplet submerged and therefore prevent dehydration. The following day, the sample was embedded in paraffin wax in a clear disposable base mould (Surgipath) for 2 hrs at 65 °C. Paraffin wax was cooled over ice between the mould and a plastic embedding cassette (Simport). 5 μm sections of paraffin-embedded tissue were taken using a Leica RM 2135 microtome and mounted

on poly-L-lysine slides (VWR). Sections were adhered to these slides by placing them at 37 °C overnight.

2.4.3 Immunofluorescence

Sections were dewaxed in Histoclear (two 5 minute incubations) and rehydrated in a series of decreasing concentrations of ethanol (100%, 95% and 70%, 2 minutes in each). Antigen retrieval was performed by boiling slides for 20 minutes (replenishing evaporated buffer with distilled water to its original volume every 5 minutes) in either Citrate buffer (10 mM citric acid, pH 6.0) or Tris buffer (0.1M, pH 10.0) with 5% (w/v) urea. Slides were cooled over ice and washed in PBS. Non-specific binding of antibody was reduced by incubating sections with serum block supplemented with 4% BSA (Cat no A7906, Sigma-Aldrich) for 30 minutes. 20% normal goat or donkey serum was used to block depending on which species the secondary antibody used is made in i.e. if using a goat secondary, block in normal goat serum. Sections were then incubated in primary antibody or a negative isotype control overnight at 4 °C. Negative isotype controls were either IgG from rabbit (Cat no I8140), mouse (Cat no I5381) or goat (Cat no I9140) serum (all Sigma). Details and optimal conditions of all antibodies characterised in this study are summarized in table 2.2. Excess unbound primary antibody was then washed off with three 10 minute washes of PBS before incubating the sections with secondary antibodies conjugated with either Alexa Fluor 488, Alexa Fluor 555 or Alexa Fluor 633 (Invitrogen) for 1 hour, at room temperature, in the dark. Excess unbound secondary antibody was washed off sections in two 5 minute PBS washes before counterstaining in 1 µg/mL DAPI (Invitrogen) in the dark for 3 minutes. Sections were mounted in Prolong Gold medium containing DAPI (Invitrogen). Digital images were recorded

using a Leica inverted SP5 confocal laser-scanning microscope (Leica Microsystems, Wetzlar, Germany).

Table 2.2 *Summary of the various targets and optimal conditions of the antibodies characterised in this project.*

Antibody species and clonality	**Immunogen sequence**	**Antigen Retrieval buffer**	**Optimal concentration (μg/ml)**	**Catalog Number, Company**
Rabbit anti-PDGFRα, mc	Withheld	Citrate	0.014	3174, Cell Signaling Technology
Rabbit anti-PDGFRβ, mc	Withheld	Citrate	0.15	3169, Cell Signaling Tech
Rabbit anti-PDGF-BB, pc	TEVFEISRRL IDRTNA, corresponding to amino acids 101-116 of Human PDGF B	Citrate	2.0	Ab21234, Abcam
Goat anti-PDGF-C, pc	E. coli-derived rmPDGF-CC (aa 235 - 345)	Citrate	2.5	AF1147, R&D systems
Rabbit anti-EGFR, mc	Withheld	N/A	N/A	4267, Cell Signaling Technology
Rabbit anti-EGFR, pc	region between residue 1150 and the C-terminus (residue 1210) of human EGFR	N/A	N/A	IHC-00005, Bethyl Laboratories
Rabbit anti-EGFR, pc	mapping within the region of amino acids 970 to 1020	N/A	N/A	sc-03, Santa Cruz Biotechnology
Rabbit anti-ErbB2, mc	Withheld	Tris	0.0545	4290, Cell Signaling Technology
ErbB2	residues surrounding tyrosine 1248 of human ErbB2 protein.	Tris	0.945	2165, Cell Signaling Technology
ErbB2	a synthetic peptide (TAENPEYLGLDVPV) corresponding to amino acids 1242-1255 from the C-terminal domain of human c-ErbB2/c-Neu	Tris	2.5	OP15L, Calbiochem, Millipore
Rabbit anti-TOB1, pc	KLH conjugated synthetic peptide between 61~91 amino acids from the N-terminal region of human TOB1	Citrate	2.5	T3262, Epitomics
Rabbit anti-pTOB1, pc	human TOB around the phosphorylation site of serine 164 (A-V-SP-P-T)	Citrate	10	Ab78915, Abcam

2.4.4 Immunohistochemistry

Day 1 of immunohistochemistry protocol was identical to that of immunofluorescence, as described in the previous section (2.4.3). On day two, unbound primary antibody was removed with three 10 minute PBS washes before incubating sections with Biotinylated secondary antibodies (Vector laboratories) at room temperature for 1 hr. While the secondary antibody was binding, the ABC complex that binds to, and effectively amplifies the signal from, the biotinylated secondary antibody was made from the reagents in the Vectastain® Universal Elite ABC kit (Cat no PK-6200, Vector Laboratories). After washing off unbound secondary antibody with two 5 minute PBS washes, sections were incubated with ABC complex at room temperature for 30 minutes. Unbound ABC complex was washed off before the incubation of sections with DAB (3, 3' –diaminobenzidinie) HRP (horseradish peroxidase) substrate to produce a brown reaction product wherever ABC complex-bound biotinylated secondary antibodies are bound. Sections were incubated for no longer than 5 minutes in DAB, in the dark, at room temperature. Once adequate immunolabelling was achieved, sections were washed in distilled water, and nuclei were counterstained in Haematoxylin (Leica Biosystems). Finally, sections were dehydrated through a series of increasing ethanol concentrations (70%, 95% and 100%, 2 mins in each), incubated in Histoclear (2 x 5 mins) and mounted in DPX mounting medium (VWR) in a fume hood.

2.4.5 Haematoxylin and Eosin staining

5 µm sections were dewaxed in Histoclear (two 5 minute incubations), rehydrated through a series of decreasing concentrations of ethanol (100%, 95%, 70% 2 mins each) and finally distilled water. Nuclei were stained in Harris Haematoxylin

(Leica Biosystems) for approximately 4 minutes, before being washed in tap water. Excess haematoxylin was leached out of sections using Acid Alcohol 1% solution (Leica Biosystems) and then washed in Scotts tap water substitute (Leica Biosystems). Cytoplasm was labelled using Eosin Y (Leica Biosystems) for 5 minutes and then washed in tap water before being dehydrated in an ethanol series (70%, 95%, 100% ethanol, 2 mins each), incubated with Histoclear (two 5 minute incubations) and mounted in DPX mounting medium (VWR).

2.4.6 Classification of immunolabelled follicles in ovarian sections

Stage of follicle development was classified by GC shape and extent of multilayering as described previously (Fenwick et al., 2011) and as illustrated in figure 2.2. A *primordial* follicle consists of a small oocyte surrounded by a single layer of flat GCs; some but not all GCs have cuboidalised in a *transitional* follicle; oocytes in *primary* follicles have begun to grow and are surrounded by a single layer of cuboidal GCs; *primary plus* follicles have an incomplete second inner layer of GCs; this second layer is completed in *secondary* follicles; *secondary plus* are classified as follicles with further GC multilayering but no antrum formation; *Antral follicle* development was classified according to development of the antrum.

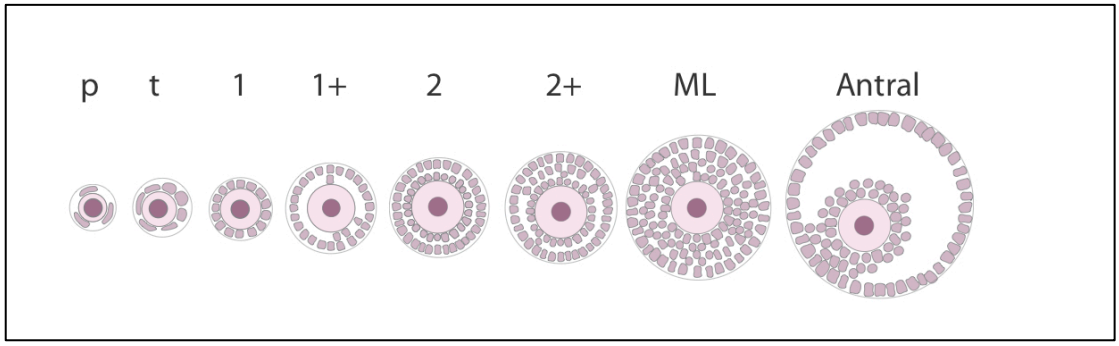


Figure 2.2. *Diagram illustrating the morphology used to classify different stages of follicle development. Key: p; primordial, t; transitional, 1; primary, 1+; primary plus, 2; secondary, 2+; secondary plus, ML; multilayered.*

2.4.7 Quantification of immunofluorescence by follicle stage

A central section from three d16 ovaries was immunolabelled with an antibody to the protein of interest as described in section 2.4.3. Sequential and overlapping images of the entire section were taken using a Leica inverted SP5 confocal laser-scanning microscope (Leica Microsystems, Wetzlar, Germany) with either a x40 or x63 oil objective. These images were compiled in DoubleTake (http://echoone.com/doubletake/) to create a high-resolution single image of the entire section, which is at the same scale as the original images. This composite image was opened in Image J (version 1.42) on a 'primary computer'. An iPad was connected via wifi, using the programme AirDisplay (http://avatron.com/apps) to the primary computer, which allowed us use the iPad as a second monitor showing ImageJ, and enable us to quickly and accurately delineate the GCs using a stylus (Bamboo stylus, Wacom) for touch screen. Protein expression was quantified by splitting the DoubleTake image, in which the scale was set to pixels/μm^2, into a 'RGB stack'. A threshold level of expression, specific to each ovary, was set that defined the boundary between presence/absence of expression. The threshold of presence/absence was set manually by matching the threshold labelling in the RGB stack with the green labelling observed in the original RGB image. For all follicles with a visible oocyte, the GC area was delineated using the stylus and the cursor tool in ImageJ and the number of pixels that met or exceeded the threshold value were measured. Additionally, the total GC area was measured and each follicle measured was given a unique ID so results in excel could be correlated with Image J tiff files.

2.4.8 Quantification of Immunofluorescence by follicular location

Protein expression was quantified as described above in section 2.5.1. However, for each follicle measured, xy co-ordinates for that follicle were simultaneously measured. After all follicles had been measured, regular XY co-ordinates around the OSE were acquired, to allow calculation of the distance of follicles from the surface. These data were processed using a custom built MATLAB programme (courtesy of Dr Carina Dunlop, University of Surrey), which generated the distance of the centre of each analysed follicle from the OSE.

2.5 EGFR protein analysis

2.5.1 Protein extraction for Western blot analysis

Follicles were pooled into groups of either 50 or 100. Whole tissue (adult ovary and liver) and pooled follicles were washed in ice cold PBS, collected into radioimmunoprecipitation assay/ sodium dodecyl sulfate (RIPA/SDS) buffer (1% Nonidet P-40 Substitute, 1% Triton X-100, 0.1% SDS, 150 mM $NaCl_2$, 10 mM Tris-HCl pH 8.0, 2 mM NaF, 0.2 micron filtered) and snap frozen in liquid nitrogen. Once thawed, samples were lysed in RIPA buffer supplemented with PhosSTOP phosphatase inhibitor cocktail tablets (Roche, Sussex, UK) and Complete mini protease inhibitor cocktail tablets (Roche, Sussex, UK). Tissue was physically disrupted using a pestle, whereas follicle samples underwent sonication in a sonicating waterbath (Bioruptor, Diagenode, Belgium) for 3 cycles of 30 seconds on, 90 seconds off. Subsequently, all samples (tissues and follicles) were agitated at 4 °C for 20 minutes on a rotary wheel before being centrifuged 13 000 RPM for 5 minutes at 4 °C and stored at -80 °C.

2.5.2 Determination of protein concentration

Protein quantification was determined by Pierce TM BCA Protein Assay Kit (Pierce, Thermo Scientific, Cheshire, UK). This kit relies on the principle that a protein in an alkaline solution causes the reduction of Cu+2 to Cu+1. This cupruous cation (Cu+1) chelates with bicinchoninic acid (BCA) causing the formation of a purple complex. The intensity of this colour, and therefore the concentration of total protein, is determined by reading the absorbance of this water-soluble complex at 562 nm using an OPTI*max*^{TM} microplate reader (Molecular devices). Total protein content of the samples are calculated by reference to a set of BSA-containing standards of known protein concentrations (25-2000 µg/mL).

2.5.3 SDS polyacrylamide gel electrophoresis (SDS-PAGE)

Samples were added to equal volumes of Laemmli buffer and heated to 100 °C for 5 minutes. Denatured proteins were then resolved on discontinuous polyacrylamide gels. As EGFR is a large (175 kDa) protein, an 8% acrylamide resolving gel was used. The resolving and stacking gels were made as shown in table 2.3. APS and TEMED were added last to the mixture as these catalyse polymerisation of the gel. Immediately after adding TEMED, the resolving gel was poured into premade 1.5 mm plastic gel cassettes (Invitrogen, Paisley, UK) to approximately 6.5 cm deep. A small amount of water saturated Butan-2-ol was poured over the top to cover the resolving gel to ensure the gel polymerises level and did not dehydrate. Once the resolving gel had set, the Butan-2-ol was removed and the cassette dried before adding the stacking gel and a comb. Once the stacking gel was set, the cassette was placed in an Xcell Surelock Mini cell gel electrophoresis tank (Life Technologies) filled with 1 X SDS running buffer. The comb was removed and the samples (with loading buffer) were loaded alongside a weight marker

(ColorPlus prestained protein marker, broad range, NEB, UK) and the gel was run for 90 minutes at 125V (except where otherwise stated in results). The difference in pH of the stacking and resolving gels meant that all the proteins move through the stacking/resolving gel boundary at the same time so the relative amount of movement through the resolving gel does relate to protein size. The gel was then removed from the tank for transfer.

2.5.4 Western blotting

The Mini-PROTEAN 3 cell tank (Bio-Rad) was used to transfer resolved proteins from the gel onto a Hybond ECL nitrocellulose membrane (Amersham/GE Healthcare). The gel and membrane were sandwiched between Whatman filter paper (Fisher Scientific) in electrotransfer buffer (containing glycine, tris base, SDS and 20 % methanol) and the transfer was run for 2.5 hours at 100 V, 350 mA at 4°C, unless otherwise stated in results. Complete and even transfer was assessed by Ponceau stain (0.1% w/v Ponceau S Red powder, 5% v/v Acetic Acid) of the membrane between washes with distilled water and Coomassie Blue (BDH labs) staining of the gel. The membrane was then blocked with 5% milk (Marvel) at room temperature before overnight incubation with Rabbit anti-EGFR antibody (4267, Cell Signaling) in 5% BSA at 4°C. On day 2, following three 5 minute washes in 1x TBST, the membrane was incubated in goat anti-rabbit HRP-conjugated secondary antibody (P0448, DAKO) in 2.5% milk at room temperature for 1 hr. Following three 1x TBST washes again, protein bands were visualised by enhanced chemiluminescence using Luminata Forte Western HRP (horse radish peroxidase) substrate (Millipore) and the membrane was exposed to high performance chemiluminescence film (Amersham/GE healthcare) in a hypercassette (Amersham/GE Healthcare, Buckinghamshire, UK).

Table 2.3 *Recipe for Resolving and Stacking gels for SDS-PAGE*

	10 mL RESOLVING gel	10 mL STACKING gel
Water	4.6	6.8
30 % Acrylamide mix	2.7	1.7
1.5 M Tris (pH 8.8)	2.5	0
1.5 M Tris (pH 6.8)	0	1.25
10% SDS	0.1	0.1
10% APS	0.1	0.1
TEMED	0.006	0.01

2.6 Isolated follicle culture studies

A minimum of 5 follicles were cultured per treatment group in each plate. Each plate represented follicles from one ovary. A minimum of 4 plates (4 ovaries) were used in each culture experiment. With the exception of experiment presented in Figure 7.15, isolated follicles were cultured for 72 hours.

2.6.1 Isolated follicle culture in the presence of insulin

Preantral follicles were isolated from d15-16 ovaries (minimum of 4 ovaries) and cultured individually in 100 µl of culture medium in 96 well plates at 37°C, 5% CO_2 for up to 72 hrs. Basal culture medium was made as follows: α-MEM media (Gibco, Invitrogen, UK) supplemented with 0.1% BSA (cat no A7030, Sigma-Aldrich), 5 µg/mL Insulin Transferrin Selenium (ITS, Sigma), 120 U/mL Penicillin (Sigma) and 100 µg/mL Streptomycin Sulphate (Sigma). This mixture was then filter sterilized and aliquotted into culture wells. Plates were placed at 37 °C, 5% CO_2 for approximately 1 hour to equilibrate before follicle isolations.

2.6.2 Isolated follicle culture in the absence of insulin

Preantral follicles were cultured as described in previous section (2.6.1) with the exception of the culture medium. The culture medium used in experiments conducted in the absence of insulin was as follows: α-MEM media (Gibco,

Invitrogen, UK) supplemented with 0.1% BSA (cat no A7030, Sigma-Aldrich), 5 μg/mL Transferrin (Sigma), 5 ng/mL Sodium Selenite (Sigma), 1 μg/mL Linoleic acid, 75 μg/mL Penicillin and 100 μg/mL Streptomycin Sulfate.

2.6.3 Exogenous ligand

Powdered receptor grade EGF, extracted and purified from mouse submaxillary glands (cat no 01-102, Millipore) was reconstituted in α-MEM medium. An initial EGF dose response (5, 10, 100 ng/mL EGF) was performed in the presence of insulin as described in section 2.6.0 and 2.6.1 (Figure 7.3, n=4 ovaries) for 72 hours. In all subsequent experiments involving EGF stimulation in the presence of insulin, isolated follicles were stimulated with 10 ng/mL EGF. An EGF dose response (5, 10, 100 ng/mL EGF) was also performed in the absence of insulin as described in section 2.6.0 and 2.6.2 (Figure 7.7, n=4). All subsequent experiments involving EGF stimulation in the absence of insulin, isolated follicles were stimulated with 100 ng/mL EGF.

2.6.4 ErbB2 inhibition

The two small molecule tyrosine kinase inhibitors specific to ErbB2 used in this study were AG-825 (Cayman Chemical, Cambridge, UK) and ErbB2 inhibitor II (Millipore). Both inhibitors were reconstituted in Dimethyl Sulfoxide (DMSO). The effect of varying concentrations of AG-825 was tested on unstimulated (section 2.6.1, Figure 7.1, 1-20 μM AG-825, n=4) and EGF stimulated (section 2.6.3, Figure 7.4, 5-25 μM AG-825, n=6) isolated follicles over 72 hours in the presence of insulin. The effect of various concentrations of ErbB2 inhibitor II was tested on unstimulated (section 2.6.1, Figure 7.1, 0.5-10 μM ErbB2 inhibitor II, n=6) and EGF-stimulated (section 2.6.3, Figure 7.4, 5-10 μM ErbB2 inhibitor II, n=4) isolated follicle growth over 72 hours in the presence of insulin . The effect of 5 and 10 μM of both AG-825

(Figure 7.8, n=5) and ErbB2 inhibitor II (Figure 7.8, n=4) was investigated over 72 hours. All treatment groups, including vehicle control, contained equal concentrations of DMSO.

Antibody-mediated inhibition of ErbB2 was achieved using Trastuzumab, clinically known as Herceptin. Powdered Trastuzumab (kindly donated to us by the Ovarian Cancer Action Research Centre led by Professor Hani Gabra) was reconstituted in α-MEM medium. The effect of 10, 25 and 100 μg/mL Trastuzumab on EGF-stimulated isolated follicle growth in the presence of insulin was investigated over 72 hours (Figure 7.11, n=6). This experiment was repeated with the exception that EGF was only added subsequently at 24 hr (Figure 7.12, n=6) to allow Trastuzumab to block dimerisation before EGF was added.

2.6.5 Dual ErbB inhibition

Lapatinib Ditosylate is a small molecule tyrosine kinase inhibitor that is specific to both EGFR and ErbB2. Lapatinib Ditosylate (sc-202205, Santa Cruz Biotechnology) was reconstituted in DMSO. Lapatanib was tested in EGF-stimulated follicles both in the presence (0.5 and 1.0 μM Lapatinib, Figure 7.10, n=10) and absence (5 and 10 μM, Figure 7.9, n=4) of insulin over 72 hours. All treatment groups, including vehicle control, contained equal concentrations of DMSO.

2.6.6 EGFR inhibition

AG1478 (cat no 658552, Millipore) was used to inhibit EGFR in isolated preantral follicles. The effect of AG1478 was tested on unstimulated (2-10 μM AG1478, Figure 7.13, n=5) and EGF-stimulated (5 and 10 μM, Figure 7.14, n=8) isolated follicle growth in the presence of insulin over 72 hours. All treatment groups, including vehicle control, contained equal concentrations of DMSO.

2.6.7 Assessment of in vitro follicle growth and morphology

Images of follicles cultured in EGF ligand and/or EGFR and ErbB2 inhibitors were taken at 0, 24, 48 and 72 hr using a Nikon digital camera DXM 1200 attached to a Nikon Eclipse E600 light microscope. Follicle area was measured by drawing around the edge/outer limit of the follicles using the 'free hand' tool (either the basal lamina or proliferating cells depending on which defined the outer limit of the follicle) using Image J software (version 1.42).

Images and measurements were imported into a custom made FilemakerPro v11.0 (FileMaker, FileMaker Inc) database. This was a powerful tool that allowed the visualization and inspection of follicle morphology of each follicle throughout the culture period (Figure 2.3), allowing consistent exclusion of follicles that did not fulfil our inclusion criteria (see below). Each follicle is given a unique number allowing tracking back of any anomalous data during analysis. It also allowed error-free automatic calculation of $\log_{10}$ follicle area at each time point, as used previously by Fenwick et al. (Fenwick et al., 2013) for analysing follicle growth data. The difference in $\log_{10}$ follicle area (ie cumulative growth for each follicle compared to its starting size) between 0h and 24h, 48h, and 72h respectively, was also automatically calculated - this was termed "log relative area". Finally, the database facilitated easy sorting and export of growth data for follicles of different initial sizes (Figure 2.4).

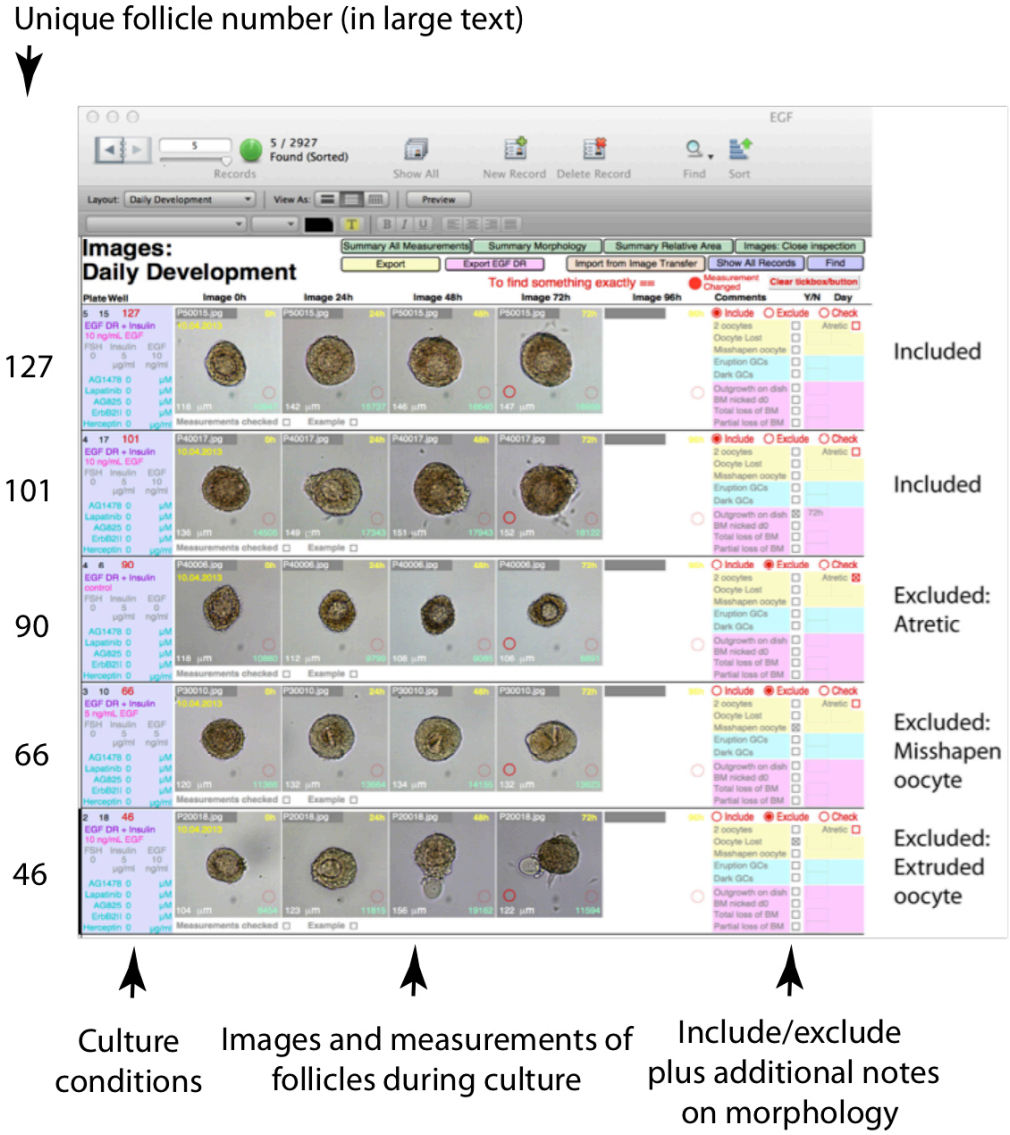


Figure 2.3. *Screen shot of FileMaker Pro follicle culture database illustrating the instances in which cultured follicles are excluded from analysis based on their morphology over the 72 hour culture period. The images and area measurements of every cultured follicle is entered into this database, assigned a unique follicle/data entry number, labelled as to what conditions it was cultured in (i.e. presence/absence of EGF or insulin or ErbB inhibitor) and then either included or excluded from further analysis based on images of the follicle in culture. The first entry shown (follicle number 127) is included as it has a spherical, centrally located oocyte, surrounded by proliferating GCs and an intact basal lamina. The basal lamina of the second entry (follicle number 101) is slightly ruptured at 24 hrs but the GCs that are 'escaping' are not dark and atretic at any point during culture and the oocyte is still spherical and centrally located by the end of culture. Therefore, this follicle is also included in analysis. The GCs of the third entry (follicle number 90) are very dark and atretic, and this follicle was therefore excluded. The oocyte of the fourth entry (follicle number 66) is not spherical at 24 hrs and this follicle was therefore excluded. The oocyte in the fifth entry (follicle number 46) is expelled from the follicle (extruded oocyte) and this follicle was therefore excluded from analysis.*

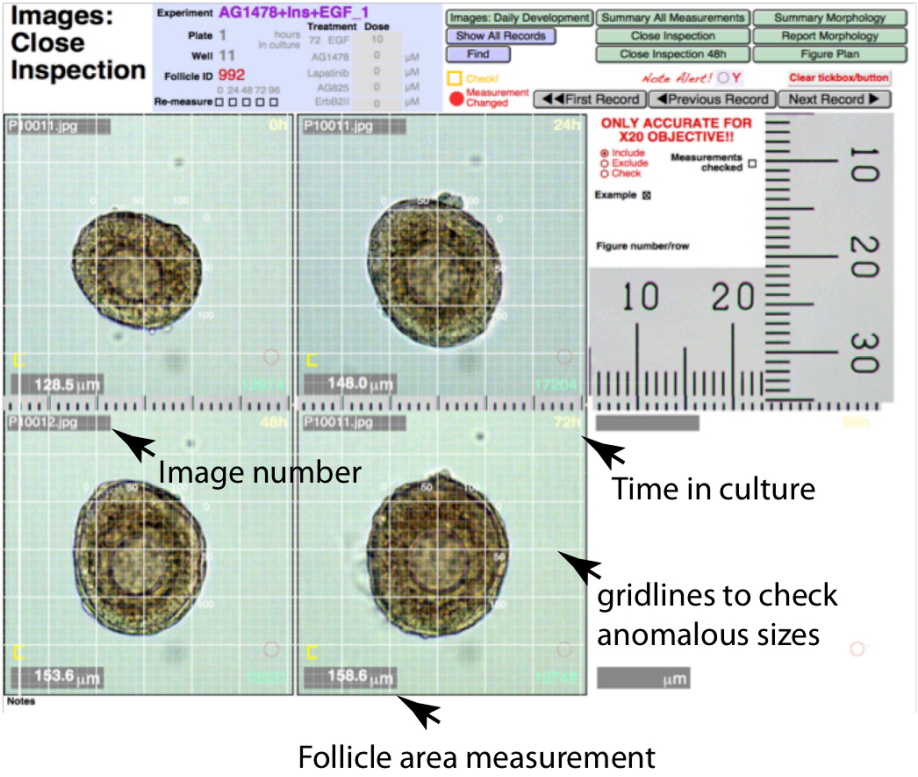


Figure 2.4. *FileMaker Pro layout with a measurement grid allowing close inspection of follicle development and checking of anomalous sizes. The follicle area measured is shown in turquoise in the bottom right, and the diameter that is calculated from this is shown in grey in the bottom left.*

Unhealthy follicles were excluded from analysis. Precise exclusion criteria were used (Figure 1.5). Unhealthy follicles were defined as those that (i) did not have a centrally located oocyte i.e. had an extruded oocyte (Figure 2.3, Follicle 46), (ii) did not have a spherical oocyte i.e. had a collapsed or misshapen oocyte (Figure 2.3, Follicle 66), or (iii) had dark GCs that are indicative of pyknotic nuclei and atresia (Figure 2.3, Follicle 90). Follicles were not excluded based on their follicle areas i.e. if follicle area decreased during culture, it was not automatically assumed that this follicle was dying. Follicles with a ruptured basal lamina were also included in analysis if they did not extrude their oocyte as (Figure 2.3, follicle 101) they remained

roughly intact and spherical and GCs usually carried on proliferating indicating it did not affect follicle growth.

2.7 Whole d4 mouse ovary culture studies

2.7.1 In vitro culture of whole d4 mouse ovary

Whole d4 ovaries were dissected out of ovarian bursa and away from extraovarian tissue and cultured under a thin film of Waymouth medium MB 752/1 (Gibco, Invitrogen, UK) on a Costar Transwell membrane (3.0 μm pore size, 24 mm diameter) above 1.5 mL of the same medium in 6 well plates (cat no 3414, Corning Inc, USA) as shown in figure 2.5. The thin film of Waymouth medium is thought to allow adequate oxygenation of the ovary and prevent necrosis. This Waymouth medium was supplemented with 0.23 mM sodium pyruvate, 75 μg/mL penicillin, 10 μg/mL streptomycin sulfate and either 10% FBS (as for the Lapatinib Ditosylate dose response experiment in Chapter 8.2.1) or 2% FBS (as for the EGF dose response experiment in Chapter 8.2.5) and changed every 48 hours. In the instances where either EGF or Lapatinib Ditosylate were added to the medium at 0 hr, they were also added to the medium at every medium change. Whole ovaries were cultured for a maximum of 8 days (EGF dose response ovaries collected at d5 of culture, Lapatinib dose response ovaries collected at d8 of culture) 37 °C and 5% CO_2 and photographed every day. They were subsequently processed for histology.

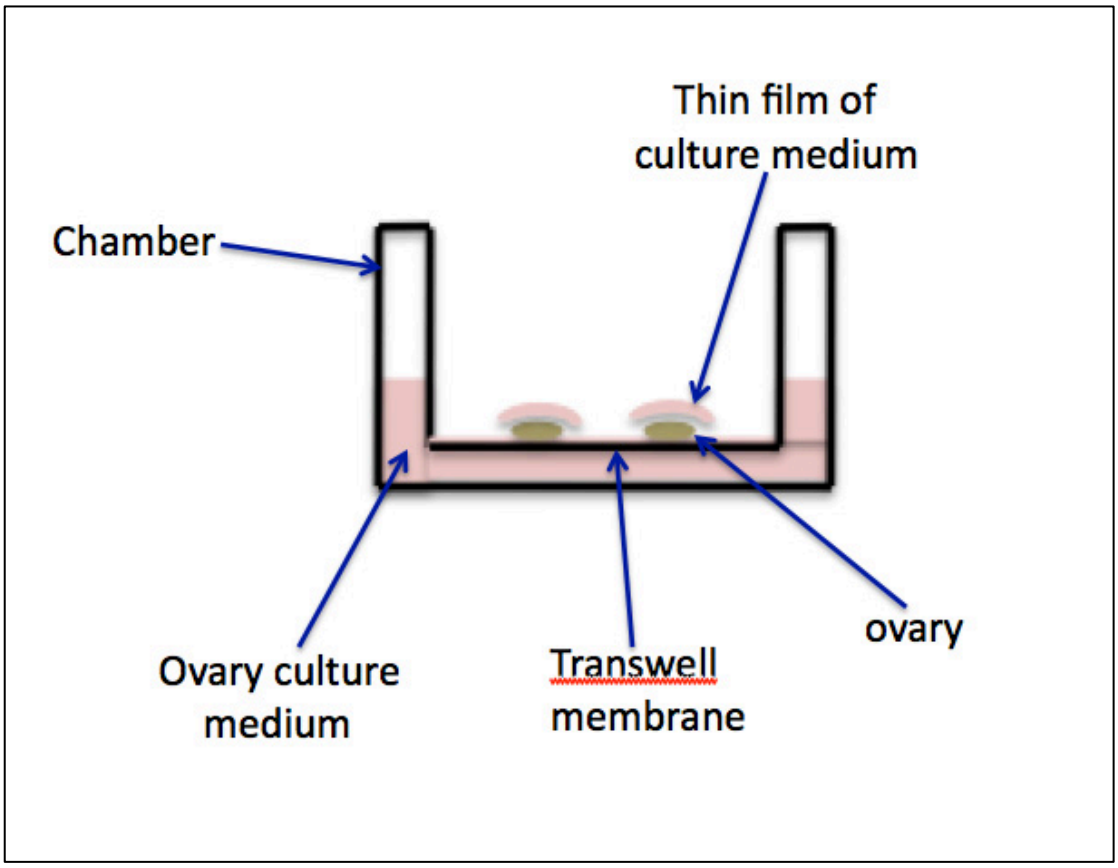


Figure 2.5. *Diagram depicting two ovaries cultured in an individual well of a 6 well plate. d4 ovaries were placed on polycarbonate Transwell® membrane inserts in a thin film of medium to allow adequate oxygenation of the ovary, above 1.5mL medium to support the ovaries nutritional and metabolic requirements for 48 hours.*

2.7.2 Fixing and processing of cultured ovaries

Cultured ovaries were carefully removed from the membrane using a 230 mm glass Pasteur pipette (VWR) and fixed in formalin for 3.5 hours. Following a wash in PBS, ovaries were incubated with Nuclear Fast Red solution (Sigma) for 20 minutes or until they had turned pink in colour. Following another wash in PBS these ovaries were incubated in 70% ethanol in which they could be stored for a few weeks. Ovaries were then dehydrated through an ethanol series: 70% for 30 minutes, 90% for 30 minutes, 100% for 3 x 10 minutes before being submerged in Histoclear for 1.5 hours. Finally, cultured ovaries were embedded in paraffin wax in plastic cassettes (as described in previous section) at 65 °C for 1.5 hours, then cooled on ice.

2.7.3 Double immunolabelling for VASA and laminin in cultured ovaries

5 μm sections from cultured ovaries were dewaxed in Histoclear (2 x 5 mins), rehydrated through a series of decreasing concentrations of ethanol (100%, 95%, 70% 2 mins each, and 5 minutes in distilled water). Antigen retrieval was performed by boiling slides for 20 minutes (replenishing evaporated buffer with distilled water to its original volume every 5 minutes) in Citrate buffer (10 mM citric acid, pH 6.0). Slides were cooled over ice and washed in PBS. Non-specific binding of antibody was reduced by incubating sections with 20 % normal goat serum for 30 minutes. Sections were then incubated in primary antibodies (simultaneously) overnight at 4 °C. Sections were incubated with (i) a rabbit anti-VASA antibody (cat no ab13840, Abcam) at a concentration of 3 μg/mL and (ii) a polyclonal rabbit anti-laminin antibody (cat no ab11575, Abcam) at a concentration of 6.9 μg/mL. The source of laminin used to generate the laminin antibody contained alpha, beta and gamma types of laminin and so it is probable that the antibody reacts to all three types, though this has not been directly tested at Abcam. Unbound primary antibody was removed in three 10 minute PBS washes the following day, before incubating sections with a goat anti-rabbit secondary antibody conjugated either Alexa Fluor 488 (Invitrogen). Excess unbound secondary antibody was washed off sections in two 5 minute PBS washes before counterstaining in 1 μg/mL DAPI (Invitrogen) for 3 minutes. Sections were mounted in Prolong Gold medium containing DAPI (Invitrogen). Sequential and overlapping digital images of the entire section were taken using a Leica inverted SP5 confocal laser-scanning microscope (Leica Microsystems, Wetzlar, Germany).

2.7.4 Follicle classification, counting and exclusion during analysis of VASA/laminin labelled cultured ovary sections

Follicle development in vivo and in vitro is not identical. Therefore, different methods of follicle classification and counting are used. As primordial activation is, in part, characterised by oocyte growth, the oocyte area as an indicator of follicle growth. Characterisation of primordial activation in vivo (Kate Hardy and Mark Fenwick, unpublished observations) revealed that the vast majority of primordial follicles had an oocyte area of less than 350 μm^2. Therefore, 350 μm^2 was used as the threshold area for non-growing/growing follicles i.e. all follicles with an oocyte area of this value or below were classified as non-growing and all follicles with an oocyte area above this value were classified as growing.

Follicles showing signs of cell death (pyknotic and/or fragmented nuclei, absence of VASA labelling in oocyte) were excluded. Additionally, follicles that had oocytes containing more than one DAPI-stained nucleus in the oocyte or immediately 'attached' to the oocyte were not included. Follicles in the OSE basal lamina were not included. Follicles containing multiple oocytes were included and every oocyte in these follicles was measured and included in analysis.

2.7.5 Measurement of area of VASA-labelled oocytes in cultured ovary

Images of immunofluorescent labelling in cultured ovaries were taken using a Leica inverted SP5 confocal laser-scanning microscope (Leica Microsystems, Wetzlar, Germany) with either a x40 or x63 oil objective. These images were compiled in DoubleTake (http://echoone.com/doubletake/) to create a high-resolution single image of the entire section, which is at the same scale as the original images. This composite image was opened in Image J (version 1.42) on a 'primary computer'.

An iPad was connected via wifi, using the programme AirDisplay (http://avatron.com/apps) to this computer which allowed us to quickly and accurately draw round oocytes using a stylus (Bamboo stylus, Wacom) for touch screen. The scale was set to pixels/μm^2 and follicles were selected, drawn around, measured, and then labelled with an oocyte number. Therefore, oocyte area measurements recorded on an Excel spreadsheet can be matched to these images.

2.8 Statistical analysis

All data was (initially) analysed using Graphpad Prism software (Graphpad software Inc, USA).

For the quantification of protein immunolabelling according to follicle stage described in Materials and Methods section 2.5.1 and results chapter 5, statistical analysis was achieved using one-way analysis of variance (ANOVA) with a post hoc Tukey's multiple comparisons test. For the quantification of protein immunolabelling according to follicular location described in Materials and Methods section 2.5.2 and results chapter 5, statistical significance was assessed by performing the Mann Whitney U test. Graphs presented the means and standard error of the means (SEM).

For the comparison of treatment groups in the isolated follicle culture experiments (see Materials and Methods section 2.7 and results chapter 7), one-way analysis of variance was initially used with a post-hoc Tukey's multiple comparisons test. However, the availability of a statistical programme, Stata 10 allowed correction for the fact that cultured follicles come from different ovaries. Therefore, more robust statistical analysis was performed by Professor Kate Hardy using Stata 10 for the Macintosh, as described below.

2.8.1 Statistic analysis of isolated preantral follicle and whole ovary culture experiments

Statistical analysis of follicle growth was carried out on $\log_{10}$ transformed data using $\log_{10}$ relative area (i.e. the difference in follicle area between 0h and 24h, 48h, and 72h respectively), using Stata 10 for the Macintosh (Stata Corporation, College Station, TX) by Professor Kate Hardy. The effect of treatment on follicle area was analysed at each timepoint using ordinary regression (regress command), using robust standard errors with clustering by ovary (using the 'cluster' command) (as previously described, Da Silva-Buttkus, 2008). This takes account of possible within-ovary correlation in follicle development, and the fact that follicles come from different ovaries, adjusting the errors (95% confidence intervals) accordingly. Multiple comparisons (for example, comparison of follicle area in five different treatment conditions) were corrected for multiple comparisons by multiplying the p value by the number of comparisons made.

In the whole ovary cultures, the proportions of growing follicles in the central sections were compared using logistic regression (logit command), with robust errors.

Chapter 3: PDGF family expression in the mouse ovary

N-cadherin is the major CAM in preantral follicles and it is upregulated during GC cuboidalisation (Mora et al., 2012). The PDGF family were considered a good candidate for regulation of N-cadherin during GC cuboidalisation as firstly, previous expression analysis in rat ovaries detected PDGFRα expression in cuboidalised GCs (Sleer and Taylor, 2007) and secondly, PDGFRα regulates N-cadherin during chick gastrulation (Yang et al., 2008). Expression of the PDGF family was characterised in rat ovaries by assessing mRNA expression in whole pre-pubertal rat ovaries by PCR and in situ hybridisation (ISH) and assessing protein localisation in formalin-fixed, paraffin-embedded and frozen sections of pre-pubertal rat ovaries using immunohistochemistry and light microscopy. In our experience, immunofluorescence and confocal microscopy allows higher resolution visualisation of immunolabelling and therefore, a better understanding of which specific cell compartment or microdomain a protein localises to. This is very important for this project as RTKs are known to intermingle with CAMs in the cell membrane to mutually regulate each other (Comoglio et al., 2003) and this project aims to investigate whether this is the case for N-cadherin in mouse GCs. Furthermore, the previous study in rat did not thoroughly examine primordial and transitional follicles that are the focus of my project. Therefore, we sought to characterise PDGF family (members of which are illustrated in Figure 3.1) expression in earliest follicle stages of the mouse ovary. PDGF mRNA expression was characterised in the mouse ovary in this project by assessing the presence or absence of PDGF transcripts in isolated preantral oocytes and follicles, antral GCs as well as whole ovary by PCR. Furthermore, protein was

localised in pre- and post-pubertal mouse ovaries using immunofluorescence and images were taken using a x63 objective (with optical zoom) on a Leica inverted SP5 confocal laser-scanning microscope (Leica Microsystems, Wetzlar, Germany) to assess the likelihood of PDGF-regulation of N-cadherin and primordial activation, a key step in follicle development that determines reproductive lifespan, in the mouse ovary.

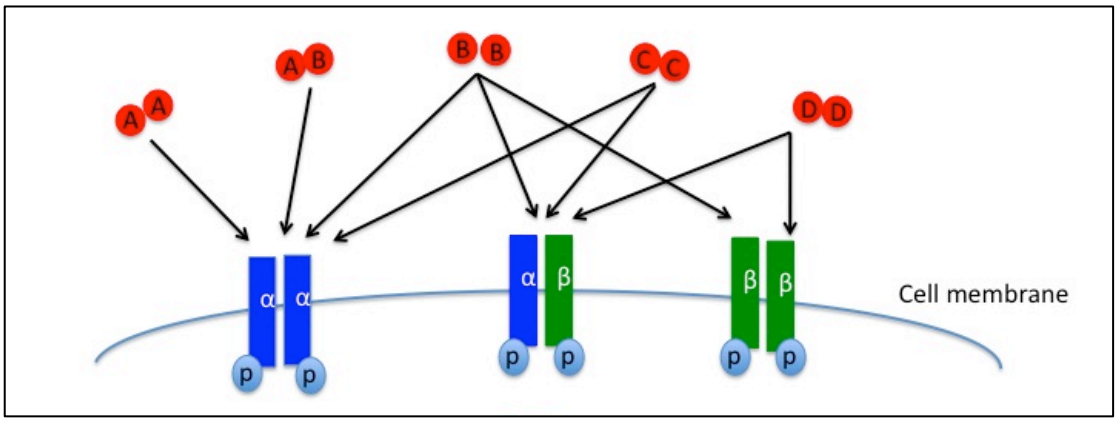


Figure 3.1. *Diagram showing all the possible dimeric combinations of PDGF ligand and receptors, and their specificity for one another.*

3.1 Results

3.1.1 PDGF receptor expression

3.1.1.1 PDGF receptor mRNA expression in the mouse ovary

An RT-PCR screen was performed to assess presence or absence of PDGF receptor and ligand transcripts in the mouse ovary by cell type and follicle stage, as described in materials and methods section 2.3.3. RT-PCR screen material consisted of primary, secondary and secondary plus stage follicles, and oocytes isolated from a d21 mouse, GCs from an antral follicle of an adult mouse and a whole ovary (d21) positive control and whole d21 oviduct control.

As seen in rat ovaries (Sleer and Taylor, 2007), *Pdgfrα* and *Pdgfrβ* mRNA transcripts were expressed in whole mouse ovary (d21). *Pdgfrα* transcripts were detected in all follicle stages, GCs and oviduct but not oocytes. *Pdgfrβ* was only convincingly detectable after 34 cycles of amplification in d21 ovary and oviduct (Figure 3.2). Expression of *Pdgfrα* in preantral follicles but not preantral oocytes suggests expression in preantral GCs. Therefore, PDGF receptor protein expression was investigated in whole mouse ovary using immunofluorescence.

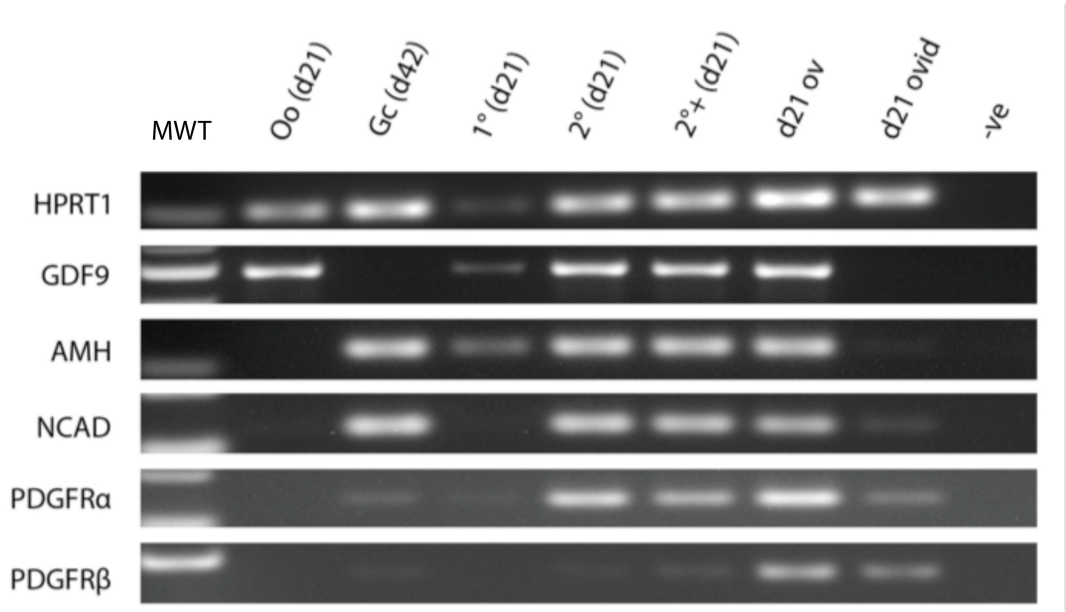


Figure 3.2. *RT-PCR screen showing presence or absence of transcripts for PDGF receptors and N-cadherin in oocytes, GCs, preantral follicles at the primary, secondary or secondary plus stages of development, ovary and oviduct. Gdf9 and AMH are included as control genes that are specific to the oocytes and GCs, respectively. Key: Oo; oocytes (~65-70 µm in diameter), Gc: antral GCs, 1°; primary follicles, 2°; secondary follicles, 2°+; secondary plus follicles, ov; ovary, ovid; oviduct, -ve; water control, MWT; molecular weight tracker.*

3.1.1.2 PDGF receptor protein expression in the mouse ovary

Spatiotemporal PDGF receptor protein expression was characterised in formalin-fixed, paraffin embedded ovarian sections obtained from pre- (d4, d12, d21) and post-pubertal (d42) mice by immunofluorescence as described in materials and methods section 2.4.3. Images from a minimum of 2 central sections from different

aged ovaries (n=8) were captured via confocal microscopy and at least 10 representative follicles at different stages were analysed. The stage of follicle development was classified as described in materials and methods section 2.4.6. This allowed characterisation of PDGF receptor protein expression with respect to (preantral) follicle stage (Figure 3.3) and ovarian age i.e. pre- or post-pubertal (Figure 3.5). Additionally, incubation of a control section with a Rabbit IgG control revealed that PDGF receptor immunolabelling was specific (Figure 3.4).

PDGFRα and PDGFRβ protein is expressed in a similar pattern (Figure 3.3). Both receptors are expressed in the membrane of theca cells in mice at all ages examined with the exception of d4 as on day 4 follicles are at the primordial and transitional stages, hence theca has not yet formed. All follicle stages that have a defined theca layer express PDGF receptors including secondary stage follicles (Figure 3.3A, 3.4A, B), large multilayered/early antral follicles (Figure 3.3C, C') and antral follicles (data not shown). However neither receptor is theca specific: both are also expressed in the membrane of stromal cells in some (Figure 3.3A, A', B', 3.4B, 3.5F), but not all (Figure 3.3B, 3.4A, 3.5E), ovaries. Furthermore, both PDGF receptors were expressed in the membrane of extrafollicular cells immediately adjacent to the basal lamina of primary follicles (Figure 3.3B, B') and also in a ring around primordial follicles in all age mice examined except d4 (Figure 3.3A, A'). It is not clear which compartments PDGF receptor is labelling in these primordial and primary follicles. We are unable to determine whether the immunoreactive cells surrounding primary follicles are theca or stroma as there is no established marker of theca formation. The smoothness of the ring of labelling in primordial follicles suggests that this might be the basal lamina, though it not as tightly enclosed around

the GC nuclei as you might expect. It is not possible to precisely determine if this is the case as an appropriate anti-Laminin antibody for double labelling is unavailable.

PDGFRα and PDGFRβ protein expression only differed significantly in d4 ovaries; PDGFRα is expressed in the rete ovarii only (Figure 3.5A, C) whereas PDGFRβ is expressed in the interstitial cells (Figure 3.5B) as well as the rete ovarii (Figure 3.5D).

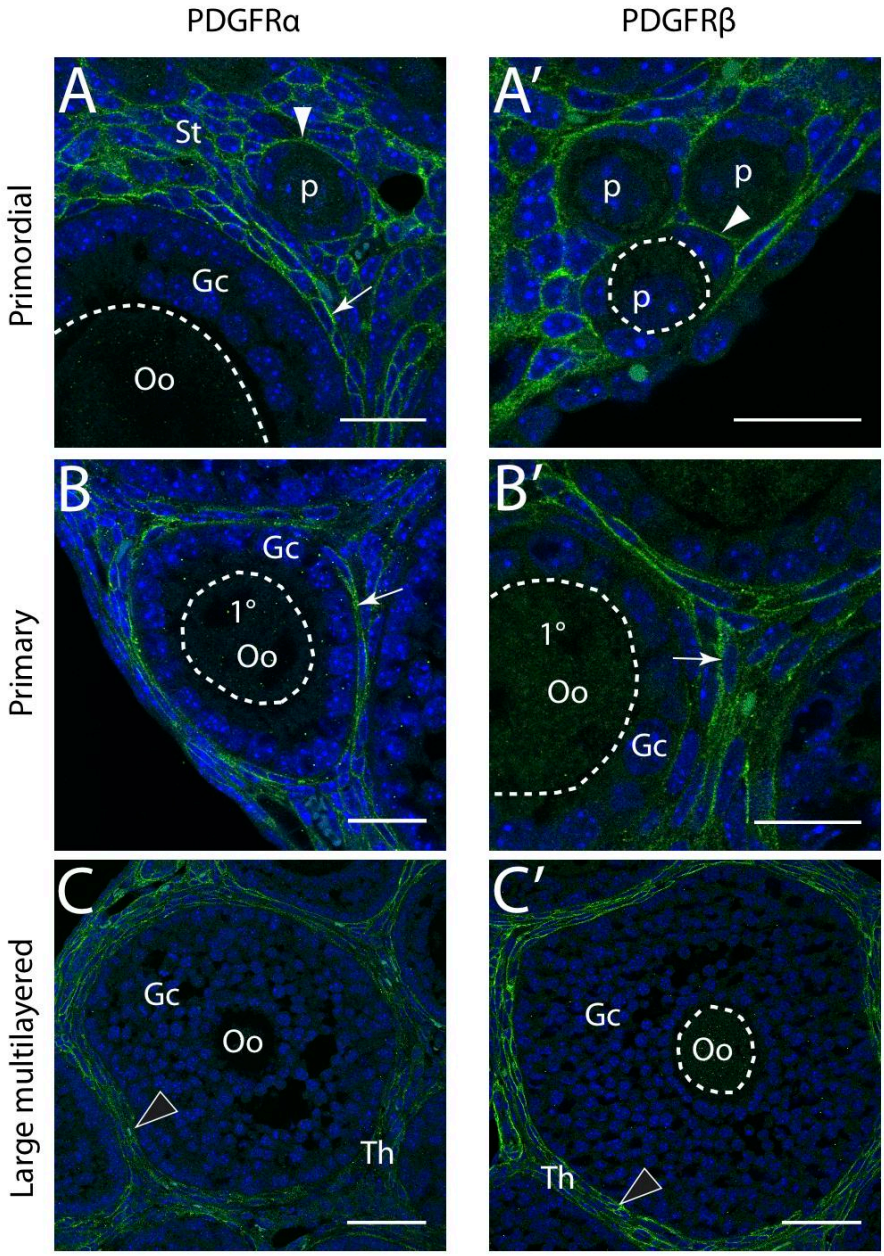


Figure 3.3. *Comparison of PDGF receptor isoforms (α and β) expression in pre-pubertal mouse ovaries. (A, A') PDGFRα and PDGFRβ were expressed in a ring around primordial follicles. (B, B') PDGFRα and PDGFRβ were expressed in putative theca cells of primary follicles. (C, C') PDGFRα and PDGFRβ were expressed in the morphologically identifiable theca of large multilayered follicles. PDGF receptor expression is shown in d12 (A-B') and d21 (C, C') ovaries. Key: Oo; oocyte, Gc; granulosa cell, Th; theca, St; stroma, p; primordial follicle, 1°; primary follicle. Scale bars represent 20 µm (A, A', B, B') and 50 µm (C, C'). White arrowheads represent PDGF receptor expression around primordial follicles. Black arrowheads represent PDGF receptor expression in mature theca. White arrows represent PDGF receptor expression in putative theca. Dotted lines represent oocyte/GC boundary.*

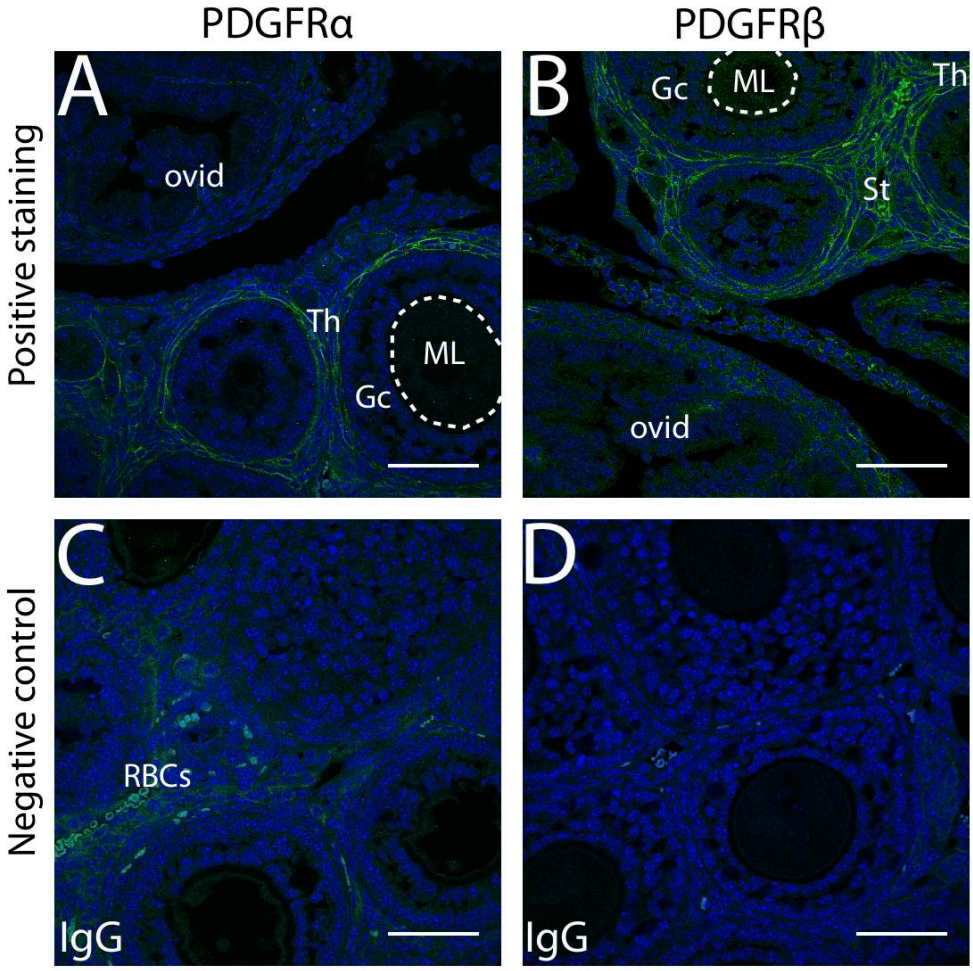


Figure 3.4. *PDGF receptor expression and IgG controls in d21 mouse ovary. PDGF receptor protein was localised to preantral follicles (green, A-B). Nuclei were stained with DAPI (blue). Key: Gc; granulosa cell, Th; theca, St; stroma, ML; multilayered follicle, ovid; oviduct, RBCs; red blood cells. Scale bars represent 50 μm. Dotted lines represent oocyte/GC boundary.*

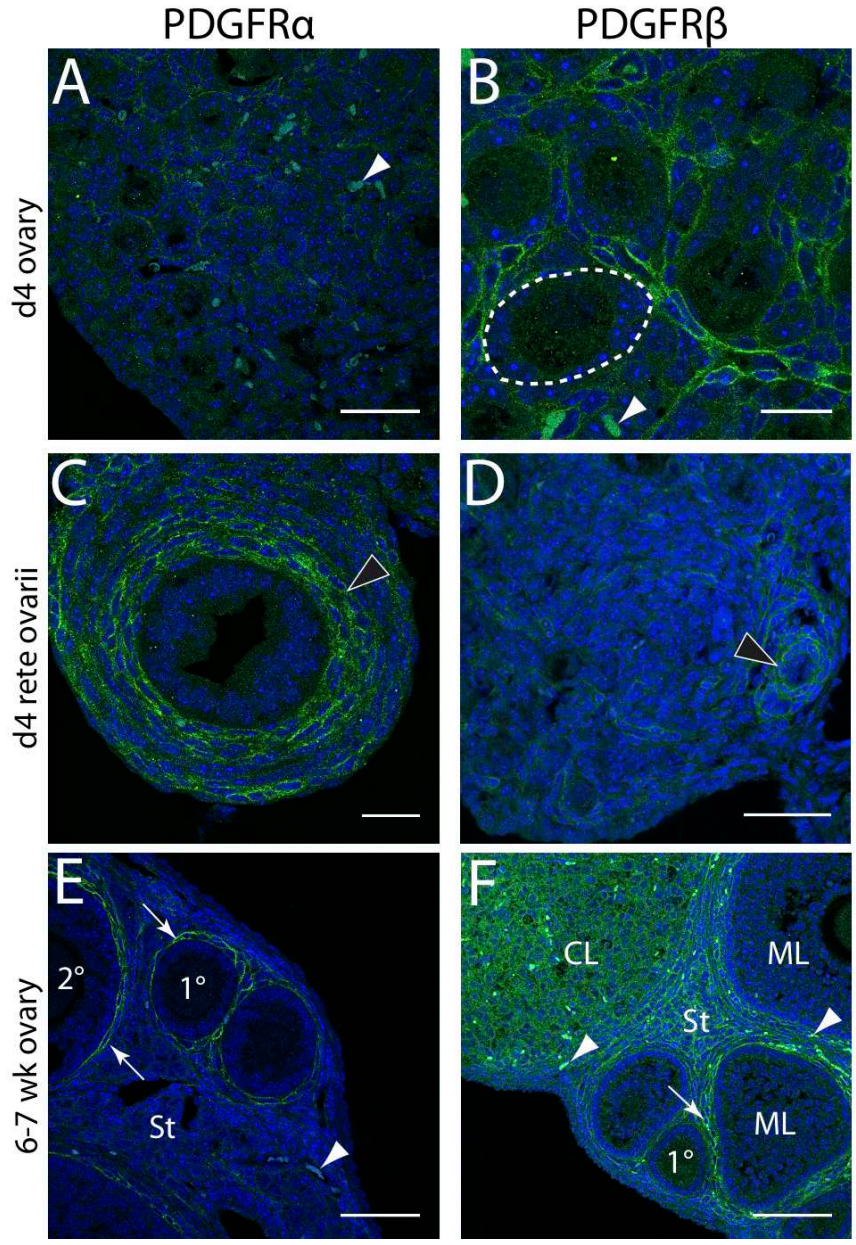


Figure 3.5. *PDGF receptor protein expression in mouse ovaries of various ages post-partum. PDGF receptor protein localisation in ovaries of 12 and 21 dpp is shown in a previous figure (Figure 3.3). PDGFRα was localised in the rete ovarii of a d4 ovary (green, C) but was not expressed in any other structure of the 4 ovary (green, A). PDGFRα also localised to theca in 6-7 week ovaries (green, E). PDGFRβ was localised to interstitial cells (green, B) and the rete ovarii (green, D) of a d4 ovary. PDGFRβ was also expressed in the theca of 6-7 week ovaries (green, F). Nuclei are labelled with DAPI (blue). Key: 1°; primary follicle; 2°; secondary follicle, ML; multilayered follicles, St; stroma, CL; corpora lutea. Scale bars represent 20 µm (B, C), and 50 µm (A, D-F). Nuclei are labelled with DAPI (blue). White arrowheads represent non-specific staining in red blood cells. Black arrowheads represent staining in the rete ovarii. White arrows represent staining in the theca or putative theca. Dotted lines represent basal lamina.*

Despite the indication from the RT-PCR screen that PDGFRα was expressed in GCs, PDGFRα and PDGFRβ protein was never observed in GCs of any follicle stage in mice of any age. This could suggest that there is untranslated PDGF receptor mRNA in GCs and follicles. Alternatively, it could suggest that mechanically isolated follicles still have theca cells attached which is likely to be responsible for *Pdgfrα* and *Pdgfrβ* expression in GCs. Recent confocal images of isolated follicles taken in our lab (M. Fenwick, unpublished observations; Figure 3.6) clearly show a single layer of very flat theca cells around the follicle so this scenario is possible. While PDGF receptor expression in the theca and stroma is consistent with previous expression analysis in rat ovaries, we did not observe PDGFRA protein in the membrane of GCs and oocyte cytoplasm as the previous study did (Sleer and Taylor, 2007). Closer examination of Figure D, E and F in the paper by Sleer and Taylor (2007) suggest that it is likely that PDGFRA is expressed in the GCs of antral follicles, and that no labelling was visible in follicles that were clearly preantral (Figure 2C, Sleer and Taylor, 2007). The previous study localised PDGF receptor protein to rat ovary sections using immunohistochemistry in both formalin-fixed and cryostat sections whereas this study localised PDGF receptor protein to formalin-fixed mouse ovary sections by immunofluorescence using a different antibody to the one used in the rat study. Therefore, the observations from these two studies are unlikely to be identical. However, neither study localises PDGF receptor protein to preantral GCs.

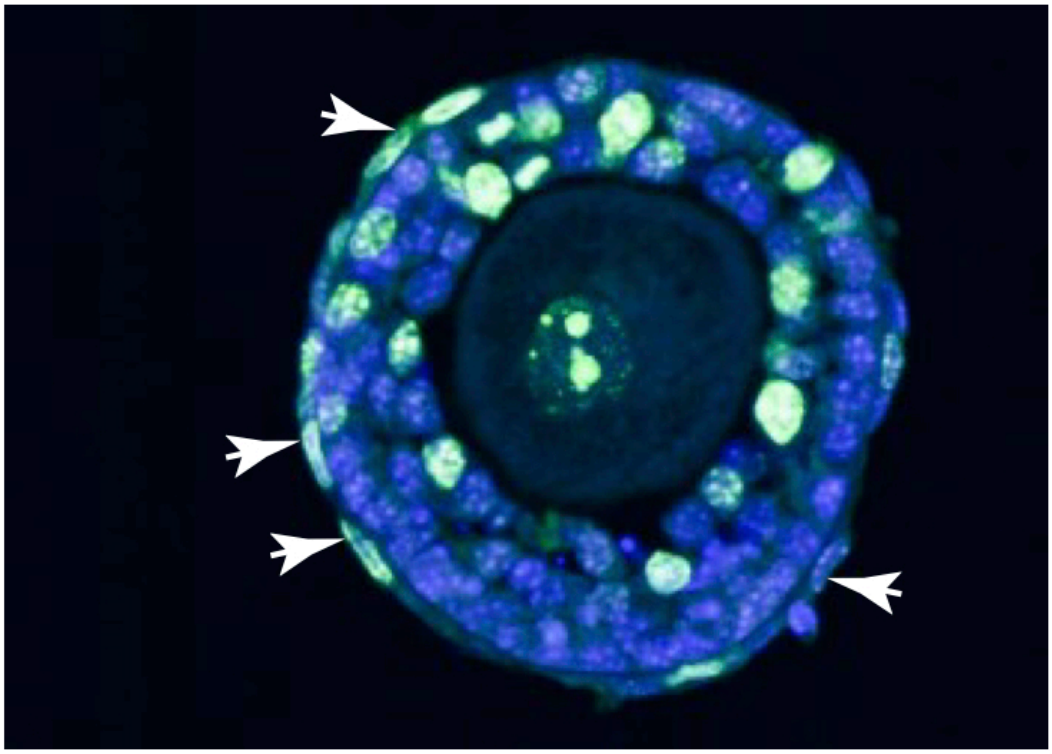


Figure 3.6. *An isolated preantral follicle, immunolabelled with antibodies to Ki67, with a single layer of flat (putative) theca cells around the basal lamina. White arrows represent putative theca cells. Image courtesy of Mark Fenwick.*

As PDGFRA protein was only observed on the stromal side of the basal lamina we wanted to examine whether *Pdgfrα* expression in preantral follicles was due to theca 'contamination' of follicle samples or untranslated *Pdgfrα* message in preantral GCs. Therefore, we repeated the RT-PCR screen and included *Cyp17α* as a marker of mature theca (Figure 3.7). Two of each of the following samples were used: oocytes from preantral follicles, GCs aspirated from an antral follicle, multilayered follicles and whole d21 ovaries. *Pdgfrα* and *Pdgfrβ* expression was as before; *Pdgfrα* message was detected in preantral follicles and d21 ovary whereas *Pdgfrβ* was only convincingly detectable in d21 ovary. A faint product for *Cyp17α* was barely detectable in the first GC sample and both follicle samples indicating slight theca contamination of these samples. However *Pdgfrα* was clearly expressed

in preantral follicles. This could be due to *Pdgfrα* mRNA expression in immature, or putative, theca that express PDGF receptor protein but not *Cyp17α*. It is therefore still unclear whether there is untranslated PDGF receptor mRNA in GCs and follicles or theca 'contamination' of GC and follicle samples. However, the absence of receptor protein in GCs suggests that PDGF does not play a role in GC cuboidalisation.

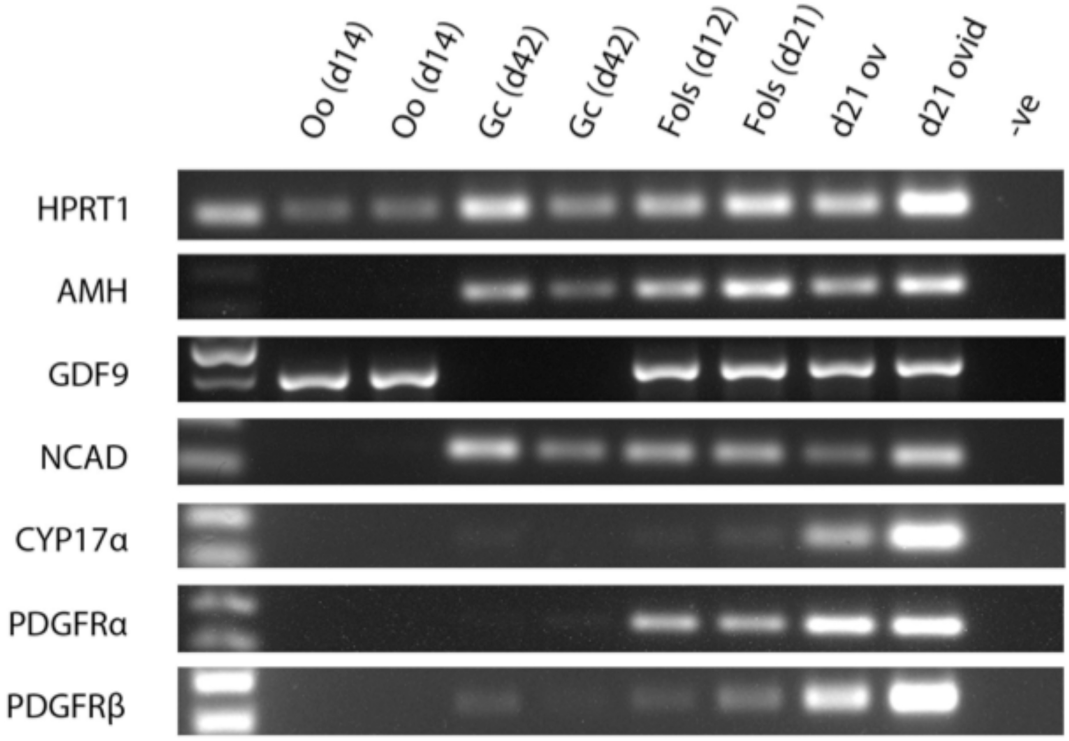


Figure 3.7. *RT-PCR screen of oocytes, GCs, follicles and ovaries showing presence or absence of transcripts for the PDGF family and N-cadherin. Gdf9 and AMH and Cyp17α are included as control genes that are specific to oocytes, GCs, and theca, respectively. Key: Oo; oocyte, Gc; granulosa cells, ov; ovary, ovid; oviduct, -ve; water control, NCAD; N-cadherin.*

3.1.2. PDGF ligand expression in the mouse ovary

3.1.2.1 PDGF ligand mRNA expression in the mouse ovary

Similar to rat ovaries (Sleer and Taylor, 2007), mRNA for all PDGF ligands were expressed in whole ovary (Figure 3.8). No PDGF ligand mRNA was detected in oocytes, however, *Pdgf-b* and *Pdgf-c* were both expressed in antral GCs. All PDGF

ligands were amplified in preantral follicle samples. Despite the absence of PDGF receptor protein in GC membranes we investigated PDGF ligand protein expression as GCs of recently activated follicles are hypothesized to secrete a Theca Differentiating Factor (TDF) (Skinner, 2005) and transcripts for *Pdgf-b* and *Pdgf-c* are detected in GC samples.

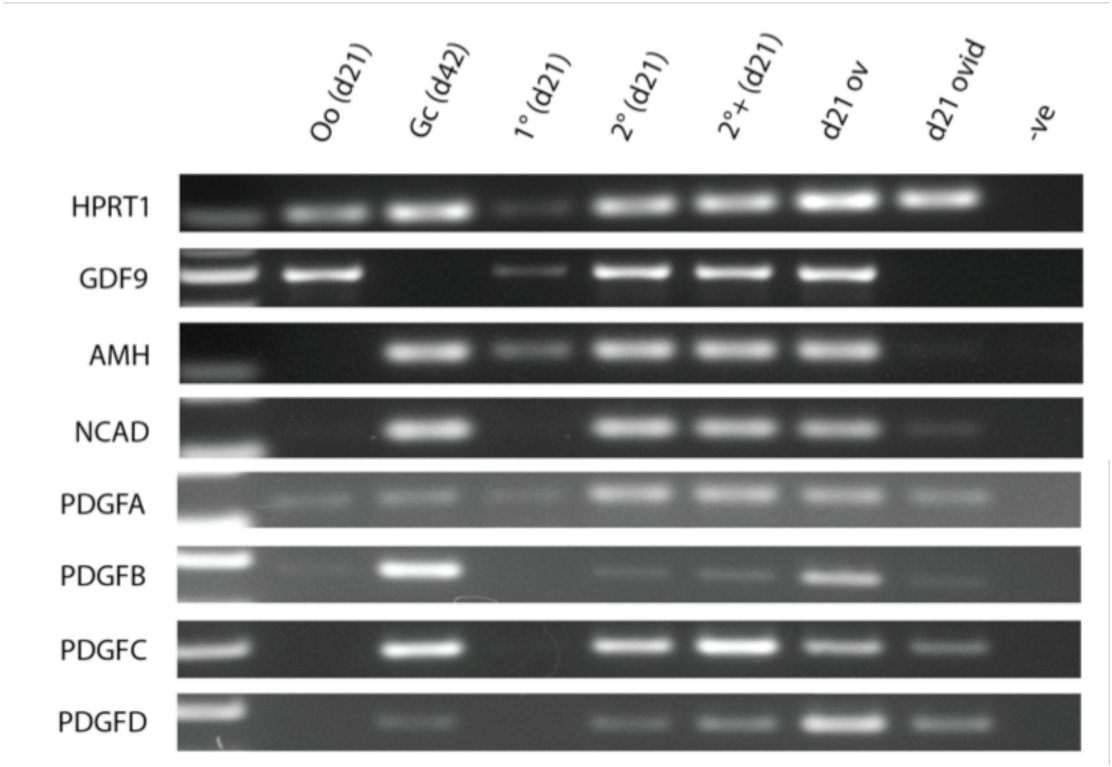


Figure 3.8. *RT-PCR screen of oocytes, GCs, follicles and ovaries and oviduct showing presence or absence of transcripts for the PDGF ligands and N-cadherin. Gdf9 and AMH and Cyp17α are included as control genes that are specific to oocytes, GCs, and theca, respectively. Key: Oo; oocyte, Gc; granulosa cells, ov; ovary, ovid; oviduct, -ve; water control, NCAD; N-cadherin.*

Table 3.1. *Summary of PDGF family mRNA expression in the mouse ovary*

	Receptor		**Ligand**			
	PDGRα	PDGFRβ	PDGFA	PDGFB	PDGFC	PDGFD
Oocytes	-	-	-	-	-	-
Antral GCs	+/-	+/-	+/-	+/-	+/-	+/-
Preantral follicles	+	+/-	+	+/-	+	+/-
Pre-pubertal ovary	+	+	+	+	+	+

Key: -; absence of transcript, +/-; faint/ambigious band, +; presence of transcript.

3.1.2.2 PDGF B ligand protein expression in the mouse ovary

Suitable commercial antibodies were available for PDGF-B and PDGF-C only. No immunolabelling was observed using a rabbit anti-PDGF-A polyclonal antibody (Cat no 07-1436, Millipore) or a rabbit anti-PDGF-D polyclonal antibody (Cat no 40-2110, Invitrogen). Therefore, only the protein expression of PDGF-B and PDGF-C was characterised.

Spatiotemporal PDGF-B protein expression was characterised with respect to preantral follicle stage (Figure 3.9), ovarian age (Figure 3.10) using immunofluorescence as described in Materials and methods section 2.4.3. Additionally, incubation with a control section with an IgG control revealed that PDGF-B staining was specific (Figure 3.11).

Consistent with data from the RT-PCR screen, PDGF-B protein was expressed in all stages of preantral follicle development (Figure 3.9, 3.10, 3.11) and d21 oviduct

(Figure 3.11A). There are three different isoforms of PDGF-B: a minor secreted form, a major cytoplasmic form, and a transient membrane form (Ostman et al., 1992). As PDGF-B staining sometimes appeared as though it might be labelling the membrane (Figure 3.9A, C), ovary sections were double labelled with antibodies to PDGF-B and β-CATENIN (Figure 3.9D). β-catenin is a linker protein (between cadherin protein and the actin cytoskeleton) that labels GC membranes in the mouse ovary (Mora et al., 2012). This double labelling demonstrated that PDGF-B expression was cytoplasmic. This was expected given that the antibody recognises the 24 kDa cell-associated form. Cytoplasmic PDGF-B staining was not homogenous but rather appeared as thin streaks, strongly suggesting that this is not background staining. These thin streaks are often lying close to the nucleus (Figure 3.9E) with the exception of GCs in a primary uni-layered follicle (Figure 3.9C, 3.10C) in which the nucleus is towards the basal lamina and PDGF-B is towards the oocyte.

PDGF-B was expressed in all ages of mouse ovaries examined but not in the same pattern. In pre-pubertal ovaries PDGF-B was expressed in the oocyte, GC, theca and stroma cytoplasm (Figure 3.9A-E, Figure 3.10A, C, E) and the basal lamina (Figure 3.9B, C, E, Figure 3.10A, C, E) whereas in adult 6-7 wk ovaries PDGF-B immunoreactivity was observed in the basal lamina only (Figure 3.10B, D, F). In pre-pubertal ovaries PDGF-B staining was observed in GC cytoplasm of all stages of preantral follicle development (Figure 3.9A-E, Figure 3.9A, C, E) including the early primordial stage (Figure 3.9A, B, Figure 3.10A). Primordial follicle formation has not yet been completed in a d4 ovary and so therefore ‘nests’ of naked oocytes and pre-GCs are still present. In d4 ovaries, PDGF-B is expressed in GC cytoplasm, as streaks, independent of whether they have been incorporated into follicles or not (Figure 3.9B). PDGF-B also labelled the basal lamina surrounding oocyte nests but

distinct PDGF-B immunolabelling in the basal lamina of primordial follicles was rare (Figure 3.9B). It was not possible to co-localise PDGF-B with laminin due to lack of an appropriate antibody combination and so it is unclear whether absence of PDGF-B in the basal lamina of primordial follicles is because the basal lamina has not completely formed around the primordial follicles yet.

PDGF-B immunolabelling also appeared punctate in preantral oocytes of ovaries from pre-pubertal mice (Figure 3.9E and Figure 3.10C). *Pdgf-b* transcripts were not detected in oocytes. It is possible that PDGF-B is only expressed in smaller oocytes compared to the ones used in the RT-PCR screen, which were, on average 67 μm in diameter and likely to have come from large multilayered or small antral follicles in pre-pubertal mice (Griffin et al., 2006). Manual collection of a pure sample of preantral oocytes is technically challenging, due to their small size, and when attempted did not provide sufficient RNA for analysis.

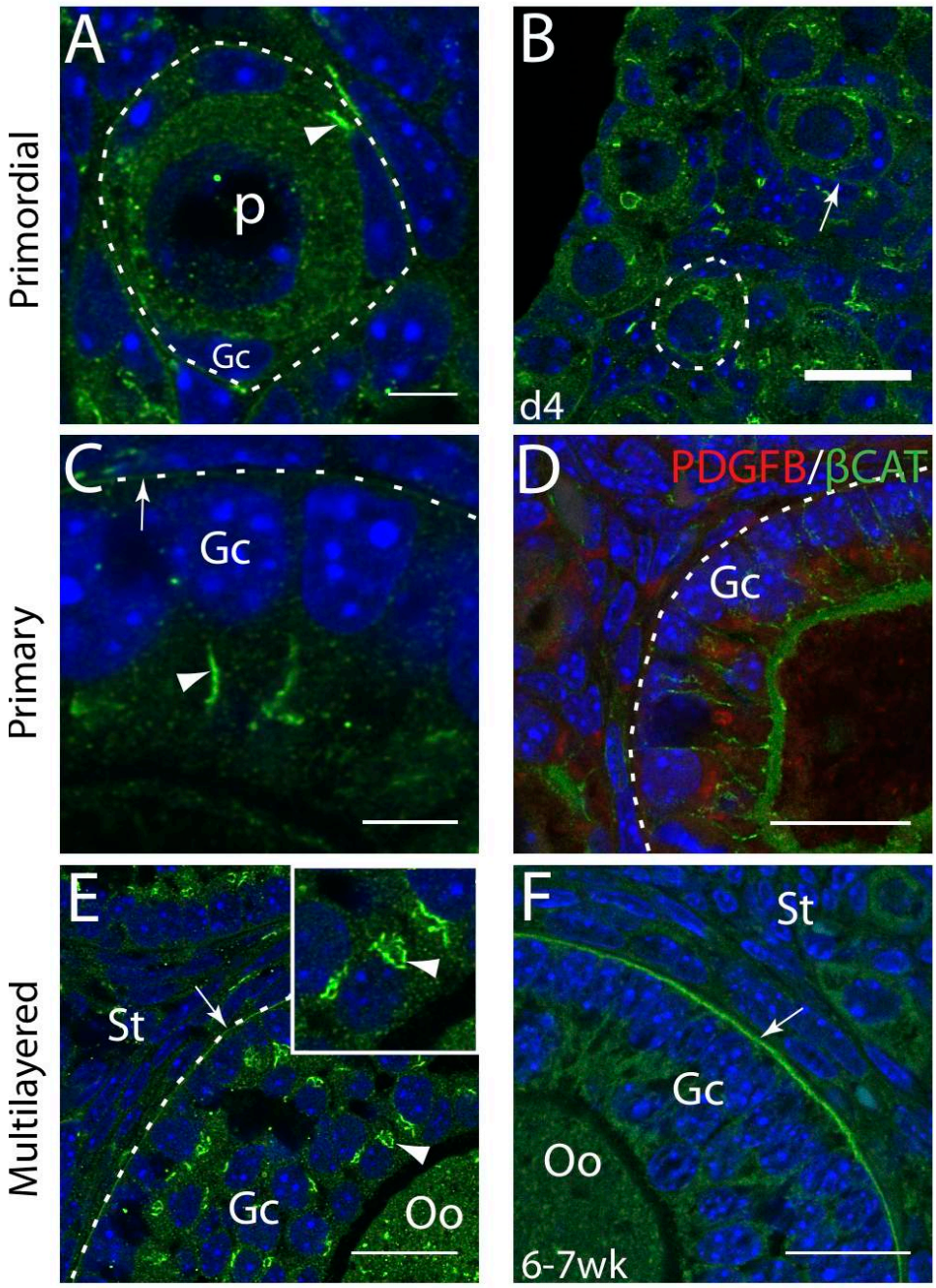


Figure 3.9. *PDGF-B expression (green) at successive stages of follicle development, in mouse ovaries of various ages post-partum. PDGF-B was localised in d4 (B), d21 (A, C-E) and 6-7 week (F) ovaries. PDGF-B was present in the basal lamina of follicles at all stages of preantral development, though only clearly in multi-layered follicles (E). PDGF-B was expressed as thin streaks in the GC cytoplasm of primordial (A, B), primary (C) and multilayered (E) preantral follicles in prepubertal ovaries but not preantral follicles of adult ovaries (F). Double immunolabelling with antibodies to PDGF-B and β-catenin confirmed that GC expression was indeed cytoplasmic (D). Punctate labelling was also observed in the oocytes of preantral follicles (E). Key: Oo; oocyte, Gc; granulosa cell, St; stroma, p;primordial follicle. Scale bars represent 5 µm (A, C) and 20 µm (B, D-F). White arrowheads represent cytoplasmic expression of PDGF-B. White arrows represent PDGF-B expression in the basal lamina. Dotted lines represent the basal lamina.*

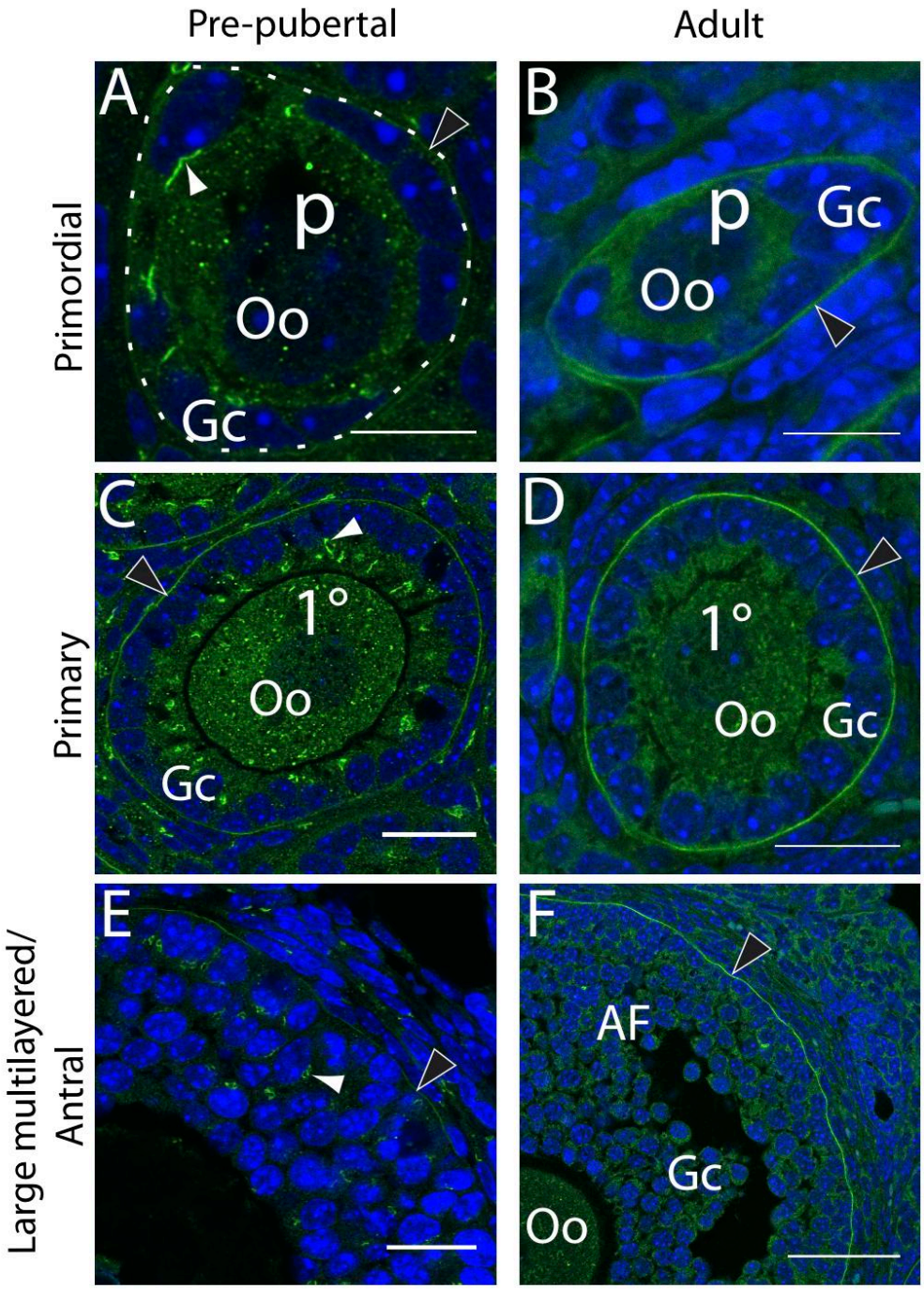


Figure 3.10. *PDGF-B protein expression in pre-pubertal and adult mouse ovaries. PDGF-B immunolabelling (green) was present in the GC cytoplasm and basal lamina of primordial (A), primary (C) and multilayered (E) preantral follicles in pre-pubertal mice but only the basal lamina of primordial (B), primary (D) and antral (F) follicles of an adult ovary. PDGF-B immunolabelling also appeared punctate in preantral oocytes in pre-pubertal ovaries (A, C). Nuclei are labelled with DAPI (blue). Key: Oo; oocyte, Gc; granulosa cell, p; primordial follicle, 1°; primary follicle, AF; antral follicle. Scale bars represent 10 µm (A, B), 20 µm (C, D) and 50 µm (E, F). White arrowheads indicate cytoplasmic PDGF-B expression. Black arrowheads show PDGF-B expression in the basal lamina.*

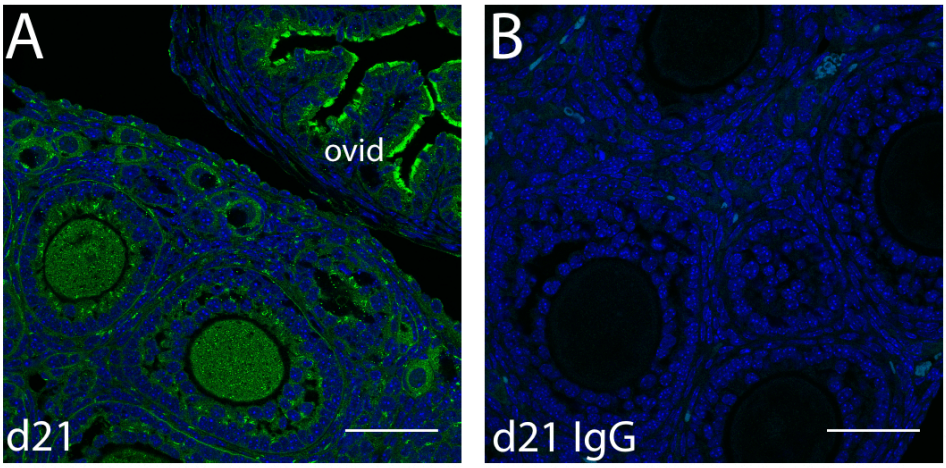


Figure 3.11. *PDGF-B expression in positive (A) and negative IgG (B) controls. PDGF-B was localised in d21 ovary and oviduct (green, A). Nuclei are labelled with DAPI (blue). Key: ovid; oviduct. Scale bars represent 50 µm.*

3.1.2.3 PDGF C ligand protein expression in the mouse ovary

Spatiotemporal PDGF-C protein expression was characterised with respect to cell type (Figure 3.12), and follicle stage (Figure 3.13) using immunofluorescence, as described in Materials and Methods section 2.4.3.

In contrast to the results of the RT-PCR screen, which clearly showed strong expression of *Pdgf-c* in antral GCs from a d42 mouse ovary and in isolated preantral follicles, but not in oocyte, PDGF-C protein was observed in the oocyte periphery (Figure 3.12A, C). Only oocytes of growing follicles express PDGF-C, the majority of which is localized to the cortex of the oocyte in a punctate pattern (Figure 3.12A, C). However, there are a small number of oocytes in which punctate PDGF-C is observed throughout the entire oocyte cytoplasm (Figure 3.12B). This is unlikely to be due to the section skimming the surface of these particular oocytes as the nucleus has been sectioned through. PDGF-C was never observed in non growing primordial follicles (Figure 3.13A-C) or newly activated transitional follicles (Figure 3.13B) indicating PDGF-C expression is not related to primordial activation. There are a few

instances, however, where the number of PDGF-C puncta steeply increases with the addition of a second layer of GCs (Figure 3.13C), indicating that the onset of PDGF-C expression is related to multilayering. However, PDGF-C protein expression does not appear to be upregulated with the addition of further GC layers (Figure 3.13D) and there are also cases where a uni-layered primary follicle has similar levels of PDGF-C protein as a multilayered follicle (Figure 3.13E). Therefore, the relationship between PDGF-C expression and multilayering is unclear. No change in PDGF-C protein expression was observed upon differentiation of these GCs as antral follicles displayed similar patterns of PDGF-C puncta as preantral follicles (Figure 3.13F). As a small number of dots of PDGF-C protein appeared as though they may be traversing the zona pellucida (ZP) (Figure 3.12B), ovary sections were co-labelled with PDGF-C and ZP-specific wheat germ agglutinin (WGA). This demonstrated that PDGF-C protein was restricted to the oocyte (Figure 3.12C).

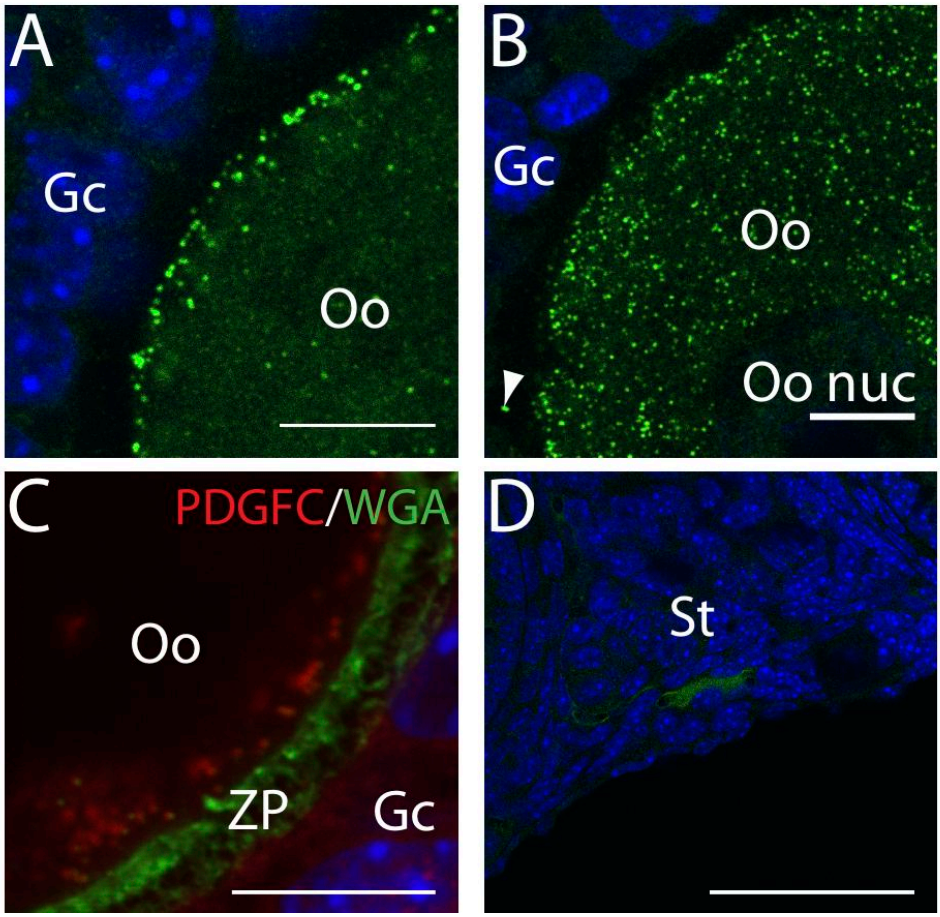


Figure 3.12. *PDGF-C expression in d21 mouse ovaries with respect to cell type and compartment. In the vast majority of follicles PDGF-C expression localised to the periphery of the ooplasm (A). However, there were a small number of oocytes in which PDGF-C was expressed throughout the ooplasm (B). Sometimes, puncta of PDGF-C expression appeared to be traversing the zona pellucida (arrowed, B). However, PDGF-C immunolabelling did not co-localise with WGA labelling (C) indicating that PDGF-C expression is restricted to the oocyte. (D) PDGF-C immunolabelling was occasionally observed in the stroma. Nuclei are stained with DAPI (blue). Key: Oo; oocyte, Gc; granulosa cell, St; stroma, Oo nuc; oocyte nucleus, ZP; zona pellucida, WGA; wheat germ agglutinin. White arrowheads represent PDGF-C expression that appears to be traversing the zona pellucida. Dotted lines represent the basal lamina. Scale bars represent 10 µm (A-C) and 50 µm (D).*

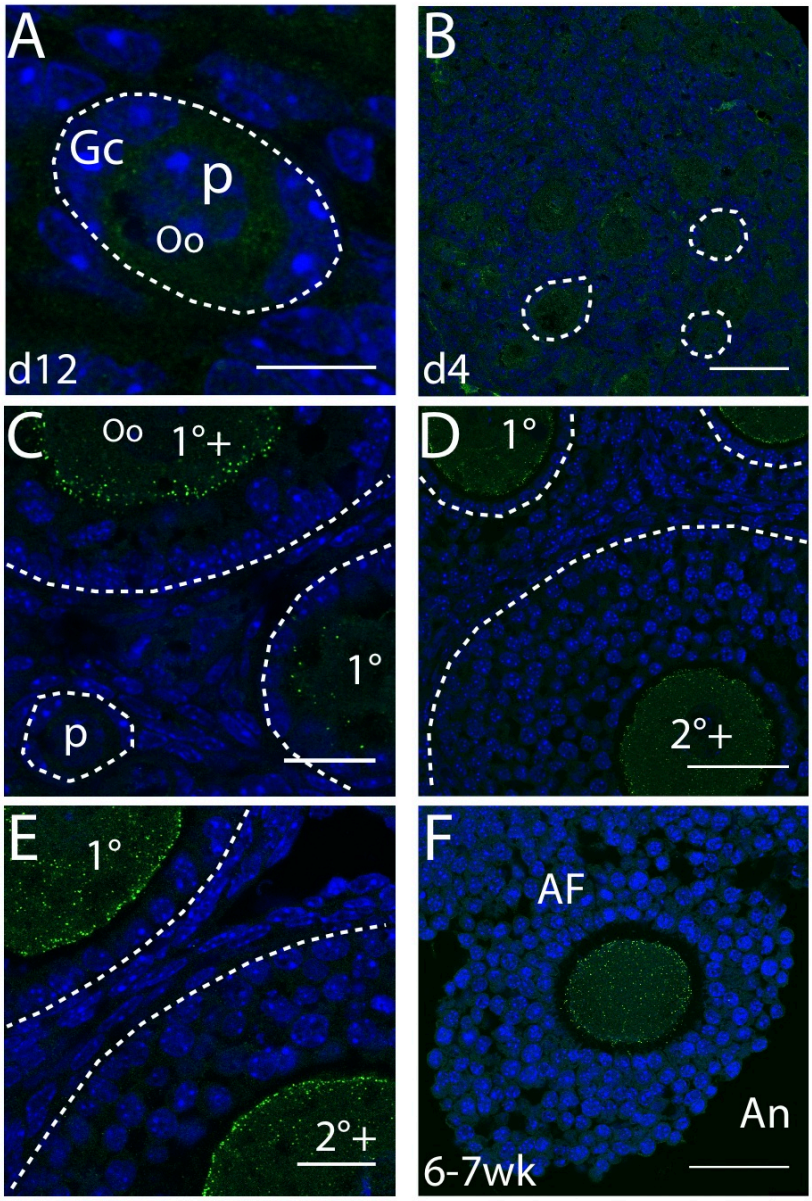


Figure 3.13. *PDGF-C expression in follicles at different stages of development. PDGF-C was not detected in primordial follicles in a d12 (A) or d4 (B) ovary. PDGF-C was expressed in the oocyte cytoplasm of growing preantral follicles from the primary stage onwards (C-E). There were instances in which the level of PDGF-C expression appeared to be related to multilayering (C) and those in which it didn't (D, E). PDGF-C was also expressed in the oocyte cytoplasm of antral follicles (F). Nuclei are labelled with DAPI (blue). Key: Oo; oocyte, Gc; granulosa cell, p; primordial follicle, 1°; primary follicle, 1°+; primary plus follicle, 2°+; secondary plus follicle, An; antrum, AF; antral follicle, cGC; cumulus granulosa cells. Dotted lines represent the basal lamina. Scale bars represent 10 µm (A) , 20 µm (C, E) and 50 µm (B, D, F)*

3.1.3 Summary of PDGF family results

- PDGF receptor expression
    - No protein observed in GCs at any follicle stage or mouse age investigated
    - In theca of multilayered follicles but also in somatic cells immediately adjacent to the basal lamina of primary follicles and in a ring around primordial follicles. These early stage follicles are not expected to have developed theca.
    - PDGFRα and PDGFRβ are also expressed, differentially, in the d4 ovary in which there is no theca present as follicles are all at the primordial or transitional stages of development. PDGFRα is expressed in the rete ovarii only while PDGFRβ is expressed in the rete ovarii and interstitial cells of the d4 ovary.
- PDGF ligand expression
    - PDGF-B expressed in the cytoplasm of oocytes, GCs, theca, and stroma and also the basal lamina in pre-pubertal ovaries.
    - Expression was not specific to a stage of follicle development
    - PDGF-C mRNA was amplified in GC samples but PDGF-C protein was localized to oocytes.
    - Only oocytes from growing follicles express PDGF-C.

3.1.4 Summary of comparisons of PDGF family expression in the mouse and rat ovary

The PDGF family were considered a good candidate for regulation of N-cadherin during GC cuboidalisation as firstly, previous expression analysis in the rat

ovary described PDGFRα expression in GCs (Sleer and Taylor, 2007) and secondly, PDGFRα regulates N-cadherin during chick gastrulation (Yang et al., 2008). Closer inspection of the PDGF receptor immunolabelling presented by Sleer and Taylor (2007) suggest that it is likely that PDGFRA is expressed in the GCs of antral follicles, and that no labelling was visible in follicles that were clearly preantral (Figure 2C, Sleer and Taylor, 2007). Therefore, PDGF receptors are expressed in the theca of pre-pubertal mouse and rat ovaries but not preantral GCs, hence, this family is unlikely to regulate N-cadherin. As PDGF receptor immunoreactivity was detected immediately surrounding primordial and transitional follicles and the GCs of recently activated follicles have been hypothesized to secrete a theca differentiating factor (TDF) (Skinner, 2005) we explored the possibility that PDGF ligands may be this hypothetical TDF. However, it seems unlikely that this is the case as PDGF-C protein was not observed in GCs and while PDGF-B protein was, it was not specific to this follicular cell type or stage.

Immunolabelling of PDGF-B and PDGF-C ligands localised to different compartments of the mouse and rat ovary. Specifically, while PDGF-B expression was previously observed in the theca, stroma and basal lamina of rat ovarian follicles, this study also localised PDGF-B protein to the GCs of the mouse ovary. Furthermore, this study only detected PDGFC protein in the oocyte and in very occasional bits of stroma, whereas Sleer and Taylor (2007) also observed PDGFC in theca. The previous study localised PDGF family protein to rat ovary sections using immunohistochemistry whereas this study localised PDGF family protein to mouse ovary sections by immunofluorescence using different antibodies. Therefore, the ‘disparity’ between these results may be due to either true species differences in

PDGF expression, the higher resolution employed when using confocal microscopy to image immunofluorescence or differences in antibody targets.

3.2 Discussion

3.2.1 The PDGF family are unlikely to be regulators of N-cadherin

Immunofluorescence for the PDGF receptors demonstrated PDGFRα and PDGFRβ expression in the theca and stroma of all ages of mouse ovaries analysed and also in a ring around primordial follicles of d12, d21 and 6-7 week ovaries but not d4. *Pdgfrα* was faintly detectable in GC samples but this is likely due to either slight contamination of samples with theca cells and/or use of too high a cycle number in PCR protocol (which enables non-specific amplification) or to small amounts of untranslated mRNA. The absence of PDGF receptor protein in the GC membranes means they are unlikely to be regulators of GC-specific N-cadherin. We would expect such a protein to colocalise with N-cadherin in GC membranes as AJs are often enriched in signalling molecules (Comoglio et al., 2003) and examples of growth factor regulation of N-cadherin in other cell types involved co-localisation of the growth factor receptor with N-cadherin (Theisen et al., 2007). We therefore ruled out the PDGF family as candidates in regulation of N-cadherin and GC cuboidalisation.

It has been hypothesized that GCs secrete a Theca Differentiation Factor (TDF) that recruits theca precursors to the follicle during the primordial-to-primary transition (Hirshfield, 1991a; Hirshfield, 1991b; Skinner, 2005). Therefore, a relationship between GC cuboidalisation and theca recruitment is in accordance with this hypothesis. As PDGF receptors are expressed in theca, we examined PDGF ligand expression to establish whether their expression pattern is compatible with the hypothesis that they are a TDF. Suitable commercial antibodies were only available

for PDGF-B and PDGF-C. PDGF-B was localised to GCs but it was not specific to a specific follicle stage suggesting onset of PDGF-B expression does not drive a distinct step in follicle development. PDGF-C protein was never observed in primordial or transitional follicles and only occasionally in primary follicles suggesting it is not involved in the primordial-to-primary transition. These are therefore unlikely to function, at least solely, as TDFs in the mouse ovary. We were unable to assess the likelihood of the remaining PDGF family ligands.

As both PDGF-B and PDGFRβ are expressed in primordial follicles, it is possible that PDGF-B/PDGFRβ signalling could be regulating primordial activation. However primordial activation begins as soon as follicles are formed, around 2-4 dpp in the mouse, and PDGF receptor is not expressed in a ring around primordial follicles of a d4 ovary. Therefore, it is unlikely that the PDGF family regulates the initial 'burst' primordial activation in the d4 ovary. It is possible that the PDGF family has a role in growth initiation of cortical primordial follicles in later life. The generally accepted, though not proven, model of primordial activation is that the GCs receive an initiation stimulus and then signal the oocyte to start growing. Therefore, PDGF signalling in the theca does not fit into this model. However, the role of extra-follicular cells on primordial activation has not been thoroughly investigated, mainly due to the difficulty in separating small primordial follicles from the rigid cortical stroma they are embedded in, in addition to their small size. Therefore, further investigation into PDGF signalling onto primordial activation could be an interesting avenue of future work.

3.2.2 PDGF receptors are candidate markers of theca formation

Immunofluorescence detection of PDGF receptors demonstrated their expression in the theca. This is consistent with previous studies in which these receptors have been localised to theca of rodent ovaries (Garnett et al., 2002; Sleer and Taylor, 2007) and PDGF receptors have also been demonstrated to regulate the steroidogenic activity of theca (Schmahl et al., 2008; Taylor, 2000). The data presented in this study suggests that PDGF receptors may have an additional role, earlier in development, in theca formation.

Theca formation is a poorly understood process, particularly in terms of when and from where theca progenitors arise. As yet, a marker for theca formation has not been identified. Theca cells are only clearly morphologically identifiable once they have differentiated into the plump steroid producing theca interna cells and the compact collagen-rich theca externa (Hirshfield, 1991b; Young and McNeilly, 2010). Both PDGF receptors are expressed in these theca cells. However, they are also expressed in cells surrounding earlier stage follicles. PDGFRα and PDGFRβ are both expressed in extrafollicular cells immediately adjacent to the basal lamina of primary follicles. These cells do also appear distinct from stroma cells even in the absence of immunofluorescent staining as they form a single tight ring of cells with approximately equally spaced, shaped and sized nuclei in an ordered fashion, that lie flat on the external face of the basal lamina. These cells are not typical of the stroma population. PDGF receptor labelling is able to completely de-lineate this compartment from the adjacent stromal cells in some, but not all, ovaries. In those ovaries in which it does not label the stroma, PDGF receptor does label cells

surrounding primary follicles. This suggests that these cells may be early or putative theca cells.

[^{3}H] thymidine infusion has been used to label the theca compartment in rat ovaries (Hirshfield, 1991b) and this predominantly, though not specifically, labelled theca in late stage follicles. Consistent with this study, [3]thymidine was also incorporated into the putative theca of primary follicles in rat. Therefore, PDGFR and [3]thymidine labelling in rodent ovaries suggests that a layer of theca has been recruited by the primary stage of follicle development. This would then suggest that theca recruitment is associated with, and perhaps of importance to, primordial activation. This is consistent with the previously discussed idea that GCs of recently activated follicles secrete a TDF. Interestingly, follicle development in Gdf9-deficient mice is blocked at the primary, uni-layered stage and a theca layer does not form around these follicles (Carabatsos et al., 1998). It would be interesting to see where PDGF receptor protein is expressed in these ovaries. Furthermore, the importance of theca recruitment to primordial activation could be approached by localising PDGF receptor in ovaries that have perturbed follicle initiation such as mice deficient for PTEN (Reddy et al., 2008) or Foxl2 (Schmidt et al., 2004).

The origin of the theca lineage is also poorly understood. Theca progenitors are presumed to originate in the stroma but whether a signal causes adjacent stroma cells to differentiate into theca (a TDF) or programmed theca progenitors are recruited from the surrounding stroma is unknown. If there are cells already programmed to become theca cells it is certainly not clear at what point theca progenitors arise in the previously homogenous stromal population (Young and McNeilly, 2010). Interestingly, while PDGF receptor expression is mainly characterized by consistent expression in the theca in d12, d21 and 6-7 wk ovaries, both PDGF receptors are also

expressed in d4 ovaries in which there is no theca as follicles are at the early primordial and transitional stages. PDGFRα and PDGFRβ are both expressed in the rete ovarii while only PDGFRβ is expressed in interstitial cells. It may be that theca cells originate from these immunoreactive rete ovarii and interstitial cells. However, it is also entirely possible that PDGF receptors have a separate role in the d4 ovary distinct from a role in the theca.

Further work involving lineage tracing would be required to fully validate the candidacy of these receptors as markers of theca lineage and theca recruitment.

3.2.3 PDGF family expression in the d4 ovary

Immunofluorescence detection of PDGF receptors revealed that only PDGFRβ was expressed in the interstitial cells of a d4 ovary. This is strongly suggestive that PDGFRβ is homodimerising in the d4 ovary. PDGF-BB, and PDGF-DD and PDGF-AB bind PDGFRβ homodimers (Figure 3.1). The homodimers PDGF-BB and PDGF-DD are high affinity ligands whereas PDGF-AB binds PDGFRβ homodimers with low affinity and is unlikely to be physiologically relevant (Fredriksson et al., 2004). PDGF-B protein was detected in d4 ovaries. All possible dimeric combinations are produced when both PDGF-A and PDGF-B chains are present (Hammacher et al., 1988; Hart et al., 1990; Heldin and Westermark, 1999). This suggests that PDGF-BB/PDGFRβ signalling is present in the d4 ovary. Suitable commercial antibodies to PDGF-A and PDGF-D were unavailable and meant we were unable to assess whether PDGF-BB was the only ligand present in the d4 ovary. The perinatal lethality of mice deficient in either PDGF-B (Leveen et al., 1994), or PDGFRβ (Soriano, 1994) precludes the investigation into the roles of PDGF-B and PDGFRβ in ovaries at 4 dpp in these mice. Conditional knock-outs can be generated

under the control of a specific promoter. As PDGF receptors are expressed in the theca, it would be sensible to conditionally knockout PDGFR expression is cells expressing a theca marker such as 17 alpha-hydroxylase/C17-20 lyase (P450(17 alpha)) enzymes (Cyp17α) (Gelety and Magoffin, 1997). However, as theca formation is poorly understood it is not possible to specifically ablate PDGFR expression in the cells of earlier stage follicles that PDGF receptor is localised to.

3.2.4 Regulation of PDGF-B biosynthesis and secretion

In contrast to PDGF receptor expression, the entirety of which is outside the basal lamina, PDGF ligands are also expressed in the oocyte and GC compartments enclosed in the basal lamina. Therefore paracrine signalling from specific cell types within the follicle (Oo- and GC-derived PDGF-B and Oo-derived PDGF-C) to multiple target cells outside the follicle (theca and stroma) is likely to occur in the mouse ovary. Cells and tissues can employ several methods to ensure a secreted ligand is delivered solely to its target cell, one of which is immobilisation/sequestration by the ECM (Schultz and Wysocki, 2009). Immunofluorescent detection of PDGF-B suggests that this may be the case in the mouse ovary as PDGF-B is present in the basal lamina and several somatic cell types of prepubertal ovaries whereas in adult ovaries PDGF-B expression is restricted to the basal lamina. It is possible that ECM components of the basal lamina of these follicles may be sequestering PDGF-B. The various laminin and collagen isoforms change during development (Irving-Rodgers et al., 2010) but this proposed sequestration event is specific to mouse age (adult ovaries) not follicle stage. Therefore, this suggests that the proposed sequestration event is more likely regulated by the fluctuating gonadotrophin levels during estrous cycles of the adult mice. This

is consistent with previous microarray data from FSH receptor knockout (FORKO) mice that demonstrated FSH regulation of PDGF family members (Chen et al., 2006).

In prepubertal ovaries, PDGF-B expression appeared as thin streaks or coils in the cytoplasm of GCs, theca and stroma as well as labelling the basal lamina. This suggests that PDGF-B is labelling a very specifc compartment of these somatic cells. This compartment may be an organelle involved in the processing of PDGF-B. PDGF-AA and PDGF-AB are quickly secreted following synthesis (Heldin and Westermark, 1990; Ostman et al., 1988) whereas only the minor 30 kDa form of PDGF-BB is processed in this way. In contrast, the major cytoplasmic form of PDGF-BB undergoes further proteolytic processing in the Golgi before being slowly degraded in lysosomes (Ostman et al., 1992). The antibody used to immunofluorescently detect PDGF-B recognises both PDGF-BB and PDGF-AB. Specifically, it recognises the 24 kDa cell associated form of PDGF-BB rather than the 30 kDa secreted form. This is consistent with PDGF-B expression labelling an organelle involved in it's processing. Lysosomal immunolabelling would be expected to be vesicular rather than 'streaky' suggesting the Golgi is a more likely candidate. Absence of a Golgi marker means we are unable to confirm this.

3.2.5 Discordance between PDGFC mRNA and protein expression

RT-PCR demonstrated GC-specific *Pdgf-c* expression whereas immunofluorescence revealed oocyte-specific PDGF-C expression. Nucleotide BLAST searches of the primer sequences and protein BLAST searches of the antibodies immunogen sequence show these irregularities are unlikely due to off target detection (data not shown). We cannot exclude the possibility that *Pdgf-c*

transcripts are only expressed in small oocytes, less than 65 μm in diameter, which are too small to isolate cleanly.

One possibility that was entertained during investigation of PDGF-C expression by immunofluorescence was that PDGF-C expression might only appear to be expressed in oocytes and actually be expressed in GCs towards the oocyte/GC interface. However double labelling with zona-pellucida specific WGA and PDGF-Cs expression throughout the entire ooplasm in some follicles suggests this isn't the case.

The proximity of PDGF-C protein to the zona pellucida is intriguing, however, when considering very recent work that has demonstrated that mRNA's can be trafficked from the GCs to the oocyte through TZP's in the transcriptionally silent mature oocyte (Macaulay et al., 2014). This raises the interesting possibility that *Pdgf-c* mRNA is synthesized in GCs, trafficked to the oocyte and translated into protein near the oocyte surface. However, it is unclear as to what the purpose of utilising this mechanism would be in an immature oocyte that is transcriptionally active. In situ hybridisation is a technique that allows spatial localisation of RNA in an ovarian section. However, this technique may not achieve a high enough resolution to detect mRNA traversing the zona pellucida. The localisation of PDGF family mRNA transcripts uniformly to the cytoplasm of specific cells by Sleer and Taylor (2007) suggests that this is the case. This is an interesting concept that is worthy of further investigation.

3.2.6 Possible regulation of PDGF-C expression by Cingulin

Cingulin is a protein that localises to, but is not required for assembly of, tight junctions and is involved in regulating gene expression and signalling (Citi et al.,

2009). Cingulin localises to the oocyte membrane in the mouse ovary (Mora et al., 2012), in a similar area to PDGF-C, although there are no functional tight junctions in mouse ovarian follicles. The role of cingulin in mouse ovarian follicles is unknown. However, PDGF-C gene expression is downregulated in cingulin knockout mice (Citi et al., 2009). Therefore, it is possible that cingulin may be regulating PDGF-C expression in the mouse ovary. This is an interesting hypothesis that is worthy of further investigation and future work will involve double labelling of mouse ovarian sections with antibodies to PDGF-C and cingulin.

3.3 Conclusions

It was concluded that the PDGF family were unlikely to regulate N-cadherin and the change in cell shape during cuboidalisation and therefore the next candidate family, the EGF family, was investigated.

Chapter 4: EGF family expression in the mouse ovary

The majority of research concerning the role of the EGF family in the mouse ovary is focused on the established role of betacellulin (BTC), amphiregulin (AREG), and epiregulin (EREG) stimulation of the EGFR in pre-ovulatory follicles to mediate the effects of the LH surge (Conti et al., 2006; Park et al., 2004). Consequently, EGF receptors have only been localised in superovulated ovaries of rodents that have been injected with human chorionic gonadotrophin (hCG), an analog of LH (Garnett et al., 2002). The relative contributions of the other ErbB receptors in follicle development are less understood but have been explored predominantly in the context of mediation of the LH surge (Kim et al., 2011; Noma et al., 2011). These later stages are clearly critical in reproductive biology and elucidation of the mechanism has been key to developing and improving the success of In Vitro Fertilisation (IVF). However, primordial activation is a much earlier step that is critical in determining the length of reproductive lifespan in women and elucidation of the mechanisms involved at this stage could allow us to tap into the abundant supply of primordial follicles outside the mammalian ovary and therefore offer women a potentially more fruitful alternative to IVF. Despite this, the expression and function of EGF family members in preantral follicles has been largely overlooked. Furthermore, the evidence so far as to whether the EGF family has a role in rodent primordial activation is much more sparse and not conclusive (Kezele et al., 2002; Li-Ping et al., 2010). We sought to address this imbalance by characterising the expression of the EGF family of receptors (the ErbBs) and ligands in the pre-pubertal mouse ovary and establish whether these

proteins were likely to have a role in GC cell shape change and proliferation during primordial activation.

4.1 Results

4.1.1 ErbB receptor mRNA expression profile in the mouse ovary

The first step towards characterisation of the EGF family in the mouse ovary sought to localise receptor mRNA. The presence or absence of ErbB1-4 mRNA transcripts was assessed in preantral oocytes, antral GCs, various stages of preantral follicles and whole pre-pubertal ovary and oviduct samples by RT-PCR as described in materials and methods section 2.3.3. As the amount of RNA that was extracted from pooled follicle, oocyte and GC samples was immeasurable by spectroscopy using the Nanodrop (Nanodrop Technologies Inc., Wilmington, DE) and we did not have access to a Bioanalyser at the beginning of my project, which can measure yield and integrity in small RNA samples, all samples were 2x diluted (in nuclease-free water) as standard protocol and appropriate detection of Gdf9 and/or AMH was used as an indication of useable yield and integrity. The multiple stages of preantral follicles that were prepared in this manner and included in the RT-PCR screen were: clusters of primordial follicles in their surrounding stroma and also isolated transitional, primary, primary plus and secondary stage follicles. ErbB expression was investigated in different aged mice, one of which should have antral follicles (d21) and two that should not (d14 and d15), in an effort to distinguish the well documented role of EGFR in antral preovulatory follicles from a possible role in preantral follicle development.

In this RT-PCR screen, only *Egfr* and *ErbB2* transcripts were expressed in prepubertal ovaries; *ErbB3* and *ErbB4* were detected in oviduct samples only (Figure

4.1). It is helpful to mention now that a subsequent RT-PCR screen of the ErbB receptors performed during the final stages of my project using a slightly different protocol, outlined in section 2.3.2 and 2.3.3, did detect ErbB3 mRNA and suggested it was expressed at low levels (Figure 4.9). Absence of *ErbB4* in the mouse ovary has previously been described (Elenius et al., 1999; Elenius et al., 1997). *Egfr* and *ErbB2* were both expressed in all stages of preantral follicles and both absent from oocytes but only *Egfr* was detected in antral GCs. The presence of *ErbB2* in all stages of preantral follicles but not oocytes or antral GCs suggests expression in preantral GCs. Therefore, as the initial RT-PCR screen suggests both *Egfr* and *ErbB2* expression in GCs we investigated their expression at the protein level by immunofluorescence. As ErbB3 was not detected in this initial screen, protein expression was not investigated. Consequently, I focused on investigating the expression and role of EGFR and ErbB2, which were consistently and readily detectable by PCR, in the mouse ovary and did not study ErbB3 due to time constraints.

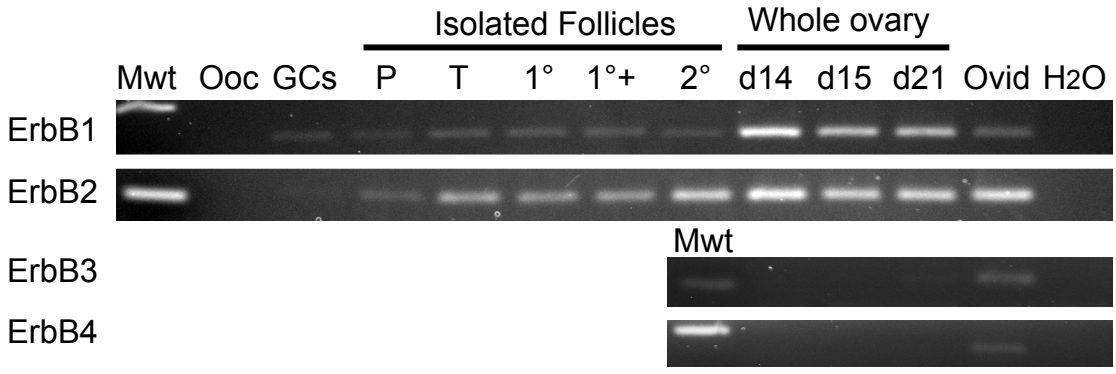


Figure 4.1. *RT-PCR screen of oocytes, GCs, different stages of preantral follicles, different ages of pre-pubertal ovaries and oviduct control showing presence/absence of transcripts for ErbB family members. ErbB3 and ErbB4 mRNA was not investigated in all follicle samples, oocytes or GCs as their transcripts were not present in ovary samples. Key: Mwt; molecular weight tracker, Ooc; oocyte, GCs; granulosa cells, p; primordial follicles, t; transitional follicles, 1°; primary follicles, 1°+; primary plus follicles, 2°; secondary follicles, Ovid; oviduct, H2O; negative water control.*

4.1.2 ErbB1 (EGFR) protein expression in the mouse ovary

There were no good EGFR antibodies available to localize EGFR in the mouse ovary. This was determined by incubating several commercial EGFR antibodies with paraffin-embedded sections taken from FSH-primed ovaries (courtesy of Jaya Nautiyal and Jenny Steel) that were fixed in formalin 4 hours post hCG injection. Injection with hCG mimics the LH surge and therefore immunoreactivity for EGFR would be expected in the cumulus GCs of antral follicles in ovaries from these mice (Park et al., 2004). None of the following antibodies tested labelled the cumulus GCs of superovulated ovaries: rabbit anti-human EGFR polyclonal antibody (cat no 4267, Cell Signaling), rabbit anti-human EGFR polyclonal (cat no sc-03, Santa Cruz Biotechnology) and rabbit anti-human EGFR polyclonal antibody (IHC-00005, Bethyl Laboratories). β-CATENIN immunolabelling was observed in GC membranes of these ovaries, however, indicating that they were suitable sections to use. Cell Signaling technology and Santa Cruz Biotechnology consider the exact immunogen sequences used to raise their antibodies as company proprietary information. However, Santa Cruz Biotechnology were able to tell us that their immunogen sequence maps to a different region of the EGFR protein C-terminus from the sequence used to raise the Bethyl Laboratories antibody. Laboratories involved in elucidating the function of EGFR during the LH surge also believe there is not a suitable EGFR antibody available (personal communication from Marco Conti).

4.1.3 ErbB2 protein expression in the mouse ovary

Although ErbB2 has been implicated in both early (Li-Ping et al., 2010) and late (Kim et al., 2011) follicle development, spatiotemporal ERBB2 expression has

not been characterized in the ovary. We sought to address this using immunofluorescence as described in materials and methods section 2.4.3.

Consistent with the RT-PCR screen, ERBB2 was expressed in preantral GCs (Figure 4.2A) and tranzonal processes (Figure 4.2E) in the ovary and also in epithelial cells of the oviduct (Figure 4.2B). In the ovary, ERBB2 was specific to a subset of GCs. ERBB2 immunoreactivity was observed in cuboidalised GCs of preantral follicles (Figure 4.2E); ERBB2 was not distinctly expressed in flattened GCs of primordial follicles (Figure 4.2C) or (cuboidalised) GCs of antral follicles (Figure 2.2F) in any age examined.

Crucially, by follicle stage, ERBB2 was first observed in cuboidalising GCs of transitional follicles (Figure 4.2D). ERBB2 is not uniform along the membrane of GCs of transitional follicles as it is in later stages; it is only observed in the elongating membrane between two cuboidalising GCs with strongest expression at the most apical contact and weaker, discontinuous expression towards the basal lamina. This is similar to N-cadherin expression and therefore consistent with ErbB2 regulation of N-cadherin during primordial activation.

As there is very little published on spatiotemporal expression of ErbB2 in non-cancerous tissues we confirmed ErbB2 expression by immunofluorescence with a further two chemically distinct antibodies (Figure 4.3). Both these antibodies are targeted against the carboxyl domain of ERBB2 whereas the epitope of the antibody initially used to localise ERBB2 in this study mapped to the amino terminus, as summarised in materials and methods table 2.2. All three ERBB2 antibodies (cat no 4290 Cell Signaling, Cat no 2165 Cell Signaling, Cat no OP15L Calbiochem) used in this study localised ERBB2 to the same follicle stages and cell compartments.

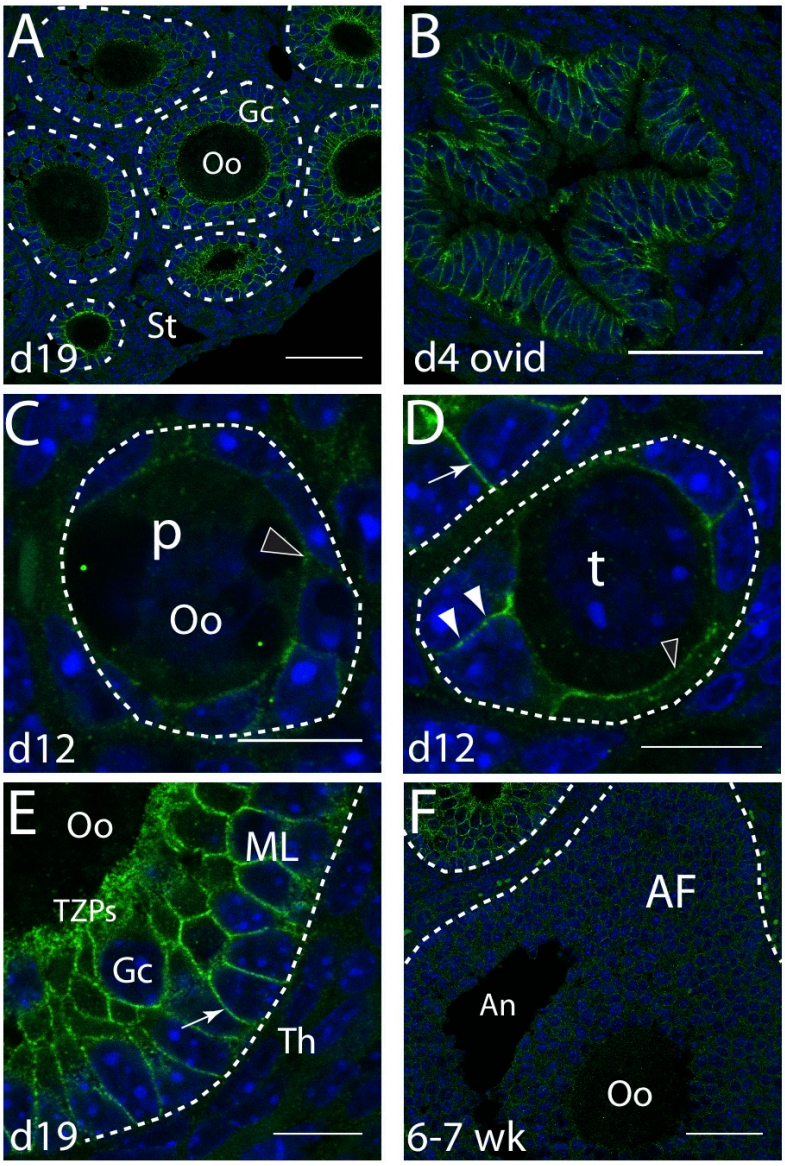


Figure 4.2. *ErbB2 protein expression in mouse ovaries of various ages post-partum. (A) d19 ovary section showing GC-specific ERBB2 expression. (B) d4 oviduct showing ERBB2 expression in epithelial cells. (C) Primordial follicle in a d12 ovary showing faint ERBB2 immunolabelling between the oocyte and flat GCs. (D) A transitional follicle beside a primary follicle in a d12 ovary showing how ERBB2 immunolabelling becomes continuous in GC membranes as they change shape from flat to columnar. (E) ERBB2 expression in GC membranes and TZPs of a multilayered follicle in a d19 ovary. (F) Downregulation in ERBB2 expression in antral GCs, as compared to neighbouring preantral GCs. Nuclei are labelled with DAPI (blue). Key: Oo; oocyte, Gc; granulosa cell, TZPs; transzonal processes, St; stroma, Th; theca, p; primordial follicle, t, transitional follicle, ML; multilayered follicle, An; antrum, AF; antral follicle, ovid; oviduct. Scale bars represent 10 µm (C-E) and 50 µm (A, B, F). White arrowheads represent punctate ErbB2 expression between cuboidalising cells. Black arrowheads represent faint immunolabelling between oocyte and GCs in non-growing or newly activated follicles. White arrows represent strong continuous and membranous ErbB2 protein expression in columnar GCs. Dotted lines represent the basal lamina.*

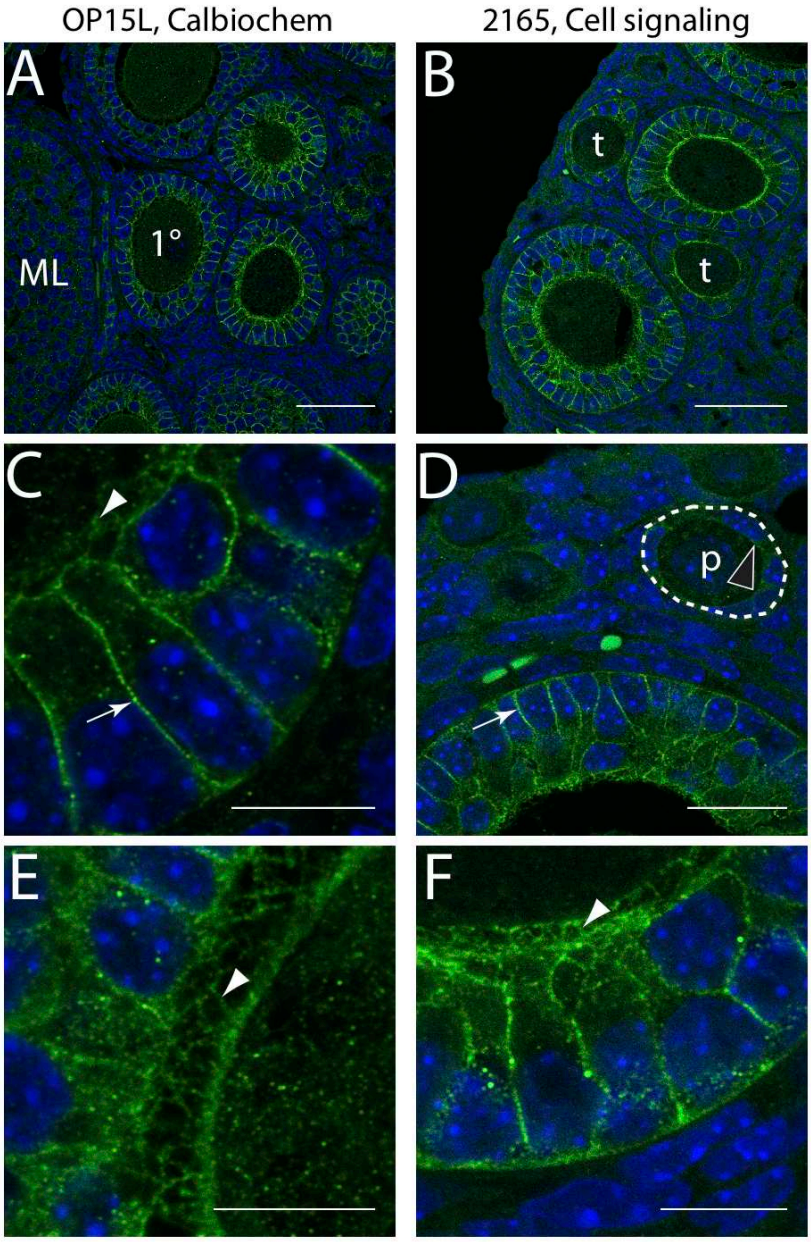


Figure 4.3. *GC-specific ErbB2 protein expression (green) confirmed with two antibodies in d19 ovary. ErbB2 was localised to GC membranes and tranzonal processes of growing preantral follicles by OP15L, Calbiochem antibody (green, A, C, E) and 2165, Cell signalling antibody (B, D, F). Nuclei are labelled with DAPI (blue). Scale bars represent 10 µm (C-F), and 50 µm (A-B). White arrowheads represent ErbB2 expression in tranzonal processes. Key: p; primordial follicle, t; transitional follicle, 1°; primary follicles. Black arrowheads represent faint immunolabelling between oocyte and GCs in non-growing or newly activated follicles. White arrows represent strong continuous and membranous ErbB2 protein expression in columnar GCs.*

As ERBB2 expression is very similar to N-CADHERIN expression in early follicle stages of development, sections of mouse ovary were co-labelled with ERBB2 and either N-CADHERIN (Figure 4.3A-F) or its associated linker protein β-CATENIN (Figure 4.3G-I). As expected, ERBB2 colocalised with both these membrane markers. Importantly it colocalised with N-CADHERIN in GCs that were cuboidalising (Figure 4.4D-F). This is consistent with a role of ERBB2 in GC cuboidalisation.

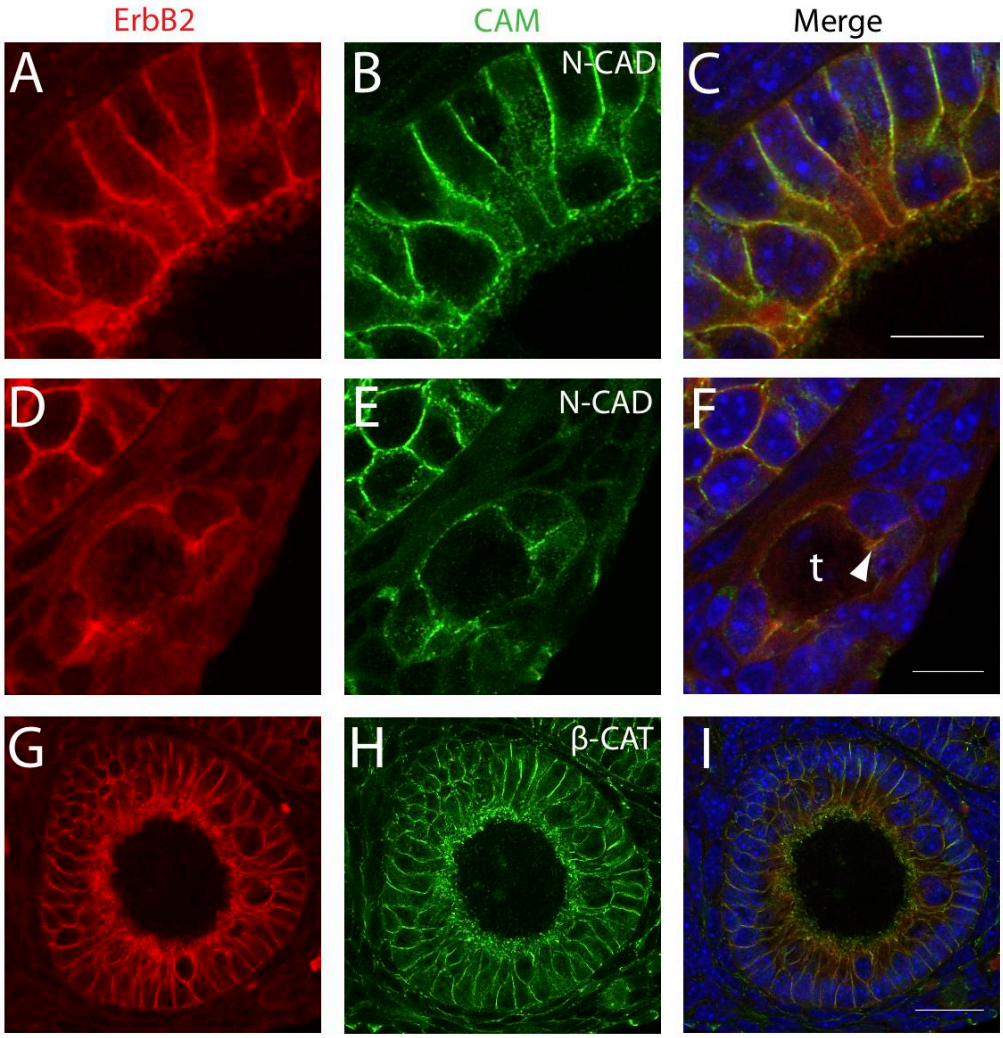


Figure 4.4 *Co-localisation of ErbB2 protein (red, A-I) with that of N-cadherin (green, A-F) and β-catenin (green, G-I). Nuclei are labelled with DAPI (blue). Key: t; transitional follicle. White arrowheads represent ERBB2 and N-CADHERIN co-localisation between cuboidalising GCs. Scale bars represent 10 μm (A-F) and 25 μm (G-I).*

4.1.4 Expression of proteins downstream from ErbB2

As immunofluorescence detection of ErbB2 is consistent with a role of ErbB2 in primordial activation, as first proposed by Li Ping et al (Li-Ping et al., 2010) based on siRNA experiments, and primordial activation is marked by an increase in GC proliferation we examined the expression of an anti-proliferative protein downstream from ErbB2 called TOB1 (Matsuda et al., 1996). The anti-proliferative activity of TOB1 is determined by its phosphorylation status: unphosphorylated TOB1 is active and localised to the nucleus while phosphorylated TOB1 (pTOB1) is inactive and cytoplasmic. ErbB2 expression causes phosphorylation of TOB1 via a downstream kinase (Helms et al., 2009; Kawamura-Tsuzuku et al., 2004).

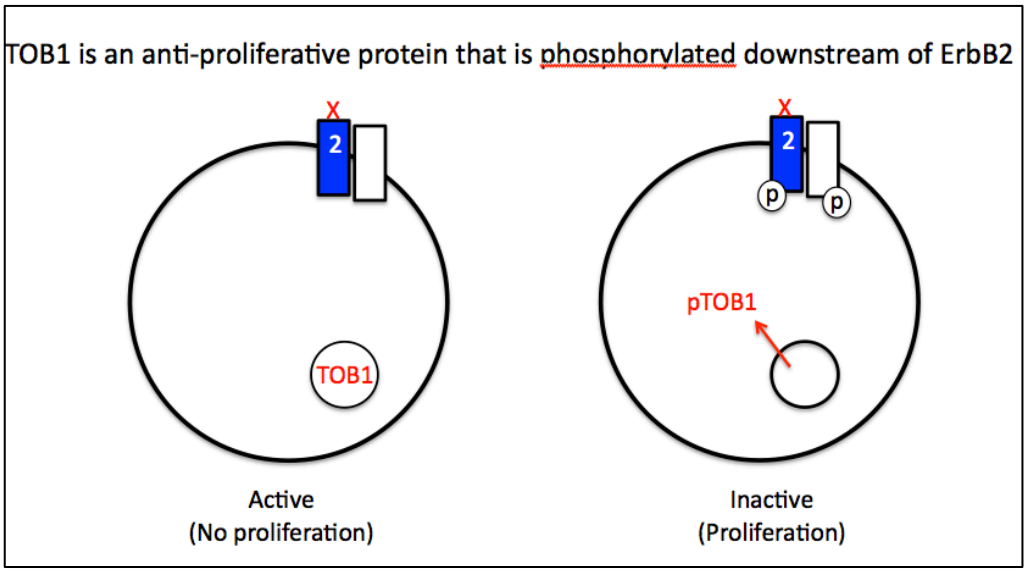


Figure 4.5. *Diagram illustrating the phosphorylation status and localisation of the active and inactive forms of TOB1, as regulated by ErbB2. ErbB2 (blue rectangle) is inactive in the cell membrane on the left diagram and hence, TOB1 is active in the nucleus. In contrast, ErbB2 is autophosphorylated and signalling in the diagram on the right and hence, TOB1 is phosphorylated and exported from the nucleus to the cytoplasm. Therefore, the brake on proliferation is lifted upon ErbB2 activation.*

We sought to characterize both the inactive and active forms of TOB1 in prepubertal mouse ovaries by immunofluorescence (pTOB1, section 2.4.3) and immunohistochemistry (TOB1, section 2.4.4). pTOB1 was expressed in the same

pattern as ErbB2; pTOB1 protein was observed in the cuboidalised GCs and TZPs of preantral follicles (Figure 4.6 A, B, E). Importantly it was not observed in flattened GCs of primordial follicles (Figure 4.6 C,D). Unlike ErbB2, pTOB1 immunolabelling appeared at a similar level in all growing preantral follicles in the d21 ovary (Figure 4.6 A). pTOB1 expression was punctate in the membranes of GCs and TZPs (Figure 4.6 B). As pTOB1 protein sometimes appeared as though it might be labelling the membrane of GCs (Figure 4.6 E), ovary sections were double labeled with antibodies for pTOB1 and the membrane marker β-catenin (Figure 4.6 F). pTOB1 and β-catenin did not co-localise although pTOB1 did track alongside the membrane.

In contrast to pTOB1 and ERBB2 expression, active non-phosphorylated TOB1 was not specific to GCs; it was also localized to a proportion of theca and stromal cells (Figure 4.7 A-D). Crucially, it was also unlike pTOB1 and ERBB2 in that it was also expressed in the flattened GCs of primordial follicles (Figure 4.7 D), suggesting it is partly responsible for maintaining primordial follicles in growth arrest. Active TOB1 protein localised to the nucleus (Figure 4.7 A-D) as expected, suggesting it is actively inhibiting proliferation via interactions with transcription factors.

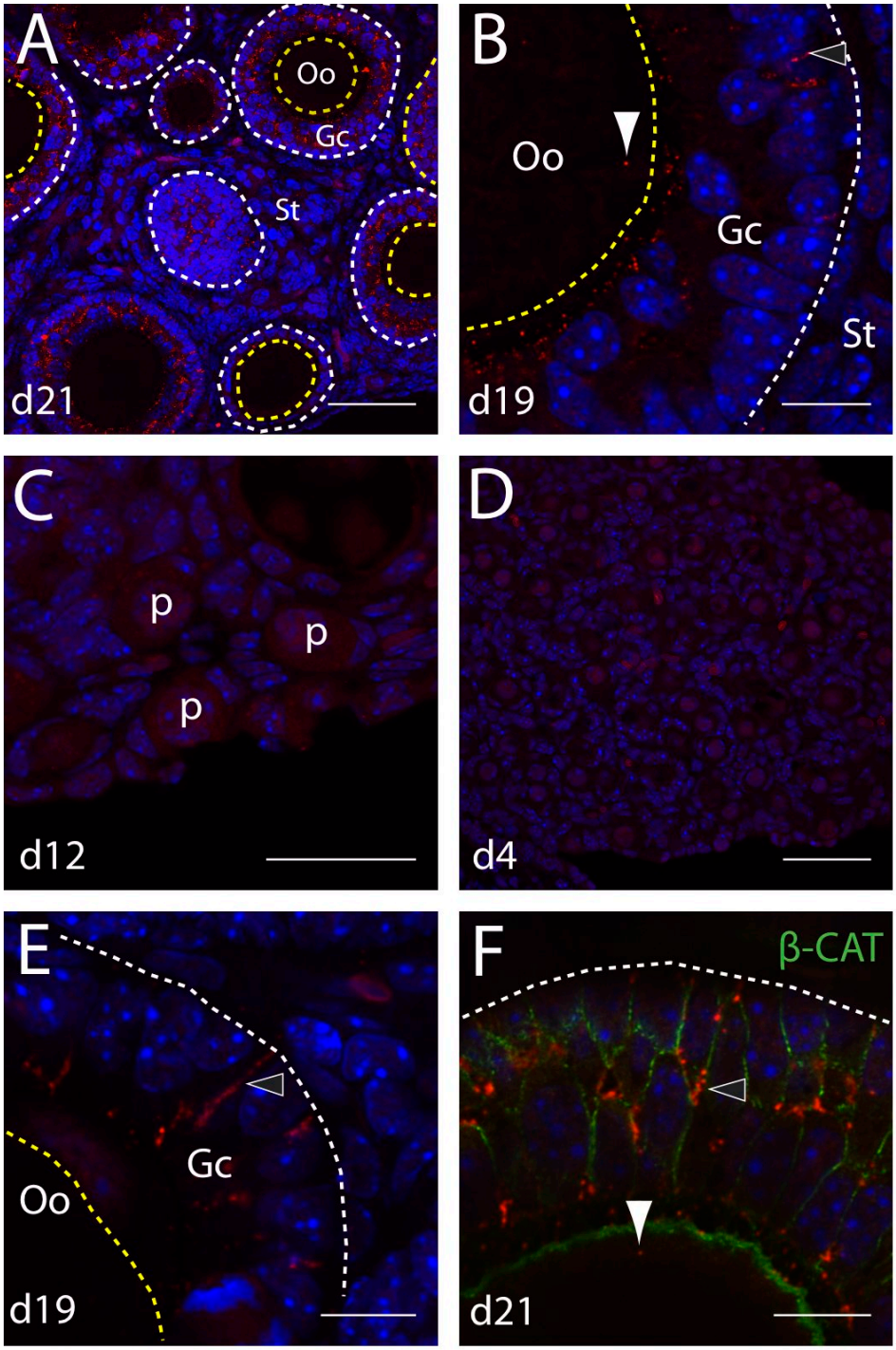


Figure 4.6. *Expression of the inactive form of TOB1, pTOB1, in mouse ovaries of various ages post-partum. (A) d21 ovarian section showing GC-specific pTOB1 expression. (B) High power image of pTOB1 expression in cuboidal GCs of a secondary follicle. (C, D) pTOB1 is not expressed in primordial follicles. (E) pTOB1 expression sometimes appears as though it may be labelling the membrane. (F) pTOB1 and β-catenin did not co-localise indicating that pTOB1 was not, in fact, membranous. Key: Oo; oocyte, Gc; granulosa cell, St; stroma, p; primordial. Nuclei are labelled with DAPI (blue). White arrowheads represent pTOB1 expression in tranzonal processes. Black arrowheads represent pTOB1 expression in GCs that appears to be membranous. Scale bars represent 10 µm (B, E-F), 25 µm (C) and 50 µm (A, D). White dotted lines represent basal lamina. Yellow dotted lines represent oocyte/Gc boundary.*

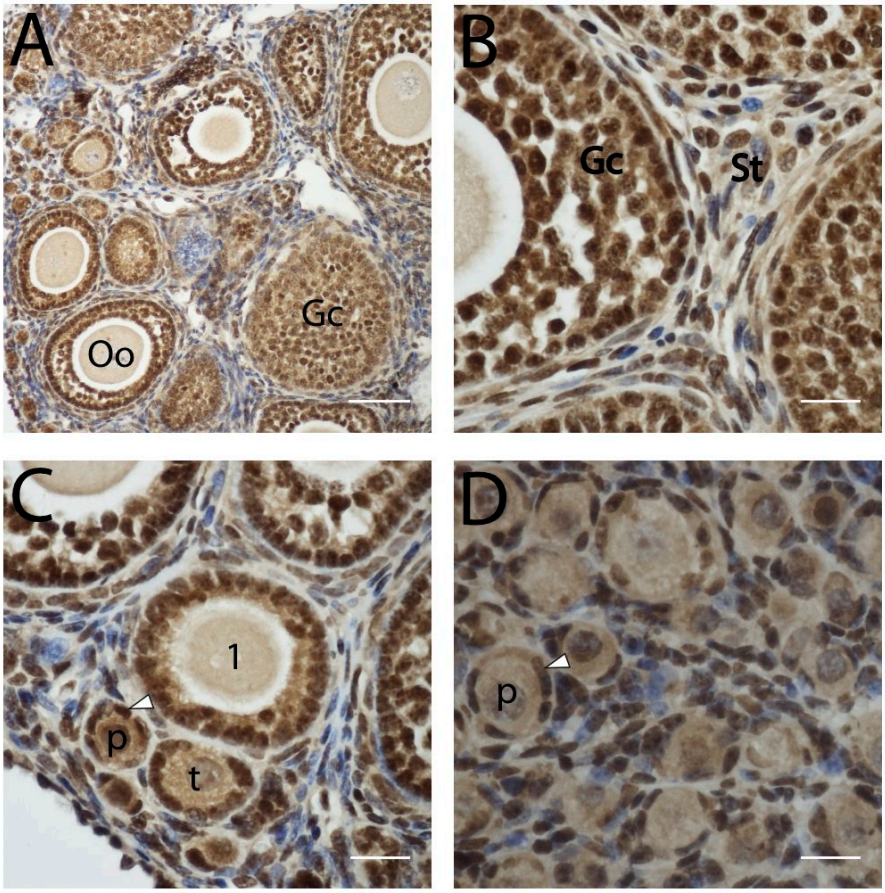


Figure 4.7*. Expression of the active, unphosphorylated form of TOB1 in mouse ovaries of various ages post-partum. Active TOB1 localises to the nucleus of GCs and some thecal and stromal cells (brown, A-D). Crucially, active TOB1 localises to the nucleus of flat GCs in non-growing primordial follicles (arrowed) in d21 (C) and d4 (D) ovaries. Nuclei are counterstained with Haematoxylin (blue) Key: oo; oocyte, Gc; granulosa cell, St; stroma, p; primordial, t; transitional, 1; primary follicle. Scale bars represent 10 µm.*

4.1.5 ErbB ligand mRNA expression profile in the mouse ovary

Egfr and *ErbB2* were the only ErbB receptors detected by PCR in the screen shown in Figure 4.1. No known ligand binds ErbB2. Therefore, the presence or absence of EGFR ligands in mouse ovarian tissue and cells was assessed by PCR. As only two ligands (*Hbegf* and *Tgfα*) were convincingly detected in an initial presence/absence screen in a single pre-pubertal ovary (data not shown), EGFR ligand mRNA expression was assessed in several other tissues to establish that the primers worked. Appropriate positive control tissues, specific for each gene, were chosen

using the online gene annotation portal, BioGPS. BioGPS allows the user to examine the relative abundance of a given gene in all the tissues that have so far been collectively examined in your species of interest. Based on this data the following positive controls were included: kidney (*Btc*, *Egf*), eye (*Tgfα*, *Hbegf*, *Epgn*) and stomach (*Areg, Ereg)* and intestine (additional control for *Areg* and *Ereg)*. However, *Egf, Areg and Ereg* have not yet been detected in positive control tissue. GCs from an FSH-primed ovary stimulated with a hCG injection could be used as a positive control for *Areg* and *Ereg* as these are upregulated following the LH surge in mice in vivo (Park et al., 2004). Therefore, the presence or absence of EGFR ligand *(Btc, Epgn, Hbegf and Tgfα)* transcripts was assessed in adult ovary, pre-pubertal (d16) ovary, pooled preantral follicles, pooled preantral oocytes, and antral GCs and the positive control tissue, specific for each gene, by PCR as described in materials and methods 2.3.3.

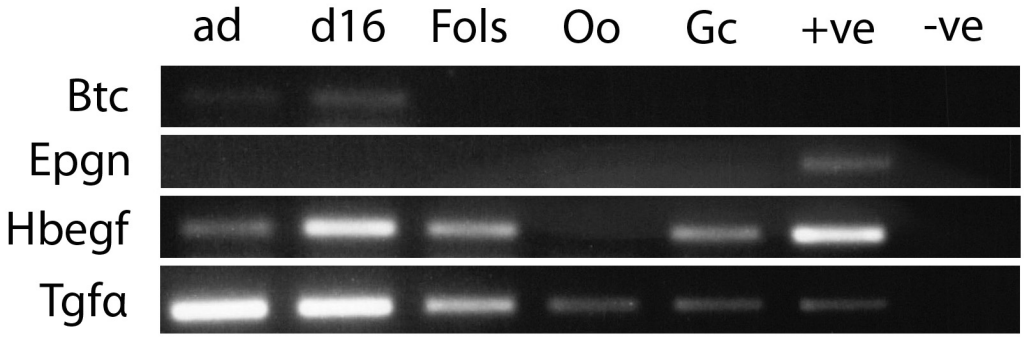


Figure 4.8*. PCR screen showing presence or absence of transcripts for Btc, Epgn, Hbegf and Tgfα in adult ovary (ad), d16 ovary (d16), pooled preantral follicles (Fols), pooled preantral oocytes (Oo), antral GCs (Gc), positive control specific for each gene (+ve) and negative water control (-ve). The following positive control tissues were used: kidney (Btc) and eye (Epgn, Hbegf, Tgfα).*

Consistent with the initial presence/absence screen conducted in pre-pubertal ovary only (data not shown), *Hbegf* and *Tgfα* were expressed in the d16 ovary (Figure 4.8). They were also both detected in adult ovary, preantral follicles and antral GCs,

whereas *Tgfα* but not *Hbegf* was detected in preantral oocytes. The presence of *Hbegf* in preantral follicles but not preantral oocytes suggests expression in preantral GCs. *Epgn* was not detected in any ovarian tissue or cells or follicles but it was detected in eye, indicating the primer set is able to amplify *Epgn* transcripts. *Btc* was not detected in the positive control. However, it was faintly detected in whole ovary samples (Figure 4.8).

4.1.6 ErbB receptor PCR screen using bioanalysed samples

The ErbB receptor mRNA expression profile shown in Figure 4.1 shows the presence or absence of ErbB1-4 mRNA transcripts in 2x diluted cDNA samples of unknown concentration and integrity, as the amount of RNA that is extracted from follicle/oocyte/GC/small pre-pubertal ovary samples is immeasurable by Spectroscopy using the Nanodrop (Nanodrop Technologies Inc., Wilmington, DE) and there is not enough RNA to run on an agarose gel and check for degradation. At a late stage in my project, a bioanalyser (Agilent 2100 Bioanalyser), which enables RNA yield and integrity to be examined in small samples, became available. cDNA samples made from pooled preantral follicles, pooled preantral oocytes, antral GCs, adult ovary, pre-pubertal (d16) ovary and lung tissue were bioanalysed (RNA pico analysis service, Clinical Sciences Centre, Imperial College London), and RNA quality was confirmed. In contrast to the PCR screen shown in Figure 4.1, cDNA samples were not diluted 2x. To summarise, the presence or absence of ErbB1-4 mRNA transcripts was repeated, and assessed in adult ovary, pre-pubertal (d16) ovary, pooled preantral follicles, pooled preantral oocytes, antral GCs and positive control tissue (lung) by PCR as described in materials and methods section 2.3.3.

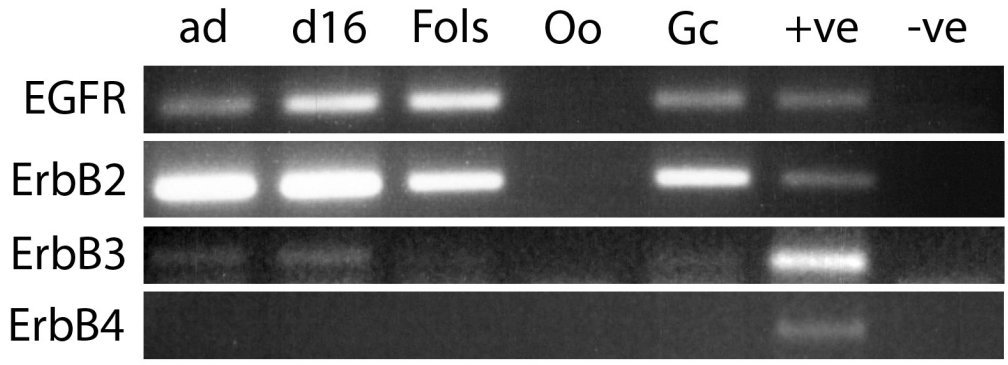


Figure 4.9. *PCR screen showing presence or absence of transcripts for ErbB1-4 in adult ovary (ad), d16 ovary (d16), pooled preantral follicles (Fols), pooled preantral oocytes (Oo), antral GCs (Gc), lung tissue (+ve) and negative water control (-ve).*

Consistent with the PCR screen shown in Figure 4.1, *Egfr* and *ErbB2* were detected in pre-pubertal ovary, preantral follicles but not preantral oocytes. This confirms my previous observation that *Egfr* and *ErbB2* mRNA is expressed in preantral GCs. As shown earlier, this was confirmed to be the case for ErbB2, as immunolabelling of ERBB2 was detected in preantral GCs of pre-pubertal ovaries (Figure 4.2). In contrast to the results of the previous ErbB PCR screen (Figure 4.1), *ErbB2* mRNA was also detected in antral GCs. It is not clear whether this disparity reflects differences in the concentration or integrity of sample used or true differential ErbB2 expression between GCs from different antral follicles. Crucially, *ErbB3* transcripts were faintly detectable in adult ovary, pre-pubertal ovary, pooled pre-antral follicles and antral GCs (as well as lung control). This is in contrast to the earlier results shown in figure 4.1. The faintness of the band suggests that the reason *ErbB3* transcripts were detected in this PCR screen and not the initial PCR screen is because it is expressed at such low levels that it becomes undetectable when cDNA samples are diluted. *ErbB4* transcripts, however, were never detected in ovarian

tissue or cells (Figure 4.1 and Figure 4.9). *ErbB4* transcripts were detected in positive control tissue (lung), however.

4.1.7 Neuregulin 1 protein expression

ErbB3 was detectable in undiluted cDNA made from isolated follicles and GCs aspirated from an antral follicle, therefore, it was possible that ERBB3 protein was expressed in GCs and dimerised with ERBB2. Due to time constraints, we were not able to localise ERBB3. However, an antibody to Neuregulin-1 (NRG-1), a ligand of ErbB3 (Schneider and Wolf, 2009), was available within the time constraints. Therefore, NRG-1 was localised in mouse ovaries to determine the likelihood that its receptor was also expressed at the protein level.

Spatiotemporal NRG-1 expression was characterised in ovaries obtained from pre- (d4, d21) and post-pubertal ovaries by immunohistochemistry (section 2.4.4). Similar to ERBB2, NRG-1 was expressed in GCs (Figure 4.10). In contrast to ERBB2, cytoplasmic NRG-1 expression was not restricted to a subset of GCs, but rather, distinct NRG-1 expression was observed in all stages of preantral GCs (Figure 4.10A, B) and also antral GCs (Figure 4.10D). Importantly, it localised to primordial and transitional follicles of d4 (Figure 4.10C) and d21 (Figure 4.10A) ovaries. The ooplasm is often non-specifically labelled and therefore it is difficult to judge whether this staining of the oocyte reflects NRG-1 expression in the mouse without accompanying PCR data. As primordial follicle formation has not yet completed in a d4 ovary, it is difficult to interpret whether the labelling observed in d4 ovaries is of somatic or germ cells or both. It is interesting, however, that there are 'threads' of somatic cells that are completely devoid of NRG-1 labelling and extend through the ovary between oocyte nests (Figure 4.10C).

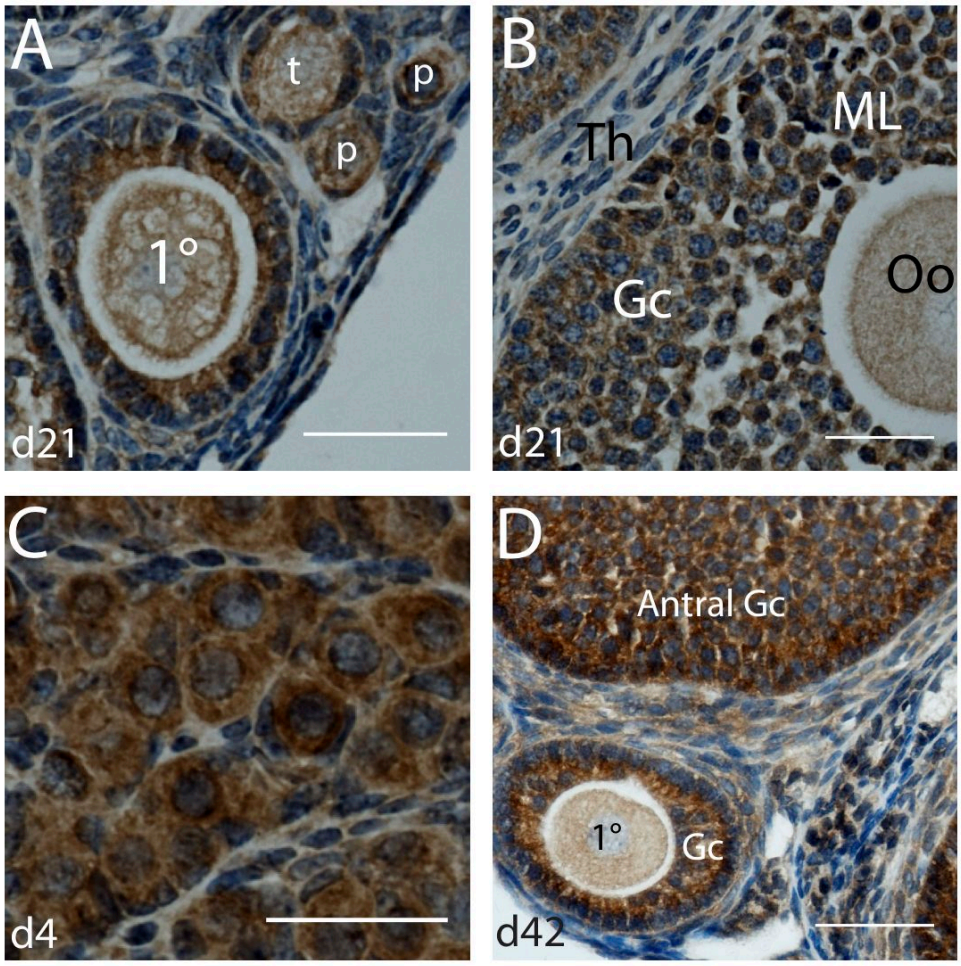


Figure 4.10. Neuregulin-1 protein expression (brown) in mouse ovaries of various ages post-partum. (A) NRG-1 expression in primordial, transitional and primary follicles. (B) NRG-1 expression in GC cytoplasm of large multilayered follicle. (C) NRG-1 expression in oocyte nests in d4 ovary. (D) NRG-1 expression in GCs of antral follicle in adult ovary. Key: Oo; oocyte, Gc; granulosa cell, Th; theca, p; primordial, t; transitional, 1°; primary, ML; multilayered follicle. Scale bars represent 50 µm.

Crucially, this result suggests that ERBB3 protein is expressed in the mouse ovary as NRG-1 does not bind EGFR or ErbB2 (Schneider and Wolf, 2009).

4.1.8 Summary of EGF family expression results

- Egfr expression
    - *Egfr* mRNA amplified in GC samples but we have not been able to detect protein by immunofluorescence
- ErbB3 and ErbB4 expression

    - Initially, *ErbB3* and *ErbB4* mRNA were not detected in ovarian tissue by PCR. However, very recent studies have suggested that *ErbB3* is expressed at low levels.
- ErbB2 expression
    - ERBB2 is GC specific.
    - ERBB2 first appears between cuboidalising GCs and co-localises here with N-cadherin
    - *ErbB2* mRNA and protein is absent from GCs of antral follicles
    - ERBB2 is only expressed in peripheral follicles of d12, d19 and d21ovaries.
- EGFR ligand expression
    - *Hbegf* and *Tgfα* are the only EGFR ligands to be detected in pooled preantral follicles so far. Furthermore, the presence of *Hbegf* and *Tgfα* transcripts in preantral follicles but not preantral oocytes suggests their expression in preantral GCs.
    - *Btc* transcripts were detected in adult ovary and pre-pubertal ovary.
- TOB1 expression
    - Similar to ErbB2, pTOB1 expressed in GCs of growing preantral follicles.
    - Active TOB1 is expressed in these GCs but it is also expressed in flattened GCs of primordial follicles and a subset of theca and stroma cells.
- NRG-1 protein expression
    - NRG-1 expressed in GC cytoplasm at all stages of follicle development
    - NRG-1 expression in oocyte is ambiguous

4.2 Discussion

4.2.1 ErbB2 may have a role in GC cell shape change during primordial activation

Spatiotemporal localisation of ErbB2 and a downstream protein, TOB1, suggests that ErbB2 may positively regulate both GC cuboidalisation and GC proliferation during primordial activation.

ERBB2 first appears between cuboidalising GCs and colocalises to the membrane with N-cadherin. The concomitant upregulation of ERBB2 and N-CADHERIN during GC cuboidalisation suggests that these proteins are associated with GC cuboidalisation. It has previously been suggested that AJ assembly is

important in GC cuboidalisation (Mora et al., 2012). It is therefore intriguing that between cuboidalising GCs, high intensity ERBB2 immunoreactivity predominantly localises towards the oocyte as this is likely the initial point of GC-GC contact that presumably coincides with AJ assembly, at the points where flattened GCs lying on the oocyte surface are in contact with each other. Furthermore, the discontinuous, almost punctate ERBB2 expression between wedge-shaped GCs of transitional follicles and subsequent uniform expression in columnar GCs of primary follicles is compatible with a model in which ERBB2 regulates assembly of N-CADHERIN based AJs during GC cuboidalisation.

While the expression data suggests that ERBB2 and N-CADHERIN are both recruited to the same points of GC-GC contact during cuboidalisation, co-localisation of ERBB2 and N-CADHERIN co-localisation does not confirm that they interact. However, it is established that receptor tyrosine kinases often do interact with components of junctional complexes (Kirkpatrick and Peifer, 1995). Techniques to examine direct interactions between proteins, such as co-immunoprecipitation, are not a viable option to investigate the possible interaction between ERBB2 and N-CADHERIN as we cannot feasibly extract sufficient protein from follicles. Co-immunoprecipitation may be viable with the amount of protein we can extract from ovaries, however. Another option could be to co-localise ERBB2 and N-CADHERIN to a specific domain of the GC membrane. There are cell structures and molecules that are known to recruit and restrict proteins to specific compartments within the cell or membrane and co-localisation of N-CADHERIN and ERBB2 with these structures/molecules would be informative. Lipid rafts are dynamic structures composed of sphingolipids and cholesterol that organise signalling proteins into rafts in the phospholipid bilayer and are able to move in the membrane. Therefore, it is

possible that lipid rafts may organise ERBB2 and N-CADHERIN into specific microdomains of the membrane. This is an interesting idea in terms of this project as lipid rafts are known to regulate (i) ErbB2 dimerisation properties (Nagy et al., 2002) and (ii) N-cadherin assembly into junctions at sites of cell-cell contact in C2C12 myoblasts (Causeret et al., 2005; Chartier et al., 2011). There are lipid raft markers available (Galbiati et al., 2001; Ishitsuka et al., 2005) and this is a possible avenue of future work. There are also proteins that are known to specifically interact with and sequester ERBB2 in epithelial membranes. ERBB2 immunolabelling is strongest at the primary and primary plus stage of follicle development (see chapter 5 for quantitative analysis). The GCs in follicles at this stage of development have been described as epithelial-like cells (Mora et al., 2012). The mucin, Muc4 (Ramsauer et al., 2006) and the PDZ protein, ERBIN (Borg et al., 2000) have both been shown to directly and specifically interact with ErbB2 in epithelial membranes. In true epithelia, Muc4-mediated translocation of ErbB2 from the basolateral membrane to the apical membrane is associated with a polarised phenotype (Ramsauer et al., 2006). Therefore, localisation of these proteins is also another possible avenue of future work.

While this chapter did not aim to examine the effect of ErbB2 on N-cadherin expression or vice versa, it offers the intriguing prospect that ErbB2 and N-cadherin may mutually regulate each other in GCs during primordial activation. The possibility that ErbB2 could regulate N-cadherin- mediated cell adhesion and N-cadherin could regulate signalling by the proto-oncogene ErbB2 is particularly interesting given the upregulation in GC proliferation following their cuboidalisation during primordial activation (Da Silva-Buttkus et al., 2008). RTKs and CAMs in cell signalling centres organised at cell-cell junctions are known to physically and

functionally interact in many diverse ways (Jamora and Fuchs, 2002; Kirkpatrick and Peifer, 1995). One of the most obvious points of regulation is expression. Cadherin expression is often the rate limiting step in cadherin-catenin complex formation (Gumbiner, 2000) and it is entirely possible that ErbB2 may regulate this aspect as it is known to induce EMT (Jenndahl et al., 2005) which involves switching off E-cadherin expression and switching on N-cadherin expression. However, visual inspection of N-CADHERIN and ERBB2 co-localisation demonstrates that N-CADHERIN is observed in more primordial follicles than ERBB2 is i.e. N-CADHERIN expression appears to be switched on earlier in follicle development than ERBB2 suggesting ErbB2 does not switch on N-cadherin expression but may modulate it. Further investigation is required, including quantitative analysis of co-localisation and assessing the level of *ErbB2* and *N-cadherin* transcripts in clusters of primordial follicles.

Therefore, while further studies are needed to elucidate any functional relationship or physical interaction between ErbB2 and N-cadherin- and Nectin-2 based AJs, spatiotemporal localisation of ERBB2 has identified it as a strong candidate for a role in GC cuboidalisation.

4.2.2 ErbB2 may have a role in GC proliferation during primordial activation

ErbB2 may also regulate GC proliferation via a downstream protein, Tob1. Tob1 is an anti-proliferative protein that is negatively regulated by kinase-active ErbB2. Crucially, only the active form of Tob1 was observed in the nuclei of flattened GCs of primordial follicles strongly suggesting that Tob1 may function in the ovary, along with other factors, to maintain the primordial pool in a quiescent state until ErbB2 is expressed at the onset of follicle growth. Expression of the

inactive (phosphorylated) form of Tob1 coincides with the appearance of ERBB2 in cuboidalised GCs, supporting this notion. However, active Tob1 was not solely expressed in these flattened GCs; it was also expressed in nuclei of cuboidalised GCs, theca and stroma. Tob1 expression in cuboidalised GCs demonstrates that only a proportion of Tob1 available in a cell is phosphorylated in the presence of ErbB2. Tob1 expression in theca is also interesting as it has long been known that theca proliferation must be tightly regulated (Culiner and Shippel, 1949), indeed, theca cell hyperplasia is associated with Polycystic Ovarian Syndrome (PCOS), a common cause of infertility (Hughesdon, 1982). Therefore these results suggest Tob1 may function at two stages of follicle development; firstly, during the release of primordial follicles into the growing pool and secondly, in maintaining the optimal size of the theca compartment.

In conclusion, this study strongly supports the contention that ErbB2 regulates two key aspects of primordial activation in the mouse (Figure 4.11). This theory is consistent with studies in rat that found that silencing ErbB2 expression with siRNAs in vitro inhibited spontaneous initiation of follicle growth. The individual expression data suggest two different mechanisms, however. Li Ping et al (2010) localise ErbB2 mRNA to rat ooplasm. In contrast, ErbB2 mRNA and protein was specific to GCs in the mouse ovary, confirmed with several antibodies and repeated PCRs.

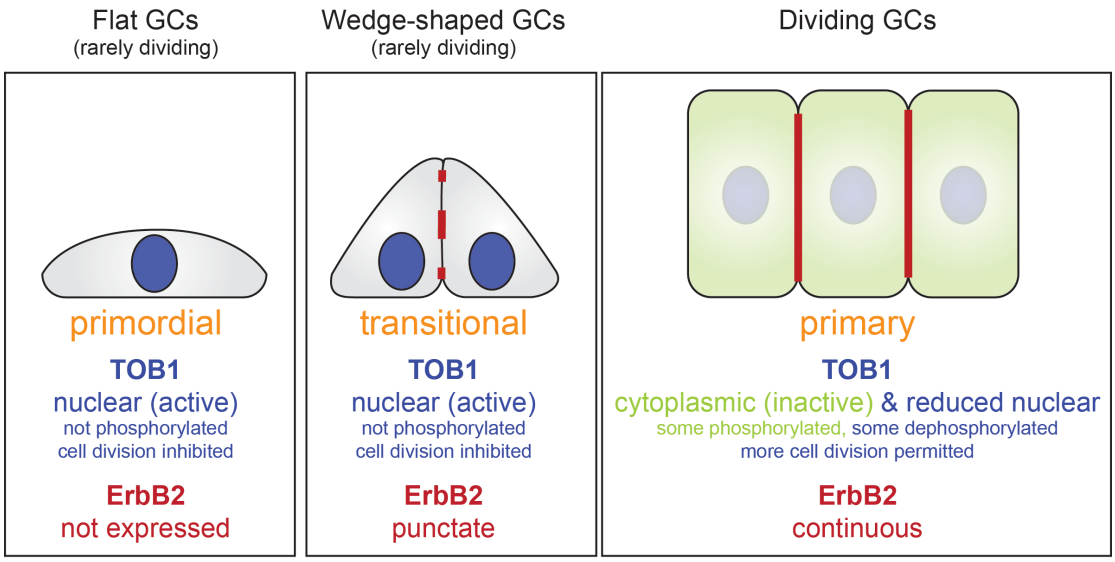


Figure 4.11. *Model of how ErbB2 may regulate the onset of GC proliferation during primordial activation. Active TOB1 may maintain the primordial pool until the onset of ErbB2 signalling in cuboidal GCs. ErbB signalling therefore may be responsible for releasing the break on proliferation.*

4.2.3 ErbB2 is downregulated in late stage follicles

Distinct ERBB2 immunolabelling was never observed in GCs of antral follicles. *ErbB2* mRNA transcripts were not detected in GCs of antral follicles in the initial PCR screen, but they were detected in the second PCR screen. It is not clear whether this is due to real differences in expression between samples or due to the differences in cDNA preparation protocol used. Further investigation is required to establish a profile of *ErbB2* expression in GCs from different antral follicles.

We have discussed the implication that ERBB2 is involved in early follicle development. ERBB2 protein expression in polarised GCs of primary uni-layered follicles and downregulation in the loosely associated GCs of antral follicles suggests ErbB2 may have a role in the EMT event that is proposed to occur during preantral follicle development in a partial (GCs do not migrate during follicle development) and contained (to the GCs within a follicle) manner (Da Silva-Buttkus et al., 2008).

Distinct ERBB2 immunolabelling was not observed in cumulus GCs in ovaries from superovulated mice (data not shown). Therefore, ERBB2 may not have a role in mediating the LH surge in mice, as EGFR does (Park et al., 2004) and as it has previously suggested to have in EREG-deficient mice (Kim et al., 2011).

4.2.4 EGFR protein was not detected in mouse ovary

Following extensive attempts to localise EGFR with several antibodies by immunofluorescence and personal communication with Marco Conti, it was concluded that there is no suitable antibody available to localise EGFR in the mouse ovary using immunofluorescence. Future chapters address EGFR expression using western blotting (see chapter 6) and functional studies (see chapter 7).

4.2.5 Future studies should examine possible ErbB3 protein expression

ErbB3 mRNA transcripts were only detected in ovary, follicle and GC samples very recently in my project. Therefore, much of the experiments in my project were based on the initial ErbB receptor PCR screen. As the recently appreciated possibility of ERBB3 protein expression is of critical importance with respect to how ErbB2 signals in the ovary, future studies will investigate ERBB3 expression. The expression of the soluble NRG-1 protein, an ErbB ligand that binds ErbB3 and ErbB4 but not EGFR or ErbB2, strongly suggests that ERBB3 protein is present in the mouse ovary. It is intriguing that NRG-1 was expressed in a d4 ovary as this suggests it could stimulate ERBB2/ERBB3 dimers to form, which are the most mitogenic ErbB dimer possible, during primordial activation (Yarden and Sliwkowski, 2001). A previous study has suggested that NRG-1 does not affect primordial activation (Nilsson et al., 2006). However, this was in rat so it would be

interesting to examine the effect of NRG-1 on primordial activation in mouse d4 ovary cultures in future work.

4.2.6 Only HB-EGF and TGFα transcripts have been detected in preantral follicles so far

As *ErbB3* transcripts were only detected very recently, the neuregulin ligands, which bind ErbB3 and ErbB4 only, were not included in the PCR screen. Future studies will examine neuregulin mRNA and protein expression. Of the seven ligands that bind EGFR, only *Hbegf* and *Tgfα* were detected in preantral follicles. However, of the remaining five EGFR ligands, only *Epgn* and *Btc* were detected in other samples. Therefore, the expression of *Areg, Ereg* and *Egf* in the mouse ovary cannot be commented on based on these results, due to the inability so far to find suitable positive controls to confirm primer functionality. *Areg* and *Ereg* transcription is induced in mural GCs following the LH surge (Park et al., 2004), therefore 'superovulated' ovaries from mice injected with hCG (human chorionic gonadotrophin, LH analog) would be an ideal control to examine *Areg* and *Ereg* expression in. Unfortunately, this was not possible during my project. The online gene annotation portal, BioGPS, indicated that the kidney was a good control tissue. However, *Egf* transcripts have not been detected in control tissues so far, so the salivary gland would be a tissue worth investigating, as it is a major source of circulating EGF. The collective data presented on BioGPS does indicate, however, that *Egf* is not expressed in the ovary. This does not preclude EGF from having a role in ovarian follicle development, however. Indeed, as the majority of circulating EGF is produced in the salivary glands, this systemic may regulate follicle development as it regulates Sertoli cell function in the testes (Liu et al., 1994).

The expression of *Hbegf* and *Tgfα* transcripts in pre-pubertal is intriguing for several reasons. Firstly, both have been suggested to be valuable molecular targets in ovarian cancer (Bauknecht et al., 1991; Miyamoto et al., 2004; Wang et al., 2012). Therefore, the interactions and cellular responses between these ligands and their proto-oncogenic receptors in the normal ovary may complement those that are inappropriately occurring in cancerous ovaries. Secondly, HB-EGF and TGFα are both able to interact with EGFR in a juxtacrine manner. The expression of *Hbegf* and *Tgfα* in preantral follicles but not preantral oocytes suggests expression in preantral GCs. Therefore, it would be particularly interesting to localise HB-EGF and TGFα protein expression in pre-pubertal ovaries by immunofluorescence to assess whether they are membranous in GCs of pre-antral follicles undergoing primordial activation i.e. do they co-localise with N-CADHERIN and ERBB2. HB-EGF expression has been investigated in ovaries from adult cycling rats using immunohistochemistry. They do describe GC expression (Pan et al., 2004), but HB-EGF immunolabelling is much more distinct in the theca of these ovaries. Furthermore, immunofluorescence would be required to examine which compartment HB-EGF is expressed in at higher resolution. The expression and role of HB-EGF and TGFα has not been investigated in pre-pubertal mouse ovaries. Therefore, this would be a novel focus of future work.

4.3 Conclusions

Immunolabelling for ERBB2 revealed that it was likely to have a role in GC cuboidalisation. Therefore, subsequent experiments focused on how its expression is regulated (chapter 5), what ErbB2 dimerises with (chapter 6) and the effect of inhibiting this (chapter 7 and chapter 8).

Chapter 5: Quantification of ErbB2 expression

Since histological examination of ovarian sections has been available, dramatic differences between the periphery and the centre of the ovary have been observed. The most obvious feature is that the blood vessels are in the medulla and the first follicles to grow are always towards the medulla whereas non-growing follicles cluster in the cortex of the ovary, adjacent to the OSE. Blood vessels enter the ovary at the hilum and extend through the medulla whereas the periphery of the ovary, where the primordial follicles lie, has historically been considered avascular (Hirshfield, 1991a).

As already discussed, the invariable clustering of primordial follicles near the surface of the ovary has been the focus of much research, as answering the question of why non-growing follicles cluster together will help answer the question of why certain follicles initiate growth. The recent elucidation of GC origin has been our most recent major leap in our understanding of why the follicles at the centre of the ovary are the first to grow, as the initial synchronous burst of activation is associated with central follicles that were enveloped in GCs in the first wave of ingression, but the molecules involved in this process remain elusive (Mork et al., 2012).

The simultaneous activation of follicles in cortical pieces of primate ovary in vitro (Fortune et al., 1998) combined with spatial analysis of follicle stages in the juvenile mouse ovary (Da Silva-Buttkus et al., 2009) suggest an inhibitor maintains the primordial pool in cell cycle arrest. Recent unpublished studies in our laboratory suggest that Smad 2/3 are the intracellular signalling molecules involved. Smad 2/3 is expressed in the nuclei of primordial and early preantral follicles, but intriguingly is

generally absent from nuclei that have entered the cell cycle and express Ki67. This suggests that Smad2/3 is involved in the maintenance of primordial follicle arrest (Kate Hardy, unpublished observations). Intriguingly, despite the gradient of follicle development observed in human and rodent ovaries and the established role of growth factor regulation in this development, Smad 2/3 is the only molecule so far described as being in a gradient in the juvenile mouse ovary (Fenwick et al., 2013). Smad2/3 expression is strongest in primordial follicles and gradually declines as follicles grow. It is not clear whether/to what extent SMAD 2/3 expression is regulated according to follicle stage or follicular location in the ovary.

Immunolocalisation of ERBB2 revealed a similar gradient of expression in juvenile mouse ovaries. Therefore, the relationship of ERBB2 immunolabelling with follicle stage, follicular location and TGF-β superfamily was examined qualitatively and quantitatively in order to understand whether ErbB2 signalling is associated with or related to the heterogeneity in primordial activation and follicle development observed in the mammalian ovary that has long been observed but not understood.

5.1 Results

5.1.1 Immunolocalisation of ErbB2 in d4, 8, 12, 19 and adult ovaries

As described in chapter 4, ERBB2 was first observed between GCs that were cuboidalising during primordial activation. Primordial follicle formation is not completed until after birth in mice. Therefore, the second wave of GC ingression from the OSE is still ongoing in a d4 mouse ovary and oocyte nests are still present. In addition, the intraovarian rete system of the rete ovarii is lined with cuboidal epithelium and persists in the medulla of the mouse ovary for about a week after birth (Byskov and Lintern-Moore, 1973; Wenzel and Odend'hal, 1985). Therefore,

although ERBB2 immunolabelling clearly localises to the membrane of cuboidal somatic cells in a d4 mouse ovary (Figure 5.1A), it is not clear, for the majority of cells, whether these are GCs that have yet to be incorporated into follicles or are the vestigial epithelium of the rete ovarii.

Initiation of follicle growth begins as soon as the first primordial follicles are formed in the centre of the ovary. Therefore, within the first week of postnatal life in the mouse, there is an initial, synchronous 'burst' of primordial activation in the centre of the ovary. ERBB2 is expressed in all cuboidal GCs of these growing follicles in a d8 mouse ovary (Figure 5.1B).

In contrast to ERBB2 immunolabelling in a d8 ovary, ERBB2 expression in d12 and d19 ovaries is not equivalent in all growing preantral follicles. ERBB2 immunolabelling is much stronger in growing preantral follicles that are located in the peripheral cortex of the ovary in d12 (Figure 5.1C), d19 (Figure 5.1D, E) and d21 (data not shown) ovaries. In contrast, follicles of a similar stage in development that are located more towards the centre of the ovary have dramatically weaker ERBB2 immunolabelling. In Figure 5.1D, five secondary follicles are shown in a d19 ovary but only the three closest to the OSE have strong ERBB2 expression. Furthermore two follicles that are developing a second layer of GCs in a d12 ovary are shown in Figure 5.1C but the most central one has weaker ERBB2 expression. The weak immunolabelling of ERBB2 in a centrally located primary plus stage follicle in a d12 ovary and strong immunolabelling in a peripherally located secondary stage follicle in an older d19 ovary suggests follicle stage is not responsible for this pattern of expression. Therefore, ERBB2 immunoreactivity of GCs in d12, d19 and d21 mouse ovaries may be determined by both follicle stage and location in the ovary.

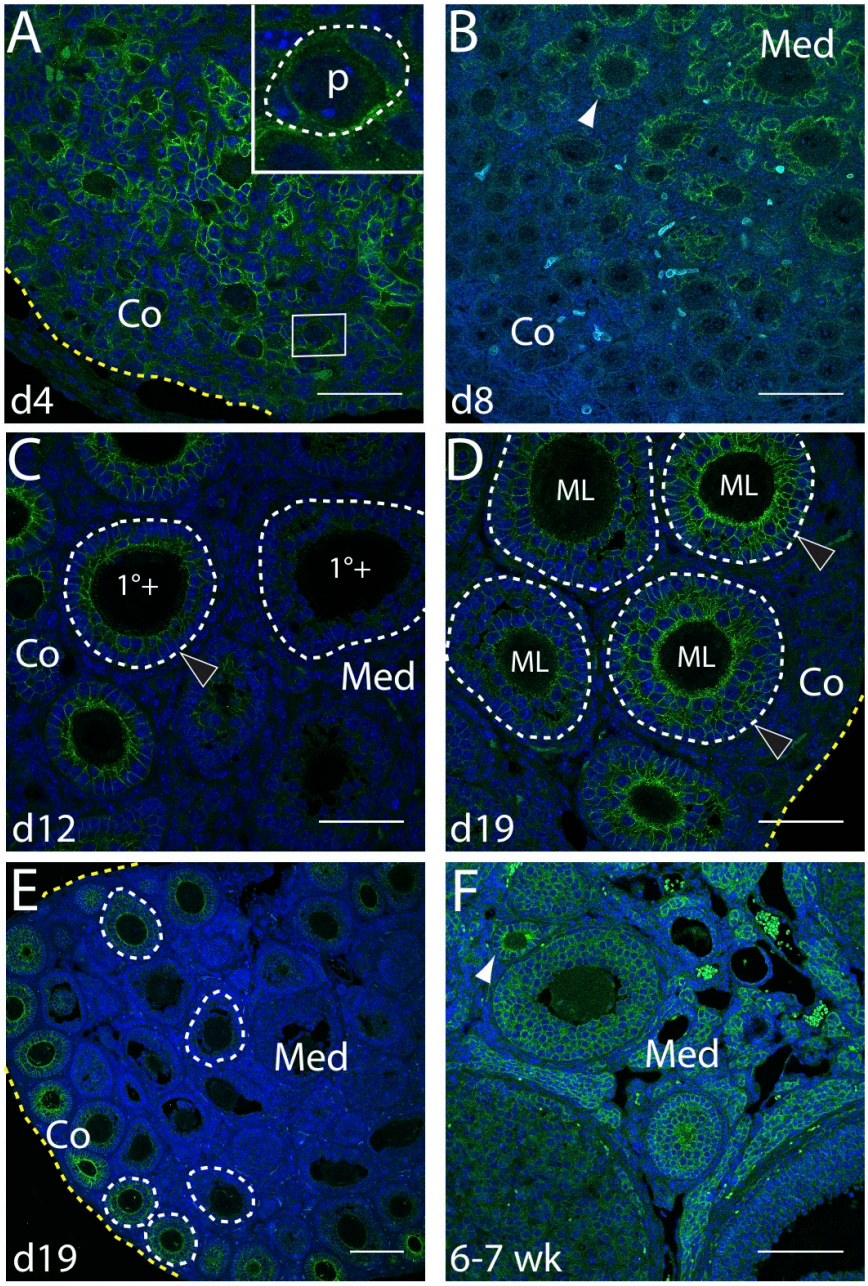


Figure 5.1. *ERBB2 protein expression in mouse ovaries of various ages post-partum. In d4 ovaries, ERBB2 labels GCs and also cuboidalised somatic cells of unknown classification (green, A). ERBB2 immunolabelling is strong in all central follicles of a d8 ovary (green, B), but only strong in peripheral growing follicles of d12 and d19 ovaries (green, C-E). Note the stronger ERBB2 immunolabelling in the two arrowed (black arrowheads) multilayered follicles close to the OSE in d12 (green, C) and d19 (green, D) ovaries. In adult ovaries, ERBB2 localises to growing preantral follicles including those that are towards the centre (green, F). Key: Med; cortico-medullary border, Co; cortex, 1°+; primary plus, ML; multilayered. Dotted lines represent the basal lamina. White arrowheads represent growing, centrally located preantral follicles expressing ERBB2. Black arrowheads represent stronger ERBB2 immunolabelling in peripheral follicles. Scale bars represent 50 µm (A-D) and 100 µm (E-F).*

ERBB2 also localises to cuboidal GCs of growing preantral follicles in adult mouse ovaries (Figure 5.1F). As described in chapter 4, ERBB2 was not expressed in flattened GCs of primordial follicles or cuboidal GCs of antral follicles. There are far fewer preantral follicles observed in a central section taken from an adult ovary, compared to that of a juvenile ovary. Therefore, it is more difficult to examine whether follicular location is affecting ERBB2 expression. However, ERBB2 immunolabelling was observed in columnar GCs of a primary follicle that was located towards the centre of an ovarian section from an adult mouse (Figure 5.1F).

To summarise, qualitatively, it appears that ERBB2 expression is regulated by both follicle stage and follicular location. Therefore, quantitative analysis of ERBB2 stained sections with respect to follicle stage and follicular location was examined.

5.1.2. Quantitative analysis of ERBB2 immunolabelling

Quantitative analysis of fluorescent ERBB2 immunolabelling in three d16 ovaries was performed as described in materials and methods section 2.4.7 and 2.4.8. Briefly, a threshold level of expression, specific for each ovary, was set and the number of pixels that met this threshold level of expression in GCs was measured. The percentage of GC area that was positive for ErbB2 immunolabelling, as determined by the threshold, was investigated with respect to follicle stage and distance of follicle from OSE. The sections used for analysis are shown in Figure 5.2 and an image of the section, as it appears during analysis using ImageJ is shown in Figure 5.3.

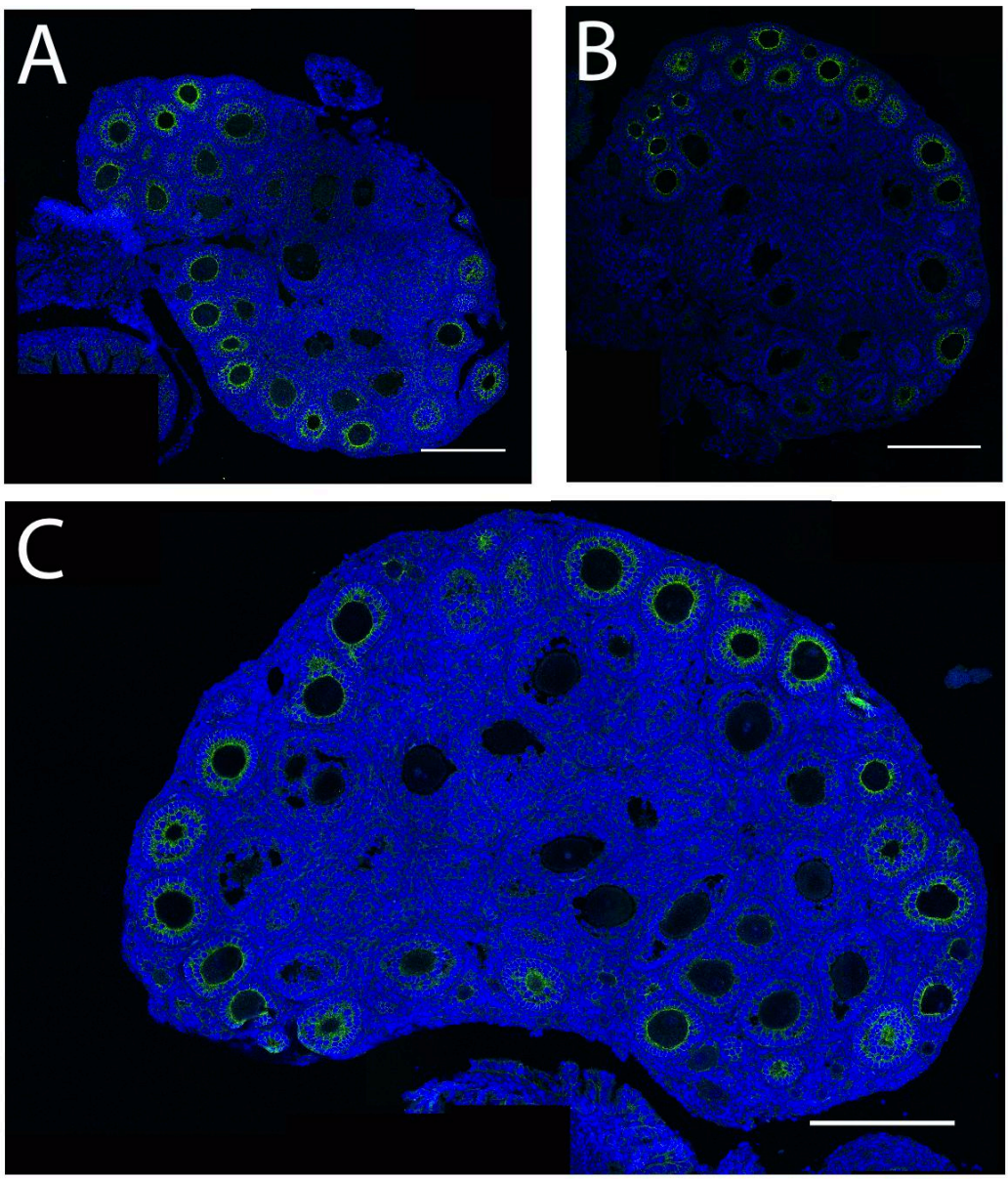


Figure 5.2. *ERBB2 immunolabelling in central sections from three d16 ovaries. Sequential, overlapping, high power images taken using a x63 oil objective were collated into one image of the entire section using DoubleTake (EchoOne.com). ERBB2 immunolabelling consistently appeared stronger in peripheral follicles of these ovaries. Scale bars represent 200 µm.*

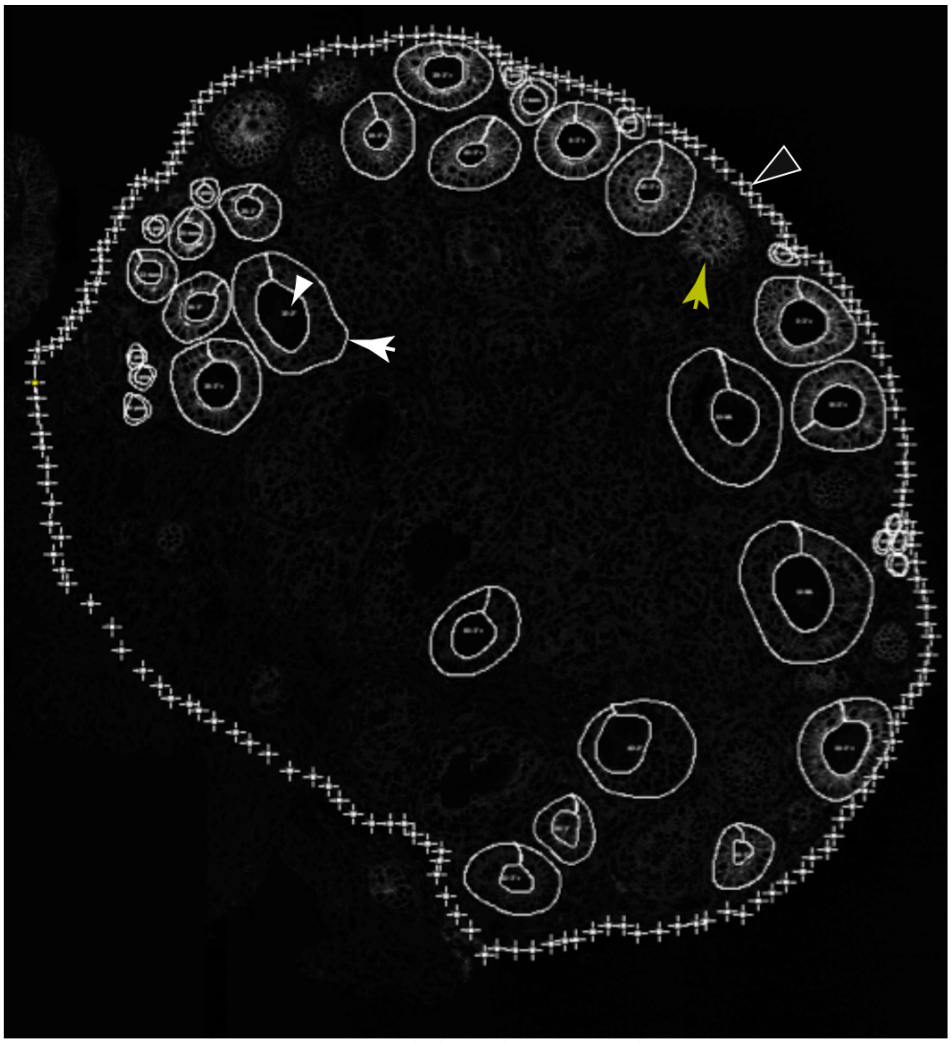


Figure 5.3. *Image showing an ovarian section used to measure ERBB2 immunolabelling intensity with respect to distance from OSE. This is achieved by delineation of the GC layer (white arrow) with the cursor tool in Image J. The number of pixels that meet or exceed the threshold labelling for presence of ERBB2 are measured. Subsequently, the xy co-ordinates and the area of the entire GC layer is measured and this follicle is labelled by follicle stage and with a unique chronological number (white arrowhead) before moving on to the next follicle. Once all follicles are measured and labelled, regular xy co-ordinates of the OSE are measured (black arrowheads). Yellow arrow shows ERBB2 immunolabelling in a follicle without a clear visible oocyte that was excluded from analysis.*

5.1.2.1 How does the level of ERBB2 immunolabelling differ with follicle stage?

The degree of ERBB2 immunolabelling was examined with respect to preantral follicle stage, as described in Materials and Methods section 2.4.7. Intensity of ERBB2 immunolabelling was expressed as the percentage of the area of the GCs only (excluding the oocyte) and these were compared between primordial, transitional, primary, primary plus and secondary follicles (Figure 5.4)

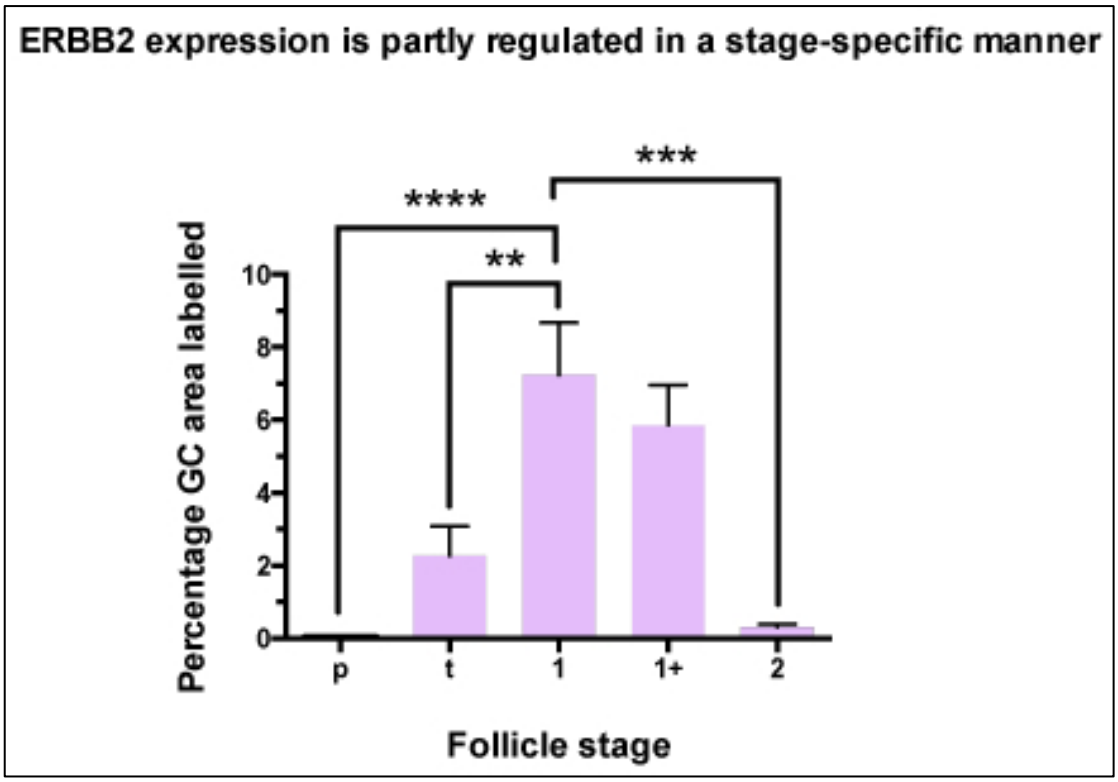


Figure 5.4. *Relationship between degree of ERBB2 immunolabelling and follicle stage. ERBB2 immunolabelling significantly increases during the primordial to primary transition and significantly decreases as GCs multilayer. A single central section from three d16 ovaries was used for this analysis and the number of follicles measured for each follicle stage were: primordial (p); 37, transitional (t); 8, primary (1); 7, primary plus (1+); 15, secondary (2); 4 follicles. Bars represent means and error bars represent standard error of the means (SEM). ANOVA was performed on the raw data using Prism 6 with a Tukeys multiple comparison post hoc test. Key: p; primordial, t; transitional, 1; primary, 1+; primary plus, 2; secondary stage follicle.*

The values for level of immunolabelling are low (less than 10%) in all stages. This is because ErbB2 is a membranous protein and therefore, the larger compartments of GCs; the cytoplasm and nucleus, are 'blank' even in follicles expressing the highest levels of ERBB2. However, it is still possible to detect significant changes between different follicle stages.

As expected, there was neglible ERBB2 immunolabelling detected in primordial follicles. ERBB2 immunolabelling increased significantly from the primordial to the primary stage and from the transitional to the primary stage. Subsequently, it decreased significantly between the primary and the secondary stage. This suggests that ErbB2 is important in primordial activation but not GC multilayering.

As the first follicles to form are in the centre of the ovary, central follicles will reach the multilayered stage of development first. The consequence of this is that multilayered follicles are more likely to be located centrally in a d16 ovary. Therefore, it is not clear whether the reduction of ERBB2 immunolabelling at the secondary stage is due to stage-dependent regulation of ERBB2 expression or is instead related to follicular location. This analysis did not address whether secondary follicles that were located in the periphery expressed more ERBB2 than secondary follicles located towards the medulla.

The next analysis examined the extent to which ERBB2 expression was regulated by follicular location.

5.1.2.2 How does the level of ERBB2 immunolabelling differ with follicular location?

The intensity of ERBB2 expression in follicles was analysed in three d16 formalin-fixed ovaries, as described above (section 5.1.2). d16 ovaries were analysed because this age is the most often used for the isolated follicle culture model. In culture experiments preantral follicles of a similar stage are isolated and cultured individually in 96 well plates. It is assumed that follicles of a similar stage will respond similarly to treatment. However, where analysis of ErbB2 function is concerned this may not be the case.

As mentioned in section 5.1.2.1, ERBB2 expression is upregulated upon GC cuboidalisation and throughout the primordial-to-primary transition therefore primordial and transitional follicles were excluded from spatial analysis, as this aspect of ERBB2 expression appears to be wholly regulated by follicle stage. Furthermore, all primordial and transitional follicles are in the periphery and so the effect of follicular location on these follicles cannot be examined in this analysis. The remaining follicles were classified as primary, primary plus, secondary and multilayered.

The intensity of ERBB2 immunolabelling (as determined by % GC area labelled) was displayed according to whether it was in a follicle that (i) was either less or more than 100 μm from the OSE and (ii) had either less than 2, or 2 or more layers of GCs (Figure 5.5). This demonstrates that ERBB2 immunolabelling vastly decreases in follicles further than 100 μm from the OSE and this affect is more pronounced in multilayered follicles (Figure 5.6).

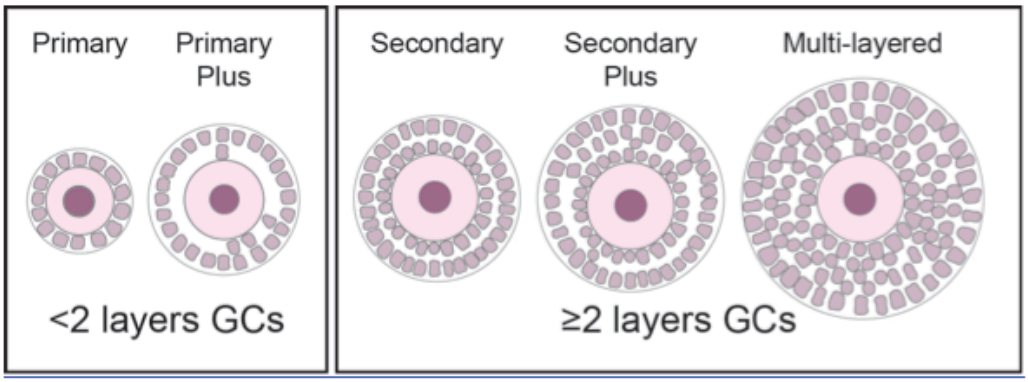


Figure 5.5. *Diagram illustrating how growing follicles were staged and separated for analysis. Primordial and transitional follicles were not included as these are only ever found in the periphery of the ovary. Primary and primary plus follicles that have a visible oocyte were grouped (as follicles with less than 2 layers of GCs) and secondary, secondary plus and multilayered follicles were grouped (as follicles with 2 or more layers of GCs).*

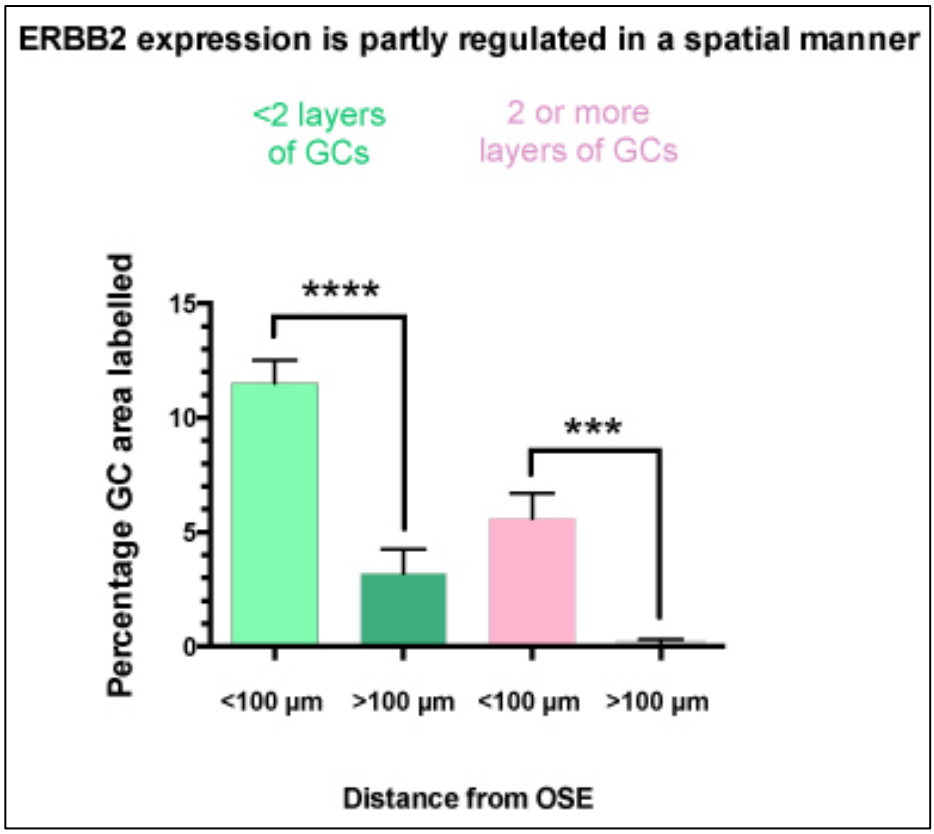


Figure 5.6. *Graph showing the effect of follicular location on intensity of ERBB2 immunolabelling. ERBB2 immunolabelling significantly decreases as you move further than 100 µm from the OSE for both follicles with less than 2 or 2 or more layers of GCs. Bars show mean and error bars represent standard error of the mean (SEM). Statistical significance was determined using the Mann Whitney test. The number of follicles analysed in total from the three ovaries were 33 follicles with <2 layer of GCs that were <100 µm from OSE, and 12 of a similar stage further than 100 µm from OSE, 4 follicles with 2 or more layers of GCs that were <100 µm from OSE and 19 follicles of a similar stage that were >100 µm from OSE.*

Quantitative analysis of ERBB2 expression demonstrated that follicles of a similar stage i.e. either primary and primary plus follicles with at least 1 but not 2 layers of GCs or secondary and multilayered follicles with at least 2 layers of GCs had differential ERBB2 expression depending on where they were in the ovary (Figure 5.6). Specifically, the average percentage of GC area positive for ERBB2 significantly decreased as you moved 100 μm in from the surface to negligible levels in the case of follicles with 2 or more layers of GCs. In fact, of the 21 follicles measured that were over 150 μm away from the OSE only 2 had an ERBB2 intensity measurement of over 1% and these were both primary plus follicles. No follicles with more than 2 layers of GCs ever had significant ERBB2 expression.

The level of expression in the first set of analysis (Figure 5.4) that examined how ERBB2 immunolabelling differed in different follicle stages appears to produce a lower value for % area stained in secondary follicles than this second set of analysis (Figure 5.6). This is due to the large amount of secondary follicles in the centre of the section that express neglible levels of ERBB2 in comparison to those secondary follicles in the periphery of the section of which there are comparatively fewer. These central and peripheral secondary follicles are grouped together in Figure 5.4 and separated in Figure 5.6.

To summarise, ERBB2 expression in growing preantral follicles of ovaries from mice of approximately 2-3 week old mice differs between follicles of a similar stage dependent upon their location within the ovary. It is not yet clear why this is the case.

5.1.3. How does ERBB2 immunolabelling in a d16 ovary compare to that of other proteins?

Activation of TGF-β signalling leads to phosphorylation and nuclear translocation of either Smad 2/3 or Smad 1/5/8, depending on which ligand:receptor pair are stimulated (Wrana, 2013). Gdf9 and AMH both have critical roles in follicle development (Dong et al., 1996; Durlinger et al., 2002) and they activate the Smad 2/3 and Smad 1/5/8 intracellular cascades, respectively (Wrana, 2013). Cross talk between Gdf9 and EGFR signalling has been reported in the mouse ovary (Sasseville et al., 2010). An indirect association between AMH and EGFR expression may exist as it is established that AMH becomes downregulated at around the same stage of development at which EGFR expression is critical to mediate the LH surge (Park et al., 2004; Salmon et al., 2004). Furthermore, Smad 2/3 (Fenwick et al., 2011) and AMH have been localised in our laboratory. There was not a good Gdf9 antibody available to us. Therefore, we double labelled 5 μm sections from formalin-fixed, paraffin-embedded d16 ovaries with antibodies to ErbB2 and also either (i) AMH or (ii) Smad 2/3 as described in materials and methods section 2.4.3.

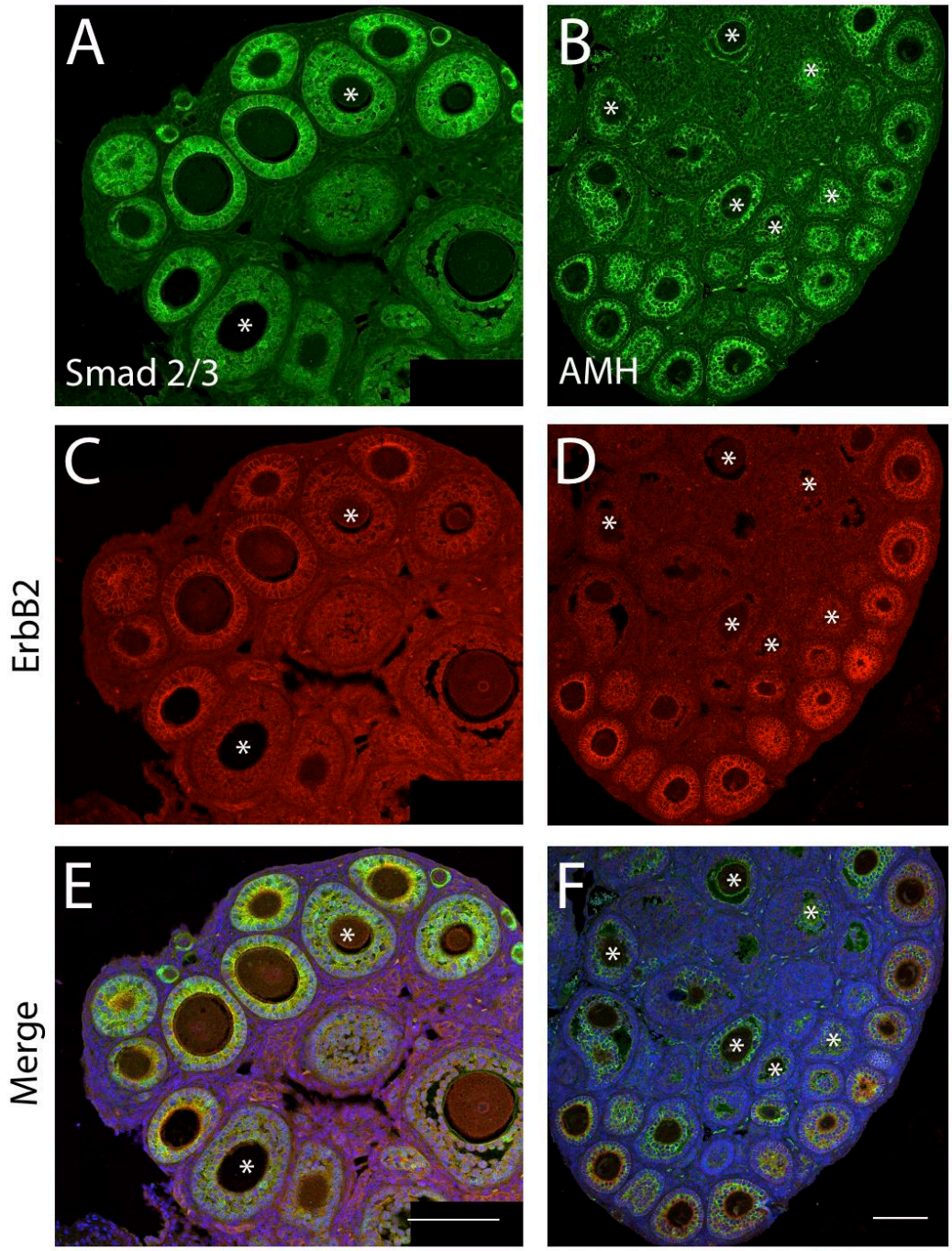


Figure 5.7. *The relationship between ERBB2 immunolabelling and that of proteins from the TGF-beta superfamily signalling pathway. Co-localisation between ERBB2 (red, C-F) and either Smad 2-3 (green, A, E) or AMH (green, B, F) was assessed in preantral follicles. Stars indicate follicles in which the relative levels of ERBB2 and either Smad 2/3 or AMH are not similar and do not indicate a relationship with ERBB2. Nuclei are labelled with DAPI (blue, A-F). Scale bars represent 100 µm.*

The spatial localisation of ERBB2 was compared to that of Smad 2/3 and AMH. The amount of co-localisation was not measured as these molecules are

expressed in different compartments: ErbB2 is membranous whereas AMH is cytoplasmic and Smad 2/3 molecules translocate between the cytoplasm and the nucleus. However, the number of follicles that express (i) high levels of ERBB2 only, (ii) high levels of both ERBB2 and Smad 2/3 or AMH, or (iii) high levels of Smad 2/3 or AMH only can be compared.

It is unclear whether there is a relationship between ERBB2 and AMH expression (Figure 5.7B, D, F). There is a substantial proportion of follicles that express both AMH and ERBB2 but these are all in the periphery. In contrast to ERBB2 immunolabelling, which is detected strongly in a peripheral ring of follicles, AMH immunolabelling also localised strongly to the majority of follicles situated closer to the medulla (Figure 5.7D). Therefore, the number of follicles that distinctly express AMH but not ERBB2 is approaching the number of follicles that distinctly express both AMH and ERBB2. It is not clear, therefore, whether ERBB2 and AMH expression is directly related or whether they coincidentally overlap based on this co-expression data alone.

The likelihood of a relationship between ERBB2 and SMAD 2/3 expression was not as clear either. There are definitely fewer follicles that have strong SMAD 2/3 expression only (Figure 5.7C) compared to those that had strong AMH expression only (Figure 5.7D). However, it is entirely possible that there is no relationship between ERBB2 and SMAD 2/3 and the similarity in pattern of expression is a coincidence peculiar to this age of ovary i.e. the initial wave of follicle activation from birth onwards in mice may cause the follicular complement of a d16 ovary to be such that SMAD 2/3 is expressed in the same follicles as ERBB2 to a comparable level even though they may be regulated by completely distinct processes.

5.2 Discussion

In contrast to the uniform level of expression of ERBB2 in cuboidalised GCs of a d8 ovary, the cuboidalised GCs of peripheral follicles in d12, d16, d19 and d21 ovaries express much more ERBB2 than similar-stage follicles in the centre of these ovaries. Therefore, ERBB2 expression is downregulated in a proportion of centrally located follicles between 8 and 12 dpp. Between 8 and 12 dpp secondary follicles become more prevalent in the centre. However, the results described in this chapter demonstrate that differential ERBB2 expression between follicles in the peripheral cortex and central cortico-medullary border in d12-d21 ovaries is not dependent on follicular stage.

5.2.1 ERBB2 expression may be regulated by something in the blood supply

The medulla of the ovary is vascularised and although there is not an exact stage of development described at which follicles become enveloped by capillaries, although that is probably linked to theca formation, central follicles closest to the medulla are likely to acquire a blood vessel network first. Therefore, it may be that ERBB2 is negatively regulated by something in the blood such as the gonadotrophins FSH and LH. However, it is not clear what the purpose of this would be. ERBB2 immunolabelling in a superovulated ovary (formalin fixed 4 hours post hCG injection) was not visibly different to that in an adult ovary (data not shown). Further research is required to establish whether a substance in the blood supply affects ERBB2 expression, such as culture of whole d4 ovaries that lack a blood supply, but preliminary observations have not yet indicated this is the case.

5.2.2 ERBB2 expression may be regulated by ECM components

An alternative hypothesis is that ovarian rigidity is regulating ERBB2 expression. There is a higher density of ECM components in the cortex of the ovary compared to the peri-medullary region and the density of ECM components is known to have an affect on follicle development in vitro (Woodruff and Shea, 2011). Interestingly, the development of a 3D follicle culture model environment with a soft collagen centre and a stiff alginate outer ring has facilitated in vitro ovulation in the absence of LH and EGF (Choi et al., 2014). Based on these and other observations, Woodruff and Shea (Woodruff and Shea, 2011) propose that the ovary is composed of a 'non-permissive' cortex, in which it is difficult for follicles to initiate growth, and a 'permissive' peri-medullary region in which is it easier for follicles to initiate growth. Woodruff and Shea conclude that work in the immediate future should focus on investigating whether different signalling pathways exist in the permissive and non-permissive environments of the ovary. Therefore, it may be that ERBB2 expression is associated with a high density of ECM component and is required to overcome the physical constraints imposed upon the peripherally located primordial pool and early stages of follicle growth. Integrins are transmembrane cell adhesion molecules that mediate physical forces and signalling between the cell and ECM. Cross-talk between ErbB2 and various integrin proteins is well documented (Wakatsuki et al., 2014; Wang et al., 2014; Wang et al., 2010) and this is a possible mechanism by which ERBB2 expression could respond to and mediate the heterogeneous mechanical signals in the mouse ovary. Several integrins have been localised in the mouse ovary. Immunofluorescent labelling of Integrin-β3 in pre-pubertal mouse ovaries in our laboratory demonstrated that Integrin-β3 protein localises to theca, stroma and preantral GC membranes (Akansha Garg and Mhairi Laird, unpublished

observations). In addition, Integrin-α6 mRNA has been localised to GCs of primary follicles (Burns et al., 2002). Therefore, it is possible that these integrins interact with ErbB2. To the best of my knowledge, none so far have been localised specifically or predominantly to follicles or stroma in the periphery of the ovary.

5.2.3 ERBB2 expression may be regulated by another growth factor family

A gradient or pattern of expression of another protein has been observed in our lab recently (Fenwick et al., 2011). The TGF-β superfamily, to which Gdf9 and BMP15 belong, signal intracellularly by different SMAD signalling proteins. Gdf9 activation acts through the SMAD2/3 pathway whereas AMH activation triggers the SMAD1/5/8 cascade. Recent studies in our lab have shown that peripheral follicles at the primordial to primary stage of development express SMAD2/3 whereas centrally located follicles at a later stage of development in which GCs are multilayering express SMAD1/5/8. However, while it appears that the gradient of SMAD2/3 expression in the mouse ovary is entirely due to the gradient of follicle development caused by the central follicles initiating growth first this does not mean that there is not cross-talk or mutual regulation between the TGF-β family and the EGF family. Indeed, this has in fact been demonstrated in the mouse ovary. Gdf9 signalling via Smad3 has been shown to require EGFR activation of ERK1/2 in COC's (Sasseville et al., 2010). Furthermore, recent preliminary results from our laboratory have also indicated that the TGF-β family may regulate ErbB2 in preantral follicles. Oocytectomised follicles, in which the oocyte has been mechanically removed, were cultured in either basal culture medium or that supplemented with BMP15 and GDF9. *ErbB2* expression is reduced in follicles lacking an oocyte compared to intact follicle controls. Interestingly, it is further reduced in oocytectomised follicles that have been

cultured in the presence of BMP15 and GDF9 (Jocelyn Mora, unpublished observations). This strongly suggests that ErbB2 is regulated by factors in the oocyte, although it appears that GDF9 and BMP15 are not the only factors involved. This result may reflect the antagonism of GDF9 and BMP15 on other oocyte-derived factors that act to positively regulate *ErbB2* expression. At the protein level, ERBB2 immunolabelling in preantral follicles (either isolated or within ovarian cross sections) was not visibly different with respect to distance from oocyte or basal lamina. However, quantitative analysis of this was not examined. Culture experiments do suggest that oocyte-derived factors are involved in ErbB2 regulation in some way and it is therefore possible that factors in the oocyte may be responsible for the peripheral pattern of ERBB2 expression.

It is also possible that GC-derived members of the TGF-β superfamily, or another family, regulate or act in conjunction with ErbB2. For example, AMH and ERBB2 are co-expressed in peripheral follicles but AMH is also expressed in a number of central follicles. AMH inhibits primordial activation in the mouse (Durlinger et al., 2002) whereas this project is proposing that ErbB2 positively regulates primordial activation in the mouse. It would be interesting to investigate whether the function of AMH and/or ErbB2 changes when they are co-expressed. BMP15 and GDF9 have different effects in vitro depending on whether they are combined or not; BMP15 on it's own has an inhibitory effect on follicle growth but when combined with GDF9 it stimulates follicle growth to a greater extent than GDF9 alone (Fenwick et al., 2013).

5.2.4 ERBB2 expression may be regulated according to GC origin

It is established that there are two populations of GCs and therefore two populations of primordial follicles that behave differently (Mork et al., 2012; Zheng et al., 2014b). A first wave of GCs ingress from the OSE to surround central oocytes and form the primordial follicles that synchronously initiate growth at birth. A second postnatal wave of GCs surround the cortical oocytes and form the primordial follicle stock that forms the entire reproductive lifespan (Mork et al., 2012; Zheng et al., 2014a). One possible idea was that the follicles that were downregulating ERBB2 expression in d12, d16, d19 and d21 mouse ovaries were those belonging to this first wave of follicle initiation. This would suggest that the follicles that maintain strong ERBB2 immunolabelling in these ovaries are those from the cortical primordial follicles activated later. However, Zheng et al (2014) demonstrated that secondary follicles derived from cortical primordial follicles do not appear in the ovary until approximately 23 or 24 dpp. Therefore, this is does not quite align with this hypothesis. However, it can certainly not be ruled out that GC origin may regulate ERBB2 expression.

5.3 Conclusions

To the best of my knowledge, ERBB2 is the only protein that has been localised in this particular pattern. Furthermore, I am not aware of any other protein whose expression is believed to be regulated by follicular location. Therefore, further study into ERBB2 expression could yield information on a previously unknown or not fully understood dynamic of follicle development in the mouse ovary.

The relationship between ErbB2 expression and ovarian rigidity and the extracellular matrix environment is worthy of further investigation. The role of the

ovary's physical environment has been appreciated relatively recently in comparison to the role of hormonal and intraovarian factors on follicle development. Several groups are developing new and exciting 3D follicle culture models, and the investigation of ErbB2 in these models would be an exciting possibility. It would also be interesting to examine whether the gradient of ERBB2 immunolabelling is maintained in cultured day 12 ovaries (if these can be supported in vitro), as these lack a blood supply.

To summarise, the role of the differential ErbB2 protein expression could be an exciting avenue of future work.

Chapter 6: Localisation of EGFR protein by Western blot

We have localised *Egfr* mRNA to preantral follicles but were not able to localise EGFR protein to GCs, as there is no good commercially available antibody for immunofluorescence or immunohistochemical detection of EGFR (confirmed by personal communication with Conti). As EGFR has an established role in cumulus GCs during the LH surge we determined whether an antibody was suitable by examining whether EGFR immunolabelling was detected in cumulus GCs of pre-ovulatory follicles in superovulated ovaries fixed 4 hours post hCG injection. None of the three antibodies to EGFR tested labelled cumulus cells, or any other cells, in these ovaries. Sensitivity of isolated follicles in culture to both EGF stimulation and to inhibition of EGFR, as described in results chapter 7, strongly suggests that EGFR must be present in isolated preantral follicles. The absence of EGFR message from preantral oocytes indicates that it is the GCs that express EGFR protein. The evidence accumulated so far strongly suggests EGFR is present, but we have so far been unable to visualise the protein. Visualisation of EGFR protein is key to determining whether it heterodimerises with ErbB2 in follicles initiating growth.

Proteins can also be detected by Western blot analysis. In this technique, you lyse proteins out of your cell/tissue of interest, separate these proteins according to size by denaturing sodium dodecyl sulfate polyacrylamide gel electrophoresis (SDS-PAGE), transfer the proteins from a gel to a membrane and probe this membrane with an antibody specific to your protein of interest. Western blot analysis is widely used

in laboratories studying cells/tissues that you are able to extract a reasonable amount of protein from, however, we are restricted to the number of follicles we are able to isolate and pool together for these experiments. However, a recent publication detected proteins in lysates from 50 pre-implantation mouse blastocysts (Sun et al., 2014). Therefore, we hypothesized we should be able to detect EGFR protein in a similar number of isolated preantral follicles, which contain more cells.

6.1 Results

6.1.1 Can we detect EGFR protein in positive mouse tissue controls by Western blot analysis?

The majority of western blots are performed on approximately 30-50 μg of protein and while it is just not feasible to prepare this much protein from follicles, it is possible with whole ovaries. EGFR has a critical role during the LH surge, therefore an ideal control would be a superovulated ovary 4 hours post hCG injection. However, as these were not immediately available to us, we prepared lysates from adult mouse ovaries. While EGFR expression may vary during different stages of estrous cycle in the mouse we are likely to detect EGFR in adult mouse ovary if we are preparing lysates from several adult mice, presumably at different stages of estrous.

Protein lysates were prepared from five ovaries obtained from 3 adult mice, as described in materials and methods 2.5.1. Ovaries were dissected away from extraovarian tissue and promptly snap frozen in a small amount of RIPA buffer by liquid nitrogen. Upon thawing of the tissue, approximately 500 μL of RIPA buffer supplemented with protease and phosphatase inhibitors was added. The tissue was mechanically dissociated with a plastic pestle while it thawed and was subsequently agitated for 30 minutes at 4°C on a rotary wheel. Yield was determined using a BCA

(bicinchoninic acid) protein assay reagent that allows you to calculate total protein content from colourimetric change, as measured on a spectrophotometer. As the aim of these experiments was just to demonstrate that we are able to detect EGFR by western blot, we loaded approximately 50 μg of protein each from five adult ovaries. As EGFR is a large protein of 175 kDa, protein was loaded onto an 8% polyacrylamide gel. In this first, preliminary western blot, the electrophoresis tank was run at 60V until the samples have reached the resolving gel (approximately 30 minutes) at which point the voltage is increased to 130V for the final 90 minutes. Protein was transferred onto a nitrocellulose membrane for 1.5 hours at 100V, 350mA at 4°C. The membrane was then blocked with 5% milk (Dried milk powder, Marvel) before overnight incubation with Rabbit anti-EGFR antibody (cat no 4267, Cell Signaling). On day 2, the membrane was incubated with a horse radish peroxidase-(HRP-) conjugated secondary antibody for 1 hour, washed in 1X TBST and briefly incubated with a peroxidase substrate for enhanced chemiluminescence (ECL). Product was visualised on chemiluminescence film in a dark room. EGFR was indeed detectable in these lysates (Figure 6.1). The amount of product varied between each sample. As a loading 'control' such as α-tubulin or β-actin was not used in this preliminary experiment, it is not clear whether this was entirely due to uneven loading or whether it also reflects the developmentally regulated levels of EGFR protein during the mouse estrous cycle. It was concluded that the antibody and protocol used in this Western blot analysis were suitable to detect EGFR in 50 μg of adult mouse ovary. Therefore, the same antibody and protocol was used to probe for EGFR in lysates made from 50 pooled preantral follicles.

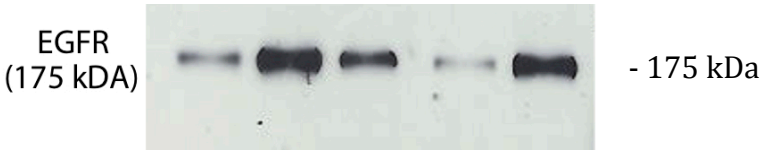


Figure 6.1. *Lysates from five adult ovaries were immunoprobed with antibodies to EGFR (175 kDa).*

6.1.2 Can we detect EGFR in pools of 50 isolated preantral follicles?

To establish whether the protocol we had used to detect EGFR protein was sufficient to detect EGFR in follicles, we isolated 250 preantral follicles from several d16 ovaries and prepared lysates from these using the same protocol as described above. 50 follicles (n=5) were pooled into 20 μL lysis buffer (RIPA buffer plus protease and phosphatase inhibitors), agitated at 4 °C for 30 mins on a rotary wheel, and then centrifuged at 13,000 RPM at 4 °C. As there was only 20 μL sample and our total protein content assay required 10 μL we did not assay for total protein content and instead loaded the entire supernatant of all 5 samples onto a western blot and probed for EGFR as before. We also loaded 30 μg of protein lysate prepared from HELA cells kindly donated by Rakhee Chauhan of Dr Nick Dibbs group (Cell signalling in gynaecological malignancy group, IRDB). Ponceau staining of the membrane revealed multiple bands of varying sizes indicating we had managed to extract some protein. EGFR, or indeed any other labelling, was not detected in any sample however (data not shown). Immunoprobing the membrane for α-Tubulin, a popular loading control in western blotting due to its ubiquitous and abundant nature, demonstrated that the Western blot had worked (Figure 6.2 A). The failure to detect EGFR in the HELA cells positive control may be due to protein degradation in an old sample. Importantly, α-tubulin was indeed detected in follicles demonstrating it is possible to detect protein in preantral follicles by western blot. However, it was unclear as to whether it was possible to detect a protein that is not expressed as highly

as α-tubulin, of which there are few. Therefore, the membrane was immunoprobed with antibodies to β-catenin, a membrane protein that is of physiological significance to this project. To allow for multiple re-probing the membrane was cut in half and one half re-probed for β-catenin. Crucially, β-catenin (92 kDa) was detected in both follicle samples probed, therefore demonstrating we can detect a membrane associated protein in preantral GCs by western blot (Figure 6.2B). It therefore seemed likely that the reason EGFR was not detected in these follicles was due to low abundance of EGFR in GCs.

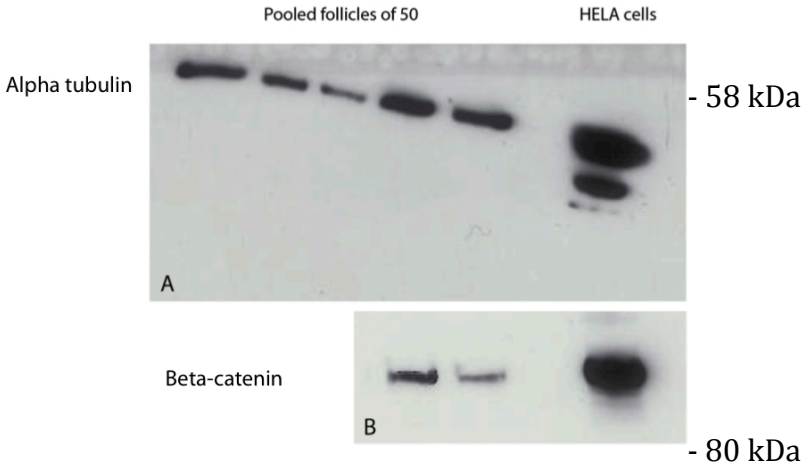


***Figure 6.2**. Lysates from pooled preantral follicles (50) and HeLa cells (positive control) were immunoprobed with antibodies to α-tubulin (A) and β-catenin (B). This demonstrated that protein, and more specifically, a membrane bound protein can be detected in lysates made from pooled preantral follicles.*

6.1.3 How much protein can we extract from pooled preantral follicles?

As it was suspected that EGFR protein was not very abundant in GCs, the next experiments focused on increasing and measuring the amount of protein extracted from pooled follicles. Visual inspection during the lysate preparation process during the previous experiment suggested that follicles remained intact following freeze-thawing and agitation on the rotary wheel. This indicates that the lysate preparation was not harsh enough. Therefore, a different protocol for lysate preparation was

tested. To further enhance the protein yield larger pools of follicles (100) were collected. To establish that the failure to detect EGFR in preantral follicles was not lack of expression we also prepared lysates from both whole d16 ovaries and also the tissue left over following follicle isolation from an ovary. This tissue consists of stroma and follicles that are resistant to mechanical isolation.

The following samples were collected: pools of 50 follicles, pools of 100 follicles, whole pre-pubertal (d16) ovaries, the tissue left over following follicle isolation from an ovary and (d16) oviduct. The following protocol was used to prepare lysates from follicle samples and the stromal tissue: samples pooled into appropriate volume of lysis buffer (20-50 μL), snap frozen in liquid nitrogen and then thawed (one freeze thaw cycle), sonicated in a sonicating waterbath for 3 cycles of 30 seconds on, 90 seconds off, agitated at 4°C for 30 minutes and finally centrifuged at 4°C for 5 minutes. The BCA total protein assay was used to determine yield and these values are summarised in Table 6.1. Importantly, we managed to extract at least 5 μg from all samples.

Table 6.1. *Protein content for juvenile ovary, preantral follicles, and oviduct as determined by BCA total protein assay.*

Lysate	Concentration of protein (microg / microL)	Approximate volume of lysate
Oviduct	1.279804878	40
Stroma	1.594926829	30
50 follicles	0.353219512	20
100 follicles	0.510780488	20
d15 ovary	1.037731707	40
d17 ovary	0.643829268	40

6.1.4 Is our Western blotting protocol optimal?

To ensure an optimal protocol was being used for Western blot analysis, we sought further advice from within our institution. The following small changes to the protocol were suggested for enhancing the likelihood of detecting EGFR in preantral

follicles. The Xcell Surelock Mini cell gel electrophoresis tank was run at 125V for 90 minutes. Protein was transferred for longer (2.5 hrs) and complete and even transfer was assessed by Ponceau stain of the membrane and Coomassie Blue staining of the gel. EGFR was immunoprobed in adult ovaries using this protocol and found that EGFR was detectable using this protocol although no obvious enhancement was observed (data not shown). As protein was detected and transfer was even and complete, this protocol (as described in materials and methods 2.5.4) was used from this point onwards.

6.1.5 How much protein from adult ovaries is needed to detect EGFR?

As the total amount of protein extracted from 100 pooled follicles was only a fraction of the protein normally loaded for Western blot analysis, the next analysis determined whether EGFR could be detected in as little as 1 μg of adult ovary control. Therefore, one EGFR-expressing adult ovary was diluted with RIPA buffer to 10, 5, 2 and 1 μg and immunoprobed with antibodies to EGFR as before. As there was difficulty in detecting EGFR in follicles in previous experiments, we used a different substrate for enhanced chemiluminescence (ECL) detection of EGFR (but not α-tubulin) that was developed to detect lower levels of antibody bound protein. As expected, α-tubulin was detected in all samples with increasing band intensity from 1 to 50 μg. Crucially, EGFR (175 kDa) was also detected in 2, 5, 10 and 50 μg but not 1 μg of adult ovary (Figure 6.3). EGFR is highly expressed in adult ovary and so while it is detectable in 2 μg of adult ovary, it may not be detectable in 2 μg of another sample i.e. follicles that do not express as much EGFR. However, this experiment at least demonstrates that it is possible to detect EGFR in a small amount of protein using this antibody and this protocol.

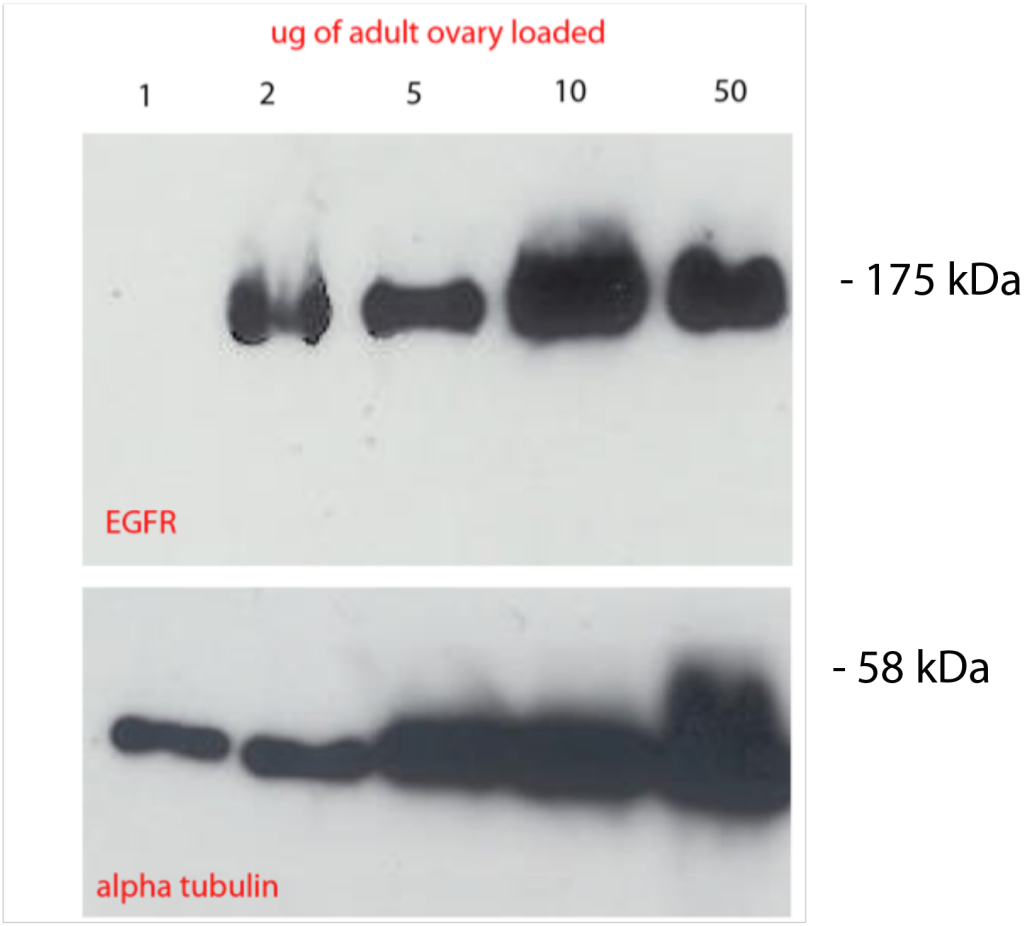


Figure 6.3. *Lysates from one adult ovary were serially diluted in RIPA buffer to 50, 10, 5, 2 or 1 µg and immunoprobed with antibodies to EGFR (A) and α-tubulin (B). α-tubulin was detected in all samples. However, EGFR was not detected in 1 µg of ovary.*

6.1.6 Can we detect EGFR in protein lysate prepared from 100 follicles?

EGFR is detectable in 2 µg of protein from an adult ovary and 10 µg of protein has been extracted from pooled preantral follicles. As 30 µg of protein is commonly loaded in western blots it was decided this was a reasonable amount of protein with which to attempt to detect EGFR. As half the sample had been used to measure the total protein content of the lysate prepared from 100 follicles, another lysate that had been prepared in the same manner at the same time and therefore presumably has the same protein content was used. There was enough of the juvenile

and adult ovaries, however, to load more of the exact same sample used in the dilution curve.

In a final attempt to localise EGFR to preantral follicles the entire supernatant of a pool of 50 and a pool of 100 follicles, 10 μg of 'stroma', d15 ovary, and 2 separate adult ovaries and 50 μg of adult ovary as a positive control was loaded into the polyacrylamide gel. The only bands detected were from adult and pre-pubertal ovaries (Figure 6.4 A). No EGFR was detected in follicles or stroma. The membrane was probed for α-tubulin to check the western blot had worked (Figure 6.4 B) and β-catenin (data not shown) to check the lysing protocol had not been too harsh for a membrane bound protein. Although, the 55 kDa band for α-tubulin appeared slightly warped in the pool of 50 follicles and very faint in the 'stroma' samples, crucially they were both detected as expected in the adult ovary controls and the pool of 100 follicles. Therefore EGFR is not detectable in pools of preantral follicles using this antibody and this protocol. It is not clear whether this is due to non-optimal protocol or low abundance of EGFR in follicles.

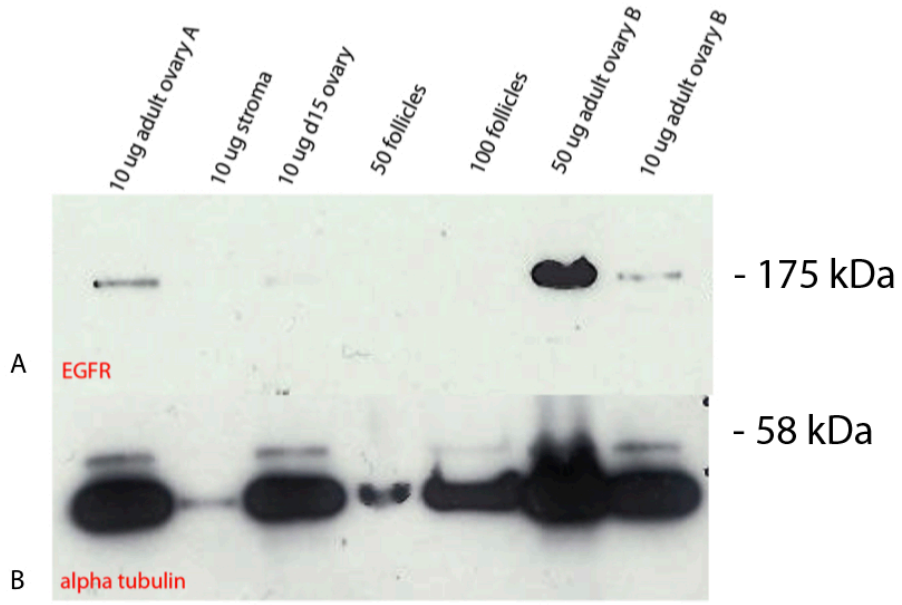


Figure . EGFR and alpha tubulin loading control shown.
Importantly no EGFR band was detected in 100 follicles.

Figure 6.4. *Lysates from adult ovary (10 and 50 µg), pre-pubertal ovary, remnant tissue from a pre-pubertal ovary following follicle isolation ('stroma'), 50 pooled preantral follicles, and 100 pooled preantral follicles were immunoprobed with antibodies to EGFR (A) and α-tubulin.*

6.2 Discussion

EGFR was not detected in lysates prepared from 50 or 100 pooled preantral follicles but it was detected in positive controls. The sensitivity of isolated preantral follicles to both EGF stimulation and inhibition of EGFR (see results chapter 7) suggests that the lack of detection is not due to lack of expression. Previous studies investigating the activin receptor have shown that only 100 molecules of occupied receptor are required to cause changes to gene transcription (Dyson and Gurdon, 1998). This illustrates the possibility that the level of EGFR protein in isolated follicles is sufficient to generate a signal but not high enough to be detected in these experiments. Additionally, further optimisation of the protocols used to prepare

lysates may be required. As ErbB3 was detected at a later point during this project, future studies would also examine ERBB3 expression by Western blot analysis.

Chapter 7: ErbB inhibition during in vitro preantral follicle growth

Immunolocalisation of ERBB2 and TOB1, an anti-proliferative protein downstream of ErbB2, suggested that ErbB2 might have a role in regulating GC cuboidalisation and proliferation during primordial activation (see chapter 4 for details). ErbB2 has been validated as a molecular target in several types of cancers in human and, as such, several inhibitors to ErbB2 signalling have been developed. We sought to address whether ErbB2 was involved in regulating GC cell shape and proliferation using these inhibitors.

The most robust culture model available in our laboratory at the beginning of this project was the isolated follicle culture model. In this model, preantral follicles from a d15 or d16 mouse are mechanically isolated and cultured individually in 100 μL of medium in 96 well plates for 72 hours. Photographs are taken at 0, 24, 48 and 72 hours. GC proliferation can only be directly quantified once follicles are collected and fixed at a specific timepoint in culture and immunolabelled for proliferation markers, such as Ki67. However, an increase in GC proliferation will result in an increase in follicle area, which can easily be measured using ImageJ software (materials and methods section 2.6.7). Preantral follicles that we isolate from d15 and d16 ovaries have undergone GC cuboidalisation and multilayering. However, we can still examine whether the height of the GC layers differs between treatment groups by substracting the oocyte diameter from the follicle diameter. Additionally, cultured follicles can be processed for histology and immunolabelled for junctional molecules involved in cell shape change and integrity. Only follicles that met the criteria to be

defined as 'healthy' are included in analysis (section 2.6.7). Therefore, we sought to examine the effect of ErbB2 inhibition in this culture model.

There are two small molecule ErbB2 inhibitors commercially available that inhibit the tyrosine kinase domain. AG-825 (Cayman Chemical, Cambridge) and ErbB2 inhibitor II (Millipore, East Midlands) both block ErbB2 signalling by targeting the ATP-binding site of the tyrosine kinase domain of ErbB2 (as outlined in Chapter 1.11). They compete with ATP at the ATP-binding cleft and therefore reduce phosphorylation. ATP-binding sites are highly conserved among receptor tyrosine kinases, especially those from the same family. These inhibitors, however, are highly specific to ErbB2, as demonstrated by their IC_{50} values for ErbB2 and EGFR. This is the concentration of the drug/inhibitor that elicits a half maximal effect i.e. that reduces ErbB2 signalling or ErbB2-induced mitogenic response by 50%. The IC_{50} values of AG-825 for ErbB2 and EGFR are 0.15 and 19 μM, respectively. In contrast, ErbB2 inhibitor II reduced ErbB2 phosphorylation in a mammary carcinoma cell line with an IC_{50} of 6.6 μM but did not affect phosphorylation of overexpressed EGFR in these cells at concentrations as high as 100 μM. Therefore, AG-825 blocks ErbB2 signalling with higher efficacy but ErbB2 inhibitor II is more specific for ErbB2 in the cell lines examined. Neither of these is used in a clinical setting but have both been used in a large number of studies (Cheng et al., 2007; Long et al., 2010; Murillo et al., 2001; Osherov et al., 1993; Tsai et al., 1996). Therefore, we sought to examine the effect of these inhibitors in our preantral follicle culture model.

7.1 Results

7.1.1 The effect of ErbB2 inhibition on preantral follicle growth in the presence of insulin

7.1.1.1 Do ErbB2 inhibitors affect preantral follicle growth?

To address whether these inhibitors affected follicle growth in vitro, a preliminary dose response curve was carried out. Follicles were cultured in basal follicule culture medium supplemented with 1, 5, 10 and 20 μM AG-825 or DMSO control in one experiment and 1, 5 and 10 μM ErbB2 inhibitor II or DMSO control in another experiment (Figure 7.1), as described in materials and methods section 2.6.1. Neither inhibitor had an effect on follicle growth at any dose tested.

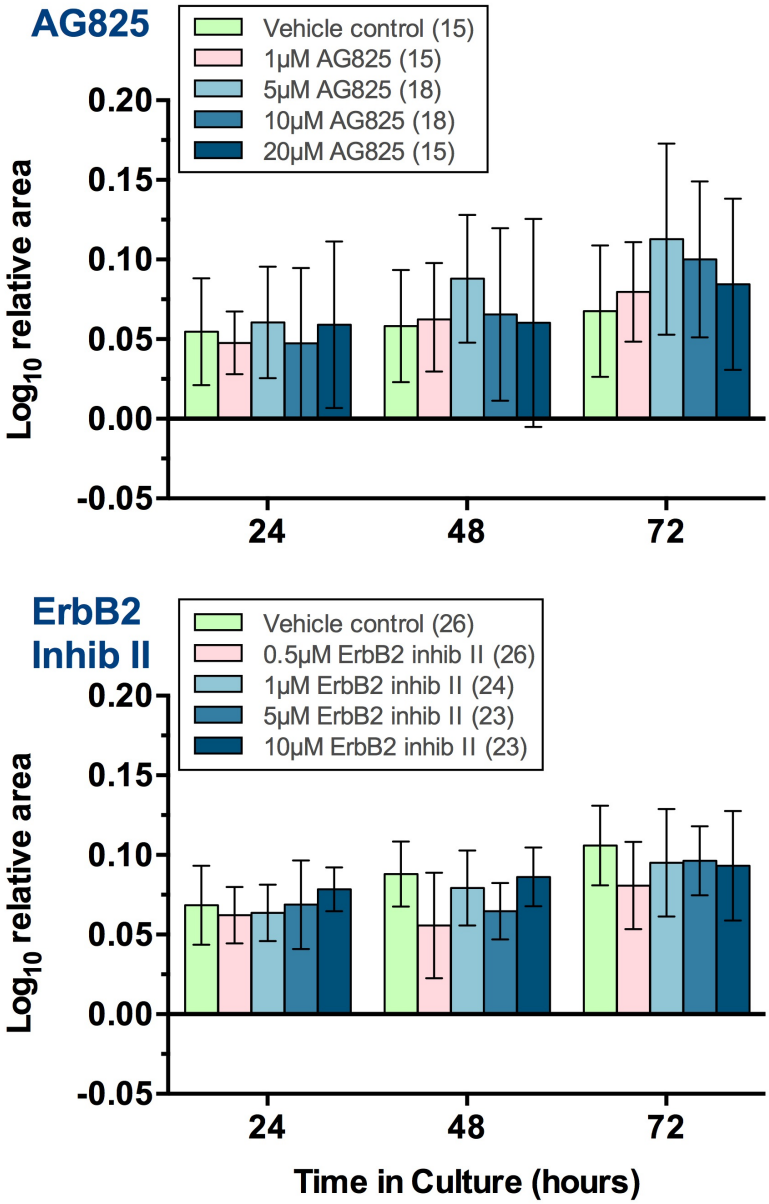


Figure 7.1. *The effect of the small molecule ErbB2 tyrosine kinase inhibitors AG-825 and ErbB2 inhibitor II on in vitro follicle growth over 72 hours. Numbers in parentheses are the number of follicles cultured in each condition. Follicles were isolated from d16 (ErbB2 inhibitor II dose response, n=6) or d17 ovaries (AG-825 dose response, n=4). Bars are mean and 95% CI.*

7.1.1.2 Is the isolated follicle culture model suitable to examine ErbB2?

One possible reason why ErbB2 inhibitors may have no affect on preantral follicle growth is that the follicles that are being placed in culture may express low levels of ErbB2. Follicles from the medullary region of the ovary are more readily

mechanically isolated from the juvenile ovary whereas those in the stiffer, collagen-dense cortex appear more adherent and are not so easily isolated. ERBB2 immunolabelling in a d16 ovary revealed that central follicles close to the medulla expressed a significantly reduced amount of ErbB2 compared to cortical follicles adjacent to the OSE (see chapter 5 for details).

To establish whether follicle culture was in fact a suitable model for examination of ErbB2 function, between 20-30 follicles were isolated from three d16 ovaries and immediately fixed and processed for histology. Immunolabelling of these follicles revealed that they all expressed ERBB2 (Figure 7.2). Furthermore, another project in our laboratory analysing possible interaction between signalling by ErbBs and androgens demonstrated that ERBB2 protein is expressed in control follicles that have been cultured for 72 hours (Kacie Thomson, unpublished observations). Therefore, it was concluded that the follicles put into culture do express ERBB2 and are therefore a suitable model to examine ErbB2 function.

Another possible reason why ErbB2 inhibitors would not affect preantral follicle growth is that there may be insufficient or no endogenous ligand in isolated preantral follicles to activate ErbB dimerisation. Therefore, the effect of exogenous ligand stimulation on preantral follicle growth was examined.

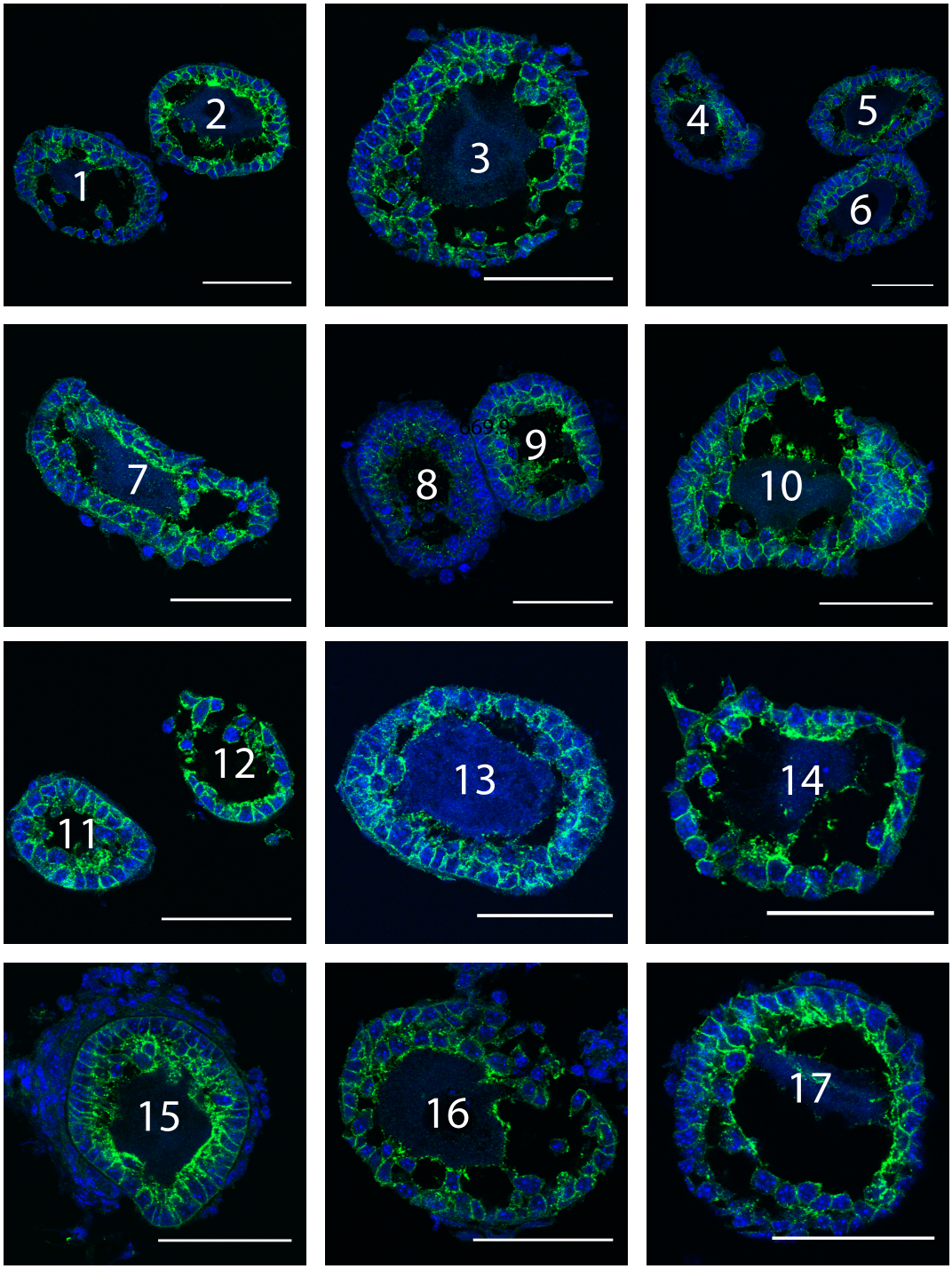


Figure 7.2 *Follicles isolated from a d16 ovary, immediately processed for histology and immunolabelled for ErbB2 (green). Nuclei are labelled with DAPI (blue). Scale bars represent 50 µm.*

7.1.1.3 Do exogenous ErbB ligands affect preantral follicle growth in vitro?

ErbB2 is unique among the ErbB receptors as no known soluble ligand binds it. Therefore, it is reliant upon heterodimerisation to signal. As EGFR was initially the only other ErbB to be detected in ovary tissue by PCR, the effect of an EGFR ligand on in vitro growth of preantral follicles was examined. A dose response study was performed with the cognate ligand of EGFR; isolated follicles were incubated with 5, 10 or 100 ng/mL EGF. This range of concentrations was chosen based on those used previously in mouse COC, follicle and ovary cultures previously (Choi et al., 2014; Ding et al., 2012; Eppig and O'Brien, 1996; Kezele et al., 2002; Wang et al., 2013). The effect of EGF stimulation was examined over 72 hours (Figure 7.3). At 24 hours follicles exposed to EGF were significantly larger than control follicles ($p<0.05$). Following the 24 hour timepoint follicle growth plateaued; follicles exposed to 5 or 10 ng/mL EGF did not grow significantly bigger at 48 or 72 hours compared to 24 hours. This plateau is likely caused by a negative feedback loop as EGF is known to rapidly induce endocytosis and lysosomal degradation of EGFR (Ebner and Derynck, 1991; Vlodavsky et al., 1978). Although 5 ng/mL EGF was sufficient to stimulate a significant increase in follicle growth at 24 hours, 10 ng/mL EGF was used for all future experiments as only follicles exposed to 10 ng/mL EGF remained significantly larger than control follicles for the entire culture period.

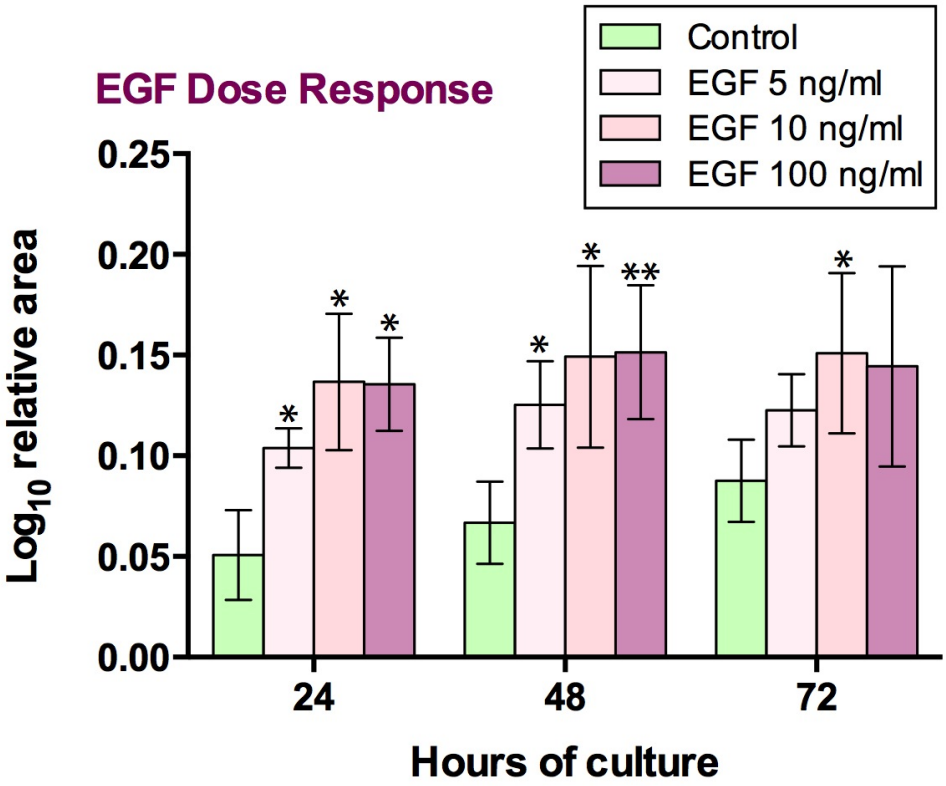


Figure 7.3. *EGF dose response in isolated preantral follicles. Preantral follicles were incubated with 5, 10 or 100 ng/mL EGF for 72 hours, photographed every 24 hours and their follicle areas measured. Follicles were isolated from d16 ovaries (n=5). Key: *; p<0.05, **; p<0.01. Bars are mean and 95% CI.*

The EGF dose response in follicles strongly suggests that EGFR protein must be present in follicles as (i) many studies examining ErbB ligand specificities and affinities have demonstrated that EGF binds EGFR but not ErbB2-4 (Graus-Porta et al., 1997; Yarden and Sliwkowski, 2001) and (ii) to the best of my knowledge, there are no studies demonstrating EGF binding and activation of another protein that does not belong to the EGF family. Therefore, based on the literature, EGFR must be present for EGF to elicit a response.

7.1.1.4 Do ErbB2 inhibitors affect EGF-stimulated preantral follicle growth in vitro?

EGF-stimulation of follicle growth strongly suggests that EGFR is expressed in isolated follicles. As ERBB2 is expressed in GCs of these isolated follicles, we hypothesize that EGFR/ErbB2 heterodimers form in preantral GCs. It is not possible to directly demonstrate that EGFR and ErbB2 hetorodimerise by co-immunoprecipitation experiments as it would require many ovaries, and a substantial amount of time, to extract sufficient protein from preantral GCs to perform this technique. To indirectly examine whether EGF was stimulating follicle growth by inducing EGFR/ErbB2 heterodimers to signal, we examined whether ErbB2 inhibitors could block EGF-stimulated growth.

Preantral follicles isolated from a d16 ovary were cultured in either (i) vehicle control (DMSO, inhibitor diluent), (ii) 10 ng/mL EGF or (iii) 10 ng/mL EGF plus ErbB2 inhibitor. As we were not able to elicit a dose response of the ErbB2 inhibitors in follicle culture in the absence of exogenous ligand stimulation (Figure 7.1), we included several concentrations of two ErbB2 inhibitors. EGF-stimulated follicles were exposed to 10 and 20 μM ErbB2 inhibitor II in one experiment and to 5, 10 and 20 μM AG-825 in another.

No concentration of ErbB2 inhibitor II or AG-825 was able to block EGF-stimulated growth in these experiments (Figure 7.4). One possible scenario is that the insulin present in the basal follicle culture medium is stimulating mitogenic intracellular signalling pathways that are common to ErbBs, such as MAPK and PI3-K. Therefore, our next set of experiments examined whether insulin signalling was compensating for ErbB2 inhibition.

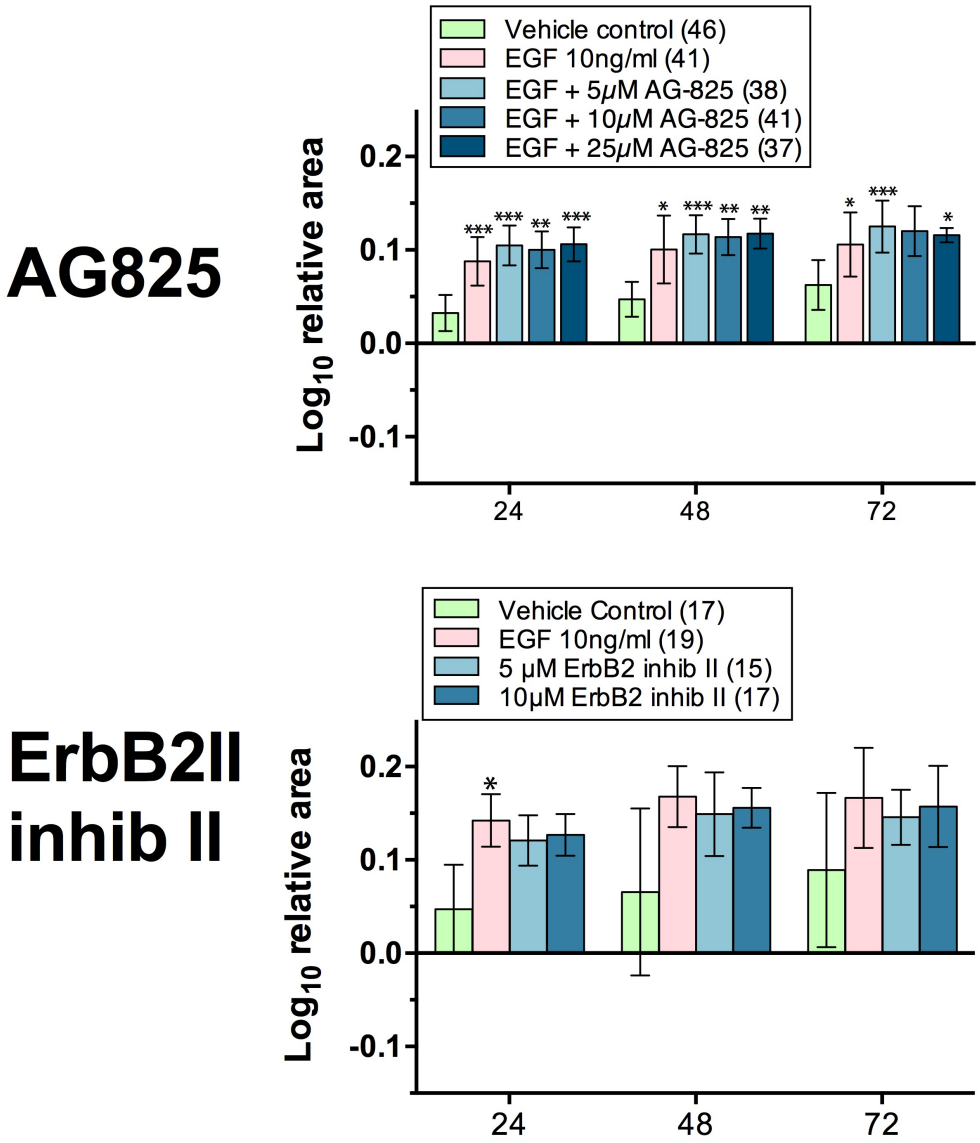


Figure 7.4. *The effect of ErbB2 inhibition on EGF-stimulated growth. Preantral follicles were incubated in basal follicle culture medium supplemented with either vehicle control (DMSO), 10 ng/mL EGF, or 10 ng/mL EGF plus either AG-825 or ErbB2 inhibitor II. Several concentrations of AG-825 and ErbB2 inhibitor II were included in this experiment. None had any effect on EGF-stimulated follicle growth. Follicles were isolated from d15 (AG-825 dose response, n=6) or d16 ovaries (ErbB2 inhibitor II, n=4). Key: *; p<0.05, **; p<0.01, ***; p<0.001, ****; p<0.0001.*

7.1.2 The effect of ErbB2 inhibition on follicle growth in the absence of insulin

7.1.2.1 Can isolated preantral follicles survive in vitro culture in the absence of insulin?

Activation of either the insulin or ErbB receptors leads to diverse intracellular signalling pathways. Some of these pathways, including the MAPK and PI3-K are common to both (Rahmouni et al., 2004; Yarden and Sliwkowski, 2001). All follicle culture experiments previously described in this chapter have used medium supplemented with ITS in which insulin is at a concentration of 5 μg/mL. Previous studies in our laboratory have demonstrated that 10 ng/mL insulin is sufficient to induce phosphorylation of Akt (of the PI3-K pathway) and ERK (of the MAPK pathway) in KK1 cells, a GC cell line (Jalini Joharatnam, unpublished observations). Furthermore, 5 ng/mL insulin was sufficient to affect the rate of primordial activation in whole rat ovaries during culture (Kezele et al., 2002). To examine whether insulin signalling was compensating for inhibition of ErbB2 signalling, first we needed to establish whether follicles could survive in culture without insulin. Therefore, follicle growth in an insulin dose response experiment was examined. The growth of follicles cultured in the medium used previously (supplemented with ITS) was compared to those cultured either (i) with 1 μg/mL insulin or (ii) without insulin, as described in Materials and Methods sections 2.6.1 and 2.6.2.

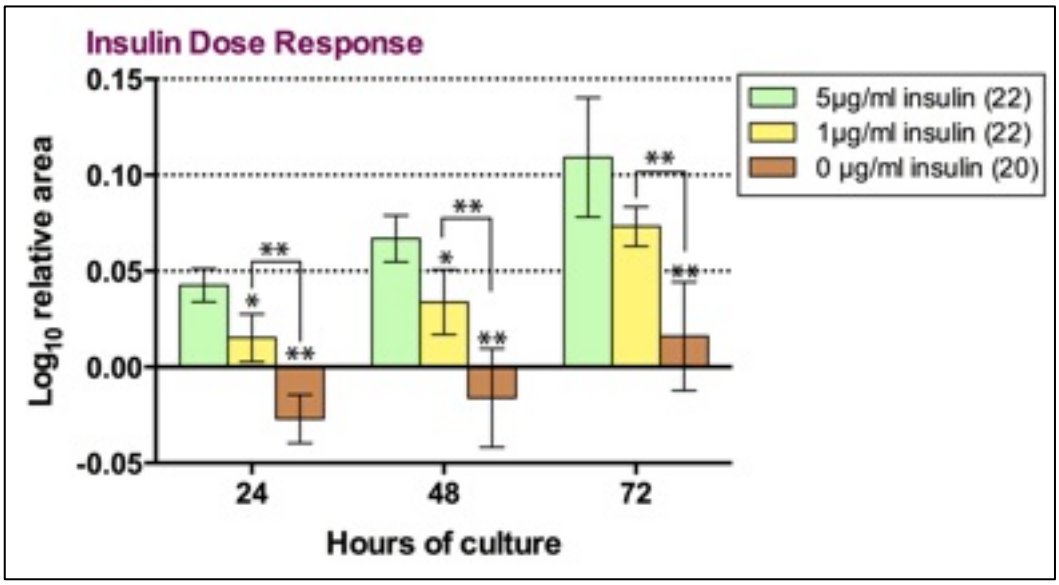


Figure 7.5. *Insulin dose response in preantral follicles. Numbers in parentheses are the number of follicles cultured in each condition. Follicles were isolated from d17 ovaries (n=5). Key: *; p<0.05, **; p<0.01. Bars are mean and 95% CI.*

All follicles, including those cultured in the absence of insulin, had grown in size by 72 hours (Figure 7.5). There was a dose response to insulin in preantral follicles; those cultured in 5 µg/mL grew significantly more than those cultured in 1 µg/mL and these grew significantly more than those cultured without insulin. In contrast to follicles cultured in the presence of insulin, those cultured in the absence of insulin appeared to shrink in the first 24 hours of culture. It is not clear why this is, but it was not associated with unhealthy morphology (Figure 7.6). This reduction in follicle area cannot be due to follicle death as the follicles have grown by 72 hours. Atresia can be visualized in cultured follicles, and is characterised by darkening of the GCs and, in extreme cases, by loss of basal lamina integrity as described in materials and methods section 2.6.7. Furthermore, TUNEL (Terminal deoxynucleotidyl transferase) labelling in follicles cultured in the presence and absence of insulin for 72 hours revealed no significant difference in cell death (Figure 7.6). TUNEL staining was not assessed at 24 hrs, the timepoint at which follicles appear to shrink.

However, follicles cultured in the absence of insulin did not show morphological signs of cell death during culture (data not shown). Therefore, the insulin-free culture system was considered appropriate for the study of EGF stimulation and ErbB2 inhibition. It is possible that follicles shrink slightly after placing in culture, and this is overcome in culture conditions that support appropriate levels of GC proliferation. Previous studies in our lab have shown that ovaries can shrink by approximately 20% after placing in culture (S. Stubbs, personal communication).

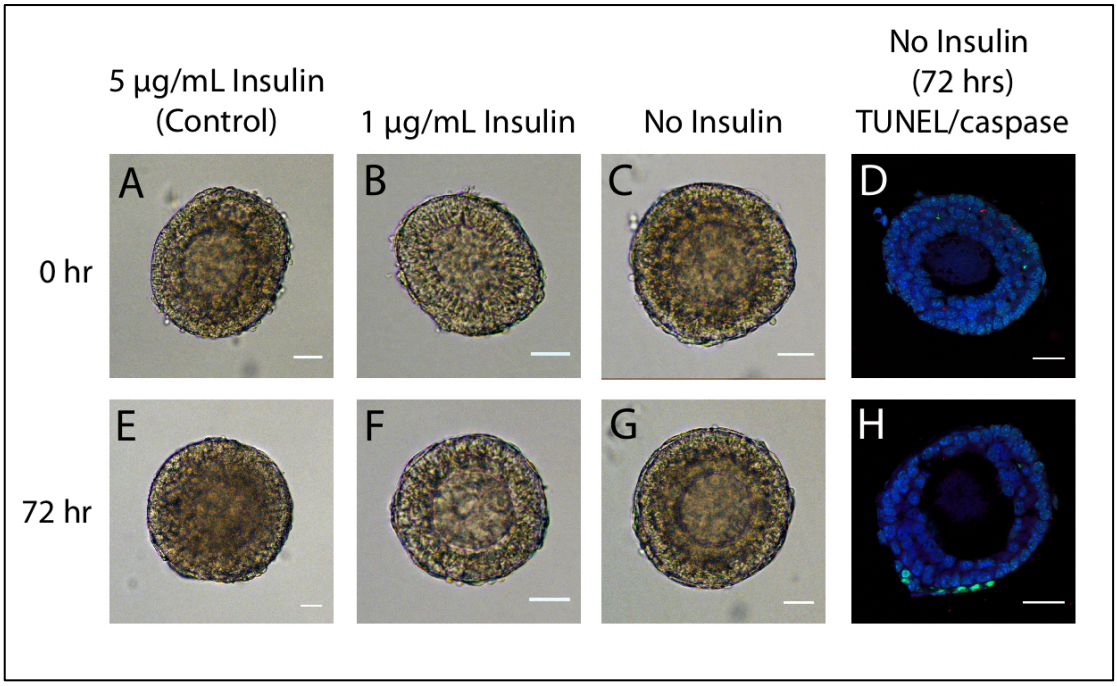


Figure 7.6. *Follicles cultured in the absence of insulin do not show signs of cell death and atresia. General morphology of isolated preantral follicles cultured in either 5, 1, or 0 µg/mL insulin at the beginning (0 hr) and end (72 hr) of culture. TUNEL (green, D, H) and active-Caspase 3 (red, D, H) immunolabelling in follicles fixed after being cultured for 72 hours in the absence of Insulin. Scale bars represent 20 µm (D, H) 30 µm (A-C, E-G).*

7.1.2.2 Can EGF stimulate follicle growth in insulin-free conditions?

Follicles cultured without insulin did not die but did not grow as much as those cultured in the presence of insulin. To establish whether they were suitable for examining the effect of ErbB2 inhibition on EGF-stimulated follicle growth, an EGF dose response in insulin-free conditions was performed. As before, the following concentrations were used: 5, 10 and 100 ng/mL EGF.

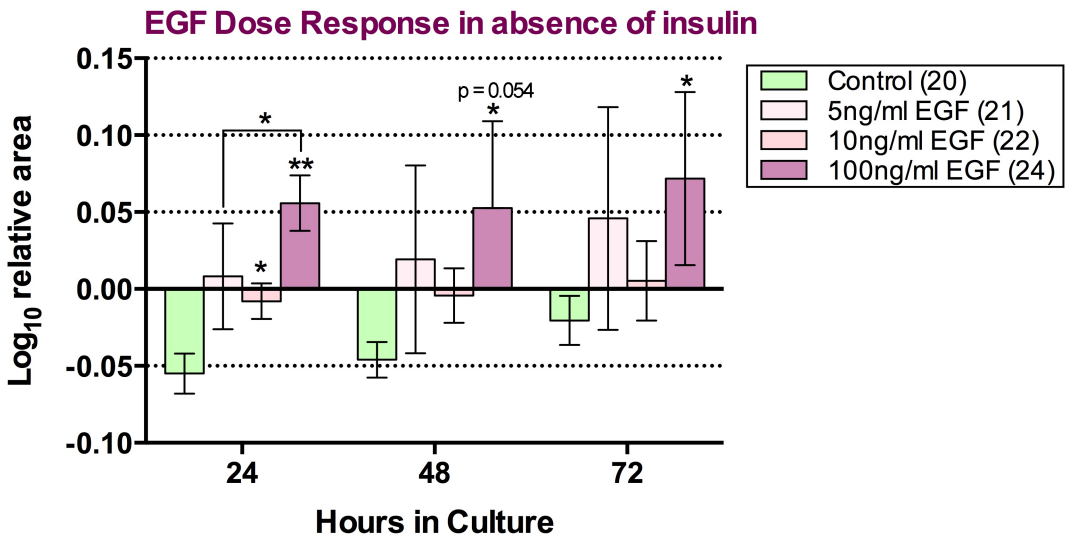


***Figure** 7.7. EGF dose response in isolated preantral follicles in the absence of Insulin. Numbers in parentheses are the number of follicles cultured in each condition. Follicles were isolated from d17 ovaries (n=4). Key: *; p<0.05. Bars are mean and 95% CI.*

Only follicles that were exposed to 100 ng/mL EGF grew significantly more than controls in insulin-free conditions (Figure 7.7). Therefore, EGF is capable of stimulating growth in an insulin-free environment. 5 ng/mL EGF is sufficient to stimulate follicle growth in the presence of insulin. The reason why a higher concentration of EGF is required in insulin-free culture to stimulate growth is not clear, but it may be due to a synergistic effect of the two.

As was found in figure 7.6, follicles that were not exposed to 100 ng/mL EGF, including control follicles, had shrunk by 24 hours. As these follicles did not show signs of atresia during culture they were not excluded from analysis on the basis of our exclusion criteria outlined in materials and methods section 2.6.7. Follicles in all treatment groups grew, albeit very slightly, at the subsequent 48 and 72 hour timepoints. Therefore, it is unlikely these follicles are dying.

To summarise, follicles survive in insulin-free media and 100 ng/mL EGF is sufficient to stimulate follicle growth. It was therefore concluded that this model was suitable for examining the effect of ErbB2 inhibition on EGF-stimulated follicle growth.

7.1.2.3 Do ErbB2 inhibitors block EGF-stimulated follicle growth in insulin-free conditions?

The ErbB2 inhibitors AG-825 and ErbB2 inhibitor II had had no effect, at the concentrations tested, on follicle growth when either (i) insulin is present and EGF is absent (Figure 7.1), or (ii) insulin and EGF are both present (Figure 7.4). One hypothesis was that this might be due to either insulin signalling compensation for inhibited ErbB2 signalling or lack of exogenous ligand stimulation or both. We now have an insulin-free model, in which 100 ng/mL EGF is capable of stimulating follicle growth. To address whether the above-mentioned hypothesis was correct, the effect of AG-825 and ErbB2 inhibitor II on EGF-stimulated follicle growth was examined in insulin-free conditions. As control follicles in these conditions either stay the same size or shrink and they require a much higher concentration of EGF to grow than those cultured in the presence of insulin, we anticipated that they might be more sensitive to DMSO, the inhibitor diluent. Therefore, follicles were only exposed to either 5 or 10 μM AG-825 or ErbB2 inhibitor II, levels that should have an

inhibitory effect, according to the pharmaceutical companies that supplied these inhibitors and from the published literature. Therefore follicles were cultured either in vehicle control, 100 ng/mL EGF or 100 ng/mL EGF plus 5/10 µM AG-825/ErbB2 inhibitor II in insulin-free culture medium.

As was the case for when insulin was present in the culture medium, 10 µM of AG-825 or ErbB2 inhibitor II had no effect on EGF-stimulated preantral follicle growth in insulin-free conditions.

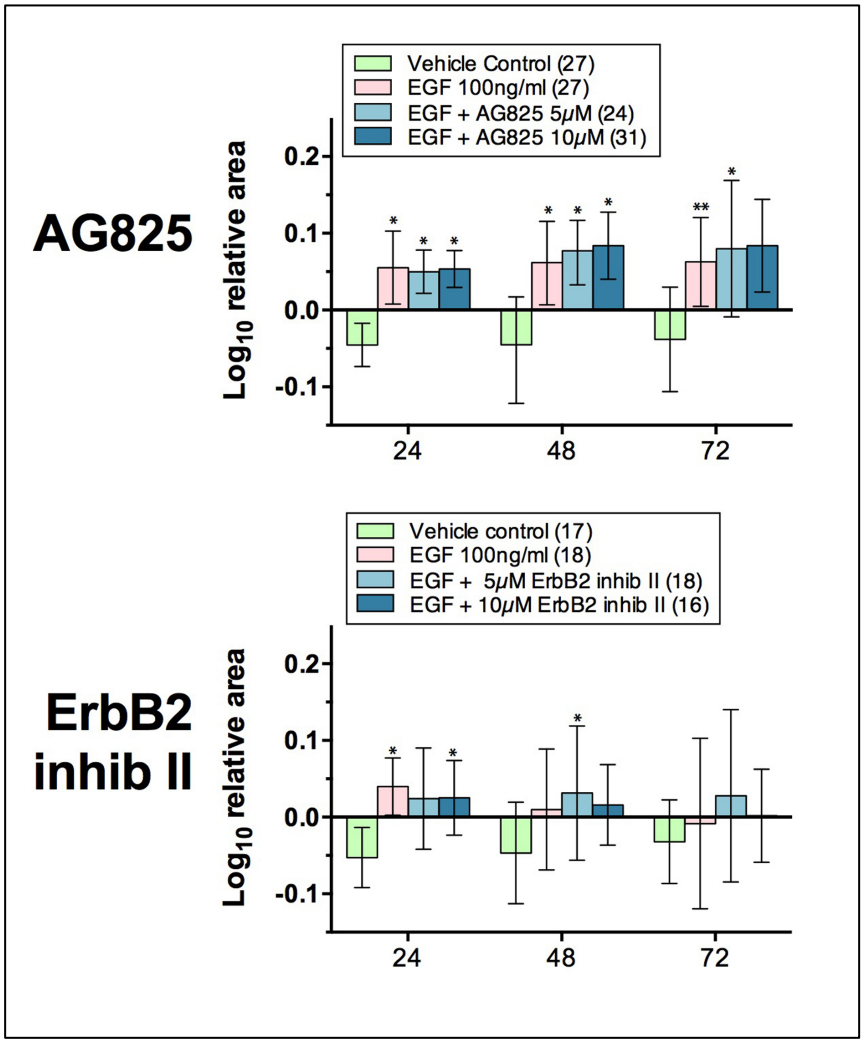


Figure 7.8. *The effect of ErbB2 inhibition on isolated preantral follicle growth in insulin-free conditions in vitro. Numbers in parentheses are the number of follicles cultured in each condition. Follicles were isolated from d15 (ErbB2 inhibitor II dose response, n=4) and d17 ovaries (AG-825 dose response, n=5). Key: *; p<0.05, **; p<0.01. Bars are mean and 95% CI.*

To summarise, the data so far has not demonstrated an effect of ErbB2 inhibition on follicle growth in vitro. The sensitivity of isolated preantral follicles to EGF suggests that EGFR is expressed in preantral GCs and therefore is likely to heterodimerise with ErbB2. Therefore, the next experiment examined the effect of a dual inhibitor of EGFR and ErbB2.

7.1.2.4. Does Lapatinib Ditosylate have an effect on EGF-stimulated follicle growth in insulin-free conditions?

All follicle culture experiments so far have only used inhibitors specific to ErbB2. None of these affected follicle growth in vitro. EGF stimulation of follicle growth strongly suggests that EGFR must also be expressed in isolated follicles. Therefore, in the next set of experiments we examined whether Lapatinib Ditosylate, a dual inhibitor of EGFR and ErbB2, affected EGF-stimulated follicle growth in insulin-free culture. The IC_{50} values of Lapatinib for EGFR, ErbB2 and the unrelated c-Src in a mammary carcinoma cell line are 9.2 nM, 10.8 nM and 3.5 μM, respectively. Lapatinib has also been used to inhibit ErbB2 signalling in vivo as well as in vitro. Lapatinib is clinically known as Tykerb and was approved by the FDA in 2007 for use on patients with HER2-overexpressing breast cancer. Elucidation of the crystal structure of EGFR bound to Lapatinib revealed that Lapatinib bound to the inactive conformation of EGFR and that this was associated with slower inhibitor off-rates (and therefore prolonged inhibition) than compounds which bind the active conformation, as described in introduction section 1.11.

As for all experiments described in this section, isolated preantral follicles were cultured individually in 96 well plates in 100 µL of insulin-free α-MEM medium for 72 hours. The following treatment groups were included: (i) vehicle control, (ii) 100 ng/mL EGF, (iii) 100 ng/mL EGF + 5 µM Lapatinib and (iv) 100 ng/mL EGF + 10 µM Lapatinib.

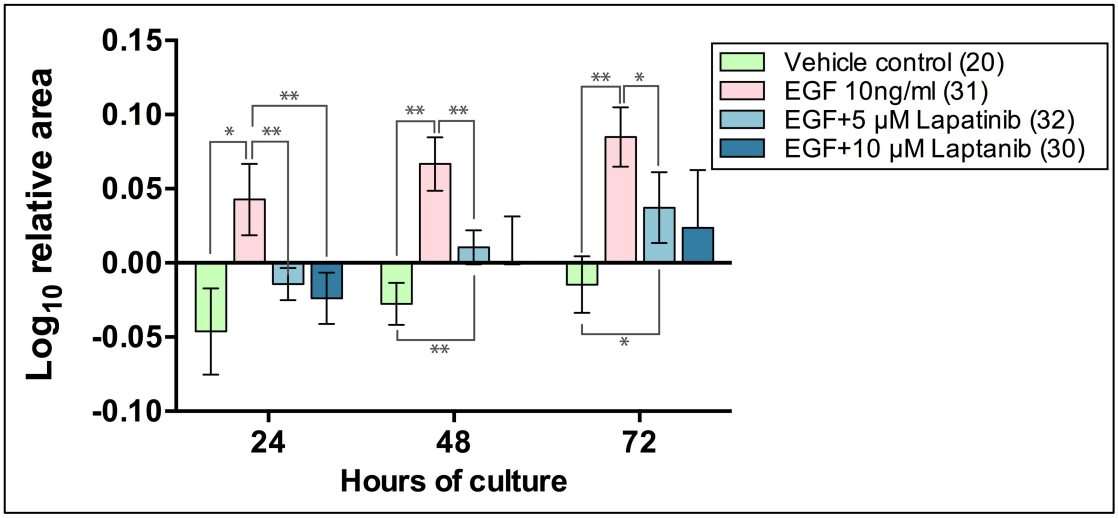


Figure 7.9. *The effect of Lapatinib on EGF-stimulated preantral follicle growth in the absence of insulin. Numbers in parentheses are the number of follicles cultured in each condition. Follicles were isolated from d16 (n=4). Key: *; p<0.05, **; p<0.01. Bars are mean and 95% CI.*

Excitingly, Lapatinib blocked the affect of EGF-stimulated follicle growth in insulin-free conditions (Figure 7.9). 5 µM Lapatinib was sufficient to completely block EGF-stimulated follicle growth at 24 hrs. Follicles exposed to Lapatinib did indeed grow over the 72 hour culture period though, indicating that the follicles were not dying. Therefore, the effect of Lapatinib on EGF-stimulated follicle growth is likely due to inhibition of mitogenic signalling stimulated by EGF, as expected.

As Lapatinib Ditosylate did inhibit EGF-stimulated follicle growth in the absence of insulin, the next experiments examined whether Lapatinib Ditosylate inhibited EGF-stimulated follicle growth in the presence of insulin.

7.1.3 Dual inhibition of EGFR and ErbB2 in the presence of insulin

7.1.3.1 Does Lapatinib Ditosylate block EGF-stimulated follicle growth in the presence of insulin?

The ErbB2 inhibitors AG-825 and ErbB2 inhibitor II had no effect on either unstimulated or EGF-stimulated follicle growth in the presence or absence of insulin. Therefore, this established that insulin signalling is not responsible for masking an effect of these inhibitors. However, it has not been established whether the presence of 5 μg/mL insulin in the follicle culture medium would mask the effect of Lapatinib. The next experiment examined whether Lapatinib blocked EGF-stimulated growth in the presence of insulin. Although follicles cultured in the absence of insulin do not die during culture, they do appear to be developmentally compromised, in that their growth is minimal compared to that in the presence of insulin. Furthermore, a lower, more physiological concentration of EGF is sufficient to stimulate further follicle growth in the presence of insulin (Figure 7.3).

Isolated preantral follicles were cultured in either (i) DMSO (inhibitor diluent, vehicle control), (ii) 10 ng/mL EGF, (iii) 10 ng/mL EGF + 0.5 μM Lapatinib and (iv) 10 ng/mL EGF + 1.0 μM Lapatinib. Lower concentrations of Lapatinib were tested in the presence of insulin, compared to those used in the absence of insulin, following advice from experts within our institution (Ovarian Cancer Action Research Centre, IRDB).

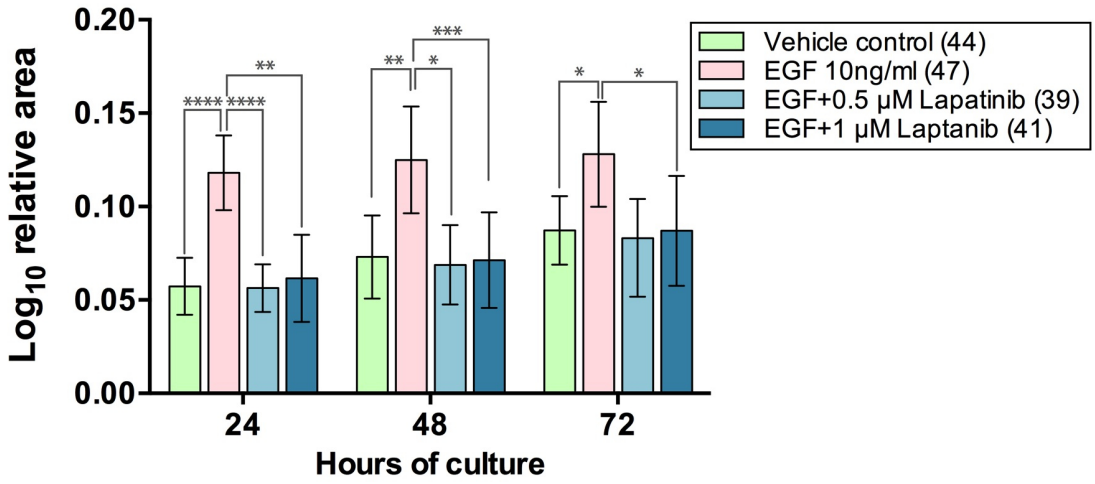


Figure 7.10. *The effect of Lapatinib Ditosylate on EGF-stimulated preantral follicle growth in the presence of insulin. Numbers in parentheses are the number of follicles cultured in each condition. Follicles were isolated from d16 ovaries (n=10). Key: *; p<0.05, **; p<0.01, ***; p<0.001, ****; p<0.0001. Bars are mean and 95% CI.*

As was the case for insulin-free culture, Lapatinib completely blocked EGF-stimulated follicle growth (Figure 7.10). 0.5 µM Lapatinib was sufficient to completely block the stimulatory effect of EGF. Therefore, a dual inhibitor of EGFR and ErbB2 can block EGF-stimulated follicle growth in vitro regardless of whether insulin is present or not.

To summarise the follicle culture experiments so far: small molecule inhibitors that were specific to ErbB2 did not affect follicle growth in the presence or absence of either insulin or EGF, whereas a dual small molecule inhibitor of EGFR and ErbB2 blocked EGF-stimulated growth in the presence and absence of insulin. This set of experiments suggests that only EGFR has a role in EGF-stimulated follicle growth in vitro. There are several alternative explanations for these results, however. Firstly, Lapatinib is known to be a very potent inhibitor of both EGFR and ErbB2. Importantly, according to the IC_{50} values cited by the pharmaceutical companies that provide these inhibitors, it is a more potent inhibitor of ErbB2 than either AG-825 or ErbB2 inhibitor II. Lapatinib is potent in both in vitro cell culture and in vivo in

patients. Therefore, it is possible that a more potent inhibitor that is specific to ErbB2 is required to block EGF-stimulated follicle growth. The next experiments sought to address whether this was the case by testing one further ErbB2 inhibitor that is known to be potent.

7.1.3.2 Antibody-mediated ErbB2 inhibition in preantral follicles

Trastuzumab, clinically known as Herceptin, is a humanized monoclonal antibody targeted towards extracellular domain IV of HER2 (human form of ErbB2), however previous studies demonstrate it does bind to the mouse homologue (Riccio et al., 2009). It has a complex mechanism of action that is entirely different to that of the small molecule inhibitors AG-825 and ErbB2 inhibitor II that target the intracellular kinase domain. Trastuzumab, on the other hand, binds to the extracellular domain therefore interfering with ErbB2 dimerisation and causing aberrant recruitment of downstream signalling molecules that target ErbB2 for degradation. In addition, the humanized portion of the antibody attracts the immune cells that then kill the antibody-bound, ErbB2-expressing cells. This latter mechanism of action is irrelevant in our culture model. Its potency can be attested to by its remarkable contribution to the improved prognosis for HER2-positive breast carcinoma patients (Baselga et al., 1999; Colomer et al., 2001; Vogel et al., 2001) as well as its published effects in vitro (Kunisue et al., 2000; Sliwkowski et al., 1999). However, Trastuzumab is much more commonly used on tumour cells, either in vivo or in vitro, and is less readily available for research laboratories studying the basic biology of ErbB2 during development. Trastuzumab was kindly donated to us by the Ovarian Cancer Action Research Centre led by Professor Hani Gabra and we chose the dose response range approximately based on experiments that this group and

others in the literature had used (Mazurek et al., 2012; Suarez et al., 2013; Thon et al., 2012).

We examined whether 10, 25 or 100 µg/mL Trastuzumab had an effect on EGF-stimulated growth of preantral follicles in the presence of insulin. Follicles were either exposed to (i) this basal culture medium only (control), (ii) 10 ng/mL EGF or (iii) 10 ng/mL EGF + 10, 25 or 100 µg/mL Trastuzumab.

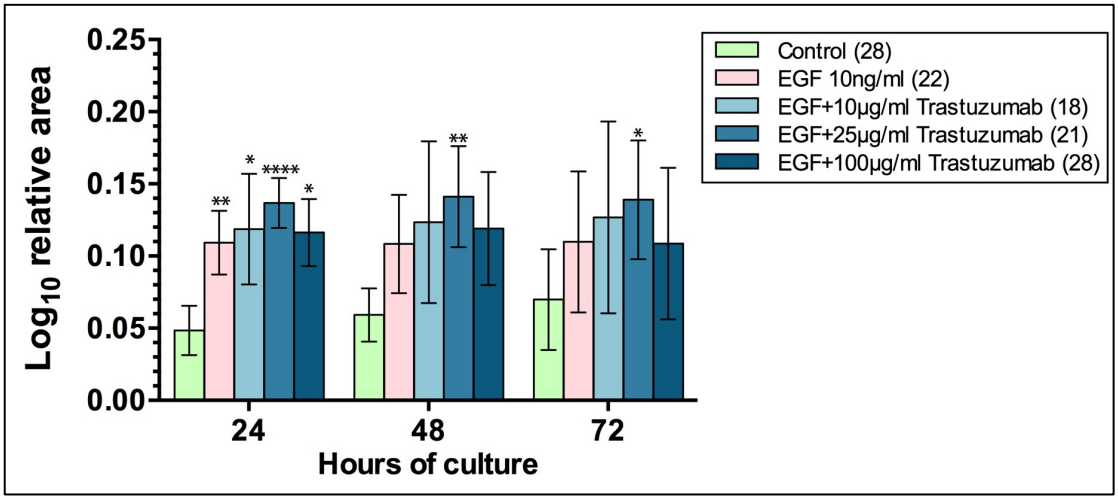


Figure 7.11. *The effect of Trastuzumab on EGF-stimulated preantral follicle growth in the presence of insulin. Numbers in parentheses are the number of follicles cultured in each condition. Follicles were isolated from d15 ovaries (n=6). Key: *; p<0.05, **; p<0.01, ***; p<0.001, ****; p<0.0001. Bars are means and 95% CI.*

In contrast to the previous experiments in this chapter, 10 ng/mL EGF does not sustain a significant increase in follicle growth at either 48 or 72 hrs (Figure 7.11). Therefore, in this case, the effect of Trastuzumab on EGF-stimulated follicle growth can only be commented on at 24 hrs. At 24 hrs, all treatment groups cause a significant increase in follicle growth, as compared to controls. However, 25 µg/mL Trastuzumab is associated with the most significant increase in follicle growth. It is difficult to interpret this result as EGF did not cause a robust effect on follicle growth as expected. It is possible to isolate primary, primary plus, secondary and secondary plus stage follicles from a d15 ovary. It is likely that these different follicle stages do

not respond equally to EGF; some follicles may not grow as much as others or at all in response to EGF. It is possible that more non- or less-responsive follicles were included in this particular experiment. It may, in future, be more appropriate to separate follicles by size, using the database, prior to analysis. Crucially, however, no concentration of Trastuzumab tested inhibited affected EGF-stimulated follicle growth (Figure 7.11).

Trastuzumab is an antibody and therefore larger than the small molecule inhibitors we have previously used. Therefore, it may be that this agent does not enter the follicle via the basal lamina as readily as Lapatinib, for example, as the basal lamina is a barrier to certain extra-follicular substances (Rodgers et al., 2000). The effects of other antibodies, of a similar molecular weight, that neutralise activity of a GC-derived protein (Nilsson et al., 2001; Parrott and Skinner, 1999), on follicle development in which the basal lamina is intact suggest that Trastuzumab should enter the follicle to some extent. Another important difference between Trastuzumab and Lapatinib is their mechanism of action. The mechanism of Trastuzumab action is not fully elucidated. However, it is known to exert its effects partly through interfering with ErbB2 dimerisation. Therefore, we thought it possible that simultaneously exposing the follicles to EGF and Trastzumab may allow EGF to actually block Trastuzumab action by stimulating dimerisation before Trastuzumab has bound the ErbB2 extracellular domain. Therefore, it was decided to pre-incubate follicles with Trastuzumab for 24 hours before stimulating with 10 ng/mL EGF to allow additional time for Trastzumab to reach the GC membranes and bind the extracellular domain of ErbB2.

7.1.3.3 Is EGF capable of stimulating growth of follicles pre-incubated with Trastuzumab?

Isolated preantral follicles were cultured for 72 hours in either (i) basal follicle culture medium (control), (ii) 10 ng/mL EGF, (iii) 10 ng/mL EGF + 10, 25 or 100 µg/mL Trastuzumab. The 10 ng/mL EGF was only added to the treatment groups described in (ii) and (iii) at 24 hours, whereas Trastuzumab was added at the beginning of culture.

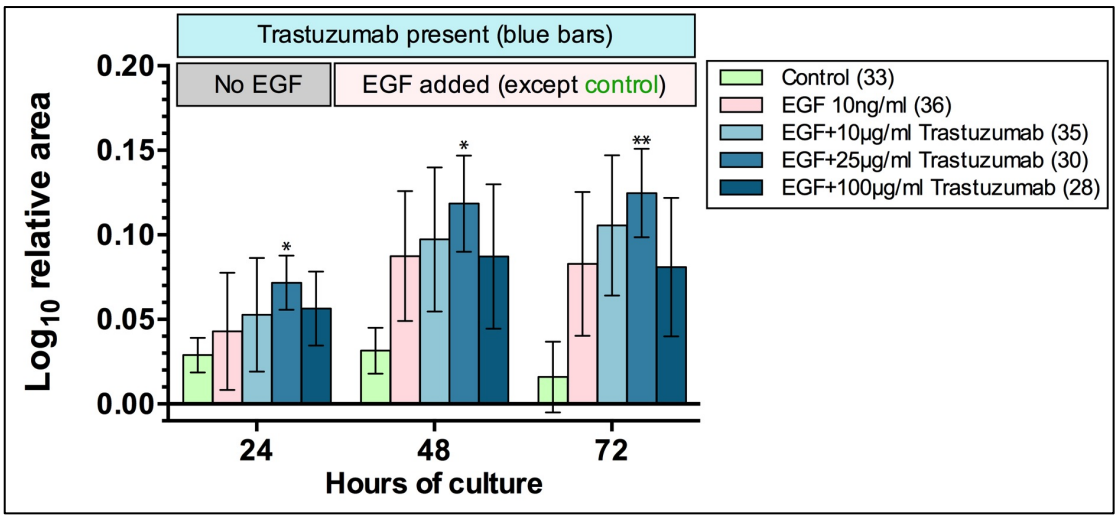


Figure 7.12. *The effect of EGF on preantral follicles pre-incubated with Trastuzumab. Numbers in parentheses are the number of follicles cultured in each condition. Follicles were isolated from d16 ovaries (n=6). Key: *; p<0.05, **; p<0.01. Bars are means and 95% CI.*

Follicles that were pre-incubated with 10, 25 or 100 µg/mL Trastuzumab and subsequently stimulated with EGF 24 hours later were not significantly smaller than follicles that had been exposed (from 24 hour time point) to EGF alone by 72 hours (Figure 7.12). Therefore, Trastuzumab does not inhibit EGF-stimulated follicle growth. However, the EGF-mediated stimulation of follicle growth in this experiment was not significant. In previous experiments in the presence of insulin, the culture medium prepared at 0 hrs was supplemented with 10 ng/mL EGF. In this experiment, 10 µL of α-MEM medium supplemented with 110 ng/mL EGF was added to each

well already containing 100 µL of medium, to give a final EGF concentration of 10 ng/mL. This may increase variability in follicle growth due to pipetting and lack of vigorous mixing. EGF does cause a non-significant increase in follicle growth, however, and those follicles that were pre-incubated with Trastuzumab are not significantly smaller than those exposed to EGF alone. Follicles pre-incubated with 25 µg/mL Trastuzumab and then subsequently stimulated with EGF were actually significantly bigger than control follicles. This is surprising, given that Trastuzumab blocks ErbB2-mediated mitogenic signalling. The underlying reasons for this curious result are not yet known. Crucially, however, this experiment demonstrated that Trastuzumab did not block EGF-stimulated follicle growth.

To summarise these experiments so far, only Lapatinib, a dual inhibitor of EGFR and ErbB2 has an effect on EGF-stimulated follicle growth. None of the inhibitors that are specific to ErbB2 alone affect EGF-stimulated follicle growth. Therefore, it is likely that inhibition of EGFR by Lapatinib is responsible for the block on EGF-stimulated follicle growth. Therefore, the next experiments aimed to check whether this was the case by examining the effect of an inhibitor specific to EGFR on EGF-stimulated follicle growth.

7.1.4 EGFR inhibition in preantral follicles

7.1.4.1 Does AG1478 affect basal follicle growth?

AG1478 is a small molecule tyrosine kinase inhibitor that works by exactly the same mechanism as AG-825 and ErbB2 inhibitor II, except that is binds to the ATP-binding site of EGFR only. Importantly, AG1478 has been shown to reduce [^{3}H] thymidine uptake in mouse secondary follicles in vitro, indicating it may have a role in preantral GC proliferation (Sasseville et al., 2010). Therefore, we exposed

unstimulated (i.e. without EGF) preantral follicles to 2, 5 or 10 μM AG1478 or DMSO (inhibitor diluent, vehicle control). We measured follicle area of follicles from photographs taken every 24 hours using Image J software, rather than measure [^{3}H] thymidine uptake.

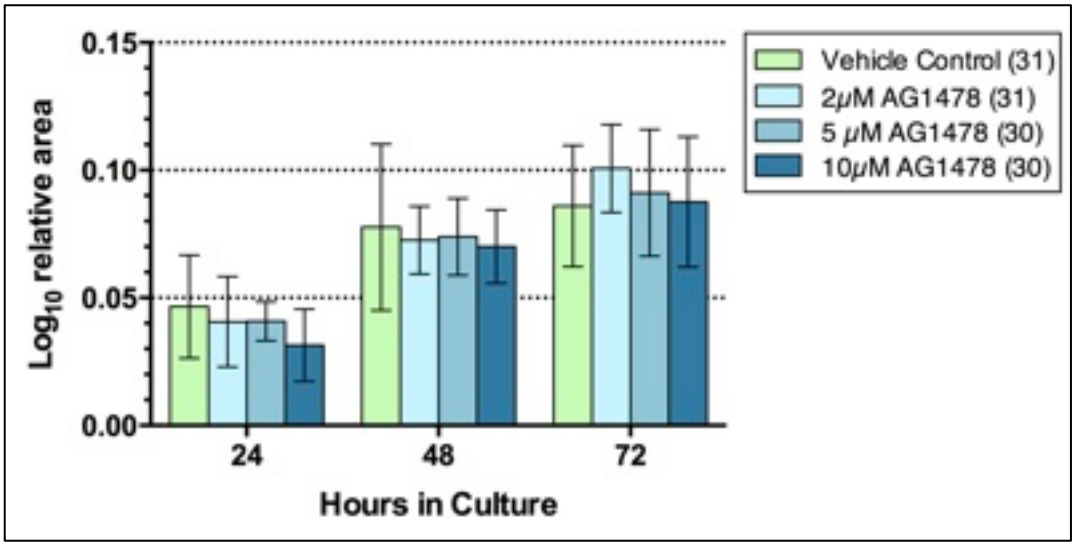


Figure 7.13. *The effect of AG1478, an EGFR inhibitor, on unstimulated preantral follicle growth in the presence of insulin. Numbers in parentheses are the number of follicles cultured in each condition. Follicles were isolated from d17 ovaries (n=5). Bars are mean and 95% CI.*

No treatment group was significantly different to another in terms of follicle areas (Figure 7.13). Therefore, based on previous experiments it was hypothesized that this was due to insufficient ligand stimulation. Importantly, AG1478 did not have a detrimental effect on follicle development.

7.1.4.2 Does AG1478 affect EGF-stimulated follicle growth?

Isolated preantral follicles were cultured in insulin-containing basal culture medium supplemented with (i) DMSO (vehicle control), (ii) 10 ng/mL EGF or (iii) 10 ng/mL EGF + 5 or 10 μM AG1478 for 72 hours. Relative follicle areas were measured and compared.

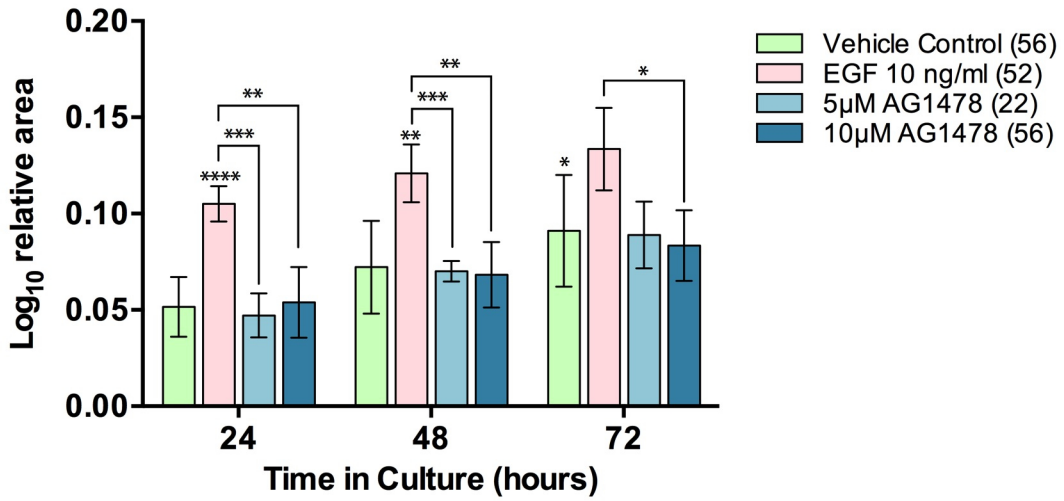


Figure 7.14. *The effect of AG1478 on EGF-stimulated preantral follicle growth in the presence of insulin. Numbers in parentheses are the number of follicles cultured in each condition. Follicles were isolated from d16 ovaries (n=8). Key: *; p<0.05, **; p<0.01, ***; p<0.001, ****; p<0.0001. Bars are mean and 95% CI.*

Similar to the effect of Lapatinib, both 5 and 10 μM AG1478 blocked EGF-stimulated follicle growth completely (Figure 7.14).

As AG1478 did not affect basal follicle growth (Figure 7.13), this suggests that the inhibition of EGF-stimulated growth is due to inhibition of EGF-stimulated EGFR dimers, rather than cytotoxicity. Furthermore, as AG-825 and ErbB2 inhibitor II did not affect EGF-stimulated follicle growth, this suggests that AG1478 and Lapatinib block EGF-induced EGFR homodimers rather than EGFR/ErbB2 heterodimers.

7.1.4.3 Are the effects of EGF and AG1478 on follicle growth due to changes in GC proliferation?

As the oocyte of multilayered follicles that we put into culture are almost fully grown, an increase in follicle area is most likely caused by an increase in GC proliferation. Furthermore, as all the inhibitors we used had no effect on basal follicle growth in the absence of EGF this suggested that the block on EGF-stimulated growth

was attributable to a block on mitogenic signalling rather than a triggering of cell death. To confirm this, we examined the expression of proliferation and cell death markers in follicles exposed to either (i) DMSO, (ii) 10 ng/mL EGF or (iii) 10 ng/mL EGF + 10 μM AG1478. Follicles were exposed to 10 μM rather than 5 μM AG1478 as this was the highest concentration ever used in our experiments, therefore if AG1478 caused cytotoxicity in any of our experiments it will be observed at this concentration. As EGF-stimulated follicle growth reached a plateau following the 24 hour timepoint, follicles were collected at 24 hours and processed for histology.

Ki67 is a widely used marker of cell division that has been used to profile proliferation in the mouse ovary (Da Silva-Buttkus et al., 2008). We can also simultaneously label for two markers of cell death. The first, terminal deoxynucleotidyl transferase dUTP nick end labelling (TUNEL) targets the termini of DNA that has fragmented during cell death. This enzyme can be simultaneously visualised on 5 μM sections of formalin-fixed, paraffin embedded follicle sections with active-caspase 3 immunolabelling. Caspase 3 is activated during apoptosis.

Ki67 staining of sections taken from these experiments immunolabelled the vast majority of GCs of follicles from all treatment groups and there was no significant difference between any treatment group. This is unlikely to be true representation of the proliferative activity of these follicles and instead suggests that either cells that are not undergoing proliferation are being non-specifically labelled for an unknown reason or cells that had undergone proliferation recently were still being labelled. Unfortunately, we are limited to the number of 5 μm sections we obtain from follicles. However, follicles from another experiment carried out in our laboratory by another PhD student, in which follicles were stimulated to 10 ng/mL in the same culture conditions, were immunolabelled with a different Ki67 antibody and

these results have demonstrated that EGF stimulates a significant increase in Ki67 immunolabelling as compared to controls (Kacie Thomson, unpublished observations).

Furthermore, TUNEL labelling did not significantly increase in follicles exposed to EGF + AG1478 compared to controls or those exposed to EGF alone (Figure 7.15). Therefore, the increase in follicle growth in response to EGF is due to increased GC proliferation.

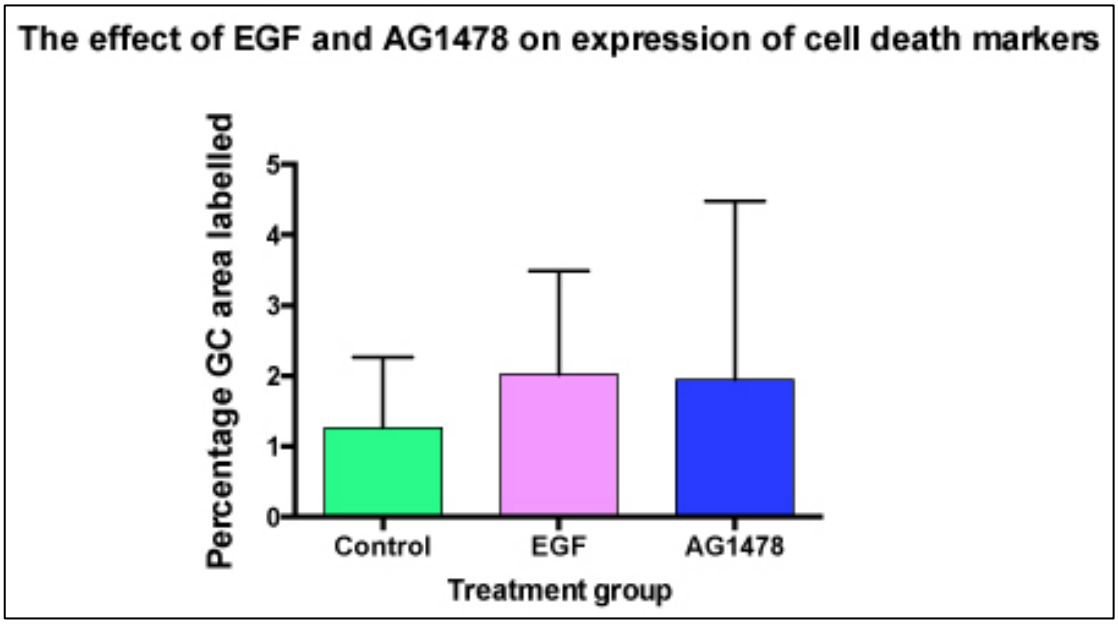


Figure 7.15. *The effect of EGF and AG1478 on TUNEL labelling. TUNEL labelling indicated that the level of cell death in follicles exposed to either EGF alone or EGF and AG1478 slightly but not significantly increased as compared to controls. These measurements are based on 10 control, 25 EGF and 23 'AG1478' (+EGF) follicles. Statistical significance was assessed by analysis of variance with a post hoc Kruskal wallis test. Bars are mean and SEM.*

7.1.5. Summary of results from follicle culture studies

- Small molecule tyrosine kinase inhibitors specific to ErbB2 had no effect on (i) basal follicle in vitro growth in either the presence of insulin or (ii) EGF-stimulated in vitro follicle growth in the presence and absence of insulin.

- 5 ng/mL EGF is sufficient to stimulate in vitro follicle growth in the presence of insulin.
- 100 ng/mL EGF is sufficient to stimulate in vitro follicle growth in the absence of insulin
- EGF-stimulated follicle growth is associated with a significant increase in Ki67 immunolabelling (proliferation marker) but not TUNEL labelling (cell death marker) in GCs.
- The mitogenic effect of EGF in preantral GCs demonstrates that EGFR must be expressed in preantral GCs.
- 5 μM AG1478, a small molecule tyrosine kinase inhibitor, is sufficient to completely block EGF-stimulated follicle growth so that EGF + AG1478 follicles are not significantly bigger than controls.
- 10 μM AG1478 does not affect basal follicle growth in the presence of insulin. Furthermore, it does not cause a significant increase in TUNEL immunolabelling (cell death marker). Therefore, the effect of AG1478 on EGF-stimulated growth is not due to cytotoxicity.
- Inhibition of EGF-stimulated follicle growth by an EGFR-specific inhibitor (AG1478) further demonstrates that EGFR protein must be expressed in preantral GCs.
- 0.5 μM Lapatinib Ditosylate, a small molecule tyrosine kinase specific to both EGFR and ErbB2, is sufficient to block the entire mitogenic effect mediated by EGF. Previous results suggest that it is the inhibition of EGFR, not ErbB2, that is responsible for this.
- 100 μg/mL Trastuzumab (Herceptin) did not inhibit EGF-stimulated growth either when added at the same time as EGF or 24 hours beforehand.

7.2 Discussion

7.2.1 Functional data indicates that EGFR must be expressed in preantral GCs

EGFR has an established role in cumulus GCs of mouse pre-ovulatory follicles; its expression is crucial to mediate the LH surge to the COC (Park et al., 2004). A possible role for EGFR in earlier, preantral, follicle development has not been thoroughly investigated although EGF incubation was found to stimulate an increase in [^{3}H]thymidine incorporation into secondary follicles (Sasseville et al., 2010). However, these groups have not localised EGFR to GCs (antral or preantral). Indeed, personal communication with Marco Conti, group leader of the studies elucidating the role of EGFR in pre-ovulatory follicles, confirm that they were not able to find a suitable EGFR antibody to do this. Our study has come to the same conclusion: there is no good EGFR antibody available to localise EGFR in the mouse ovary, as determined by absence of EGFR immunolabelling in a superovulated mouse ovary. Functional studies in this project support my mRNA expression data, and strongly suggest that EGFR protein is expressed in preantral GCs. Firstly, 10 ng/mL EGF consistently stimulates a significant increase in follicle growth, which is generally a two-fold stimulation. Secondly, 5 μM AG1478, an inhibitor specific to EGFR, was able to block this EGF-stimulated follicle growth.

Several pieces of evidence indicate that these results are not due to non-specific effects of either reagent used. Multiple studies examining ErbB ligand specifities and affinities have demonstrated that EGF binds EGFR only (Graus-Porta et al., 1997; Yarden and Sliwkowski, 2001). Furthermore, to the best of my knowledge, there are no studies demonstrating EGF binding and activation of another protein outside of the EGF family. Powdered EGF was reconstituted in αMEM

media, the same media used to culture follicles, indicating it is not the diluent responsible for the increase in follicle growth. Vehicle control follicles, which were exposed to the equivalent amount of DMSO as those exposed to the inhibitor, demonstrated that the effects observed were indeed attributable to the ligand and the inhibitor and not the inhibitor diluent. In addition, the specificity of AG1478 has been rigorously tested by the pharmaceutical companies that supply them. AG1478 is targeted against the ATP-binding domain of the kinase domain of EGFR. There is a high level of conservation in these domains among receptors of the same family and even between receptors of different families. Therefore, the IC50 values, which show the concentration of drug required to elicit a 50% or half maximal inhibition of signalling, have been cited on the data sheet. Whereas only 3 nM of AG1478 is sufficient to half maximally block EGFR signalling, over 100 μM is required to block ErbB2 and PDGFR signalling. We used 5 and 10 μM in this study and should therefore not elicit non-specific inhibition. This concentration is significantly higher than the 3 nM cited as being sufficient to block EGFR signalling by half. However, pharmaceutical companies do not test their inhibitors on 3D structures such as follicles, they test them on 2D monolayers of cells. The concentrations used in our initial dose response were chosen based on previous studies using AG1478 in follicles (Sasseville et al., 2010). Our study confirmed that these concentrations were not toxic as (i) these concentrations of AG1478 has no effect on follicle growth in the absence of EGF, (ii) atresia has a very specific morphology in cultured follicles, with darkening of GCs, and the follicles cultured in inhibitor were showing no sign of detrimental effect, (iii) TUNEL immunolabelling (a measure of cell death) was not significantly increased in follicles exposed to AG1478 compared to those exposed to EGF, and (iv) follicles exposed to AG1478, either with or without EGF, still grew to

some extent. Furthermore, EGF-stimulated EGFR is known to processed in a particular way; EGFR is rapidly cleared from the membrane following EGF incubation and targeted for degradation. Consistent with this, in our study, EGF-stimulates an initial spike in follicle growth at 24 hours and then a subsequent plateau at 48 and 72 hours. Furthermore, another study has demonstrated that ErbB2 protein is downregulated at 24, 48 and 72 hours compared to 0 hrs (Kacie Thomson, unpublished observations). This could be explained by EGF-stimulated degradation of EGFR/ErbB2 heterodimers. Therefore, we can safely conclude that it is EGF that stimulates follicle growth and inhibition of EGFR is responsible for blocking this mitogenic effect. Based on this data, therefore, EGFR must be expressed in preantral follicles from d15 and d16 mice otherwise these follicles would not respond to incubation with EGF.

Several pieces of evidence also indicate that we can pinpoint EGFR expression more specifically to the GCs. As the oocyte does not divide and we are able to cleanly isolate preantral follicles from juvenile ovaries so that attached theca/stroma cells are minimal, we are able to conclude that an increase in follicle diameter/growth is due to an increase in GC area. Increase to GC area during in vitro culture of isolated follicles is caused by increased GC proliferation rather than increase in the size of individual GCs. Qualitative inspection of these follicles during culture indicates that this is the case. Furthermore, immunolabelling for Ki67, a proliferation marker, in follicles exposed to 10 ng/mL EGF in identical treatment conditions to the follicles described in this study has demonstrated that EGF stimulates an increase in Ki67 labelling (Kacie Thomson, unpublished observations). Therefore, the simplest explanation for EGF-stimulated preantral follicle growth is that preantral GCs express EGFR and that EGF incubation stimulates activation of

mitogenic signalling downstream of EGFR in GCs. Furthermore, *Egfr* mRNA was not detected in the oocytes (see chapter 4).

Therefore, we conclude that EGFR is expressed in preantral GCs and is therefore likely to have a role in follicle development earlier to that described and elucidated in pre-ovulatory follicles.

7.2.2 It is possible that EGFR/ErbB2 heterodimers form in preantral GCs

It is well established that ErbB2 is the preferred heterodimerisation partner of all other ErbBs and its expression biases dimer formation towards ErbB2-containing heterodimers (Graus-Porta et al., 1997). The heirachy of ErbB dimerization is such that all other ErbBs prefer to dimerise with ErbB2 and ErbB2 prefers to dimerise with ErbB3. *ErbB3* mRNA transcripts and NRG-1 (an ErbB3 ligand) protein was detected in GCs suggesting that ERBB3 may be available to heterodimerise with ErbB2. Therefore, the question of whether EGFR and ErbB2 heterodimerise hinges on whether ErbB3 protein is present in the follicles and to what extent ErbB2 monomers are incorporated into ErbB3-containing heterodimers. It seems unlikely, however, that EGFR and ErbB2 would not heterodimerise at all when co-expressed.

If EGFR/ErbB2 heterodimers form following EGF stimulation and EGF is known to target EGFR for degradation, it follows that ErbB2 would also be downregulated. ErbB2 protein intensity, as determined by immunofluorescence, was found to decrease from 24 hrs onwards in EGF-stimulated follicles (Kacie Thomson, unpublished observations). ErbB2 heterodimerisation with EGFR is known to augment EGF-induced EGFR downregulation (by making EGF:EGFR interactions sensitive to the drop in pH as endosomes mature) (Lenferink et al., 1998), however,

you would still expect a proportion of EGFR/ErbB2 heterodimers to be targeted for degradation. Therefore, ErbB2 immunolabelling in isolated follicles may decrease upon EGF stimulation as a result of EGF-stimulated activation and downregulation of EGFR/ErbB2 heterodimers.

To summarise, the data from this chapter does not exclude the possibility that EGFR/ErbB2 heterodimers form but it also does not support this scenario either.

7.2.3 This data has not demonstrated a role for ErbB2 in in vitro follicle growth

Inhibitors specific to ErbB2 alone did not affect either basal or EGF-stimulated follicle growth in isolated follicle culture. It is important to note that the effect of Lapatinib on follicle growth in the absence of EGF was not investigated. This key experiment is an immediate priority for future work on this project as firstly, it will confirm that Lapatinib is not having a toxic effect on follicles and secondly, it will reveal whether Lapatinib effects basal follicle growth as it may be possible that EGF stimulation is masking an effect of Lapatinib. AG-825 and ErbB2 inhibitor II however, did not affect basal follicle growth in vitro, whereas AG1478 did. It is difficult to conclude that ErbB2 does not have role in follicle growth in vitro based on these experiments as there was no positive control confirming that AG-825, ErbB2 inhibitor II and Trastuzumab were inhibiting ErbB2 as expected. One possible technical reason why they may not have been is that a higher concentration of inhibitor is required to elicit an effect on follicle growth. The concentrations used were based on those recommended by the pharmaceutical companies that supplied them and other studies in the literature. However, the majority of this data is based on experiments in carcinoma cell lines, grown as a monolayer, that overexpress ErbB2.

Therefore, these are clearly different to follicles and may not respond in the same way. However, the same is true of Lapatinib and AG1478, which did affect EGF-stimulated follicle growth. This suggests that the reason ErbB2 inhibition did not affect EGF-stimulated preantral follicle growth while EGFR inhibition did is because ErbB2 does not have a role in, or is dispensable for, EGF-stimulated follicle growth whereas EGFR is involved and required. However, further validation of ErbB2 inhibitors is required to confirm this.

As these experiments examined the role of EGFR and ErbB2 inhibition only on EGF-stimulated preantral follicle growth, we cannot comment on the role of EGFR and ErbB2 on other processes they are known to regulate such as adhesion, EMT, steroidogenesis or cell survival. Furthermore, due to time constraints the effect of ErbB3 inhibition was not examined in preantral follicles, so the possible role of ErbB2/ErbB3 heterodimers was not investigated. The possible expression of ErbB3 protein is intriguing as ErbB3 and ErbB2 preferentially dimerise and therefore worthy of further investigation in future work.

As ERBB2 expression is regulated in a spatial manner (see Chapter 5 for details), there were concerns that the isolated preantral follicle culture model was not a suitable model to use to investigate ErbB2 function, as the majority of the follicles that we put into culture are from the cortico-medullary border. To check whether this was the case, preantral follicles were isolated from a d16 ovary and immediately fixed in formalin, processed for histology and immunolabelled with antibodies to ERBB2. This demonstrated that all follicles expressed ERBB2. Furthermore, another study revealed that ERBB2 was expressed in follicles cultured in control conditions for 72 hours (Kacie Thomson, unpublished observations). Therefore, the follicles that are put into culture do express ERBB2 and it was concluded that this model was suitable.

It is not possible to define from where in the ovary these follicles are from, but we are unlikely to mechanically isolate 20 follicles from the periphery of the follicle only. It is safe to assume that some of the follicles from this analysis were from the centre of the ovary. The intensity of ERBB2 immunolabelling in these isolated follicles appears visibly different to those in the centre of a d16 ovarian section. This is likely due to differential processing of whole ovaries and isolated follicles as well as images being taken at different settings and immunolabelling being performed at separate times as there is usually no longer than an hour between dissection of the ovary and fixation of isolated follicles and hence it is unlikely that ERBB2 expression is downregulated in this time. Therefore, while it was concluded that the isolated follicle culture model was a suitable model to examine ErbB2 function in, we cannot comment on the effect of ErbB2 inhibition specifically in peripheral preantral follicles that express the most ERBB2 (see Chapter 5).

It is interesting that Trastuzumab caused a non-significant increase in follicle growth. Growth factors can generate intracellular signalling that ultimately leads to stimulation or inhibition of many processes including cell division, cell death, cell migration, and cell shape change. However, inhibition of ErbB2, a proto-oncogene, would generally be expected to have a negative effect on growth. Among the ErbB family of receptors, it is ErbB4 that is more frequently associated with a negative effect on growth (Ishibashi et al., 2013). The mechanism of action of Trastuzumab has not been fully elucidated but it is known to bind to juxtamembrane domain and thought to cause ErbB2 internalisation (Klapper et al., 2000; Vu and Claret, 2012). It is possible that Trastuzumab may be potentiating the EGF response in some way though it is unclear how.

The co-localisation of ERBB2 with N-CADHERIN and immunolocalisation of the downstream anti-proliferative protein, TOB1, suggests that ErbB2 has dual functions during primordial activation (see Chapter 4 for details), which cannot be examined in this model. Therefore, further experiments examined the effect of ErbB2 inhibition on initiation of follicle growth during in vitro culture of whole d4 mouse ovaries (Chapter 8).

7.3 Conclusion

The data presented here suggest that EGFR is expressed in preantral GCs and is available to heterodimerise with ErbB2. Furthermore, the data suggest that EGFR has a role in EGF-stimulated GC proliferation during preantral follicle growth. The data does not suggest that ErbB2 has a role in GC proliferation during preantral follicle growth but, as earlier expression data (see Chapter 4) suggested that ErbB2 has a role in primordial activation, further experiments examined the effect of ErbB2 inhibition on initiation of follicle growth during in vitro culture of whole d4 mouse ovaries (Chapter 8).

Chapter 8: ErbB stimulation and inhibition during in vitro culture of whole d4 mouse ovaries

Immunolocalisation of ERBB2 and TOB1, an anti-proliferative protein downstream of ErbB2, suggested that ErbB2 might have a role in regulating GC cuboidalisation and proliferation during primordial activation (see Chapter 2 for details). Primordial activation is key to determining the reproductive lifespan of a female and therefore elucidation of this process could enable development and improvement of fertility treatments. During my project, a whole ovary culture model was established in our laboratory by Jocelyn Mora based on the protocol described by Eppig and O'Brien (1996). This involved culture of a whole d4 mouse ovary, in which the majority of follicles are at the primordial stage, for 8 days, at which point some follicles have reached the multilayered stage. Therefore, the role of ErbB2 in primordial activation can be investigated. In addition, there are several other advantages of the whole ovary model compared to the isolated follicle culture model in terms of studying ErbB2 function. We use d16 mouse ovaries to collect isolated follicles for culture experiments. ERBB2 expression varies significantly between follicles of a similar stage in a d16 ovary (see Chapter 5) whereas ERBB2 is expressed in all growing follicles in a d4 ovary to a similar level (see Chapter 4). The data presented here investigates the effect of ErbB inhibition and stimulation on in vitro primordial activation.

8.1 Approach

Expression analysis suggested that ErbB2 may have a role in primordial activation (see Chapter 4). Inhibitors that targeted both EGFR and ErbB2, but not

those specific to ErbB2, blocked EGF-stimulated isolated preantral follicle growth in vitro (see Chapter 7). Therefore, the effect of Lapatinib, an inhibitor of EGFR and ErbB2, and EGF was investigated in separate whole ovary culture experiments. As endogenous ligands that control primordial activation should be present in this model, no exogenous ligand was added for the first experiment.

Ovaries (day 4 post partum) were collected from a 'litter' of cross-fostered female pups (6) and dissected free of the bursa membrane. Healthy, intact ovaries were placed into culture (Eppig and O'Brien,1996; materials and methods section 2.7.1). Briefly, d4 ovaries are cultured in 6 well plates under a thin meniscus of medium on 24 mm membrane inserts (3.0 μM pore size). 1.5mL of medium is placed in the well beneath the inserts. The medium was Waymouth medium MB752/1 supplemented with 0.23 mM sodium pyruvate, 0.3% BSA and 10% FBS. Several ovaries can be placed on the same membrane and images taken during culture are 'tracked' according to their orientation in the well. d4 ovaries were cultured in either DMSO vehicle control (n=3), 1 μM (n=3) or 10 μM (n=2) Lapatinib medium. Ovaries on the membrane were not disturbed during culture until collection but the medium beneath the insert was changed every 48 hours. 1 mL of medium was removed and replaced with fresh medium supplemented with either vehicle control or Lapatinib to ensure continual inhibition of ErbB2 signalling during culture. Images were taken of these ovaries every 24 hours using an inverted microscope with a x10 objective. On day 8 of culture (equivalent to postnatal day 12 in ovarian age), ovaries were formalin fixed and paraffin-embedded. General health and morphology of the ovaries (i.e. presence of pyknotic nuclei) was assessed by Haematoxylin and Eosin staining (materials and methods section 2.4.5), while another central section was double labelled using antibodies and fluorescently-tagged secondary antibodies

against VASA and LAMININ (materials and methods section 2.7.3), markers of the oocyte and basal lamina, respectively to aid follicle identification and classification.

8.2 Results

8.2.1. Do ovaries exposed to Lapatinib appear healthy during the 8 day culture period?

Photographs of the ovaries on the membrane were taken every 24 hours. Visual inspection of ovaries during culture revealed that follicles were growing as it was possible to focus the microscope so as to visualise growing oocytes inside the ovary. The ovaries remained largely intact during culture. However, there was loss of integrity of some ovaries during the last days of culture (Figure 8.1). All ovaries, regardless of whether their surface was well, or less, defined, spread/flattened on the membrane during culture. This was very apparent when they were removed from the membrane to be processed for histology. They were thin, white whisps of tissue that required staining with nuclear fast red to make sure they are visible during processing and sectioning. As described in materials and methods section 2.7.2, our alchohol dehydration steps for histological processing protocol had to be modified for these cultured ovaries as more than 30 minutes, in total, in 100% ethanol completely dried out the ovaries so much so that they were too brittle to section. In contrast, isolated follicles that are agarose embedded prior to alcohol dehydration and paraffin embedding are capable of being sectioned following three 1.5 hour washes in 100% alcohol. This gives a reasonable idea of how fragile this tissue is.

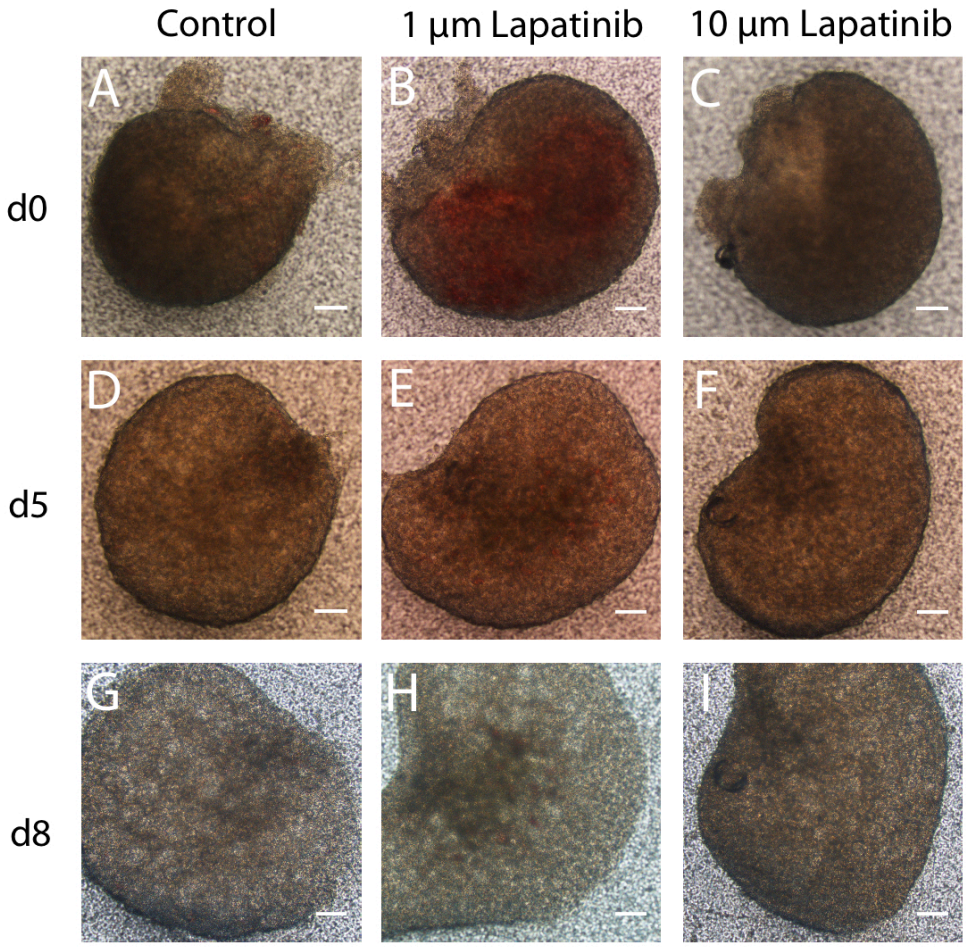


Figure 8.1. Ovaries on the membrane at days 0, 5 and 8 of culture during Lapatinib Ditosylate dose response experiment. A representative ovary from control and both treatment groups (1 µM and 10 µM lapatinib) is shown. Ovaries may still have a small amount of extraovarian tissue still attached following microdissection at the beginning of culture. At day 5 of culture, the ovaries appear entirely intact. By the last day of culture (8) ovaries have grown too big to be photographed in one image using the x10 objective. In addition, in some places the edge of these ovaries becomes less defined as it appears the OSE has not remained completely intact. Scale bars represent 100 µm.

8.2.2. How does in vitro follicle development differ from in vivo follicle development?

Haematoxylin and Eosin staining demonstrated that these ovaries were healthy (Figure 8.2); the number of pyknotic nuclei did not significantly vary between treatment groups and was similar to that seen at d12 in vivo (i.e. immediately collected and processed).

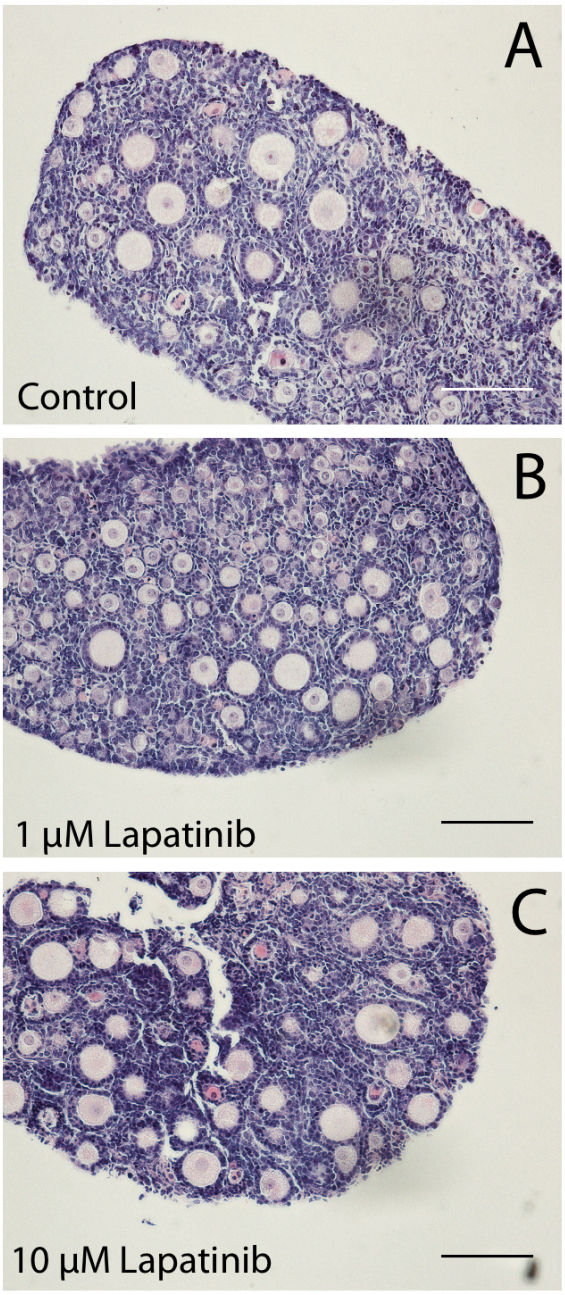


Figure 8.2. Representative sections from ovaries cultured with vehicle control (A), 1 µM Lapatinib (B) or 10 µM Lapatinib (C) stained with Haematoxylin and Eosin.

VASA and laminin double labelling revealed that several follicles reached secondary stage in which GCs are multilayering (Figure 8.3A, B). Eppig and O'Brien (1996) originally developed this technique to develop mature, developmentally competent oocytes from primordial follicles via a two-step system in which whole neonatal ovaries are cultured for 8 days and then oocytes surrounded by 1-3 layers of

GCs are isolated and cultured for a further 14 days. Although we haven't isolated follicles from these ovaries to test whether they are capable of maturing and achieving developmental competence, it is a promising sign that follicles in our cultured ovaries reach the same stage of development as those cultured by Eppig and O'Brien. Furthermore, some follicles remain as dormant, primordial follicles and the majority of these are situated near the OSE demonstrating that, as you would see in vivo, only a subset of follicles initiate growth (figure 8.3 C, D). There are several primordial follicles that appear to be at the very centre of the ovary (8.6 C). Although the ovaries remained intact and spherical on the transwell membrane insert, they did not retain the 3D structure of the ovary and rather grew almost flat. Therefore, primordials that appear in the centre of a section may actually be adjacent to the surface that is either touching the membrane or facing upwards in the well. Therefore, it was not possible to draw conclusions regarding spatial regulation of activation of follicle growth based on these sections.

VASA/laminin double labelling also revealed several features of these ovaries that appear to be specific to in vitro culture. These are summarised in figure 8.3. One feature, revealed by laminin staining, was the development of follicles with more than one oocyte i.e. it appears as though several follicles have developed inside the basal lamina (Figure 8.3E, F). The oocytes within these follicles are positive for VASA and appear healthy when stained with haematoxylin and eosin, as do the GCs. Therefore, these follicles appear to initiate growth and develop perfectly normally in every aspect other than the laying down of the basement membrane. In the vast majority of instances the follicles with multiple oocytes are enclosed within a continuous, unbroken basal lamina. A 'broken' basal lamina is much less frequently observed. The occurrence of these follicles mean that it is sometimes harder to

classify follicles at a particular stage because we use the level of GC cuboidalisation, proliferation and multilayering to stage follicles. However, in these follicle 'nests' the GCs become continuous with either each other, or the somatic cells in the stroma or both. Additionally, there are oocytes that are surrounded by somatic cells but no basal lamina. However, the vast majority of these are small, non growing oocytes within the OSE. This is also seen in vivo (Kate Hardy, unpublished observations) and was not considered a feature unique to in vitro culture, but rather a natural occurrence both in vivo and in vitro. It is not clear why follicles with more than one oocyte are more common in vitro than in vivo.

Another, more occasionally observed, feature was oocytes in which there were a small number of somatic cells (1-5) immediately adjacent to the oocyte i.e. they were not separated from the oocyte from a zona pellucida (Figure 8.3G, H). It was not considered feasible to label the zona pellucida in these sections due to the small number of sections available and how occasionally this feature was observed. However, the vast majority of GC nuclei in the vast majority of growing follicles are separated from the oocyte, suggesting the presence of a normal zona pellucida. VASA/laminin double immunolabelling was performed on one section of every ovary. The unusual oocytes described here were not observed in every section, and no more than two was observed in a single section. At least one was observed in a control and a treatment group section. Again, it is not clear why these follicles occur in vitro but it appears to be associated with the culture system rather than a specific treatment group.

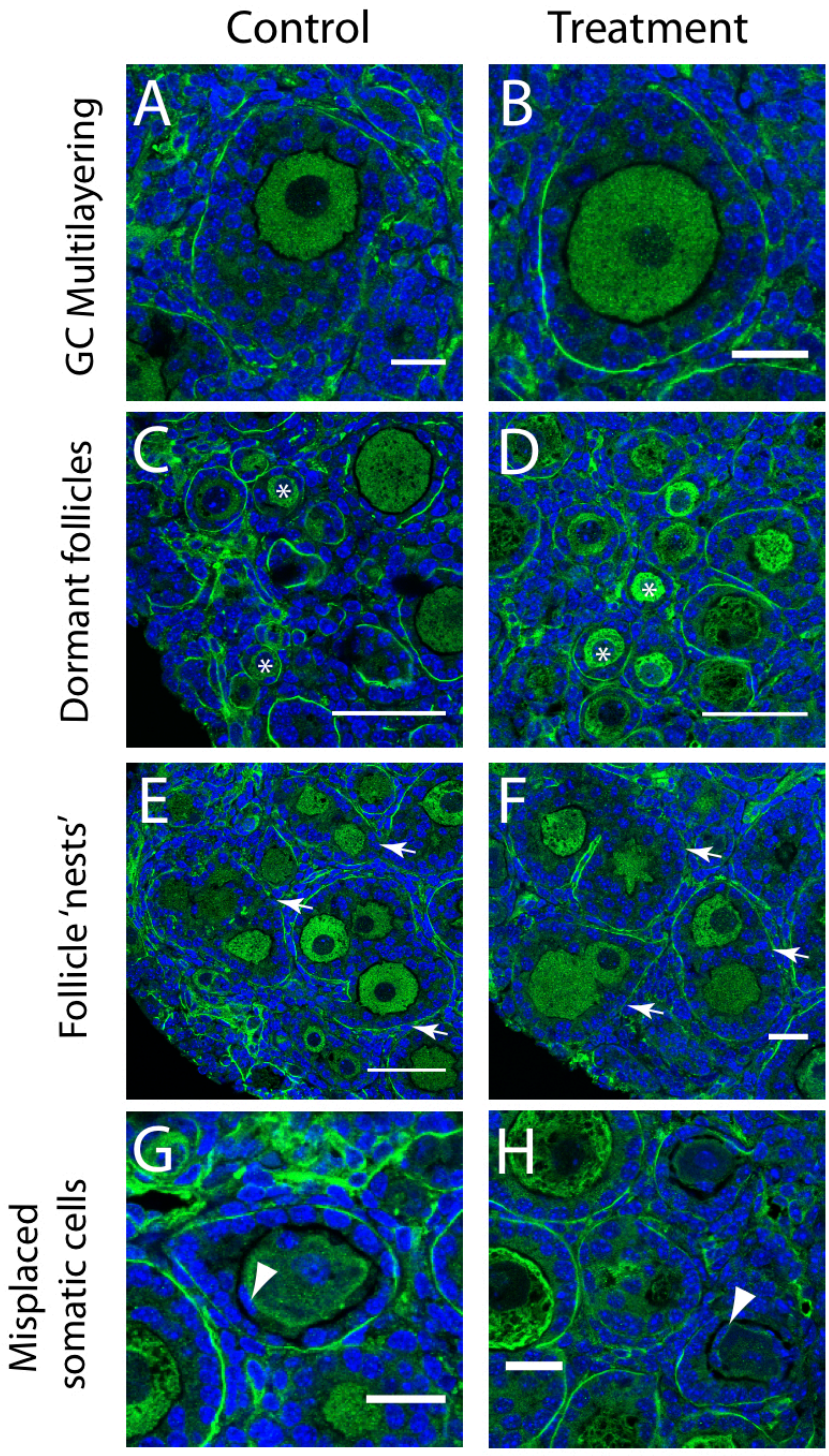


Figure 8.3. Features of follicle development during in vitro culture of whole d4 ovaries that are either similar to follicle development in vivo (A-D) or peculiar to in vitro model (E-H). Sections from whole ovaries cultured for 8 days in either vehicle control (DMSO) or Lapatinib Ditosylate were double immunolabelled for VASA and laminin (gree, A-H). Nuclei are labeled with DAPI (blue, A-H). White arrows label follicles with more than one oocyte. White arrowheads label somatic cell nuclei that are not separated from the oocyte by the zona pellucida. Stars represent primordial follicles. Scale bars represent 20 µm and 50 µm.

8.2.3 Is ErbB2 expressed in cultured ovaries?

ERBB2 expression is regulated according to both follicle stage and follicular location within the ovary (see Chapter 5). Regulation of ERBB2 is such that, in vivo, it is regulated entirely according to follicle stage in d4 ovaries (see Chapter 4), whereas in d12 ovaries it is also regulated according to follicular location within the ovary (see Chapter 5). The in vitro model described here involves the culture of d4 ovaries for 8 days (i.e. equivalent to postnatal day 12 in ovarian age). Therefore, to assess ERBB2 expression was regulated in a similar manner in cultured ovaries, we incubated a central section from each ovary with antibodies to ErbB2, as described in materials and methods section 2.4.3.

ERBB2 localised to cuboidal GCs of all growing follicles in all ovarian sections analysed from every treatment group (Figure 8.4). Therefore, it was concluded that this was a suitable model to examine ErbB2 function in. Furthermore, it appears that ERBB2 expression is regulated entirely according to follicle stage in these ovaries.

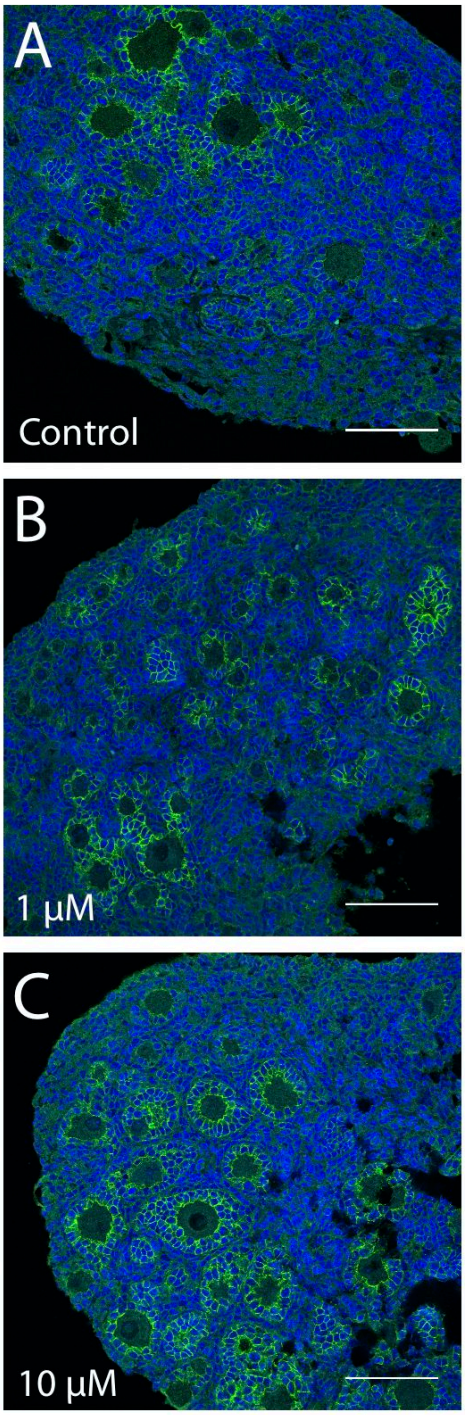


Figure 8.4. ERBB2 immunolocalised in sections from cultured ovaries. d4 ovaries were cultured in 0, 1 or 10 µM Lapatinib for 8 days. ERBB2 localised to cuboidal GCs of all follicles, in all treatment groups. Scale bars represent 50 µm.

3.2.4 How does Lapatinib treatment affect in vitro primordial activation in these ovaries?

To examine whether Lapatinib Ditosylate had an effect on follicle development we analysed one approximately central section of each ovary. A representative section from each ovary is shown in figure 8.5. The number of growing follicles in each section was counted and compared. Lapatinib was not associated with follicle loss as the average number of follicles in a central section from control, 1 μM and 10 μM Lapatinib treatment groups were 37, 52, and 40, respectively. As a feature of these cultured ovaries was the development of follicles which shared a basal lamina and this made follicle stage difficult to classify according to the criteria outlined in materials and methods section 2.6.7. Therefore, oocyte area was measured and used as a surrogate marker for activation, as this was a constant measurable parameter for all sections. An approximately central section from each cultured ovary was immunolabelled with antibodies to VASA and laminin, markers of the oocyte and basal lamina, respectively (Figure 8.6). Only oocytes that had a visible nucleus were measured to ensure all oocytes were measured at approximately their widest cross section. A threshold area that defined the point at which a follicle was classified as growing was chosen based on a large collection of nearly 900 measurements carried out for another study, measuring follicles and oocyte area for follicles at different stages in formalin-fixed, paraffin-embedded ovary sections (Kate Hardy, unpublished observations; Figure 8.5). This value was 350 μm^2. All oocytes that had an area of this value or below were classified as non-growing and all oocytes that had an area above this value were classified as growing.

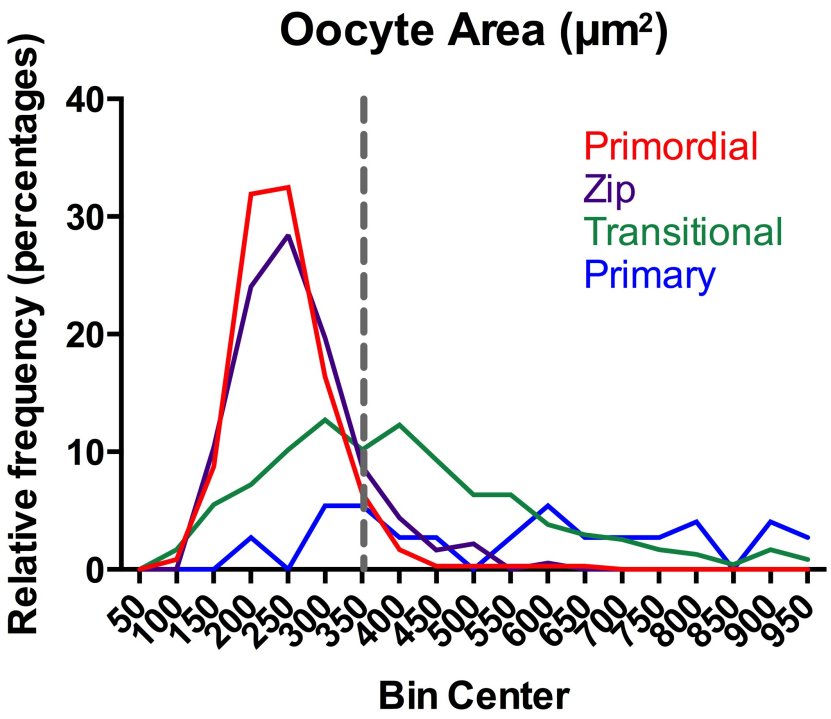


Figure 8.5. The distribution of area of oocyte in different stages of follicle development. The vast majority of primordial follicles have an oocyte area of less than 350 µm^2. Follicles which have an oocyte area of more than 350 µm^2 are more likely to have initiated growth. Therefore, 350 µm^2 was used as the cut off value to differentiate between non-growing and growing follicles in cultured ovaries. The term 'Zip' used in this analysis was used to classify follicles that had a mixture of flat GCs and wedge-shaped GCs but no cuboidal GCs. In my thesis, these follicles are classified simply as transitional follicles (Kate Hardy, unpublished observations).

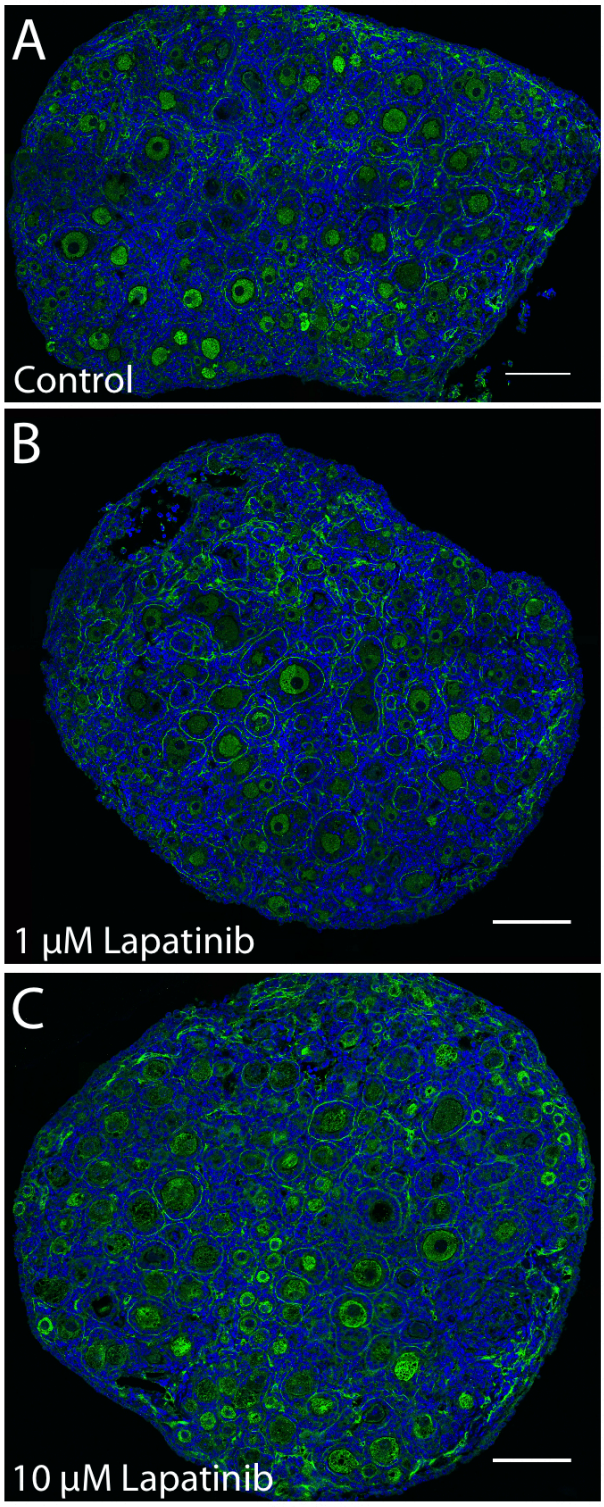


Figure 8.6. Representative sections from control and both treatment groups immunolabelled for VASA and laminin, markers of the oocyte and basal lamina, respectively. Scale bars represent 100 µm.

All oocytes with a visible nucleus were measured, as described in materials and methods section 2.7.5, and classified as growing or non-growing. The proportion of growing follicles was then compared between control and treatment groups. Excitingly, 1 µM Lapatinib (n=3) caused a significant decrease ($p<0.0001$) in the proportion of growing follicles, suggesting that ErbB signalling positively regulates primordial activation. (Figure 8.7). However, 10 µM Lapatinib does not significantly affect primordial activation, compared to vehicle control. The reason for this is unclear. This is an exciting result and further investigation with larger n numbers is required to validate this effect.

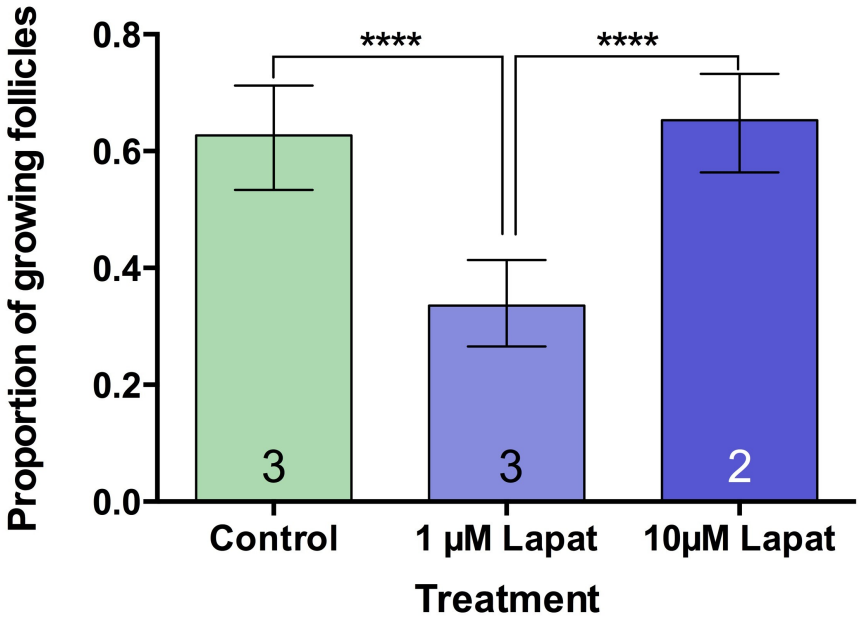


*Figure 8.7. The effect of Lapatinib on in vitro primordial activation. Whole d4 mouse ovaries were cultured in either vehicle control, 1 µM or 10 µM Lapatinib and the proportion of growing follicles was measured. The numbers in bars represent the number of ovaries. Bars are means and 95% CI. Key: ****; p<0.0001*

8.2.5 What is the effect of EGF on in vitro primordial activation?

As EGF stimulated isolated preantral follicle growth in vitro (see Chapter 7), an EGF dose response was performed in the whole ovary to determine whether stimulation of the ErbB receptors affected primordial activation. Healthy d4 mouse

ovaries were placed into culture as described in materials and methods section 2.7.1. Ovaries in the same treatment group were split over different wells (i.e. not all control ovaries were cultured on the same membrane) and ovaries were fixed on day 5 of culture as the flattening or 'spreading' of the ovaries on the membrane was quite extensive at this point. Ovaries were cultured in a thin film of either control medium or 10 ng/mL or 100 ng/mL EGF. The same features of follicle development described in Figure 8.3 were observed in this experiment (data not shown). Therefore, the same method of classification of follicles was used; oocyte area was used as an objective, surrogate marker of primordial activation. The threshold area that defined activation of growth was again 350 μm^2. The area of VASA labelled oocytes in a central section from each cultured ovary were measured, classified and compared.

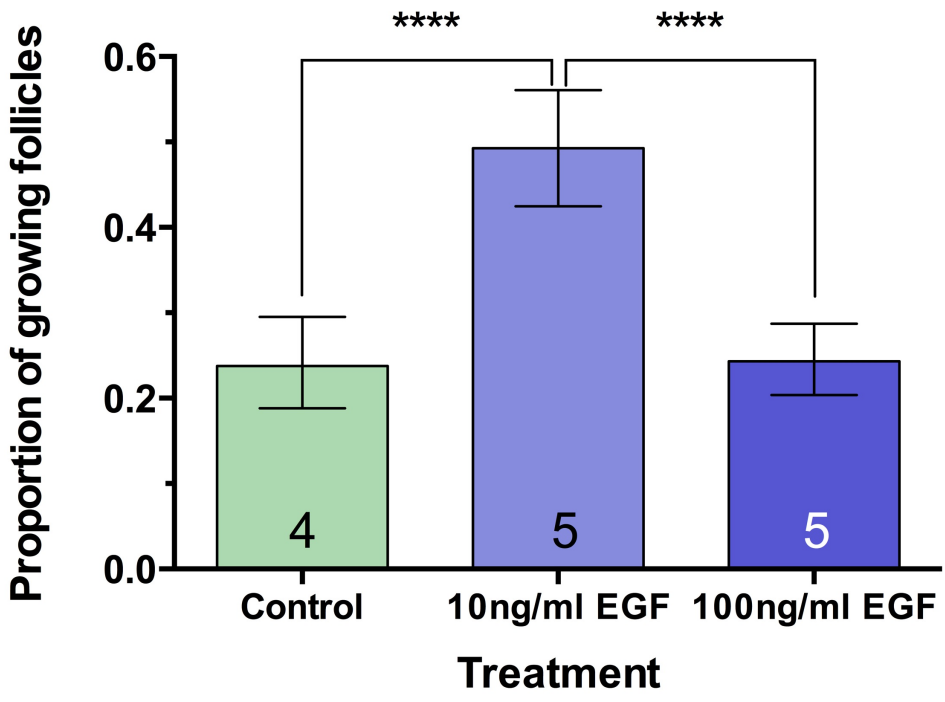


*Figure 8.8. The effect of EGF on in vitro primordial activation. Whole d4 mouse ovaries were cultured in either control, 10 ng/mL or 100 ng/mL EGF medium for 5 days and the proportion of follicles with an oocyte area of >350 μm^2 was measured. The numbers in bars represent the number of ovaries. Bars are means and 95% CI. Key: ****; p<0.0001*

Excitingly, the proportion of growing follicles in central sections of ovaries exposed to 10 ng/mL EGF (n=5) was significantly higher ($p<0.0001$) than that of controls suggesting that EGF stimulates in vitro primordial activation. The proportion of growing follicles in ovaries exposed to 10 ng/mL was also significantly higher than that of 100 ng/mL. As EGF stimulation of EGFR is known to cause rapid downregulation of EGFR from the membrane via targetting to the lysosome (Ebner and Derynck, 1991) and different doses of EGF are known to alter EGFR function (Xiao et al., 2008), this is not that surprising.

8.3 Discussion

8.3.1 Follicle development in vitro differs to that in vivo

Unsurprisingly, follicles do not develop in vitro as they would in vivo. There are several features observed during this culture that are rarely seen in vivo. The most commonly observed of which was follicles that shared a basal lamina. It is not clear what the reason for this is. However, as it is seen in both control and treatment groups, it is not due to Lapatinib exposure. DMSO and FBS and phenol red were all common to control and treatment medium. Therefore, one of these substances may be responsible. The EGF dose response in ovary culture model (Figure 8.8) was conducted in the absence of DMSO and this feature is still observed (data not shown). Ovaries cultured in 2% FBS (Figure 8.8) rather than 10% FBS (Figure 8.7) do not have visibly fewer follicles that share a basal lamina (data not shown). Whole ovary culture in the absence of phenol red has not been tested and is certainly worthy of further investigation as phenol red has been demonstrated to have estrogenic

properties (Welshons et al., 1988). While in vitro follicle development is different to in vivo follicle development, a small proportion of follicles in these cultured ovaries do reach the multilayered stage by day 8 of culture, as would be expected if these ovaries had developed until day 12 in vivo. Therefore, in vitro follicle development is certainly not impaired.

Eppig and O'Brien (1996) did not report this feature. However, they did not immunolabel sections from their cultured ovaries with antibodies to Laminin, so it may be that this feature did occur in their model. However, GCs from one follicle do appear distinct from the GCs from other follicles and stroma in their sections, in the absence of Laminin labelling. The only major difference between our protocols is that Eppig and O'Brien placed neonatal ovaries into culture whereas d4 ovaries were used in these experiments. Oocyte nest breakdown and primordial follicle formation is occurring between these two timepoints (Pepling and Spradling, 2001). It is possible that taking d4 ovaries from the in vivo environment and placing them into culture at this point is disturbing these processes in such a way and at such a timepoint that growing follicle nests are formed.

Alternatively, these features could be associated with the way ovaries flatten on the membrane. Laminin is a component of the ECM, and the ECM is likely to behave differently in ovaries that have developed as oval in shape compared to those in vitro that grow as thin, whisps.

8.3.2 ErbB signalling may be involved in in vitro primordial activation

The proportion of growing follicles in a central section from each cultured ovary, as determined using the oocyte area as a surrogate, objective marker for primordial activation, was significantly reduced in ovaries exposed to 1 μM Lapatinib

compared to those exposed to either vehicle control or 10 μM Lapatinib. It is exciting that ErbB signalling may have a role in primordial activation, as suggested by expression analyses (see Chapter 4). However, it is perplexing why 1 μM but not 10 μM Lapatinib would have a significant effect.

The ovaries exposed to 10 μM Lapatinib did not appear unhealthy during culture (Figure 8.1). Haematoxylin and eosin staining of ovarian sections from these ovaries confirmed this (Figure 8.2). Furthermore, the features of follicle development that were peculiar to in vitro culture of whole ovaries were seen in both control ovaries and those exposed to 10 μM Lapatinib (Figure 8.3). Therefore, the reason that 1 μM Lapatinib abrogates primordial activation but 10 μM Lapatinib doesn't is not because 10 μM Lapatinib is toxic and skews the number of follicles.

Clearly, further investigation with a large number of ovaries, analysis of multiple sections from each ovary, and the culture of ovaries within the same treatment group on different membranes is required to validate this result. It is promising, however, that a concentration of Lapatinib known to affect preantral follicle development in vitro is associated with inhibition of primordial activation in vitro.

Furthermore, the proportion of growing follicles in central sections from ovaries exposed to 10 ng/mL EGF was significantly higher than that of ovaries exposed to 0 ng/mL EGF (control) or 100 ng/mL EGF. The stimulatory effect associated with 10 ng/mLEGF and lack of an effect with a higher concentration of EGF (100 ng/mL) may be due to EGF induced downregulation of EGFR at the membrane (Ebner and Derynck, 1991). An assay for EGFR phosphorylation and signalling would confirm whether this was the case. A previous study used

pharmalogical reagents to disrupt different membrane microdomains and single-molecule fluorescence microscopy to visualise the extent of EGFR endocytosis upon pharmacological assault and concomitant activation with a low or high dose of EGF. This revealed that EGFR associated with clathrin-coated pits when stimulated by a low dose of EGF whereas when EGFR was stimulated with a high dose of EGF it also associated with caveolae (Xiao et al., 2008). This alteration to EGFR trafficking will alter it's signalling and function and therefore this may be the reason that 10 ng/mL but not 100 ng/mL of EGF may positively regulate primordial activation in vitro. Furthermore, this may be the reason a stimulatory effect was not observed in previous studies on rat ovaries (Kezele et al., 2002) in which whole d4 rat ovaries, cultured on floating filters, were incubated with 100 ng/mL EGF for 8 days. There may also be different factors involved in rat and mouse primordial activation.

Following validation of these results, the localisation of junctional molecules such as N-cadherin should be investigated. Furthermore, the effects of an N-cadherin neutralising antibody on both primordial activation and ErbB2 phosphorylation would be pertinent to this project. The results of chapter 7 indicate that these ovaries are unlikely to yield enough protein to do co-immunoprecipitation assay to assess ErbB2/N-cadherin interactions. However, it may be possible to label ErbB2 and N-cadherin in these cells with a donor and acceptor fluorophore, respectively, and assess whether they are closely associated enough to enable excitation of the acceptor fluorophore following excitation of donor with a photon via fluorescence resonance energy transfer (FRET). Furthermore, the physiological relevance of EGF:EGFR interaction in primordial activation in mice could be further examined in ovaries from mice that have had their salivary glands removed. Additionally, localisation of other

ErbB ligands, especially in light of *ErbB3* detection, is also worthy of further investigation.

8.4 Conclusion

The result of these experiments suggest that ErbB signalling may be involved in primordial activation, as was suggested by immunolocalisation of ErbB2 (see Chapter 4). Further investigation is required to confirm the effect of ErbB stimulation and inhibition and future work would also investigate the role of the recently detected ErbB3 receptor and its ligand NRG-1. Additionally, further investigation into the underlying reasons for development of the features of follicle development in this in vitro model would be interesting for future work.

.

Chapter 9: General discussion

Primordial activation, the key irreversible process that initiates a cascade of events that ultimately leads to either ovulation or atresia, and therefore defines a female's reproductive lifespan, is poorly understood. Several RTKs have been implicated in positively regulating this process. However, in the majority of cases, the particular aspect of primordial activation these receptors are promoting remains unclear (Adhikari and Liu, 2009). Few studies are concerned with investigating GC cuboidalisation, however, a recent study from our lab demonstrated that N-cadherin the major CAM associated with this change in the mouse ovary (Mora et al., 2012). As it is well established that RTKs and CAMs can mutually regulate one another (Comoglio et al., 2003), this project investigated the hypothesis that N-cadherin collaborated with RTK(s) to co-ordinate GC cuboidalisation and GC proliferation during primordial activation. The studies carried out in this thesis have provided evidence that the EGF family are likely to have an important role in GC shape change and division during initiation of follicle growth, whereas, in contrast, the PDGF family is less likely to be crucial in this process.

This project hypothesised that the change in GC shape, from flattened to cuboidal, and the accompanying upregulation of N-cadherin immunolabelling were key steps in primordial activation and that this was subject to RTK regulation. Therefore, initial studies aimed to find an RTK that co-localised with N-cadherin. This study showed that PDGF receptor did not co-localise with N-cadherin at any stage of follicle development; the receptors exclusively localised to cells 'outside' the basal lamina. Therefore, it was concluded that this family were unlikely to regulate the change in GC shape from flattened to cuboidal or GC proliferation and a second candidate family were investigated. However, absence of PDGF receptor protein

does not preclude the PDGF family from having a role in primordial activation, as has been shown in previous studies in the rat ovary (Nilsson et al., 2006). PDGFRβ and PDGF-B did localise to the rete ovarii and interstitial cells of d4 mouse ovaries, whereas, in older mice, PDGF receptor protein localised to mature theca cells of antral follicles or cells immediately adjacent to basal lamina which may be early or putative theca cells. The development of the theca layer and its relevance to primordial follicle formation/activation is poorly understood (Young and McNeilly, 2010). Furthermore, no postnatal function has been attributed to the rete ovarii, although its role in primordial follicle formation and development was much discussed several decades ago (Byskov and Lintern-Moore, 1973). The role of interstitial cells on primordial follicle formation has not been thoroughly investigated, as it is not feasible to separate these from small, fragile, firmly embedded primordial follicles or oocyte nests. However, further investigation of PDGF signalling during early ovarian development in mice may shed light on the origin of theca and its relevance to follicle formation and initiation of growth.

PDGF signalling in theca cell proliferation and steroidogenesis has been investigated (Duleba et al., 1999). Furthermore, the PDGF family has been implicated in PCOS (Scotti et al., 2014). PCOS is one of the most common causes of infertility, which is characterised by theca hyperplasia and hyperandrogenemia, among other things, but the underlying mechanisms are poorly understood. In light of the fact that PDGF receptors localise to cells of unknown origin in pre-pubertal ovaries as well as mature theca of cycling ovaries, it is possible that the mechanisms underlying pertubation of theca function in PCOS ovaries occur much earlier than anticipated.

To summarise, the PDGF family is likely to have a role in early ovarian development but how and whether this role relates to its later, more understood, function during theca development and in PCOS ovaries is unclear.

A major finding early in this thesis was that ErbB2 co-localised with N-cadherin between cuboidalising GCs. The intensity of ErbB2 expression was upregulated during primordial activation, providing strong evidence of a potential role in follicle activation. Furthermore, the co-localisation of ErbB2 and N-cadherin to specific domains of membranes of cuboidalising GCs is intriguing as it mirrors the pattern expected of N-cadherin during AJ assembly. Therefore, it is possible that ErbB2 is associated with junctional assembly during GC cuboidalisation. To the best of my knowledge, there are no factors that have been implicated in this process. The hypothesis this project investigated was that mutual regulation of N-cadherin and an associated RTK(s) co-ordinated GC cuboidalisation and proliferation during initiation of follicle growth. Therefore, the expression of an anti-proliferative protein downstream of ErbB2, TOB1, was examined. TOB1 is an anti-proliferative protein that is inactivated downstream of ErbB2 signalling. The inactive form was expressed in the same pattern as ErbB2; pTOB1 localised exclusively to cuboidal GCs of growing follicles, evidencing that ErbB2 was indeed signalling, phosphorylating and inactivating TOB1 in the mouse ovary. Crucially, the active form of TOB1 also localised to flat GCs of non-growing, primordial follicles providing strong evidence that TOB1 may have a role in maintaining the primordial pool and that ErbB2 may be involved in regulating the steady trickle of follicles entering the growing pool. As expression analyses provided evidence that ErbB2 was likely to have a role in primordial activation, the function of ErbB2 was further investigated. The focus of the majority of my project was investigating the effects of stimulating and inhibiting

these receptors on follicle development. However, future work will continue to examine the association of ErbB2 with N-cadherin more closely. Co-immunoprecipitation would demonstrate whether ErbB2 and N-cadherin are physically interacting during primordial activation. Furthermore, knockdown of either ErbB2 or N-cadherin expressing using inhibiting siRNAs and investigation into the affect of this on localisation of the other protein and primordial activation would also give a clearer idea of whether these membranous proteins mutually regulate one another.

ErbB2 is unique among the ErbB receptors as no known soluble ligand binds to it and it requires heterodimerisation to signal, as does kinase-dead ErbB3. EGFR, on the other hand, is able to signal as a homodimer. *Egfr* and *ErbB2* were the only ErbB receptors detected in an initial PCR screen. Therefore, I focused on investigating the possible role of EGFR/ErbB2 dimers on follicle development. However, a second PCR screen performed at a late stage in this project by my laboratory colleagues also detected *ErbB3*. The discrepancy between these PCR screens is likely due to the fact that *ErbB3* is expressed at low levels and a dilution of the cDNA samples used in the initial PCR screen may have diluted these transcripts beyond detection. Due to time constraints the expression and function of ErbB3 protein during follicle development was not investigated further. However, NRG-1 protein, a ligand of ErbB3, was detected in mouse ovary, suggesting that ErbB3 protein is expressed in the mouse ovary. This is of critical importance to examining the function of ErbB2 in the mouse ovary as ErbB2 requires heterodimerisation to signal and, in addition, it is the preferred heterodimerisation partner of all other ErbBs. Furthermore, ErbB2 prefers to heterodimerise with ErbB3 and form the most mitogenic ErbB dimer possible (Graus-Porta et al., 1997; Tzahar et al., 1996; Yarden

and Sliwkowski, 2001). Therefore, our deductions on the heterodimerisation and signalling of ErbB2 in the mouse ovary hinge on whether ErbB3 protein co-localises with ErbB2. Therefore, if I had more time I would focus on localising ErbB3 protein by immunofluorescence or western blot analysis. We were not able to immunolocalise EGFR protein in preantral follicles by either of these methods. However, the sensitivity of isolated preantral follicles to stimulation with EGF and inhibition of EGFR demonstrates that EGFR protein is expressed in preantral GCs. Therefore, if a similar situation arose with ErbB3, the effect of NRG-1 and ErbB3 inhibitors on isolated preantral follicles and whole d4 ovary could be examined. This may be more difficult than similar experiments with EGFR and ErbB2 as ErbB3 has a defective kinase domain. Furthermore, the role of ErbB3 in cancer progression was not appreciated as quickly as for that of EGFR and ErbB2 (Yarden and Sliwkowski, 2001). Therefore, there have been fewer agents made available to block ErbB3 signalling, and those that have are usually targeted towards the extracellular domain of ErbB3 (Jiang et al., 2012). There is a humanized anti-HER3 antibody called MM-121, however, that blocks the binding of HRG1-β to HER3. HRG1-β is a neuregulin-1 type 1 polypeptide. The antibody we used to localise neuregulin-1 recognises NRG1 type 1 polypeptides and is therefore predicted to label the NRG1 beta type I isoforms 6-8 in addition to the NRG1 alpha isoforms 1-4. Therefore, the antibody MM-121 should block the action of the neuregulin ligand we have localised in the mouse ovary. Furthermore, the antibody MM-121 blocks signalling from ErbB2 and ErbB3. However, these antibodies may not be available to groups not performing clinical studies. One agent that is available is Canertinib, a pan-ErbB inhibitor, that blocks signalling from all ErbBs. The effects of Canertinib could be compared to those of AG1478 (EGFR-specific), and Lapatinib Ditosylate (dual inhibitor of EGFR

and ErbB2). To summarise, in order to investigate a possible role of ErbB2 in primordial activation, it is very important to establish whether it is EGFR or ErbB3 that ErbB2 dimerises with. The availability of suitable antibodies, inhibitors and techniques that are feasible to perform on such small amounts of material may be limiting factors, however, as was found during the investigation of EGFR/ErbB2 signalling.

The most robust culture model available at the beginning of this project was the isolated follicle culture model. The drawback of this model is that it is only feasible to isolate follicles in which GCs have already cuboidalised and formed multiple layers. However, the role of ErbB signalling on GC proliferation, a key feature of primordial activation, can be examined. Therefore, the effect of EGF (as ErbB2 has no known ligand) and various inhibitors or ErbB2 and/or EGFR on isolated preantral follicle growth was investigated. These data demonstrate that (i) EGFR and/or ErbB2 inhibition does not effect basal isolated preantral follicle growth, (ii) EGFR but (likely) not ErbB2 inhibition completely blocks EGF-stimulated growth. This provides strong evidence that EGFR signalling is important in preantral follicle growth. The effect of salivary gland removal (the major source of circulating EGF) on preantral follicle growth would demonstrate the physiological relevance of EGF:EGFR interactions to preantral follicle growth. However, even if GC-expressed EGFR is never exposed to EGF during preantral follicle growth, the fact that it is mitogenic to GCs when bound by a ligand in follicles is strong evidence that that is its function in vivo. *Hbegf* and *Tgfα* are the only EGFR ligands that have been detected in follicles so far in this project. Therefore, investigation into the effects of these on isolated preantral follicle growth is a good idea for future work as ligands do have distinct roles and biological responses. The MAPK pathway is a mitogenic

intracellular signalling pathway activated downstream of all ErbB dimers (Yarden and Sliwkowski, 2001). Therefore, as EGFR and its ligands are expressed in preantral follicles and EGFR:EGF interactions are mitogenic to preantral GCs it is likely that EGFR signalling is important for preantral GC proliferation in vivo. These data did not suggest that ErbB2 had a role in preantral follicle growth. However, ErbB2 protein expression was regulated such that it was much higher in growing follicles in the peripheral cortex of the ovary. These follicles are unlikely to be isolated and put into culture and, therefore, the role of ErbB2 in growth of these follicles cannot be commented on based on this data.

The underlying reason for this pattern of ErbB2 expression is unclear, though very intriguing as, to the best of my knowledge, there is only one other protein that is expressed in a similar manner: Smad2/3 (Fenwick et al., 2011; Fenwick et al., 2013). Smad2/3 and ErbB2 are both regulated according to follicle stage to some extent. ErbB2 is also definitely regulated in a spatial manner. Whether, or to what extent, Smad2/3 expression is regulated according to follicular location within the ovary, remains unclear. Therefore, ErbB2 may be the only protein, so far described, to be regulated in this particular manner. Several possible underlying mechanisms were outlined in Chapter 5. Further investigation into these could shed light on why follicles towards the medulla of the pre-pubertal ovary, which initiate grow first, are different to those in the cortex of the ovary whose development appears comparatively delayed.

ErbB2 protein was expressed in all follicles of a d4 ovary however, and therefore the role of ErbB2 in primordial activation was directly examined using exogenous EGF ligand and Lapatinib, a dual EGFR/ErbB2 inhibitor. Excitingly, the proportion of growing follicles in central sections from ovaries exposed to 10 ng/mL

EGF was significantly more than that of ovaries exposed to control medium indicating EGF promotes in vitro primordial activation. Furthermore, in a separate experiment, the proportion of growing follicles in central sections from ovaries exposed to 1 μM Lapatinib was significantly smaller than that of ovaries exposed to vehicle control, suggesting that EGFR/ErbB2 signalling positively regulates in vitro primordial activation. These data provide evidence to support a model in which EGF stimulation of EGFR/ErbB2 heterodimerisation and downstream signalling promotes primordial activation. However, the higher doses included in both these experiments did not affect the proportion of growing follicles in a central section. This may be a real reflection of the effect of treatment. For example, 100 ng/mL may target EGFR for lysosomal degradation more efficiently than 10 ng/mL EGF. A previous study implicated ErbB2 in primordial activation in a rodent model (Li-Ping et al., 2010) using siRNA to ErbB2. However, they localised *ErbB2* transcripts to the ooplasm of rat primordial follicles. The data presented here demonstrate that *ErbB2* transcripts and ERBB2 protein is GC-specific. Furthermore, 100 ng/mL EGF did not affect in vitro primordial activation in rat ovaries (Kezele et al., 2002), similar to the results presented here. This technique involves the dissection of small ovaries from d4 mice and culture on a transwell membrane insert. The ovaries spread and flatten on this membrane during culture, some more than others, for a reason as yet unknown. Therefore, the extent to which this occurs during culture could be responsible for differences in follicle development between ovaries, as the spatial relationship between follicles will be altered. Future work will include experimenting with the ovary culture model to establish whether flattening of the ovaries on the membrane inserts and the extent to which follicles that share a basal lamina develop in vitro are features which can be reduced or whether they are unavoidable features of in vitro

culture of d4 mouse ovaries on membrane inserts. The establishment of an ovary culture model in which the effects of ErbB2 inhibition on GC cuboidalisation, proliferation and multilayering could be accurately classified/characterised would be greatly beneficial to future work on this project. Following any possible optimisation, future work would also include validation of the results observed in these preliminary experiments using a large number of ovaries cultured on several membranes per treatment group and analysis of every fifth section for follicle counts. If in vitro observations were validated, the role of ErbB2 signalling in vivo could be examined by either conditionally ablating ErbB2 in mouse GCs or treating live mice with ErbB2 inhibitors. It would be appropriate to specifically ablate ErbB2 in Foxl2-expressing cells of the ovary as this is a marker of pre-GCs and GCs and has been genetically targeted in the ovary. With regards to exposing live mice to inhibitors of ErbB2, Lapatinib Ditosylate would be the most easily administered as Tykerb, as it is clinically known, is an oral anti-HER2 cancer therapy. It would be interesting to examine the effect of HER2-targetted therapies on ovarian reserve in female cancer patients. The results from this project suggest that cancer therapies which block ErbB2 signalling would slow the rate of primordial activation which may lead to anovulatory cycles and delay of the onset of menopause. However, investigation into this will always be hindered by confounding factors such as the cell death caused by other chemotherapeutic agents used. To the best of my knowledge this has not been investigated so far.

To summarise, the role of ErbB2 and its possible heterodimerisation partners may provide useful avenues for further research into primordial activation and preantral follicle development.

Abel, M. H., Wootton, A. N., Wilkins, V., Huhtaniemi, I., Knight, P. G. and Charlton, H. M. (2000). The effect of a null mutation in the follicle-stimulating hormone receptor gene on mouse reproduction. *Endocrinology* **141**, 1795-803.

Adhikari, D. and Liu, K. (2009). Molecular mechanisms underlying the activation of mammalian primordial follicles. *Endocr Rev* **30**, 438-64.

Anklesaria, P., Teixido, J., Laiho, M., Pierce, J. H., Greenberger, J. S. and Massague, J. (1990). Cell-cell adhesion mediated by binding of membrane-anchored transforming growth factor alpha to epidermal growth factor receptors promotes cell proliferation. *Proc Natl Acad Sci U S A* **87**, 3289-93.

Balk, S. D. (1971). Stimulation of the proliferation of chicken fibroblasts by folic acid or a serum factor(s) in a plasma-containing medium. *Proc Natl Acad Sci U S A* **68**, 1689-92.

Baselga, J., Tripathy, D., Mendelsohn, J., Baughman, S., Benz, C. C., Dantis, L., Sklarin, N. T., Seidman, A. D., Hudis, C. A., Moore, J. et al. (1999). Phase II study of weekly intravenous trastuzumab (Herceptin) in patients with HER2/neu-overexpressing metastatic breast cancer. *Semin Oncol* **26**, 78-83.

Bauknecht, T., Kommoss, F., Birmelin, G., von Kleist, S., Kohler, M. and Pfleiderer, A. (1991). Expression analysis of EGF-R and TGFa in human ovarian carcinomas. *Anticancer Res* **11**, 1523-8.

Betsholtz, C. (2003). Biology of platelet-derived growth factors in development. *Birth Defects Res C Embryo Today* **69**, 272-85.

Borg, J. P., Marchetto, S., Le Bivic, A., Ollendorff, V., Jaulin-Bastard, F., Saito, H., Fournier, E., Adelaide, J., Margolis, B. and Birnbaum, D. (2000). ERBIN: a basolateral PDZ protein that interacts with the mammalian ERBB2/HER2 receptor. *Nat Cell Biol* **2**, 407-14.

Burns, K. H., Owens, G. E., Fernandez, J. M., Nilson, J. H. and Matzuk, M. M. (2002). Characterization of integrin expression in the mouse ovary. *Biol Reprod* **67**, 743-51.

Byskov, A. G. (1974). Does the rete ovarii act as a trigger for the onset of meiosis? *Nature* **252**, 396-7.

Byskov, A. G., Guoliang, X. and Andersen, C. Y. (1997). The cortex-medulla oocyte growth pattern is organized during fetal life: an in-vitro study of the mouse ovary. *Mol Hum Reprod* **3**, 795-800.

Byskov, A. G. and Lintern-Moore, S. (1973). Follicle formation in the immature mouse ovary: the role of the rete ovarii. *J Anat* **116**, 207-17.

Calongos, G., Hasegawa, A., Komori, S. and Koyama, K. (2009). Harmful effects of anti-zona pellucida antibodies in folliculogenesis, oogenesis, and fertilization. *J Reprod Immunol* **79**, 148-55.

Carabatsos, M. J., Elvin, J., Matzuk, M. M. and Albertini, D. F. (1998). Characterization of oocyte and follicle development in growth differentiation factor-9-deficient mice. *Dev Biol* **204**, 373-84.

Carmeliet, P., Lampugnani, M. G., Moons, L., Breviario, F., Compernolle, V., Bono, F., Balconi, G., Spagnuolo, R., Oosthuyse, B., Dewerchin, M. et al. (1999). Targeted deficiency or cytosolic truncation of the VE-cadherin gene in mice impairs VEGF-mediated endothelial survival and angiogenesis. *Cell* **98**, 147-57.

Carnegie, J. A., Byard, R., Dardick, I. and Tsang, B. K. (1988). Culture of granulosa cells in collagen gels: the influence of cell shape on steroidogenesis. *Biol Reprod* **38**, 881-90.

Causeret, M., Taulet, N., Comunale, F., Favard, C. and Gauthier-Rouviere, C. (2005). N-cadherin association with lipid rafts regulates its dynamic assembly at cell-cell junctions in C2C12 myoblasts. *Mol Biol Cell* **16**, 2168-80.

Chang, L. and Karin, M. (2001). Mammalian MAP kinase signalling cascades. *Nature* **410**, 37-40.

Chartier, N. T., Laine, M. G., Ducarouge, B., Oddou, C., Bonaz, B., Albiges-Rizo, C. and Jacquier-Sarlin, M. R. (2011). Enterocytic differentiation is modulated by lipid rafts-dependent assembly of adherens junctions. *Exp Cell Res* **317**, 1422-36.

Chen, X., Aravindakshan, J., Yang, Y., Tiwari-Pandey, R. and Sairam, M. R. (2006). Aberrant expression of PDGF ligands and receptors in the tumor prone ovary of follitropin receptor knockout (FORKO) mouse. *Carcinogenesis* **27**, 903-15.

Cheng, Z. Y., Li, W. J., He, F., Zhou, J. M. and Zhu, X. F. (2007). Synthesis and biological evaluation of 4-aryl-5-cyano-2H-1,2,3-triazoles as inhibitor of HER2 tyrosine kinase. *Bioorg Med Chem* **15**, 1533-8.

Choi, J. K., Agarwal, P., Huang, H., Zhao, S. and He, X. (2014). The crucial role of mechanical heterogeneity in regulating follicle development and ovulation with engineered ovarian microtissue. *Biomaterials* **35**, 5122-8.

Citi, S., Paschoud, S., Pulimeno, P., Timolati, F., De Robertis, F., Jond, L. and Guillemot, L. (2009). The tight junction protein cingulin regulates gene expression and RhoA signaling. *Ann N Y Acad Sci* **1165**, 88-98.

Colomer, R., Shamon, L. A., Tsai, M. S. and Lupu, R. (2001). Herceptin: from the bench to the clinic. *Cancer Invest* **19**, 49-56.

Comoglio, P. M., Boccaccio, C. and Trusolino, L. (2003). Interactions between growth factor receptors and adhesion molecules: breaking the rules. *Curr Opin Cell Biol* **15**, 565-71.

Conti, M., Hsieh, M., Park, J. Y. and Su, Y. Q. (2006). Role of the epidermal growth factor network in ovarian follicles. *Mol Endocrinol* **20**, 715-23.

Craig, J., Orisaka, M., Wang, H., Orisaka, S., Thompson, W., Zhu, C., Kotsuji, F. and Tsang, B. K. (2007). Gonadotropin and intra-ovarian signals regulating follicle development and atresia: the delicate balance between life and death. *Front Biosci* **12**, 3628-39.

Culiner, A. and Shippel, S. (1949). Virilism and theca-cell hyperplasia of the ovary; a syndrome. *J Obstet Gynaecol Br Emp* **56**, 439-45.

Da Silva-Buttkus, P., Jayasooriya, G. S., Mora, J. M., Mobberley, M., Ryder, T. A., Baithun, M., Stark, J., Franks, S. and Hardy, K. (2008). Effect of cell shape and packing density on granulosa cell proliferation and formation of multiple layers during early follicle development in the ovary. *J Cell Sci* **121**, 3890-900.

Da Silva-Buttkus, P., Marcelli, G., Franks, S., Stark, J. and Hardy, K. (2009). Inferring biological mechanisms from spatial analysis: prediction of a local inhibitor in the ovary. *Proc Natl Acad Sci U S A* **106**, 456-61.

Dean, J. (1991). The zona pellucida genes encode essential proteins for mammalian fertilization and early embryogenesis. *Proc Soc Exp Biol Med* **196**, 141-6.

Ding, T., Luo, A., Yang, S., Lai, Z., Wang, Y., Shen, W., Jiang, J., Lu, Y., Ma, D. and Wang, S. (2012). Effects of basal media and supplements on diethylstilbestrol-treated immature mouse primary granulosa cell growth and regulation of steroidogenesis in vitro. *Reprod Domest Anim* **47**, 355-64.

Dong, J., Albertini, D. F., Nishimori, K., Kumar, T. R., Lu, N. and Matzuk, M. M. (1996). Growth differentiation factor-9 is required during early ovarian folliculogenesis. *Nature* **383**, 531-5.

Dragovic, R. A., Ritter, L. J., Schulz, S. J., Amato, F., Armstrong, D. T. and Gilchrist, R. B. (2005). Role of oocyte-secreted growth differentiation factor 9 in the regulation of mouse cumulus expansion. *Endocrinology* **146**, 2798-806.

Dube, E., Dufresne, J., Chan, P. T. and Cyr, D. G. (2012). Epidermal growth factor regulates connexin 43 in the human epididymis: role of gap junctions in azoospermia. *Hum Reprod* **27**, 2285-96.

Duleba, A. J., Spaczynski, R. Z., Arici, A., Carbone, R. and Behrman, H. R. (1999). Proliferation and differentiation of rat theca-interstitial cells: comparison of effects induced by platelet-derived growth factor and insulin-like growth factor-I. *Biol Reprod* **60**, 546-50.

Durlinger, A. L., Gruijters, M. J., Kramer, P., Karels, B., Ingraham, H. A., Nachtigal, M. W., Uilenbroek, J. T., Grootegoed, J. A. and Themmen, A. P. (2002). Anti-Mullerian hormone inhibits initiation of primordial follicle growth in the mouse ovary. *Endocrinology* **143**, 1076-84.

Durlinger, A. L., Kramer, P., Karels, B., de Jong, F. H., Uilenbroek, J. T., Grootegoed, J. A. and Themmen, A. P. (1999). Control of primordial follicle recruitment by anti-Mullerian hormone in the mouse ovary. *Endocrinology* **140**, 5789-96.

Dyson, S. and Gurdon, J. B. (1998). The interpretation of position in a morphogen gradient as revealed by occupancy of activin receptors. *Cell* **93**, 557-68.

Ebner, R. and Derynck, R. (1991). Epidermal growth factor and transforming growth factor-alpha: differential intracellular routing and processing of ligand-receptor complexes. *Cell Regul* **2**, 599-612.

Elenius, K., Choi, C. J., Paul, S., Santiestevan, E., Nishi, E. and Klagsbrun, M. (1999). Characterization of a naturally occurring ErbB4 isoform that does not bind or activate phosphatidyl inositol 3-kinase. *Oncogene* **18**, 2607-15.

Elenius, K., Corfas, G., Paul, S., Choi, C. J., Rio, C., Plowman, G. D. and Klagsbrun, M. (1997). A novel juxtamembrane domain isoform of HER4/ErbB4. Isoform-specific tissue distribution and differential processing in response to phorbol ester. *J Biol Chem* **272**, 26761-8.

Eppig, J. J. and O'Brien, M. J. (1996). Development in vitro of mouse oocytes from primordial follicles. *Biol Reprod* **54**, 197-207.

Erickson, S. L., O'Shea, K. S., Ghaboosi, N., Loverro, L., Frantz, G., Bauer, M., Lu, L. H. and Moore, M. W. (1997). ErbB3 is required for normal cerebellar and cardiac development: a comparison with ErbB2-and heregulin-deficient mice. *Development* **124**, 4999-5011.

Espey, L. L. and Richards, J. S. (2002). Temporal and spatial patterns of ovarian gene transcription following an ovulatory dose of gonadotropin in the rat. *Biol Reprod* **67**, 1662-70.

Faddy, M. J. (2000). Follicle dynamics during ovarian ageing. *Mol Cell Endocrinol* **163**, 43-8.

Fenwick, M. A., Mansour, Y. T., Franks, S. and Hardy, K. (2011). Identification and regulation of bone morphogenetic protein antagonists associated with preantral follicle development in the ovary. *Endocrinology* **152**, 3515-26.

Fenwick, M. A., Mora, J. M., Mansour, Y. T., Baithun, C., Franks, S. and Hardy, K. (2013). Investigations of TGF-beta signaling in preantral follicles of female mice reveal differential roles for bone morphogenetic protein 15. *Endocrinology* **154**, 3423-36.

Fortune, J. E., Kito, S., Wandji, S. A. and Srsen, V. (1998). Activation of bovine and baboon primordial follicles in vitro. *Theriogenology* **49**, 441-9.

Fredriksson, L., Li, H. and Eriksson, U. (2004). The PDGF family: four gene products form five dimeric isoforms. *Cytokine Growth Factor Rev* **15**, 197-204.

Free, M. J., Jaffe, R. A. and Morford, D. E. (1980). Sperm transport through the rete testis in anesthetized rats: role of the testicular capsule and effect of gonadotropins and prostaglandins. *Biol Reprod* **22**, 1073-8.

Fretto, L. J., Snape, A. J., Tomlinson, J. E., Seroogy, J. J., Wolf, D. L., LaRochelle, W. J. and Giese, N. A. (1993). Mechanism of platelet-derived growth factor (PDGF) AA, AB, and BB binding to alpha and beta PDGF receptor. *J Biol Chem* **268**, 3625-31.

Galbiati, F., Razani, B. and Lisanti, M. P. (2001). Emerging themes in lipid rafts and caveolae. *Cell* **106**, 403-11.

Garnett, K., Wang, J. and Roy, S. K. (2002). Spatiotemporal expression of epidermal growth factor receptor messenger RNA and protein in the hamster ovary: follicle stage-specific differential modulation by follicle-stimulating hormone, luteinizing hormone, estradiol, and progesterone. *Biol Reprod* **67**, 1593-604.

Garrett, T. P., McKern, N. M., Lou, M., Elleman, T. C., Adams, T. E., Lovrecz, G. O., Kofler, M., Jorissen, R. N., Nice, E. C., Burgess, A. W. et al. (2003). The crystal structure of a truncated ErbB2 ectodomain reveals an active conformation, poised to interact with other ErbB receptors. *Mol Cell* **11**, 495-505.

Gassmann, M., Casagranda, F., Orioli, D., Simon, H., Lai, C., Klein, R. and Lemke, G. (1995). Aberrant neural and cardiac development in mice lacking the ErbB4 neuregulin receptor. *Nature* **378**, 390-4.

Gelety, T. J. and Magoffin, D. A. (1997). Ontogeny of steroidogenic enzyme gene expression in ovarian theca-interstitial cells in the rat: regulation by a paracrine theca-differentiating factor prior to achieving luteinizing hormone responsiveness. *Biol Reprod* **56**, 938-45.

Gosden, R. G. and Faddy, M. J. (1998). Biological bases of premature ovarian failure. *Reprod Fertil Dev* **10**, 73-8.

Gougeon, A. and Chainy, G. B. (1987). Morphometric studies of small follicles in ovaries of women at different ages. *J Reprod Fertil* **81**, 433-42.

Graus-Porta, D., Beerli, R. R., Daly, J. M. and Hynes, N. E. (1997). ErbB-2, the preferred heterodimerization partner of all ErbB receptors, is a mediator of lateral signaling. *EMBO J* **16**, 1647-55.

Gridelli, C., De Marinis, F., Di Maio, M., Cortinovis, D., Cappuzzo, F. and Mok, T. (2011). Gefitinib as first-line treatment for patients with advanced non-small-cell lung cancer with activating epidermal growth factor receptor mutation: Review of the evidence. *Lung Cancer* **71**, 249-57.

Griffin, J., Emery, B. R., Huang, I., Peterson, C. M. and Carrell, D. T. (2006). Comparative analysis of follicle morphology and oocyte diameter in four mammalian species (mouse, hamster, pig, and human). *J Exp Clin Assist Reprod* **3**, 2.

Gumbiner, B. M. (2000). Regulation of cadherin adhesive activity. *J Cell Biol* **148**, 399-404.

Hammacher, A., Nister, M., Westermark, B. and Heldin, C. H. (1988). A human glioma cell line secretes three structurally and functionally different dimeric forms of platelet-derived growth factor. *Eur J Biochem* **176**, 179-86.

Harris, R. C., Chung, E. and Coffey, R. J. (2003). EGF receptor ligands. *Exp Cell Res* **284**, 2-13.

Harris, T. J. and Tepass, U. (2010). Adherens junctions: from molecules to morphogenesis. *Nat Rev Mol Cell Biol* **11**, 502-14.

Hart, C. E., Bailey, M., Curtis, D. A., Osborn, S., Raines, E., Ross, R. and Forstrom, J. W. (1990). Purification of PDGF-AB and PDGF-BB from human platelet extracts and identification of all three PDGF dimers in human platelets. *Biochemistry* **29**, 166-72.

Heldin, C. H. and Westermark, B. (1990). Platelet-derived growth factor: mechanism of action and possible in vivo function. *Cell Regul* **1**, 555-66.

Heldin, C. H. and Westermark, B. (1999). Mechanism of action and in vivo role of platelet-derived growth factor. *Physiol Rev* **79**, 1283-316.

Helms, M. W., Kemming, D., Contag, C. H., Pospisil, H., Bartkowiak, K., Wang, A., Chang, S. Y., Buerger, H. and Brandt, B. H. (2009). TOB1 is regulated by EGF-dependent HER2 and EGFR signaling, is highly phosphorylated, and indicates poor prognosis in node-negative breast cancer. *Cancer Res* **69**, 5049-56.

Henderson, S. A. and Edwards, R. G. (1968). Chiasma frequency and maternal age in mammals. *Nature* **218**, 22-8.

Hillier, S. G. (1994). Current concepts of the roles of follicle stimulating hormone and luteinizing hormone in folliculogenesis. *Hum Reprod* **9**, 188-91.

Hillier, S. G. (2001). Gonadotropic control of ovarian follicular growth and development. *Mol Cell Endocrinol* **179**, 39-46.

Hillier, S. G., Whitelaw, P. F. and Smyth, C. D. (1994). Follicular oestrogen synthesis: the 'two-cell, two-gonadotrophin' model revisited. *Mol Cell Endocrinol* **100**, 51-4.

Hirshfield, A. N. (1989). Granulosa cell proliferation in very small follicles of cycling rats studied by long-term continuous tritiated-thymidine infusion. *Biol Reprod* **41**, 309-16.

Hirshfield, A. N. (1991a). Development of follicles in the mammalian ovary. *Int Rev Cytol* **124**, 43-101.

Hirshfield, A. N. (1991b). Theca cells may be present at the outset of follicular growth. *Biol Reprod* **44**, 1157-62.

Hirshfield, A. N. (1992). Heterogeneity of cell populations that contribute to the formation of primordial follicles in rats. *Biol Reprod* **47**, 466-72.

Hoschuetzky, H., Aberle, H. and Kemler, R. (1994). Beta-catenin mediates the interaction of the cadherin-catenin complex with epidermal growth factor receptor. *J Cell Biol* **127**, 1375-80.

Hsieh, M., Thao, K. and Conti, M. (2011). Genetic dissection of epidermal growth factor receptor signaling during luteinizing hormone-induced oocyte maturation. *PLoS One* **6**, e21574.

Hughesdon, P. E. (1982). Morphology and morphogenesis of the Stein-Leventhal ovary and of so-called "hyperthecosis". *Obstet Gynecol Surv* **37**, 59-77.

Hummitzsch, K., Irving-Rodgers, H. F., Hatzirodos, N., Bonner, W., Sabatier, L., Reinhardt, D. P., Sado, Y., Ninomiya, Y., Wilhelm, D. and Rodgers, R. J. (2013). A new model of development of the mammalian ovary and follicles. *PLoS One* **8**, e55578.

Hynes, N. E. and Dey, J. H. (2009). PI3K inhibition overcomes trastuzumab resistance: blockade of ErbB2/ErbB3 is not always enough. *Cancer Cell* **15**, 353-5.

Irving-Rodgers, H. F., Hummitzsch, K., Murdiyarso, L. S., Bonner, W. M., Sado, Y., Ninomiya, Y., Couchman, J. R., Sorokin, L. M. and Rodgers, R. J. (2010). Dynamics of extracellular matrix in ovarian follicles and corpora lutea of mice. *Cell Tissue Res* **339**, 613-24.

Ishibashi, K., Fukumoto, Y., Hasegawa, H., Abe, K., Kubota, S., Aoyama, K., Nakayama, Y. and Yamaguchi, N. (2013). Nuclear ErbB4 signaling through H3K9me3 is antagonized by EGFR-activated c-Src. *J Cell Sci* **126**, 625-37.

Ishitsuka, R., Sato, S. B. and Kobayashi, T. (2005). Imaging lipid rafts. *J Biochem* **137**, 249-54.

Jamora, C. and Fuchs, E. (2002). Intercellular adhesion, signalling and the cytoskeleton. *Nat Cell Biol* **4**, E101-8.

Jenndahl, L. E., Isakson, P. and Baeckstrom, D. (2005). c-erbB2-induced epithelial-mesenchymal transition in mammary epithelial cells is suppressed by cell-cell contact and initiated prior to E-cadherin downregulation. *Int J Oncol* **27**, 439-48.

Jiang, N., Saba, N. F. and Chen, Z. G. (2012). Advances in Targeting HER3 as an Anticancer Therapy. *Chemother Res Pract* **2012**, 817304.

John, G. B., Gallardo, T. D., Shirley, L. J. and Castrillon, D. H. (2008). Foxo3 is a PI3K-dependent molecular switch controlling the initiation of oocyte growth. *Dev Biol* **321**, 197-204.

Jones, J. T., Akita, R. W. and Sliwkowski, M. X. (1999). Binding specificities and affinities of egf domains for ErbB receptors. *FEBS Lett* **447**, 227-31.

Jones, R. B., Gordus, A., Krall, J. A. and MacBeath, G. (2006). A quantitative protein interaction network for the ErbB receptors using protein microarrays. *Nature* **439**, 168-74.

Kaipia, A. and Hsueh, A. J. (1997). Regulation of ovarian follicle atresia. *Annu Rev Physiol* **59**, 349-63.

Kananen, K., Markkula, M., Rainio, E., Su, J. G., Hsueh, A. J. and Huhtaniemi, I. T. (1995). Gonadal tumorigenesis in transgenic mice bearing the mouse inhibin alpha-subunit promoter/simian virus T-antigen fusion gene:

characterization of ovarian tumors and establishment of gonadotropin-responsive granulosa cell lines. *Mol Endocrinol* **9**, 616-27.

Kawagishi, R., Tahara, M., Morishige, K., Sakata, M., Tasaka, K., Ikeda, W., Morimoto, K., Takai, Y. and Murata, Y. (2005). Expression of nectin-2 in mouse granulosa cells. *Eur J Obstet Gynecol Reprod Biol* **121**, 71-6.

Kawamura-Tsuzuku, J., Suzuki, T., Yoshida, Y. and Yamamoto, T. (2004). Nuclear localization of Tob is important for regulation of its antiproliferative activity. *Oncogene* **23**, 6630-8.

Kendall, S. K., Saunders, T. L., Jin, L., Lloyd, R. V., Glode, L. M., Nett, T. M., Keri, R. A., Nilson, J. H. and Camper, S. A. (1991). Targeted ablation of pituitary gonadotropes in transgenic mice. *Mol Endocrinol* **5**, 2025-36.

Kezele, P. R., Nilsson, E. E. and Skinner, M. K. (2002). Insulin but not insulin-like growth factor-1 promotes the primordial to primary follicle transition. *Mol Cell Endocrinol* **192**, 37-43.

Kidder, G. M. and Mhawi, A. A. (2002). Gap junctions and ovarian folliculogenesis. *Reproduction* **123**, 613-20.

Kidder, G. M. and Vanderhyden, B. C. (2010). Bidirectional communication between oocytes and follicle cells: ensuring oocyte developmental competence. *Can J Physiol Pharmacol* **88**, 399-413.

Kim, K., Lee, H., Threadgill, D. W. and Lee, D. (2011). Epiregulin-dependent amphiregulin expression and ERBB2 signaling are involved in luteinizing hormone-induced paracrine signaling pathways in mouse ovary. *Biochem Biophys Res Commun* **405**, 319-24.

Kirkpatrick, C. and Peifer, M. (1995). Not just glue: cell-cell junctions as cellular signaling centers. *Curr Opin Genet Dev* **5**, 56-65.

Klapper, L. N., Waterman, H., Sela, M. and Yarden, Y. (2000). Tumor-inhibitory antibodies to HER-2/ErbB-2 may act by recruiting c-Cbl and enhancing ubiquitination of HER-2. *Cancer Res* **60**, 3384-8.

Kochupurakkal, B. S., Harari, D., Di-Segni, A., Maik-Rachline, G., Lyass, L., Gur, G., Kerber, G., Citri, A., Lavi, S., Eilam, R. et al. (2005). Epigen, the last ligand of ErbB receptors, reveals intricate relationships between affinity and mitogenicity. *J Biol Chem* **280**, 8503-12.

Kreeger, P. K., Woodruff, T. K. and Shea, L. D. (2003). Murine granulosa cell morphology and function are regulated by a synthetic Arg-Gly-Asp matrix. *Mol Cell Endocrinol* **205**, 1-10.

Kunisue, H., Kurebayashi, J., Otsuki, T., Tang, C. K., Kurosumi, M., Yamamoto, S., Tanaka, K., Doihara, H., Shimizu, N. and Sonoo, H. (2000). Anti-HER2 antibody enhances the growth inhibitory effect of anti-oestrogen on breast cancer cells expressing both oestrogen receptors and HER2. *Br J Cancer* **82**, 46-51.

Kuroda, H., Terada, N., Nakayama, H., Matsumoto, K. and Kitamura, Y. (1988). Infertility due to growth arrest of ovarian follicles in Sl/Slt mice. *Dev Biol* **126**, 71-9.

Lawrence, T. S., Ginzberg, R. D., Gilula, N. B. and Beers, W. H. (1979). Hormonally induced cell shape changes in cultured rat ovarian granulosa cells. *J Cell Biol* **80**, 21-36.

Lee, K. F., Simon, H., Chen, H., Bates, B., Hung, M. C. and Hauser, C. (1995). Requirement for neuregulin receptor erbB2 in neural and cardiac development. *Nature* **378**, 394-8.

Lee, Y., Ma, J., Lyu, H., Huang, J., Kim, A. and Liu, B. (2014). Role of erbB3 receptors in cancer therapeutic resistance. *Acta Biochim Biophys Sin (Shanghai)* **46**, 190-8.

Lemmon, M. A. and Schlessinger, J. (2010). Cell signaling by receptor tyrosine kinases. *Cell* **141**, 1117-34.

Lemmon, M. A., Schlessinger, J. and Ferguson, K. M. (2014). The EGFR family: not so prototypical receptor tyrosine kinases. *Cold Spring Harb Perspect Biol* **6**, a020768.

Lenferink, A. E., Pinkas-Kramarski, R., van de Poll, M. L., van Vugt, M. J., Klapper, L. N., Tzahar, E., Waterman, H., Sela, M., van Zoelen, E. J. and Yarden, Y. (1998). Differential endocytic routing of homo- and hetero-dimeric ErbB tyrosine kinases confers signaling superiority to receptor heterodimers. *EMBO J* **17**, 3385-97.

Leveen, P., Pekny, M., Gebre-Medhin, S., Swolin, B., Larsson, E. and Betsholtz, C. (1994). Mice deficient for PDGF B show renal, cardiovascular, and hematological abnormalities. *Genes Dev* **8**, 1875-87.

Li-Ping, Z., Da-Lei, Z., Jian, H., Liang-Quan, X., Ai-Xia, X., Xiao-Yu, D., Dan-Feng, T. and Yue-Hui, Z. (2010). Proto-oncogene c-erbB2 initiates rat primordial follicle growth via PKC and MAPK pathways. *Reprod Biol Endocrinol* **8**, 66.

Lintern-Moore, S. and Moore, G. P. (1979). The initiation of follicle and oocyte growth in the mouse ovary. *Biol Reprod* **20**, 773-8.

Liu, A., Flores, C., Kinkead, T., Carboni, A. A., Menon, M. and Seethalakshmi, L. (1994). Effects of sialoadenectomy and epidermal growth factor on testicular function of sexually mature male mice. *J Urol* **152**, 554-61.

Liu, Y. and Gray, N. S. (2006). Rational design of inhibitors that bind to inactive kinase conformations. *Nat Chem Biol* **2**, 358-64.

Long, J. S., Fujiwara, Y., Edwards, J., Tannahill, C. L., Tigyi, G., Pyne, S. and Pyne, N. J. (2010). Sphingosine 1-phosphate receptor 4 uses HER2 (ERBB2) to regulate extracellular signal regulated kinase-1/2 in MDA-MB-453 breast cancer cells. *J Biol Chem* **285**, 35957-66.

Luetteke, N. C., Qiu, T. H., Fenton, S. E., Troyer, K. L., Riedel, R. F., Chang, A. and Lee, D. C. (1999). Targeted inactivation of the EGF and amphiregulin genes reveals distinct roles for EGF receptor ligands in mouse mammary gland development. *Development* **126**, 2739-50.

Macaulay, A. D., Gilbert, I., Caballero, J., Barreto, R., Fournier, E., Tossou, P., Sirard, M. A., Clarke, H. J., Khandjian, E. W., Richard, F. J. et al. (2014). The Gametic Synapse; RNA Transfer to the Bovine Oocyte. *Biol Reprod*.

Martin, K. L., Barlow, D. H. and Sargent, I. L. (1998). Heparin-binding epidermal growth factor significantly improves human blastocyst development and hatching in serum-free medium. *Hum Reprod* **13**, 1645-52.

Matsuda, S., Kawamura-Tsuzuku, J., Ohsugi, M., Yoshida, M., Emi, M., Nakamura, Y., Onda, M., Yoshida, Y., Nishiyama, A. and Yamamoto, T. (1996). Tob, a novel protein that interacts with p185erbB2, is associated with anti-proliferative activity. *Oncogene* **12**, 705-13.

Mazurek, A., Luo, W., Krasnitz, A., Hicks, J., Powers, R. S. and Stillman, B. (2012). DDX5 regulates DNA replication and is required for cell proliferation in a subset of breast cancer cells. *Cancer Discov* **2**, 812-25.

McGee, E. A. and Hsueh, A. J. (2000). Initial and cyclic recruitment of ovarian follicles. *Endocr Rev* **21**, 200-14.

McLaughlin, E. A. and McIver, S. C. (2009). Awakening the oocyte: controlling primordial follicle development. *Reproduction* **137**, 1-11.

Miettinen, P. J., Berger, J. E., Meneses, J., Phung, Y., Pedersen, R. A., Werb, Z. and Derynck, R. (1995). Epithelial immaturity and multiorgan failure in mice lacking epidermal growth factor receptor. *Nature* **376**, 337-41.

Mitamura, T., Higashiyama, S., Taniguchi, N., Klagsbrun, M. and Mekada, E. (1995). Diphtheria toxin binds to the epidermal growth factor (EGF)-like domain of human heparin-binding EGF-like growth factor/diphtheria toxin receptor and inhibits specifically its mitogenic activity. *J Biol Chem* **270**, 1015-9.

Miyamoto, S., Hirata, M., Yamazaki, A., Kageyama, T., Hasuwa, H., Mizushima, H., Tanaka, Y., Yagi, H., Sonoda, K., Kai, M. et al. (2004). Heparin-binding EGF-like growth factor is a promising target for ovarian cancer therapy. *Cancer Res* **64**, 5720-7.

Mora, J. M., Fenwick, M. A., Castle, L., Baithun, M., Ryder, T. A., Mobberley, M., Carzaniga, R., Franks, S. and Hardy, K. (2012). Characterization and significance of adhesion and junction-related proteins in mouse ovarian follicles. *Biol Reprod* **86**, 153, 1-14.

Mork, L., Maatouk, D. M., McMahon, J. A., Guo, J. J., Zhang, P., McMahon, A. P. and Capel, B. (2012). Temporal differences in granulosa cell specification in the ovary reflect distinct follicle fates in mice. *Biol Reprod* **86**, 37.

Moscatello, D. K., Holgado-Madruga, M., Godwin, A. K., Ramirez, G., Gunn, G., Zoltick, P. W., Biegel, J. A., Hayes, R. L. and Wong, A. J. (1995). Frequent expression of a mutant epidermal growth factor receptor in multiple human tumors. *Cancer Res* **55**, 5536-9.

Moustakas, A. and Heldin, C. H. (2009). The regulation of TGFbeta signal transduction. *Development* **136**, 3699-714.

Muhsin, M., Graham, J. and Kirkpatrick, P. (2003). Gefitinib. *Nat Rev Drug Discov* **2**, 515-6.

Murillo, H., Schmidt, L. J. and Tindall, D. J. (2001). Tyrphostin AG825 triggers p38 mitogen-activated protein kinase-dependent apoptosis in androgen-independent prostate cancer cells C4 and C4-2. *Cancer Res* **61**, 7408-12.

Murray, A. and Spears, N. (2000). Follicular development in vitro. *Semin Reprod Med* **18**, 109-22.

Nagy, P., Vereb, G., Sebestyen, Z., Horvath, G., Lockett, S. J., Damjanovich, S., Park, J. W., Jovin, T. M. and Szollosi, J. (2002). Lipid rafts and the local density of ErbB proteins influence the biological role of homo- and heteroassociations of ErbB2. *J Cell Sci* **115**, 4251-62.

Nilsson, E., Parrott, J. A. and Skinner, M. K. (2001). Basic fibroblast growth factor induces primordial follicle development and initiates folliculogenesis. *Mol Cell Endocrinol* **175**, 123-30.

Nilsson, E. E., Detzel, C. and Skinner, M. K. (2006). Platelet-derived growth factor modulates the primordial to primary follicle transition. *Reproduction* **131**, 1007-15.

Nilsson, E. E. and Skinner, M. K. (2004). Kit ligand and basic fibroblast growth factor interactions in the induction of ovarian primordial to primary follicle transition. *Mol Cell Endocrinol* **214**, 19-25.

Nippita, T. A. and Baber, R. J. (2007). Premature ovarian failure: a review. *Climacteric* **10**, 11-22.

Noma, N., Kawashima, I., Fan, H. Y., Fujita, Y., Kawai, T., Tomoda, Y., Mihara, T., Richards, J. S. and Shimada, M. (2011). LH-induced neuregulin 1 (NRG1) type III transcripts control granulosa cell differentiation and oocyte maturation. *Mol Endocrinol* **25**, 104-16.

Ogiso, H., Ishitani, R., Nureki, O., Fukai, S., Yamanaka, M., Kim, J. H., Saito, K., Sakamoto, A., Inoue, M., Shirouzu, M. et al. (2002). Crystal structure of the complex of human epidermal growth factor and receptor extracellular domains. *Cell* **110**, 775-87.

Osherov, N., Gazit, A., Gilon, C. and Levitzki, A. (1993). Selective inhibition of the epidermal growth factor and HER2/neu receptors by tyrphostins. *J Biol Chem* **268**, 11134-42.

Ostman, A., Rall, L., Hammacher, A., Wormstead, M. A., Coit, D., Valenzuela, P., Betsholtz, C., Westermark, B. and Heldin, C. H. (1988). Synthesis and assembly of a functionally active recombinant platelet-derived growth factor AB heterodimer. *J Biol Chem* **263**, 16202-8.

Ostman, A., Thyberg, J., Westermark, B. and Heldin, C. H. (1992). PDGF-AA and PDGF-BB biosynthesis: proprotein processing in the Golgi complex and lysosomal degradation of PDGF-BB retained intracellularly. *J Cell Biol* **118**, 509-19.

Otsuka, F., Yao, Z., Lee, T., Yamamoto, S., Erickson, G. F. and Shimasaki, S. (2000). Bone morphogenetic protein-15. Identification of target cells and biological functions. *J Biol Chem* **275**, 39523-8.

Pan, B., Sengoku, K., Takuma, N., Goishi, K., Horikawa, M., Tamate, K. and Ishikawa, M. (2004). Differential expression of heparin-binding epidermal growth factor-like growth factor in the rat ovary. *Mol Cell Endocrinol* **214**, 1-8.

Pangas, S. A. (2007). Growth factors in ovarian development. *Semin Reprod Med* **25**, 225-34.

Paria, B. C., Ma, W., Tan, J., Raja, S., Das, S. K., Dey, S. K. and Hogan, B. L. (2001). Cellular and molecular responses of the uterus to embryo implantation can be elicited by locally applied growth factors. *Proc Natl Acad Sci U S A* **98**, 1047-52.

Park, J. Y., Su, Y. Q., Ariga, M., Law, E., Jin, S. L. and Conti, M. (2004). EGF-like growth factors as mediators of LH action in the ovulatory follicle. *Science* **303**, 682-4.

Parrott, J. A. and Skinner, M. K. (1999). Kit-ligand/stem cell factor induces primordial follicle development and initiates folliculogenesis. *Endocrinology* **140**, 4262-71.

Pece, S. and Gutkind, J. S. (2000). Signaling from E-cadherins to the MAPK pathway by the recruitment and activation of epidermal growth factor receptors upon cell-cell contact formation. *J Biol Chem* **275**, 41227-33.

Peluso, J. J., Pappalardo, A. and Trolice, M. P. (1996). N-cadherin-mediated cell contact inhibits granulosa cell apoptosis in a progesterone-independent manner. *Endocrinology* **137**, 1196-203.

Peng, X. R., Hsueh, A. J., LaPolt, P. S., Bjersing, L. and Ny, T. (1991). Localization of luteinizing hormone receptor messenger ribonucleic acid expression in ovarian cell types during follicle development and ovulation. *Endocrinology* **129**, 3200-7.

Pepling, M. E. (2006). From primordial germ cell to primordial follicle: mammalian female germ cell development. *Genesis* **44**, 622-32.

Pepling, M. E. and Spradling, A. C. (2001). Mouse ovarian germ cell cysts undergo programmed breakdown to form primordial follicles. *Dev Biol* **234**, 339-51.

Peter R. Smith, L. D. Q., Jennifer J. Juengel, and Peter R. Hurst. (2009). Development of the Rete Ovarii in the Sheep Ovary. In *BIOLOGY OF REPRODUCTION*, vol. 81.

Peters, H. (1969). The development of the mouse ovary from birth to maturity. *Acta Endocrinol (Copenh)* **62**, 98-116.

Picton, H. M. (2001). Activation of follicle development: the primordial follicle. *Theriogenology* **55**, 1193-210.

Raab, G., Kover, K., Paria, B. C., Dey, S. K., Ezzell, R. M. and Klagsbrun, M. (1996). Mouse preimplantation blastocysts adhere to cells expressing the transmembrane form of heparin-binding EGF-like growth factor. *Development* **122**, 637-45.

Rahmouni, K., Morgan, D. A., Morgan, G. M., Liu, X., Sigmund, C. D., Mark, A. L. and Haynes, W. G. (2004). Hypothalamic PI3K and MAPK differentially mediate regional sympathetic activation to insulin. *J Clin Invest* **114**, 652-8.

Ramsauer, V. P., Pino, V., Farooq, A., Carothers Carraway, C. A., Salas, P. J. and Carraway, K. L. (2006). Muc4-ErbB2 complex formation and signaling in polarized CACO-2 epithelial cells indicate that Muc4 acts as an unorthodox ligand for ErbB2. *Mol Biol Cell* **17**, 2931-41.

Reddy, P., Liu, L., Adhikari, D., Jagarlamudi, K., Rajareddy, S., Shen, Y., Du, C., Tang, W., Hamalainen, T., Peng, S. L. et al. (2008). Oocyte-specific deletion of Pten causes premature activation of the primordial follicle pool. *Science* **319**, 611-3.

Riccio, G., Esposito, G., Leoncini, E., Contu, R., Condorelli, G., Chiariello, M., Laccetti, P., Hrelia, S., D'Alessio, G. and De Lorenzo, C. (2009). Cardiotoxic effects, or lack thereof, of anti-ErbB2 immunoagents. *FASEB J* **23**, 3171-8.

Riethmacher, D., Sonnenberg-Riethmacher, E., Brinkmann, V., Yamaai, T., Lewin, G. R. and Birchmeier, C. (1997). Severe neuropathies in mice with targeted mutations in the ErbB3 receptor. *Nature* **389**, 725-30.

Rodgers, R. J., Irving-Rodgers, H. F. and van Wezel, I. L. (2000). Extracellular matrix in ovarian follicles. *Mol Cell Endocrinol* **163**, 73-9.

Ross, R., Glomset, J., Kariya, B. and Harker, L. (1974). A platelet-dependent serum factor that stimulates the proliferation of arterial smooth muscle cells in vitro. *Proc Natl Acad Sci U S A* **71**, 1207-10.

Salmon, N. A., Handyside, A. H. and Joyce, I. M. (2004). Oocyte regulation of anti-Mullerian hormone expression in granulosa cells during ovarian follicle development in mice. *Dev Biol* **266**, 201-8.

Sasseville, M., Ritter, L. J., Nguyen, T. M., Liu, F., Mottershead, D. G., Russell, D. L. and Gilchrist, R. B. (2010). Growth differentiation factor 9 signaling requires ERK1/2 activity in mouse granulosa and cumulus cells. *J Cell Sci* **123**, 3166-76.

Schechter, A. L., Stern, D. F., Vaidyanathan, L., Decker, S. J., Drebin, J. A., Greene, M. I. and Weinberg, R. A. (1984). The neu oncogene: an erb-B-related gene encoding a 185,000-Mr tumour antigen. *Nature* **312**, 513-6.

Schlessinger, J. (2002). Ligand-induced, receptor-mediated dimerization and activation of EGF receptor. *Cell* **110**, 669-72.

Schmahl, J., Rizzolo, K. and Soriano, P. (2008). The PDGF signaling pathway controls multiple steroid-producing lineages. *Genes Dev* **22**, 3255-67.

Schmidt, D., Ovitt, C. E., Anlag, K., Fehsenfeld, S., Gredsted, L., Treier, A. C. and Treier, M. (2004). The murine winged-helix transcription factor Foxl2 is required for granulosa cell differentiation and ovary maintenance. *Development* **131**, 933-42.

Schneider, M. R. and Wolf, E. (2009). The epidermal growth factor receptor ligands at a glance. *J Cell Physiol* **218**, 460-6.

Schultz, G. S. and Wysocki, A. (2009). Interactions between extracellular matrix and growth factors in wound healing. *Wound Repair Regen* **17**, 153-62.

Scotti, L., Parborell, F., Irusta, G., De Zuniga, I., Bisioli, C., Pettorossi, H., Tesone, M. and Abramovich, D. (2014). Platelet-derived growth factor BB and DD and angiopoietin1 are altered in follicular fluid from polycystic ovary syndrome patients. *Mol Reprod Dev* **81**, 748-56.

Skinner, M. K. (2005). Regulation of primordial follicle assembly and development. *Hum Reprod Update* **11**, 461-71.

Slamon, D. J., Clark, G. M., Wong, S. G., Levin, W. J., Ullrich, A. and McGuire, W. L. (1987). Human breast cancer: correlation of relapse and survival with amplification of the HER-2/neu oncogene. *Science* **235**, 177-82.

Sleer, L. S. and Taylor, C. C. (2007). Cell-type localization of platelet-derived growth factors and receptors in the postnatal rat ovary and follicle. *Biol Reprod* **76**, 379-90.

Sliwkowski, M. X., Lofgren, J. A., Lewis, G. D., Hotaling, T. E., Fendly, B. M. and Fox, J. A. (1999). Nonclinical studies addressing the mechanism of action of trastuzumab (Herceptin). *Semin Oncol* **26**, 60-70.

Soltoff, S. P. and Cantley, L. C. (1996). p120cbl is a cytosolic adapter protein that associates with phosphoinositide 3-kinase in response to epidermal growth factor in PC12 and other cells. *J Biol Chem* **271**, 563-7.

Soriano, P. (1994). Abnormal kidney development and hematological disorders in PDGF beta-receptor mutant mice. *Genes Dev* **8**, 1888-96.

Su, Y. Q., Sugiura, K., Wigglesworth, K., O'Brien, M. J., Affourtit, J. P., Pangas, S. A., Matzuk, M. M. and Eppig, J. J. (2008). Oocyte regulation of metabolic cooperativity between mouse cumulus cells and oocytes: BMP15 and GDF9 control cholesterol biosynthesis in cumulus cells. *Development* **135**, 111-21.

Suarez, E. R., Paredes-Gamero, E. J., Del Giglio, A., Tersariol, I. L., Nader, H. B. and Pinhal, M. A. (2013). Heparan sulfate mediates trastuzumab effect in breast cancer cells. *BMC Cancer* **13**, 444.

Sun, C., Velazquez, M. A., Marfy-Smith, S., Sheth, B., Cox, A., Johnston, D. A., Smyth, N. and Fleming, T. P. (2014). Mouse early extra-embryonic lineages activate compensatory endocytosis in response to poor maternal nutrition. *Development* **141**, 1140-50.

Sundvall, M., Korhonen, A., Paatero, I., Gaudio, E., Melino, G., Croce, C. M., Aqeilan, R. I. and Elenius, K. (2008). Isoform-specific monoubiquitination,

endocytosis, and degradation of alternatively spliced ErbB4 isoforms. *Proc Natl Acad Sci U S A* **105**, 4162-7.

Takai, Y., Ikeda, W., Ogita, H. and Rikitake, Y. (2008). The immunoglobulin-like cell adhesion molecule nectin and its associated protein afadin. *Annu Rev Cell Dev Biol* **24**, 309-42.

Takai, Y. and Nakanishi, H. (2003). Nectin and afadin: novel organizers of intercellular junctions. *J Cell Sci* **116**, 17-27.

Taylor, C. C. (2000). Platelet-derived growth factor activates porcine thecal cell phosphatidylinositol-3-kinase-Akt/PKB and ras-extracellular signal-regulated kinase-1/2 kinase signaling pathways via the platelet-derived growth factor-beta receptor. *Endocrinology* **141**, 1545-53.

Tebbutt, N., Pedersen, M. W. and Johns, T. G. (2013). Targeting the ERBB family in cancer: couples therapy. *Nat Rev Cancer* **13**, 663-73.

Theisen, C. S., Wahl, J. K., 3rd, Johnson, K. R. and Wheelock, M. J. (2007). NHERF links the N-cadherin/catenin complex to the platelet-derived growth factor receptor to modulate the actin cytoskeleton and regulate cell motility. *Mol Biol Cell* **18**, 1220-32.

Thon, J. N., Devine, M. T., Jurak Begonja, A., Tibbitts, J. and Italiano, J. E., Jr. (2012). High-content live-cell imaging assay used to establish mechanism of trastuzumab emtansine (T-DM1)--mediated inhibition of platelet production. *Blood* **120**, 1975-84.

Trolice, M. P., Pappalardo, A. and Peluso, J. J. (1997). Basic fibroblast growth factor and N-cadherin maintain rat granulosa cell and ovarian surface epithelial cell viability by stimulating the tyrosine phosphorylation of the fibroblast growth factor receptors. *Endocrinology* **138**, 107-13.

Troyer, K. L. and Lee, D. C. (2001). Regulation of mouse mammary gland development and tumorigenesis by the ERBB signaling network. *J Mammary Gland Biol Neoplasia* **6**, 7-21.

Tsai, C. M., Levitzki, A., Wu, L. H., Chang, K. T., Cheng, C. C., Gazit, A. and Perng, R. P. (1996). Enhancement of chemosensitivity by tyrphostin AG825 in high-p185(neu) expressing non-small cell lung cancer cells. *Cancer Res* **56**, 1068-74.

Tzahar, E., Waterman, H., Chen, X., Levkowitz, G., Karunagaran, D., Lavi, S., Ratzkin, B. J. and Yarden, Y. (1996). A hierarchical network of interreceptor interactions determines signal transduction by Neu differentiation factor/neuregulin and epidermal growth factor. *Mol Cell Biol* **16**, 5276-87.

Vanderhyden, B. C., Caron, P. J., Buccione, R. and Eppig, J. J. (1990). Developmental pattern of the secretion of cumulus expansion-enabling factor by mouse oocytes and the role of oocytes in promoting granulosa cell differentiation. *Dev Biol* **140**, 307-17.

Vanderhyden, B. C., Cohen, J. N. and Morley, P. (1993). Mouse oocytes regulate granulosa cell steroidogenesis. *Endocrinology* **133**, 423-6.

Vanderhyden, B. C., Telfer, E. E. and Eppig, J. J. (1992). Mouse oocytes promote proliferation of granulosa cells from preantral and antral follicles in vitro. *Biol Reprod* **46**, 1196-204.

Vlodavsky, I., Brown, K. D. and Gospodarowicz, D. (1978). A comparison of the binding of epidermal growth factor to cultured granulosa and luteal cells. *J Biol Chem* **253**, 3744-50.

Vogel, C., Cobleigh, M. A., Tripathy, D., Gutheil, J. C., Harris, L. N., Fehrenbacher, L., Slamon, D. J., Murphy, M., Novotny, W. F., Burchmore, M. et al. (2001). First-line, single-agent Herceptin(trastuzumab) in metastatic breast cancer: a preliminary report. *Eur J Cancer* **37 Suppl 1**, S25-9.

Vu, T. and Claret, F. X. (2012). Trastuzumab: updated mechanisms of action and resistance in breast cancer. *Front Oncol* **2**, 62.

Wakatsuki, S., Araki, T. and Sehara-Fujisawa, A. (2014). Neuregulin-1/glial growth factor stimulates Schwann cell migration by inducing alpha5 beta1 integrin-ErbB2-focal adhesion kinase complex formation. *Genes Cells* **19**, 66-77.

Wandji, S. A., Srsen, V., Voss, A. K., Eppig, J. J. and Fortune, J. E. (1996). Initiation in vitro of growth of bovine primordial follicles. *Biol Reprod* **55**, 942-8.

Wang, C., Lv, X., Jiang, C., Cordes, C. M., Fu, L., Lele, S. M. and Davis, J. S. (2012). Transforming growth factor alpha (TGFalpha) regulates granulosa cell tumor (GCT) cell proliferation and migration through activation of multiple pathways. *PLoS One* **7**, e48299.

Wang, C. and Roy, S. K. (2010). Expression of E-cadherin and N-cadherin in perinatal hamster ovary: possible involvement in primordial follicle formation and regulation by follicle-stimulating hormone. *Endocrinology* **151**, 2319-30.

Wang, H., Jin, H., Beauvais, D. M. and Rapraeger, A. C. (2014). Cytoplasmic Domain Interactions of Syndecan-1 and Syndecan-4 with alpha6beta4 Integrin Mediate HER2- and EGFR-dependent Motility and Survival. *J Biol Chem*.

Wang, H., Leavitt, L., Ramaswamy, R. and Rapraeger, A. C. (2010). Interaction of syndecan and alpha6beta4 integrin cytoplasmic domains: regulation of ErbB2-mediated integrin activation. *J Biol Chem* **285**, 13569-79.

Wang, Y., Kong, N., Li, N., Hao, X., Wei, K., Xiang, X., Xia, G. and Zhang, M. (2013). Epidermal growth factor receptor signaling-dependent calcium elevation in cumulus cells is required for NPR2 inhibition and meiotic resumption in mouse oocytes. *Endocrinology* **154**, 3401-9.

Webber, L. J., Stubbs, S., Stark, J., Trew, G. H., Margara, R., Hardy, K. and Franks, S. (2003). Formation and early development of follicles in the polycystic ovary. *Lancet* **362**, 1017-21.

Weenen, C., Laven, J. S., Von Bergh, A. R., Cranfield, M., Groome, N. P., Visser, J. A., Kramer, P., Fauser, B. C. and Themmen, A. P. (2004). Anti-Mullerian hormone expression pattern in the human ovary: potential implications for initial and cyclic follicle recruitment. *Mol Hum Reprod* **10**, 77-83.

Wehrman, T., He, X., Raab, B., Dukipatti, A., Blau, H. and Garcia, K. C. (2007). Structural and mechanistic insights into nerve growth factor interactions with the TrkA and p75 receptors. *Neuron* **53**, 25-38.

Welshons, W. V., Wolf, M. F., Murphy, C. S. and Jordan, V. C. (1988). Estrogenic activity of phenol red. *Mol Cell Endocrinol* **57**, 169-78.

Wenzel, J. G. and Odend'hal, S. (1985). The mammalian rete ovarii: a literature review. *Cornell Vet* **75**, 411-25.

Willert, K. and Nusse, R. (1998). Beta-catenin: a key mediator of Wnt signaling. *Curr Opin Genet Dev* **8**, 95-102.

Wong, R. W. (2003). Transgenic and knock-out mice for deciphering the roles of EGFR ligands. *Cell Mol Life Sci* **60**, 113-8.

Wong, R. W., Kwan, R. W., Mak, P. H., Mak, K. K., Sham, M. H. and Chan, S. Y. (2000). Overexpression of epidermal growth factor induced hypospermatogenesis in transgenic mice. *J Biol Chem* **275**, 18297-301.

Wood, E. R., Truesdale, A. T., McDonald, O. B., Yuan, D., Hassell, A., Dickerson, S. H., Ellis, B., Pennisi, C., Horne, E., Lackey, K. et al. (2004). A unique structure for epidermal growth factor receptor bound to GW572016 (Lapatinib): relationships among protein conformation, inhibitor off-rate, and receptor activity in tumor cells. *Cancer Res* **64**, 6652-9.

Woodruff, T. K. and Shea, L. D. (2011). A new hypothesis regarding ovarian follicle development: ovarian rigidity as a regulator of selection and health. *J Assist Reprod Genet* **28**, 3-6.

Wrana, J. L. (2013). Signaling by the TGFbeta superfamily. *Cold Spring Harb Perspect Biol* **5**, a011197.

Wu, X. and Matzuk, M. M. (2002). GDF-9 and BMP-15: oocyte organizers. *Rev Endocr Metab Disord* **3**, 27-32.

Xiao, Z., Zhang, W., Yang, Y., Xu, L. and Fang, X. (2008). Single-molecule diffusion study of activated EGFR implicates its endocytic pathway. *Biochem Biophys Res Commun* **369**, 730-4.

Yang, X., Chrisman, H. and Weijer, C. J. (2008). PDGF signalling controls the migration of mesoderm cells during chick gastrulation by regulating N-cadherin expression. *Development* **135**, 3521-30.

Yarden, Y. and Sliwkowski, M. X. (2001). Untangling the ErbB signalling network. *Nat Rev Mol Cell Biol* **2**, 127-37.

Yoshida, Y., Tanaka, S., Umemori, H., Minowa, O., Usui, M., Ikematsu, N., Hosoda, E., Imamura, T., Kuno, J., Yamashita, T. et al. (2000). Negative regulation of BMP/Smad signaling by Tob in osteoblasts. *Cell* **103**, 1085-97.

Young, J. M. and McNeilly, A. S. (2010). Theca: the forgotten cell of the ovarian follicle. *Reproduction* **140**, 489-504.

Yuzawa, S., Opatowsky, Y., Zhang, Z., Mandiyan, V., Lax, I. and Schlessinger, J. (2007). Structural basis for activation of the receptor tyrosine kinase KIT by stem cell factor. *Cell* **130**, 323-34.

Zhang, S., Zeng, Y., Qu, J., Luo, Y., Wang, X. and Li, W. (2013). Endogenous EGF maintains Sertoli germ cell anchoring junction integrity and is required for early recovery from acute testicular ischemia/reperfusion injury. *Reproduction* **145**, 177-89.

Zheng, W., Zhang, H., Gorre, N., Risal, S., Shen, Y. and Liu, K. (2014a). Two classes of ovarian primordial follicles exhibit distinct developmental dynamics and physiological functions. *Hum Mol Genet* **23**, 920-8.

Zheng, W., Zhang, H. and Liu, K. (2014b). The two classes of primordial follicles in the mouse ovary: their development, physiological functions and implications for future research. *Mol Hum Reprod* **20**, 286-92.